Sede Amministrativa: Università degli Studi di Padova
Sede Consorziata: Istituto di Ricerca Pediatrica

Dipartimento della Salute della Donna e del Bambino

SCUOLA DI DOTTORATO DI RICERCA IN MEDICINA DELLO SVILUPPO E SCIENZE DELLA PROGRAMMAZIONE SANITARIA
INDIRIZZO EMATO-ONCOLOGIA, GENETICA, MALATTIE RARE E MEDICINA PREDITTIVA
CICLO XVIII

SVILUPPO E CARATTERIZZAZIONE DI MATRICE ACELLULARE DA MUSCOLO DIAFRAMMATICO ATTRAVERSO L'USO DI STRATEGIE IN VITRO E IN VIVO

DIAPHRAGM DERIVED ACELLULAR MATRIX AS MULTISTEP STUDY: FROM DEVELOPMENT TO CHARACTERIZATION USING* IN VITRO *AND* IN VIVO *STRATEGIES

Direttore della Scuola : Prof.Giuseppe Basso

Coordinatore d'indirizzo: Prof. Giuseppe Basso

Supervisore :Dott.ssa Michela Pozzobon

Dottorando : Mario Enrique Alvarez Fallas

Declaration

I, Mario Enrique Alvarez Fallas, confirm that the work presented in this thesis is my own. Whenever information were derived from other sources, I confirm that this has been indicated in the thesis.

_____

Signature

Riassunto

Introduzione

Negli ultimi decenni, la lista di attesa dei pazienti che necessitano trapianto di organi o un intervento chirurgico mirato alla sostituzione di grandi porzioni di tessuto, è andata aumentando. Al contrario però, la disponibilità di donatori, sia vivi che cadaverici, non ha seguito lo stesso andamento. Come conseguenza, nonostante i tentativi di supplire a queste necessità, molti ancora muoiono in attesa di essere curati. La medicina rigenerativa, ovvero la combinazione di diversi elementi dell'ingegneria tissutale, nasce proprio per rispondere alla ancora pressante domanda di organi e tessuti trapiantabili. Precisamente, un approccio di medicina rigenerativa si avvale di tre componenti principali: i) le cellule (dalla terapia cellulare), ii) il supporto o impalcatura per favorirne la crescita (derivato dalla scienza dei materiali, ad esempio prostetici, comunemente chiamato scaffold o mesh) e iii) segnali molecolari (principalmente dalla biologia molecolare e della farmaceutica). Tra gli organi e tessuti che sperimentano danni tali da richiedere l'impianto/trapianto, vi è anche il muscolo scheletrico. Di conseguenza, anche per questo sono stati sviluppati diversi approcci mirati a riparare efficacemente i più comuni difetti sia pediatrici sia adulti che richiedono un intervento chirurgico: A) la perdita muscolare di un grande volume di muscolo (causato da incidenti o dalla necessità di rimuovere tumori muscolari), B) difetti della parete addominale e C) difetti del diaframma, soprattutto congeniti. A seconda del tipo di difetto, il sostituto da sviluppare dovrà avere peculiari proprietà, oltre a quelle basilari necessarie per essere considerato un approccio di ingegneria tissutale completo. Infatti, mentre A necessita di un sostituto in grado di ripristinare un grande volume, B e C richiedono un costrutto sottile ma, a seconda delle dimensioni del difetto, di una più o meno ampia superficie. Finora, per la riparazione di tali difetti per lo più sono stati utilizzati più frequentemente scaffold/mesh sintetici, ma quelli di derivazione naturale, ed in particolare ottenuti dalla decellularizzazione di un tessuto nella sua completezza, stanno rapidamente recuperando strada, ed è probabile che diverranno il metodo di elezione nel prossimo futuro. La ragione di questo potenziale

è la stretta somiglianza con l'organo o il tessuto di origine, pur possedendo caratteristiche in grado di culminare in un rimodellamento costruttivo e funzionale. Inoltre, mentre la decellularizzazione è stata ottenuta anche in organi più complessi, i prodotti derivati da tessuti più semplici sono stati anche già testati in clinica e per alcuni si è persino giunti alla commercializzazione su larga scala (ad esempio il Surgisis®).

In questo lavoro si è partiti dal considerare la patologia dell'ernia diaframmatica, ad oggi riparata chirurgicamente tramite chiusura primaria con tessuto autologo, se il difetto lo permette, oppure ancora con mesh prostetici di natura sintetica. Tuttavia, gli svantaggi di questi tipi di materiali in termini di rigidità ed inerzia, rendono conto dell'attuale ricerca di una valida alternativa.

Si è proposto quindi di derivare un costrutto muscolare partendo dalla decellularizzazione del muscolo diaframmatico utilizzabile come toppa tissutale per riparare il danno dell'ernia sia senza cellule sia con nuove cellule donatrici. Il modello studiato è stato, per la prima volta, quello murino.

Metodi

Diaframmi (topo e coniglio) sono stati decellularizati tramite esposizione ciclica alla sequenza: acqua deionizzata, sodio desossicolato, DNasi. Gli scaffold ottenuti sono stati caratterizzati per valutare l'efficienza del protocollo in termini di rimozione delle cellule (topo e coniglio), preservazione della micro architettura (topo e coniglio), componenti della matrice extracellulare (topo), proprietà meccaniche (topo). Successivamente, l'interazione ospite-scaffold (in topo) è stata testata *in vivo*, sia in topi sani che atrofici. Un ulteriore caratterizzazione è stata attuata approfondendo le proprietà angiogeniche, sia potenziali, sfruttando il noto test CAM, il trapianto sottocutaneo e rivelando il contenuto di proteine coinvolte nella angiogenesi ancora presenti dopo la decellularizzazione, sia effettive, eseguendo un impianto ortotopico, utilizzando come confronto un materiale sintetico. Per avvicinare la validazione alla pratica clinica, il diaframma decellularizato di topo precedentemente caratterizzato è stato quindi utilizzato per il riparo nel primo modello di ernia diaframmatica chirurgicamente indotta in topo. Il paragone è stato fatto anche in questo caso con il materiale più comunemente usato per la riparazione di questo difetto in clinica. Inoltre, più recentemente è stato

introdotto un controllo rappresentato dall'allotrapianto. Infine, a completamento di un approccio di ingegneria tissuatle, è stato sviluppato un metodo per combinare la componente cellulare, poi applicato a entrambi gli scaffold derivati da topo e coniglio.

Risultati

L'adattamento di un protocollo detergente enzimatico precedentemente pubblicato, al fine di ottenere uno scaffold decellularizato da diaframma, si è rivelato efficiente sia utilizzando il topo che il coniglio come fonti, ottenendo così da entrami la rimozione delle cellule preservando la somiglianza della struttura con il tessuto di origine. Inoltre, è stato confermato, solo in topo, che le proprietà meccaniche e i fattori di crescita sono stati conservati dopo la decellularizzazione. L'impianto dello scaffold di topo, ha provocato sia angiogenesi che l'attivazione dei precursori muscolari, modulando al contempo la risposta immunitaria. Nell'ambiente sano, l'effetto è stato transitorio, mentre l'impianto in un modello murino di atrofia ha portato ad effetti benefici a lungo termine. La sperimentazione nel modello chirurgico di ernia ha confermato i risultati precedentemente osservati ed in aggiunta, rispetto al materiale sintetico, ha mostrato migliori risultati, come l'assenza di erniazione recidiva, il miglioramento dell'escursione diaframmatica e, diversamente da prima, una più sostenuta risposta miogenica nel tempo. Il metodo utilizzato per ripopolare entrambi i diaframmi acellulari di topo e muscoli, dopo essere stato sviluppato, ha finora portato a risulstati positivi, mentre lo scaffold ha dimostrato di poter supportare la proliferazione, la sopravvivenza e la differenziazione delle cellule.

Conclusioni

Scaffold derivati dal muscolo di diaframma possono essere conseguiti con successo sia da topi che conigli, utilizzando un protocollo di tipo detergente-enzimatico. Tali, hanno dimostrato di possedere diverse proprietà interessanti sia *in vitro* che *in vivo*, derivate dalla loro stretta somiglianza con il tessuto di origine. Precisamente, è stato dimostrato che, mentre *in vitro* possono sostenere la

sopravvivenza, la proliferazione e la differenziazione cellulare, *in vivo* sono in grado di interagire positivamente con l'ambiente ricevente, guidando una risposta costruttiva. Quindi, è molto probabile che ulteriori passi vengano fatti nel prossimo futuro, fino a raggiungere infine l'applicazione in clinica.

Abstract

Introduction

The demand for organ transplantation has rapidly increased during the past decades, thus requiring the development of a new interdisciplinary field, aimed at supplying this demand. Branching from regenerative medicine, the combination of elements usually applied separately for same or other purposes, was named Tissue Engineering (TE). Precisely, the components combined in TE constitute the so-called TE triad, are i) cells (derived from cell therapy), ii) scaffolding material (derived from material science) and iii) molecular signals (mainly derived from molecular biology and drug research). Among the organs and tissue that experience damages such that requiring implantation/transplantation, skeletal muscle represents no exception. As result of this, several approaches developed to efficiently repair the most common defects requiring surgery: Volumetric muscle loss (VML), abdominal wall defects (AWD) and defects of the diaphragm, namely traumatic diaphragmatic hernias or congenital diaphragmatic hernias (CDHs). While the first necessitates a substitute large in volume, the other two need a thinner but, according to defect size, wider surface. Thus far, between the materials chosen for repair of such defects, mostly synthetic materials were used, but decellularized tissue are rapidly covering the gap, likely to surpass them in the next future. Reason of this potential is the close resemblance to the organ or tissue of origin, while possessing features able to endpoint to constructive and functional remodeling. While decellularization-derivates of several organs and tissue were already attained, some were even tested in clinic and further moved to large-scale production (i.e. Surgisis®). However, only recently the proposal of developing a decellularized scaffold from diaphragm muscle for autologous repair purposes was reprised, and in general, was never considered in mouse.

Methods

Diaphragms (mouse and rabbit) were decellularized by a cyclical exposure to the sequence deionised water, sodium deoxycholate, DNase. Scaffolds were characterized in order to evaluate decellularization protocol efficiency, by the means of cell removal (mouse and rabbit), maintenance of microarchitecture (mouse and rabbit), ECM components (mouse), mechanical properties (mouse). Next, the interaction host-scaffold was tested in vivo, both in healthy and atrophic mice. Subsequent, a further characterization by disclosing the angiogenetic properties, both potential, taking advantage of the well-known CAM assay and subcutaneous transplant, as well as revealing angiogenesis-related protein content whithin the scaffold, and actual, by performing an orthotropic transplant in comparison with a synthetic material. To draw nearer the clinical validation, the characterized decellularized diaphragm (DD) were thus transplanted in the first surgically created model of CDH, again compared to the most commonly used material for the repair of this defect, polytetrafluoroethylene (PTFE), with the introduction recently of an allotransplant control. Lastly, as completion of a TE approach, it was developed a method to combine the cellular component, which was then applied to both mouse and rabbit derived scaffold.

Results

The adaption of a previously published detergent-enzymatic protocol aiming at obtaining a decellularized scaffold from diaphragm, resulted successful in with both mouse and rabbit sources, as cell removal while preserving microarchitecture and ECM components was attained. Moreover, it was confirmed that mechanical properties and growth factors were preserved in the mouse-derived scaffold. Upon implantation of the latter, angiogenesis and myogenic activation, while modulating the immune response were observed. In the healthy environment, the effect was transient, whereas implantation in a mouse model of atrophy led to long-term beneficial effects. The testing of mouse scaffold in a surgical model of CDH proved the previously seen results, as, compared to PTFE, yielded better outcomes, such as no recurrence, amelioration of diaphragm excursion and, differently from before, to a sustained myogenic response through time points analysed. The method used to re-populate both mouse and acellular muscles , after being developed, thus far resulted in a successful cell delivery, while the scaffold supported cell proliferation, survival and differentiation.

Conclusions

Muscle scaffold from mice and rabbit can be successfully obtained by decellularizing the diaphragm muscle via detergent enzymatic protocol. These scaffolds were proven to have several attractive properties both *in vitro* and *in vivo*, derived from their close resemblance to the tissue of origin. Precisely, it was demonstrated that while *in vitro* can sustain cell survival, proliferation and differentiation, *in vivo* positively interact with the recipient environment, driving a constructive response. Hence, scaling up of this type of construct is likely to be happening in the next future.

Table of contents

Abbreviations

2D	Two-dimensional
3D	Three-dimensional
AB	Alcian Blue
AFSC	Amniotic fluid stem cells
AHXR	Acute humoral xenograft rejection
ASC	Adult stem cells
AWD	Abdominal wall defect
BMMC	Bone marrow mononuclear cells
BSA	Bovine serum albumin
CAM	Chicken chorioallantoic membrane
CDH-3	Congenital Diahpragmatic Hernia
CHAPS	3-[(3cholamidopropyl) dimethylammonio]-1-propanesulfonate
CM	Conditioned medium
DAPI	4',6-diamidino-2-phenylindole
DD	Decellularized diaphragm
DET	Detergent enzymatic treatment
dH_2O	Deionised water
DM	Differentiating medium
DMEM	Dulbecco's Modified Eagle Medium
DMSO	Dimethyl sulfoxide
DNA	Deoxyribonucleic acid
DNase	Deoxyribonuclease
ECM	Extracellular Matrix
EDTA	Ethylenediaminetetraacetic acid
EGF	Epidermal growth factor

ELISA	Enzyme linked immunosorbent assay
ESC	Embryonic stem cell
EVG	Elastin Van Gieson
FA	Formic acid
FACS	Fluorescent activated cell sorting
Fb	Fibroblast
FBS	Foetal bovine serum
FDA	Food and Drug Administration
FGF	Fibroblast growth factor
GAG	Glycosaminoglycans
GFP	Green fluorescent protein
GM	Growth medium
GTKO	α-1,3-Galactosyltransferase-1 knockouts
h	Human
H&E	Haematoxylin and Eosin
HAR	Hyperacute rejection
HBSS	Hank's Balanced Salt Solution
HCl	Hydrochloric acid
HGF	Hepatocyte growth factor
HSC	Haematopoietic stem cell
ICM	Inner cell mass
IF	Immunofluorescence
iPSC	Induced pluripotent stem cells
m	Murine
MABs	Mesangioblasts
MACS	Magnetic activated cell sorting
MHC	Major histocompatability complex
min	Minute

MI	Myogenic Index
MPC	Muscle precursor cell
MRI	Magnetic resonance imaging
MSC	Mesenchymal stem cell
MT	Masson's Trichrome
MyHC	Myosin Heavy Chain
NaCl	Sodium chloride
NTC	Non tissue culture
PBS	Phosphare buffered saline
p	paediatric
PCL	Poly(caprolactone)
PCR	Polymerase chain reaction
PFA	Paraformaldehyde
PG	Platelet gel
PGS	Platelet gel supernatant
PGA	Poly(glycolic acid)
PL	Plastic
PLA	Poly(lactic acid)
PLGA	Poly(D,L-lactic-co-glycolic acid)
PLLA	Poly(L-lactic acid)
PS	Penicillin - Streptomycin
qPCR	Quantitative polymerase chain reaction
r	Rabbit
RGD	Arg-Gly-Asp peptide sequence
RT	Reverse transcription
SC	Satellite cell
SDC	Sodium deoxycholate
SDF-1	Stromal derived factor-1

SDS	Sodium dodecyl sulphate
SEM	Scanning electron microscopy
SIS	Small intestinal submucosa
SMA	Smooth muscle actin
SMTE	Skeletal muscle tissue engineering
TC	Tissue Culture
TE	Tissue engineering
TEM	Transmission electron microscopy
TX100	Triton X-100
VEGF	Vascular endothelial growth factor
VML	Volumetric muscle loss
XNA	Xenoreactive natural antibodies
α-Gal	α(1-3)galactose sugar residue

List of figures

Acknowledgements

I would like to thank Dr. Michela Pozzobon, which efforts keep this laboratory a reality, along with Prof. Paolo De Coppi which ideas, constant enthusiasm, and knowledge have inspired me to begin and prosecute my path into the regenerative medicine and tissue engineering.

I am particularly thankful to Dr. Luca Urbani, Dr. Martina Piccoli, Dr. Chiara Franzin and Dr. Enrica Bertin, for they support, joy, madness, professionalism but mostly patience throughout my experience in the laboratory, equally distributed between my years in Padua and my year in London.

Additionally, I would thank Dr. Andrea Alex Schiavo, which was the only male presence after Dr. Urbani moved to London and with him showed me the ropes when I started in this lab, and the fresh PhD student Caterina, which efforts on the same topic helped me a lot developing these results.
I would also like to thank the guys of the former (2014-2015) surgery unit and institute of child health of London (Fatay, Antonio, Panos, Panicos, Laween, Claire and all the others which passed by). Kwan and Carlotta specially, for their very nature, which made my time in the lab there a joy, and formed with me the PhD alliance through the difficulties of research

I am particularly grateful to Dr. Paola Bonfanti and Dr. Anna Urciuolo, which during my London experience were constantly sources of advice and teachings. To Dr. Stavros Loukogeorgakis, I just want to say ‘Malaka!

A special thanks is also due to Dr. Arben Dedja for his amazing surgery skills, which made the surgical procedures possible, and Dr. Asllan Gjinovci, which on top of astonishing surgery skills displayed to be an incredible chef along with Prof. Giulio Cossu.

I am thankful to my mother Flor and my sisters Karla and Sofia, for simply being as well as supporting my career while answering with only ‘oh, fascinating’ to my explanation attempts, and to the ones

that I can consider by now parents-in-law, Paola and Sandro, for feeding me despite my partner's will and for supporting both.

Finally, I am indebted for life to my partner Silvia, which showed me the way to be a better man, and supported me throughout the studentship and this PhD, even though I have more than once put her patience to test with both my career choices and my behaviour. I admire her and consider her fundamental.

None of this would have been possible without standing on the shoulders of the giants.

Chapter 1 : General introduction

1.1 Regenerative medicine: why tissue engineering

1.1.1 The current issues of organ replacement

Availability of adequate candidates for organ transplantation was largely surpassed by the demand, which has rapidly increased in the past decade. This has resulted in long waiting lists, generating the need of an alternative to the shortage of healthy live or deceased donor organs.
The issue became evident as patients with both vital and non-vital organ failure were (and still are) deprived of life extension. Additionally, the increased use of alternative medical care (e.g. dialysis) markedly increased the cost/benefit ratio of these therapies to society.

Xenotransplantation, that is the transplantation of cells, tissues, or organs from different species, is one of the proposed strategies to overcome the shortage of human organs.
A major limitation to this approach though, is the presence of conserved antigens among non-human primates and mammalians, which may lead to hyper acute rejection (HAR). HAR is the consequence of the recognition of a surface antigen located on endothelial cells, α(1-3)galactose sugar residue (α-Gal), conserved among all lower mammals, by xeno-reactive natural antibodies (XNA). The cascade of events following this recognition is in a way similar to the acute haemolysis of donor erythrocytes in a mismatched blood transfusion [1]. Although reduction of HAR has been possible by genetically engineering animals that are α-Gal antigen negative [2,3], elongating graft survival from a maximum of 30 days to over 80 days [4], there is still graft failure, associated with a late thrombotic microangiopathy and ischemic injury [5].

The reason is that also other forms of rejection are still active. Acute humoral xenograft rejection (AHXR), or acute vascular rejection indeed, is triggered by anti-α Gal and anti-non-α Gal antibodies, and can lead to loss of the graft as well as HAR [6]. It has been suggested that neutrophils, natural

killer cells and macrophages are heavily involved in this mechanism [7]. This form of rejection is not typically seen with intense immunosuppressive drug regimens, but still does not fully prevents graft failure, which again still occurs, usually due to development of angiopathies.

In summary, despite the remarkable progress made in xenotransplantation field in the last decade, before making xenotransplantation a clinical reality, several hurdles of general safety must be overcome, principally represented by immunological barriers and physiological discrepancies [8].

Another proposed option is represented by auto transplantation, which vary according to the organ that's due to be replaced. For example, autologous replacement of the oesophagus involves the use of more distal parts of the gastrointestinal tract, with long-term problems associated to each technique [9–11]. In addition, a limit for this technique is the availability of autologous healthy tissue compatible with the injured.

1.1.4 Tissue engineering as possible answer

Given the issues described above, conventional transplantation offers a limited solution, still with a life-long immunosuppression being prominent. Tissue engineering (TE) was then born to offer a therapeutic alternative [12].

Indeed, a regenerative medicine approach combines and integrates into one field TE with different disciplines: cell biology, material engineering, physiology and gene-therapy, with damaged tissues and organs. To be more specific, three are the main components proposed by TE to obtain a functional organ: 1) Cells, the key for successful tissue engineering, which desired features include non-immunogenicity, non-tumourogenicity, high potency, proliferation and differentiation potential 2) A scaffold, the supporting structure necessary to help cells growth and differentiation in a tridimensional fashion, needs to meet important characteristic as well (e.g. Biocompatibility, biodegradability, adequate stiffness) 3) the signaling molecules necessary for functionalization, which

can hasten and help cell growth and differentiation (Fig. 1.1). All of these components carry out interacting roles, whose cumulative effects aim to assist, simulate or replace the function of a failing native tissue or organ. Depending of the need, a construct can be tissue engineered to take the form of tissue sheets, which may be used for structural repair of congenital (e.g. atrial septal defect) or acquired (e.g. trauma) defects or for functional assistance (e.g. pancreatic islet cell grafts). Alternatively, whole organs can be produced for surgical transplantation.

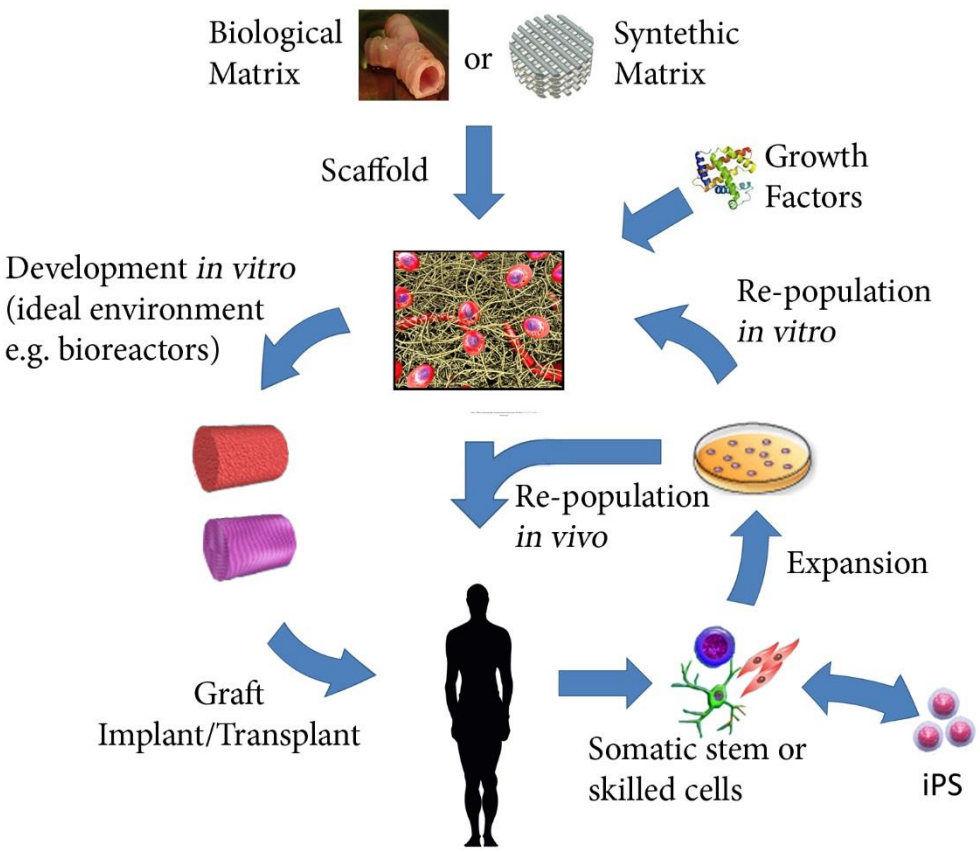

Figure 1.1 - An overview of tissue engineering/regenerative medicine

Tissue engineering with the aim of organogenesis involves the combination of appropriate cells and scaffolds, their growth in bioreactor systems and eventual transplantation.

1.2 Skeletal muscle Tissue Engineering (SMTE)

1.2.1 Skeletal muscle in clinic: incidence and significance of muscle injuries

Skeletal muscle represents no exception when it comes to organ or tissue replacement demand. Indeed, there is no current permanent solution to the many known congenital muscular diseases, which reflect the anatomical and molecular complexity of this tissue. Duchenne muscular dystrophy (DMD) or Spinal muscular atrophy (SMA) still shorten affected lifespan to an expectation that rarely surpasses the 20s [13]. While congenital diseases are still frequent but limited to genetics, acquired muscle injury represents a condition found in different fields, then covering a wider range, such as military or sports. Car accidents, gunshots [14,15] but also the insurgence of cancer[16], with the subsequent necessity to remove large amount of muscle mass, are only few examples of the many causes that lead to volumetric muscle loss (VML), defined as the loss of a sufficiently large fraction of a skeletal muscle. Whenever this loss is such that natural regeneration mechanisms are unable to compensate, patients experience a permanent loss of function [17]. Currently the only two treatment options to VML are scar tissue debridement and/or free muscle transpositions, which is the most common and usually consists in a muscle autograft transplant to the injury site, such as a free flap transfer procedure [18][19][20][21]. However, muscle graft size is often limiting for a successful incorporation into the recipient site (innervated and vascularized), resulting in difficulties avoiding necrosis, functional differences between the donor and recipient muscles, and significant donor site morbidity [22]. Though defects in the diaphragm or in the abdominal wall are still often repaired with synthetic, non-degradable mesh materials (e.g. polytetrafluoroethylene, PTFE; Dacron), these synthetic materials serve only to reinforce the remaining tissue to prevent further damage, as they elicit a chronic foreign body response (FBR) and fibrosis with no functional recovery of the injured muscle [23][24][25]. Therefore, SMTE approaches and their potential applications are various, and today solutions to muscle injury are being investigated to promote new muscle tissue growth rather than only focusing on preventing further tissue damage.

1.2.1 Skeletal muscle self-renewal and response to injury

Skeletal muscle has a great plasticity and self-renewal capacity, which ensure and maintain tissue and body homeostasis. Upon injury, unlike other tissues [26], skeletal muscle is capable of fully recapitulating normal condition, architecture and function [27].

The processes involved in muscle regeneration were well characterized both in human and mouse, in which established muscle injury models (such as cardiotoxin injection, cryoinjury, muscle excision) progress through similar cellular and molecular events [28]. Briefly, (1) inflammatory and/or non-inflammatory signals trigger the activation of resident progenitor cells, (2) which proliferate after activation, (3) commit to myogenic differentiation, and finally (4) fuse into functional multinucleate myofibers [29][30](Fig. 1.2) .

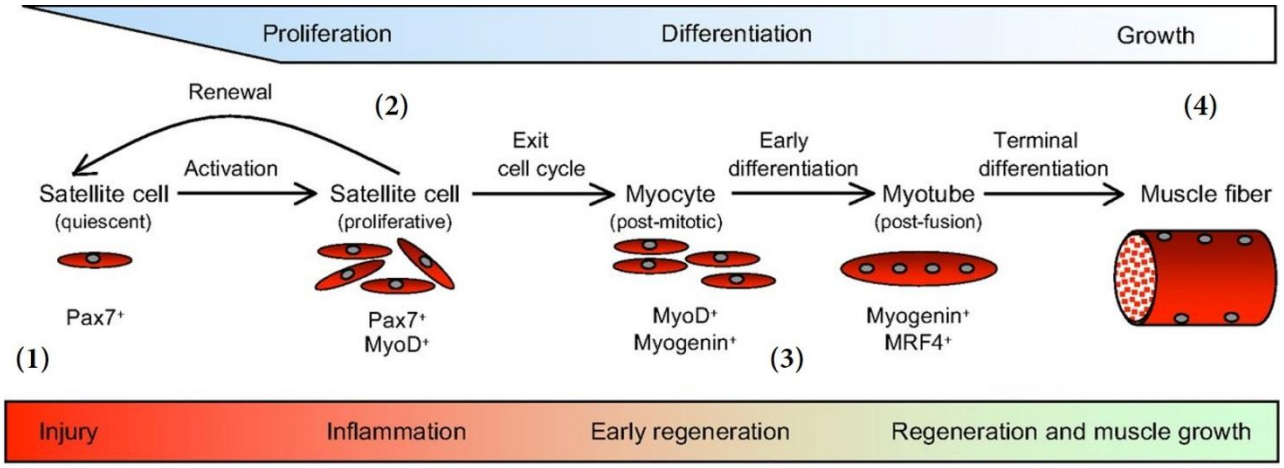

Figure 1.2 – Muscle repair phases (adapted from [30])

Tissue engineering with the aim of organogenesis involves the combination of appropriate cells and scaffolds, their growth in bioreactor systems and eventual transplantation.

The primary contributor to new muscle fibers formation, most abundant and well studied muscle progenitor is the satellite cell (SC) [31], which is characterized by the expression of the transcription factor Pax-7 [32]and by their unique anatomical position when in quiescent state. SCs in fact, during homeostasis, reside in a well-defined stem cell niche that is located directly between the myofiber cell

membrane (sarcolemma) and the basement membrane (basal lamina) of the surrounding extracellular matrix (ECM) [33].

After activation, SCs undergo asymmetrical division, to both ensure niche preservation and to generate a proliferating myogenic progenitor, known as Myoblast. After migration to the sites of injury, these cells proliferate extensively in response to mitogenic factors present in the wound environment, which is comprised of immune cell secreted cytokines and chemokines and growth factors released by damaged myofibers [29]. Further committing towards the myogenic cascade, myoblasts exit the cell cycle, downregulate MyoD and Myf5, and upregulate the transcription factor Myogenin [34][35]. Fully committed cells, now called Myocytes, are able to form cell-cell adhesions with neighboring myogenin+ cells, and finally fuse to the pre-existing damaged myofibers or form de novo myofibers (Fig. 1.2). Fusion is then accompanied by the expression of the late muscle differentiation transcription factor MRF4, cytoskeletal proteins such as dystophin and dystroglycan, as well as functional contractile proteins such as sarcomeric myosin. As remnant of cell fusion, newly formed myofibers initially display nuclei located within the center of the cytoplasm [36]. As last stage of correct muscle regeneration, muscle fibers will grow (hypertrophy) and form mature muscle-ECM adhesion complexes for force transmission, as well as developing neuromuscular junctions with innervating axons and nervous system control [37]. Indeed, functional innervation and formation of a stable neuromuscular junction is necessary for muscle fiber survival and appropriate phenotype. To summarize, since effective muscle repair is dependent on two general cell processes: the presence of progenitor cells able to proliferate and create a pool of myogenic cells, and differentiation/fusion of these to become terminally differentiated and functional myofibers, either or both of these processes may be potential targets for directing and improving muscle regeneration.

1.2.3 SMTE requirements

Given the complexity of skeletal muscle, to develop a tissue-engineered construct the combination of appropriate cellular engineering and material science is needed. Indeed, this tissue is highly organised,

thick, heavily innervated and vascularised, making those characteristics that will have to be reproduced by SMTE.

To this aim, of particular importance are external stimuli like mechanical and electrical [38] [39]. In fact, correct alignment of muscle fibers, one of the most critical factors for muscle formation, is strictly connected to both mechanical and electrical stimuli [40][41], while muscle growth, as seen in neuronal related athrophies, has been identified to be influenced by neuromuscular junctions, which are essential for directed control and in turn have been linked to full force generation [42]. Hence, scaffolds materials must assist cell alignment, promote skeletal muscle formation, and stimulate vascularization and innervation while balancing structural and mechanical support of the injury site, degrading in a fashion such that enough structural stability is present within the scaffold material to support mechanical loading until the regenerated tissue is stable enough to withstand loading independently [43–46].

On the other hand, not only cellular component should be able to proliferate and self-renew, in order to completely repopulate the scaffold and to improve the in vivo engraftment, but should be also able to differentiate giving rise to the cell types necessary to recreate an environment similar the most to skeletal muscle [47]. For example, besides the muscular cells, also fibroblasts (that secrete and remodel ECM) and endothelial cells are necessary to completely regenerate the functional tissue.

In the recellularization process, two steps are considered as the most important: the first one is the cell seeding, that is aimed at repopulating the decellularized scaffold with a mixture of cells that should redistribute mimicking the native tissue. The second is the culture that should allow the cells to proliferate or to differentiate for the subsequent in vivo functions [48]. Therefore, the quest for a correct environment (e.g. bioreactors) in the field of skeletal muscle TE is developing concomitantly with the pursuit for ideal scaffolds and cells, to eventually allow mimicking of muscle formation to the fullest.

Moreover, each TE component has to adhere to specific requirements, which must be previously satisfied before considering the use into bioreactors, in vivo and eventually into clinic. Cell and scaffold choice will be further discussed in the next chapters.

1.2.4 Current state of SMTE

While many approaches to obtain skeletal muscle constructs were developed to study skeletal muscle formation *in vitro* or as model for drug screening applications, in the last decade the use of engineered muscle was also aimed to replace or augment damaged tissue *in vivo* [49–54].

In general, the most common technique to obtain an engineered construct is to seed cells able to differentiate into muscle either onto or within a structure, commonly three-dimensional, to then allow for the compound to grow and remodel into muscle tissue *in vitro* [55–58]. While suitable for whatever purpose, i.e. as model of development, test sample for drug screening or pre-conditioning for the further delivery *in vivo*, the specific aim of supporting and repairing injured muscle, not only amended the possibility of an *in situ* approach, but also led to the use of naturally derived materials [59–63].

The continuous steps forward made by technology, along with the collaboration among different disciplines, led to remarkably results throughout the years in both cases. Muscle constructs engineered *in vitro* for example, can to date not only spontaneously contract, but also respond to both electrical and drug stimuli (e.g. tetanic contractions, calcium gradient inhibition), displaying trends that can accurately mimic skeletal muscle functions [56][64]. Some examples of *in vitro* approaches developed thus far are summarized in table 1.1

Table 1.1 | Examples of *in vitro* approaches to develop muscle

Aim	Cell source	Scaffolding material	Outcome	References
Test of patterned platform for engineered muscle formation	Rat L6 myoblasts	Collagen I crosslinked with EDC/NHS	Efficient myotube alignment	[43]
Vascularization of muscle bundle construct	Primary hMDCs; HUVECs	Molded Thrombin/Fibrinogen/Matrigel	Cells alignment; creation of a vascular network within the construct	[65]
Develop a controlled system lowering number of cells required	Human immortalized myoblasts, 3T3	Collagen/Matrigel		[66]
Increase number of bundle production	C2C12	GelMa/PEGDMA	High-throughput production, uniform loading	[67]
Creation of bundles from human primary cells and drug screening	Expanded hMDCs	Molded Thrombin/Fibrinogen/Matrigel	High number of bundles from a single biopsy, drug response similar to clinical testing	[56]
Development of scaffold material for SMTE	C2C12	PEG-MAL hydrogel	Chemical functionalization; 3D structure	[68]
Development of aligned 3D structure	Human myoblasts	poly(N-isopropylacrylamide)	Alignment, easy manipulation	[69]
Acceleration of myogenic differentiation of BMCs	mBMMSCs; C2C12	Fibrin on silicone	Mechano-driven differentiation	[52]
Development of 3D neuromuscular constructs	C2C12; Primary mNSC	Matrigel	Self-tension; NMJ formation	[70]
Development of a culture platform	hPSCs differentiated in myocites	Autologos ECM; collagen	Self-assembly; responsive to electrical stimuli	[71]
biowireEvaluation of patterning on growth and differentiation	C2C12	N/A	Microtopography	[72]
Development of a new scaffold for SMTE	Expanded hMDCs	Biodegradable bacteriostatic glass fibers; collagen	Micropatterning; self-contraction	[53]
Evaluation of culture method for bundles	C2C12; Primary hMPCs	Neutralized collagen I gel	Self-contraction; easily reproducible	[73]
Maturation of AchR in the bundles	GFP-C3H myoblasts	Fibrin gel	Laminin and agrin expression; formation of NM receptors	[58]

Aim	Cell source	Scaffolding material	Outcome	References
Evaluation of spatial geometry of bundles	Neonatal rat Myoblasts	Matrigel-fibrin hydrogel mesoscopically structured	Self-contraction	[74]
Patterning of engineered muscle	C2C12	Microstructured gelatin methacrylate	Micropatterning; response to electrical stimuli	[40]
Patterning of engineered muscle	C2C12	Patterned film (polyelectrolyte)	Micropatterning; stiffness modification	[75]
Model for Skeletal muscle ageing	Aged C2C12 (≤p54)	Collagen	Self-contraction but reduced contracting force	[76]
Evaluation of TGF β1 effects	Primary SCs from rat (F344) *Soleus*	Self-produced ECM	Response to electrical and chemical stimuli; self-contraction into 3D	[77]
Evaluation scaffold functionalization on differentiation	C2C12; C3H10T1/2	Electrospun PS	Chemical functionalization; microtomography	[78]
Evaluation of co-culture with Fbs	Primary mMyoblasts; mEF from E13/CF1	Fibrin; Self-produced ECM	Self-contraction; generation of 3D structures	[79]
Evaluation of mechanical stimuli direction	C2C12	Collagen I	Mechanical conditioning; axial conditioning	[80]
Mechanoregulation of constructs	H5V EC; C2C12	Collagen I and self-produced ECM	Self-contraction; paracrine VEGF effect on vascularization	[81]
3D organization patterning	rSCs (*Soleus)*	Self-produced ECM	Micropatterning, self-assembly into 3D	[82]
Patterning evaluation	C2C12	Degrapol	Efficient micropatterning	[83]
Evaluation of environmental stiffness	C2C12; primary human Fbs	Patterned polyacriacrylamide gel	Mechanoregulation also by cellular substrate	[84]
Evaluation of physiological properties of bundle	Primary rat SCs and Fbs	Self-produced ECM	Self-contraction, self-structuring 3D	[85,86]

EDC/NHS=1-Ethyl-3-(3-dimethylaminopropyl)-carbodiimide)/ N-Hydroxysuccinimide; hMDC=human Muscle Derived Cells; HUVEC=Human Umbilical Vein Endothelial Cell; GelMA/PEGDMA=gelatin methacrylate/polyethylene glycol di (metha) acrylate; PEG/MAL=olyethylen glycol/MALeimide; mBMMSC=mouse Bone Marrow Derived Stem Cell; mNSC=mouse; Neural Stem Cell; NMJ=Neuromuscular Junction; hPSC=human pluripotent stem cells; hMDC=human Muscle Derived Cells; hMPC=human Muscle Precursor Cells; GFP=Green Fluorescent Protein; mSC=mouse Satellite Cells; PS= polystyrene; mEF= mouse Embryonic Fibrobalsts; EC= Endothelial Cells; Fbs= fibroblasts.

While for *in vitro* purposes size does not constitute a limitation though, the application as a repair tool or even as substitute requires a larger construct. However, to increase the dimension of the muscle constructs requires additional care to cope the issues rising sideways. For example, it was shown that forcing the growth can result in the inability for nutrients to reach the innermost layers of the tissue, a condition that often cause the formation of a necrotic core, then unsuitable for implantation [64][86]. Trying to overcome this and other issues in the creation of a construct suitable for implantation (addition of a construct helping the host regeneration) or transplantation (substitution of functional tissue with an equal counterpart), several approaches with as many type of cells and constructs were developed. For example, it was tried to use an heterogeneous population obtained from muscle hind limbs [87], the co-seeding of different cell types [44,88], or to take simply advantage of the host vasculature [89–91]. Remarkably, Juhas et al. created bundles that could also repaired themselves after cardiotoxin insult in vitro, demonstrating that the SC niche was present within these constructs, whereas Fuoco et al. managed to obtain a vascularized muscle, which seemed to restore limb strenght. Even larger skeletal muscle constructs have been implanted to observe engraftment, vascularization, and functional recovery [92].

Others, managed to obtain construct called skeletal muscle units (SMUs), testing their efficiency in a model of rat VML. Although these SMU displayed some vascular and nervous tissue integration, with a significant increase in force production after 28 days, muscle functionality was still far from native condition [93]. In general, it was demonstrated that proximity to host blood vessels resulting in a better vascularization [94], can result in a significant increase of the force output of these constructs, demonstrating that these are capable of integrating with the surrounding tissue and remain thereby viable [95]. Thus, an essential feature for a successful outcome is, among the others, the ability to elicit an abundant pro-angiogenetic response in order to allow graft survival. In table 1.2 were listed some of the developed constructs tested and delivered *in vivo* until 2016.

Table 1.2| Examples of constructs for SMTE tested in vivo

Aim	Cell source	Scaffolding material	Model	References
AWD repair	Acellular	PPL	Rat	[96]
Scaffold testing/comparative study	Rat myoblasts	PGA		[46,97,98]
Scaffold testing	Acellular	PLLA	Rat	[99]
Scaffold testing/comparative study	Acellular	PLLA-PLGA	Mouse	[44,100,101]
Scaffold testing/comparative study	Myoblasts	PLLA-PLGA	Mouse	[44]
Scaffold testing-AWD repair	Tri-culture: MPCs, HUVEC, mEFs	PLLA-PLGA	Mouse	[44]
Scaffold testing-AWD repair	Co-culture: HUVEC, hFbs	PLLA-PLGA	Mouse	[101]
AWD repair	Myoblasts; Co-Culture: HUVEC, hFbs; Tri-Colture: Altogether	PLLA-PLGA	Mouse	[101]
Muscle defects	Acellular	Decellularized syngeneic scaffold	Mouse	[102,103]
Scaffold characterization/testing in atrophic model	Acellular	Decellularized syngenic scaffold	Mouse	[104]
AWD				[105,106]
VML	Acellular	Decellularized syngeneic scaffold	Rat	[25,90,107]
Scaffold Characterization				[108]
AWD repair	Acellular	Decellularized syngeneic scaffold	Rabbit	[109–111]
Scaffold characterization	Acellular	Decellularized ECM secreted *in vitro*	Rat	[108]
AWD repair	Rat SCs or myoblasts	Decellularized syngeneic scaffold	Rat	[55,112–114]
VML	MSCs	Decellularized syngeneic scaffold	Rat	[90,115]
CDH closure	MSCs	Decellularized syngeneic scaffold	Rat	[116]
VML	Acellular	Decellularized xenogeneic scaffold	Mouse	[117–119]
VML AWD repair	Acellular	Decellularized xenogeneic scaffold	Rat	[105,107,120,121] [122,123]

(continued)

Table 1.2| Continued

Aim	Cell source	Scaffolding material	Model	References
Muscle defects	Acellular	Decellularized xenogeneic scaffold	Rat	[124]
AWD repair				[96]
				[125]
Scaffolds testing	Acellular	Decellularized xenogeneic scaffold	Rat	[126]
VML	Acellular	Decellularized xenogeneic scaffold	Dog	[127]
VML	Acellular	Decellularized xenogeneic scaffold	Human	[118,128]
VML	MDCs	Decellularized xenogeneic scaffold	Mouse	[129,130]
VML	MSCs	Decellularized xenogeneic scaffold	Rats	[121]
AWD repair	Tri-culture: MPCs, HUVEC, foreskin Fbs	Decellularized xenogeneic scaffold	Mouse	[88]
AWD	Acellular	Hydrogels from decellularized xenogeneic tissues	Rat	[131,132]
VML	Autologous	Minced skeletal muscle		[25,133,134]
Scaffold characterization, hindlimb transplant	Tri-culture: MPCs, HUVEC, mEFs	Decellularized whole limb	Rat	[92]
Scaffold testing /Factor delivery	Acellular	Alginate	Mouse	[135,136]
Bladder function recovery	Acellular	Alginate	Rat	[137]
Scaffold testing	Myoblasts	Alginate	Mouse	[135,138,139]
Scaffold characaterization	Myoblast	Alginate	Rat	[46]
Bladder function recovery	MSCs; MSCs induced to muscle cells	Alginate	Rat	[137]
Factors delivery	Acellular	Collagen	Rat	[61]
VML	Acellular	Collagen	Rabbit	[140]
Factors delivery				[63]
VML	MPCs	Collagen	Mouse	[60,141]
Testing in dystrophic model				[142]
AWD repair	ECs and MSCs	Collagen	Mouse	[143]
AWD repair	Myoblasts	Collagen	Rat	[144]
Scaffold characterization	Myoblasts	Fibrin	Rat	[94,145]
AWD repair/comparative	Acellular	Fibrin	Mouse	[101]
VML	Human Myoblasts	Fibrin	Mouse	[146]
Dystrophic model				[147]

(continued

Table 1.2 | Continued

Aim	Cell source	Scaffolding material	Model	References
AWD repair/comparative study	Co-Culture: HUVEC-hFbs	Fribrin	Mouse	[101]
	Acellular	Fibrin-PLL/PLGA		
	Co-Culture: HUVEC-hFbs	Fibrin-PLLA/PLGA		
Construct characterization, CTX-injury	MPCs	Fibrin/ matrigel	Mouse	[89]
Construct characterization	Primary cells (Check)	Fibrin/Autologous ECM	Rats	[148]
Construct characerization	Tri-culture: MPCs, HUVEC, 10T1/2	Matrigel	Mouse	[149]
Scaffold characaterization	Myoblast	Hyaluronic acid gel	Rat	[46,150]
EDL transplant	MPCs	Self-Assembled ECM	Mouse	[87]
TA transplant	MPCs	Self-assembled construct	Rat	[93]
TA repair	Mesoangioblasts	PEG-Fibrinogen	Mouse	[91]
Muscle defects	Autologous muscle cells	Autograft (used as control) - minced	Rat	[25,105,116]

PPL=Polyphenyl; PGA=Polyglycolide; PLLA=Polylactic Acid; PLGA=Poly(lactic-co-glycol acid); MPC=Muscle Precursor Cell; HUVEC=Human Umbilical Vein Endothelial Cell; mEF=mouse Embryonic Fibroblast; hFb=human Fibroblast; MSC=Mesenchymal Stem Cell; EC=Endothelial Cell.

Despite the several studies made, being defects as VML extensive by their very own nature, the amount of functional tissue to be created is beyond what currently possible to reproduce through TE constructs [151]. Further, as the most complete constructs were obtained by combination of different cells population harvested separately, the complexity of these procedure s pulls them back from clinical application, not considering the time required for construct completion, likely to result in weeks or even months waiting for the surgery. Definitely, to reach the clinical use are the ones that guaranteed the fewer variables in the pre-clinical phases.

1.2.5 Clinical application of SMTE

Therapies to have reached clinical application so far use techniques belonging to TE but cannot be considered real TE approaches yet, as they lack either cell support or do not take advantage of any scaffold. Indeed, on one side we have cell therapy strategies, in which cells were injected locally or

systemically to improve syndromes originating from genetic diseases of the muscle [152,153].On the other, we have defects requiring surgery rather than cell therapy, as the flat muscles defects (i.e. abdominal wall and diaphragm hernias[154,155]) or VMLs. While in the first case several scaffold are currently in use (this topic will be further discussed in *Chapter 6*), the clinical reports for VML treatment are just two, both involving xenogeneic decellularized tissue (scaffold materials, among which decellularized tissues, will be further discussed in *Chapter 4*).

In the first case, a defect in the *quadriceps femoris*, already treated years before with a muscle flap, was repaired with an acellular porcine small intestine submucosa (SIS) scaffold [128]. More recently, a different scaffold (porcine bladder matrix) was used, showing that the treatment did not induce an adverse effect. The outcomes were further positive in three cases out of five, which displayed also improvement in strength and mobility, compared to a patient-specific baseline. Thus, even though these devices cannot be considered the result of tissue engineering according to the usually accepted definition [12], they provides evidence that a commonly used scaffold, can be a good bedrock to repair skeletal muscle injuries. Moreover, non-muscle-derived acellular scaffolds have shown applications comparable to decellularized muscle tissue in SMTE treating of VML [114,125], and their xenogeneic origin could obviate the need for human tissue as a starting material for scaffold development.

Given the reported effects of empty scaffolds on cell homing [99], suggesting that SMTE derived materials may indeed constitute a valid clinical option, there is still the need to better understand the role of the cellular component, as to whether necessary or not. Indeed, while from one side there is still the concern of host alone not being enough, evidence in other engineered tissues have proven a limited structural role for the seeded cells, which seem to be rapidly overcome and substituted [156]. While non muscle-derived acellular scaffold have shown applications in muscle defects at clinical level, muscle derived are holding higher promises when considering the amount of tissue that could be used. Indeed, not only it is the largest tissue in the body, but also the possibility of obtaining xenogeneic acellular muscles expands the sources that could be used.

Hence, decellularized scaffold represent an attractive candidate to ease and quicken translation to the clinic as the ECM derived from large mammals was and still is widely used [96,123,157,158]. Lastly, the structure and composition of the these material is known to be capable of promoting the

vascularization of the structure as it is assimilated in the body [159,160], thus the remaining concerns would rely mostly on the cell side.

Chapter 2 Main hypothesis and specific aims

Up to now, applications aiming at the repair of skeletal muscle were as many, but the majority focuses on the repair of VML However, also other defects lead to loss muscle, such as AWD and diaphragmatic hernias. Congenital diaphragmatic hernia (CDH), in particular, is a defect leading to ineffective closure of the diaphragm muscle, thus requiring surgical intervetion to ensure normal physiological condition. To date, repairs for which primary repair is not possible, are mainly performed with synthetic meshes. The general motivation of the present work is to develop an autologous natural alternative to actual CDH treatments, which could overcome the actual concerns raised by the nature and the mechanical properties of the synthetic materials. In this respect, the use of an acellular matrix derived from the diaphragm was considered an ideal choice. The central hypothesis is then: diaphragm acellular matrix, which will be possible to derive *via* decellularization using an adapted protocol, can represent an eligible material for the closure of CDH defect, since the unique reservoir these types of scaffold retain. Additionally, it would be possible to set a method towards the completion of a TE approach. Hence, aims were developed as follow.

2.1 Aim chapter 4

In this chapter, my goal was to evaluate a decellularization protocol to efficiently deliver a scaffold that would maintain macro- and micro-architecture whilst removing the antigen cellular component. The hypothesis it that adapting a detergent enzymatic treatment to suit the tissue I want to decellularize, I will be able to obtain the desired degree of cell removal and structure preservation throughout the exposure to the treatment. My expectation is that, once determined the most efficient condition, it will be possible to develop an acellular scaffold that will closely resemble native tissue. Aiming at further testing the obtained scaffold, I will analyze also outcomes in both healthy and diseased environment.

2.2 Aim chapter 5

The following chapter was developed aiming at further characterizing the developed acellular matrix, focusing on its angiogenetic potential. The hypothesis is that mild decellularization chosen, as well as the nature of the scaffold itself, will result in a pro-angiogenetic environment, as demonstrated using other types of acellular matrices. Angiogenetic potential will be essayed both with in vitro molecular biology and in vivo, where host response can be compared to PTFE to distinguish from the effects that the physiological FBR implicates.

2.3 Aim chapter 6

The aim pursued in this chapter was to evaluate the outcome after the repair of a surgical mouse model of CDH with our developed acellular matrix. I hypothesize that, in line with the several studies involving acellular matrix, as well as clinical level of evidence reached thus far, outcome of the intervention will endorse the use of such scaffold for CDH repair purposes. To confirm this hypothesis, the actual gold standard prosthetic mesh (PTFE) will be used as control

2.4 Aim chapter 7

The work described in this chapter was aimed at developing and evaluating a method to combine cells with the diaphragm derived acellular matrix obtained previously. Main hypothesis is that, even though diaphragm is a thin muscle, only seeding cells on top is not sufficient to guarantee cell growth and integration. Also, adding mechanical tension to culture condition may result in an enhancement to differentiation stimuli.

Chapter 3 : Materials and Methods

3.1 Animals and tissue harvesting

All surgical procedures and animal husbandry were carried out in accordance with University of Padua's Animal care and Use Committee (CEASA, protocol number 67/2011 approved on 21st September 2011) and were communicated to the Ministry of Health and local authorities in accordance with the Italian Law on the use of experimental animals (DL n. 16/92 art. 5). For the experiments carried out in the UK, all surgical procedures and animal husbandry were carried out in accordance with UK Home Office guidelines under the Animals (Scientific Procedures) Act 1986 and the local ethics committee.

3.1.1 Mouse

The animals used as donors were 12 weeks-old wild type (WT) C57BL/6j (B6) male and female mice. Surgical procedures (section *3.8*) were performed on 12 weeks-old WT B6, HSA-*Cre,* $Smn^{F7/F7}$, BALB/c, or BTX-GFP^{+} (GFP) mice male and female.

3.1.1.1 Mouse diaphragms

A transverse incision was made right below the xiphoid process. Then both the thorax and the abdomen where exposed by carefully detaching and pulling the skin from the incision to the opposite sides (cranial or caudal direction). Exposed *fascia* was next removed from the rib cage, along with the dorsal and costal muscles. Once cleaned, the whole rib cage was harvested by freeing, detaching and cleaning the diaphragm from all ligaments and removing the aorta, the inferior vena cava and the oesophagus from each hiatus. Finally, the rib cage was reduced to have the least amount of tissue around the diaphragm, able to provide support to it as well. Diaphragms to be used as fresh control (mFD) were stored snap frozen or treated immediately for subsequent analysis.

3.1.1.2 Mouse Extensor Digitorum Longus (EDL) and Soleus (SOL) muscles

EDL and SOL muscles were harvested from both right and left hindlimb of each mouse. A circular incision was made at the distal end of the *tibia* (above the *tarsus*), then limbs were gently skinned with a lateral incision made on the whole length. The *fascia* above the *tibialis* was removed and the distal tendon of the muscle was identified and cut. *Tibialis* was removed exposing underlying EDL muscle, which was harvested by gently detaching it from its location cutting both the proximal and distal tendons. Limb was then turned and distal tendons of the backside were freed from the *tarsus*. SOL proximal tendon was then located and picked up to gently lift the muscle from the *gastrocnemius*. Distal tendon is then cut away from the previously cut group of tendons, allowing muscle harvesting from tendon to tendon. EDL and SOL were then immediately processed for cell isolation.

3.1.1.3 Mouse whole limb

Legs were skinned as described above. Fat and connective tissue were then removed from the proximal side (femoral head) to allow harvesting of the whole limb, which was cut away at that level. *Tarsus* and paw were cut away to ensure a cleaner preparation. Limbs were then immediately processed or stored in DMEM high glucose (DMEM HG, Gibco).

3.1.4 Rabbit

Adult New Zealand rabbits were used as donors. Animals were euthanized by administration of an overdose of intravenous Pentobarbital Sodium. Then, a midline incision was made to completely expose the abdomen and the thorax. Similarly to the mouse, after removing the covering *fascia*, muscles of the chest and all the other anatomical connections were removed, allowing for the harvest of the rib cage along with the diaphragm. Finally, the rib cage was reduced as in mouse diaphragms.

Diaphragms to be used as fresh control (rFD) were stored snap frozen or treated immediately for subsequent analysis.

3.2 Human Biopsies

Skeletal muscle samples (paediatric) were obtained from Orthopedic and Pediatric Surgery Clinic. Patient tissues were collected after written informed consent. The protocol s(n. 2682P and 3030P) was approved by Local Ethics Committee.

3.3 Decellularization

Tissue was rinsed in 1x phosphate buffered saline (PBS) supplemented with 1% Penicillin/Streptomycin(P/S; PBS-P/S) before the beginning of the procedure. Both mouse and rabbit diaphragms were decellularized adapting a well-established detergent-enzymatic treatment (DET, developed by Meezan et al., then further adapted by Gamba et al.) [109,161]. Depending on the origin and dimension of the tissue, the protocol was applied as one or more cycles of sequential exposition to the reagents. Each DET cycle consisted of 3 steps. First, the diaphragms were maintained in sterile ddH2O at 4°C, for 24 hours. Then, the samples were put in 4% SDC for 4 hours at room temperature (RT) and in gentle agitation. After that, the samples were washed 3 or 4 times with sterile and deionized water, to remove the detergent that could inhibit DNase I (or could be toxic for cells if the scaffold will be recellularized or implanted *in vivo*). At last, the tissues were put in a solution with a concentration of 2000 kU DNase I (Sigma-Aldrich) in 1 M NaCl (Sigma-Aldrich) for 3 hours at RT and in gentle agitation (Fig. 3.1). Of each solution, 40ml for the mouse and 300-400ml for the rabbit were used. A complete decellularization of the mouse diaphragm was achieved with 3 cycles, whereas rabbit diaphragm required 7 cycles. Then, decellularized diaphragms (DDs; mouse: mDDs; rabbit: rDDs) were washed for at least 3 days in sterile ddH_2O and preserved at 4°C in 1X PBS with 3% penicillin/streptomycin (P/S) (Gibco-Life Technologies and finally stored snap frozen or treated immediately for subsequent analysis.

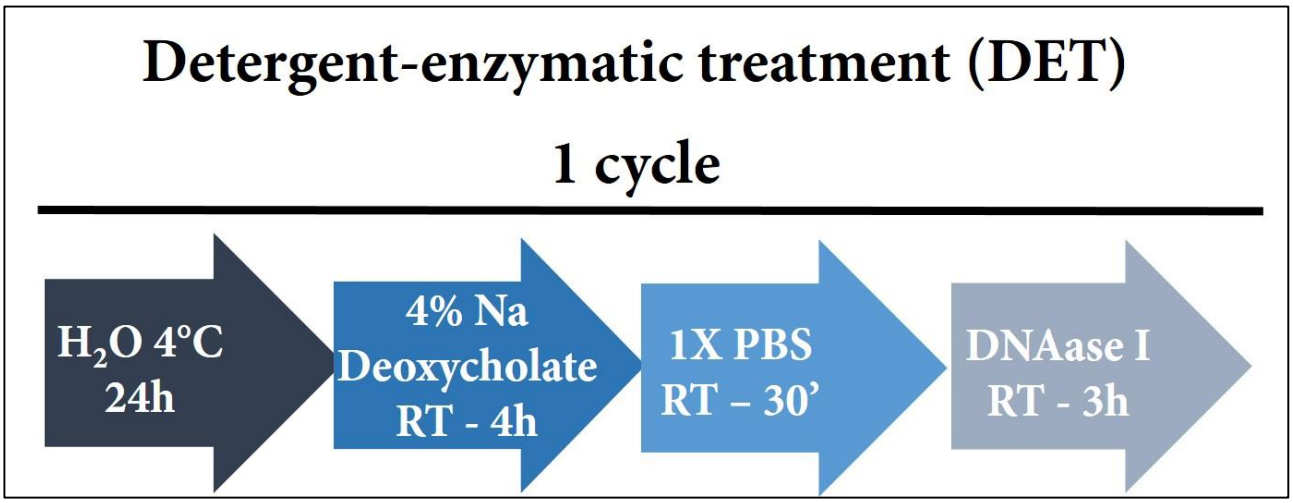

Figure 3.1 Schematic representation of DET, depicted as cycle.

3.4 DNA quantification

DNA was isolated using a tissue DNA isolation kit (DNeasy Blood&Tissue Kit, Qiagen) following the manufacturer's instructions. DNA concentration was determined by Nanodrop 2000 (Thermo Scientific).

3.5 Glycosamminoglycans quantification

The glyocosaminoglycan content of native tissue and acellular matrices was brought to solution (sGAG) and quantified using the Blyscan GAG Assay Kit (Biocolor, UK). In brief, 50 mg of minced wet tissue was weighed and placed in a micro-centrifuge tube containing 1 ml of Papain digestion buffer and incubated in a water bath at 65 °C for 18 h, with occasional tube removal and vortexing. Aliquots of each sample were mixed with 1,9-dimethyl-methylene blue dye and reagents from the kit. The absorbance at 656 nm was measured spectrophotometrically (Spectramax) and compared to standards made from bovine tracheal chondroitin-4-sulfate to determine the sGAG content.

3.6 Collagen quantification

The collagen content of native tissue and acellular matrices was quantified using the Sircol collagen assay kit (Bio-color, UK). Briefly for collagen, the samples were hydrolysed in 6N HCl at 95 °C for 20 hour, the hydrolysate were mixed with a chromogen solution staining hydroxyproline residues and color was developed at 60 °C for 1 hour. The absorbance for each sample was determined at 555 nm using a microplate reader (Spectramax) and the collagen quantity was calculated from a standard curve created with known concentrations of pure collagen hydrolysates.

3.7 Elastin quantification

The Elastin content in fresh and decellularized diaphragms was quantified using the Fastin Elastin Assay Kit (Biocolor, UK). All test samples require the conversion of the native hydrophobic elastin into a water soluble derivative (α-elastin). To extract α-elastin, samples were heated at 100 °C for one hour with 1 ml of 0.25 M oxalic acid twice. Pelleted samples were then used for the assay. Briefly, each sample was then incubated for 15 minutes with ice cold Elastin Precipitating Reagent (containing trichloroacetic and hydrochloric acids). Precipitated was then dyed with Fastin Dye Reagent (contains 5,10,15,20-etraphenyl-21H,23H-porphine tetrasulfonate (TPPS) in a citrate-phosphate buffer). After a precipitation step, Dye dissociation reagent (containing guanidine HCl and propan-1-ol) was added. The contents of each tube was transferred into a well in a 96 well plate and absorbance at 513 nm was measured using a microplate reader (Spectramax). A standard curve was set up using standards containing α-elastin from bovine neck ligament..

3.8 Scanning Electron Microscopy (SEM)

Samples were fixed in 2.5% glutaraldehyde in 0.1 M phosphate buffer and left for 24 hours at 4°C. Following washing with 0.1 M phosphate buffer, they were cut into segments of approximately 1 cm length and cryoprotected in 25% sucrose, 10% glycerol in 0.05 M PBS (pH 7.4) for 2 hours, then fast frozen in Nitrogen slush and fractured at approximately -160°C. The samples were then placed back into the cryoprotectant at room temperature and allowed to thaw. After washing in 0.1 M phosphate buffer (pH 7.4), the material was fixed in 1% OsO_4 / 0.1 M phosphate buffer (pH 7.3) at 3°C for 1½ hours and washed again in 0.1 M phosphate buffer (pH 7.4). After rinsing with dH_2O, specimens were dehydrated in a graded ethanol-water series to 100% ethanol, critical point dried using CO_2 and finally mounted on aluminum stubs using sticky carbon taps. The material was mounted to present the fractured surfaces across the parenchyma to the beam and coated with a thin layer of Au/Pd (approximately 2nm thick) using a Gatan ion beam coater. Images were recorded with a Jeol 7401 FEG scanning electron microscope.

3.9 Chicken chorioallantoic membrane (CAM) assay

To evaluate the angiogenic properties of the decellularized materials *in vivo* the CAM assay was used as previously described [162]. Fertilized chicken eggs (Henry Stewart and Co., UK) were incubated at 37 °C and constant humidity. At 3 days of incubation an oval window of approximately 3 cm in diameter was cut into the shell with small dissecting scissors to reveal the embryo and CAM vessels. The window was sealed with tape and the eggs were returned to the incubator for a further 5 days. At day 8 of incubation, 1 mm diameter mDDs were placed on the CAM between branches of the blood vessels. Polyester sections soaked overnight either in a PBS solution or in PBS with 200ng/ml VEGF (R&D systems) were used as negative and positive controls respectively. Samples were examined daily until 10 days after placement wherein they were photographed *in ovo* with a stereomicroscope equipped with a Camera System (Leica) to quantify the blood vessels surrounding the matrices. The

number of blood vessels (less than 10 μm in diameter) converging towards the placed tissues was counted blindly by assessors, with the mean of the counts being considered. Ending time-point of the experiment was 7 days.

3.10 Proteomics

3.10 Proteome profiler angiogenesis array

Before start, tissue was lysed by mechanical homogenization and protein fraction was collected in PBS with protease inhibitors (10 μg/mL Aprotinin, 10 μg/mL Leupeptin, and 10 μg/mL Pepstatin, all Sigma-Aldrich). An equal volume of 2% Triton-X (Sigma-Aldrich) in PBS was added to obtain a final concentration of 1%. Next, samples underwent a freeze-thaw passage to further lyse cells, and were immediately used for the analyses. Three tissue homogenates for each sample were pooled for analysis. Then, with the aim of loading an equal amount of protein, concentration of each homogenate pool was determined with BCA protein assay kit (Pierce, performed according to manufactures´ instructions). Proteome profiler mouse angiogenesis array ARY015 (R&D Systems) was carried out according to manufactures' instructions. Luminescence acquisition and quantification of the pixel density of each spot was determined with Alliance (UVITEC Cambridge). For data analysis, average background signal (negative control spots) was subtracted from duplicate spot signal intensity which was subsequently normalized to positive control spots and related to signals from mFD mice.

3.10 ELISA test

Tissue was lysed as described above, then immediately essayed. Three decellularized diaphragm quarters (from different samples) were pooled and used for each ELISA. Quantikine for mouse VEGF,

HGF, EGF and SDF-1α (R&D systems) were carried out according to manufactures' instructions. Luminescence acquisition and sample quantification was performed using Spectramax.

3.11 In vivo implantations

Mice were gently handled in general anesthesia with O_2 and isofluorane (Forane, Merial, IT) inhalation (3-3.5% for induction and, subsequently, 1-2% for maintenance). Analgesics (as painkillers), antibiotics and saline solution (for rehydration) were administered after each procedure.

3.11.1 Subcutaneous (SC) implantation

Mice were put in a put in a procumbent position. A medial incision was performed on the back of the mouse and skin was gently detached from the underlying *fascia.* For each animal, up to three portions (0,7x0,7 cm each) of acellular scaffold were positioned and fixed to the skin side with a Prolene 7/0 suture (Fig 3.2). Skin was then closed with a Prolene 6/0 suture and animal left to recover under a heating lamp. Samples were harvested from euthanized mice (cervical dislocation) at 7 and 15 days post implantation (p.i.)

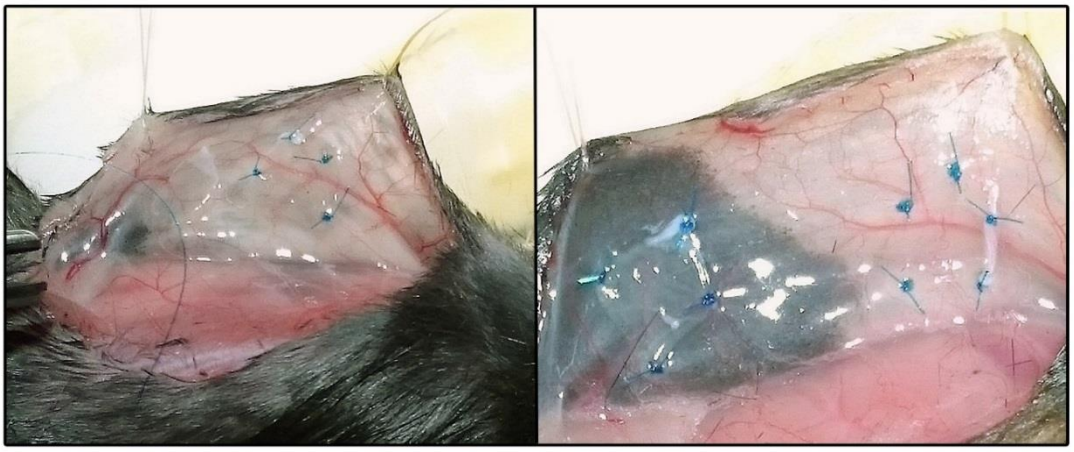

Figure 3.2 Surgical procedure /example of SC implantation

Implantation of one (left) or two (righ) mDD patches under the skin of GFP mice.

3.11.2 Orthotropic implantation

Mice were put in a put in a recumbent position. A medial incision was performed in the abdomen of the mouse, then, to visualize the diaphragm, liver and stomach were then gently moved aside with the help of a sterile gauze. Either mDD or PTFE patches (0,7x0,7 cm each) were fixed on the left side (right-hand side from operator point of view) of the recipient diaphragm with stitches of non-absorbable Prolene 9/0 (Fig. 3.3). Organs were then repositioned into the abdominal cavity, the abdominal wall was closed in two layers and the animals left to wake up under a heating lamp.

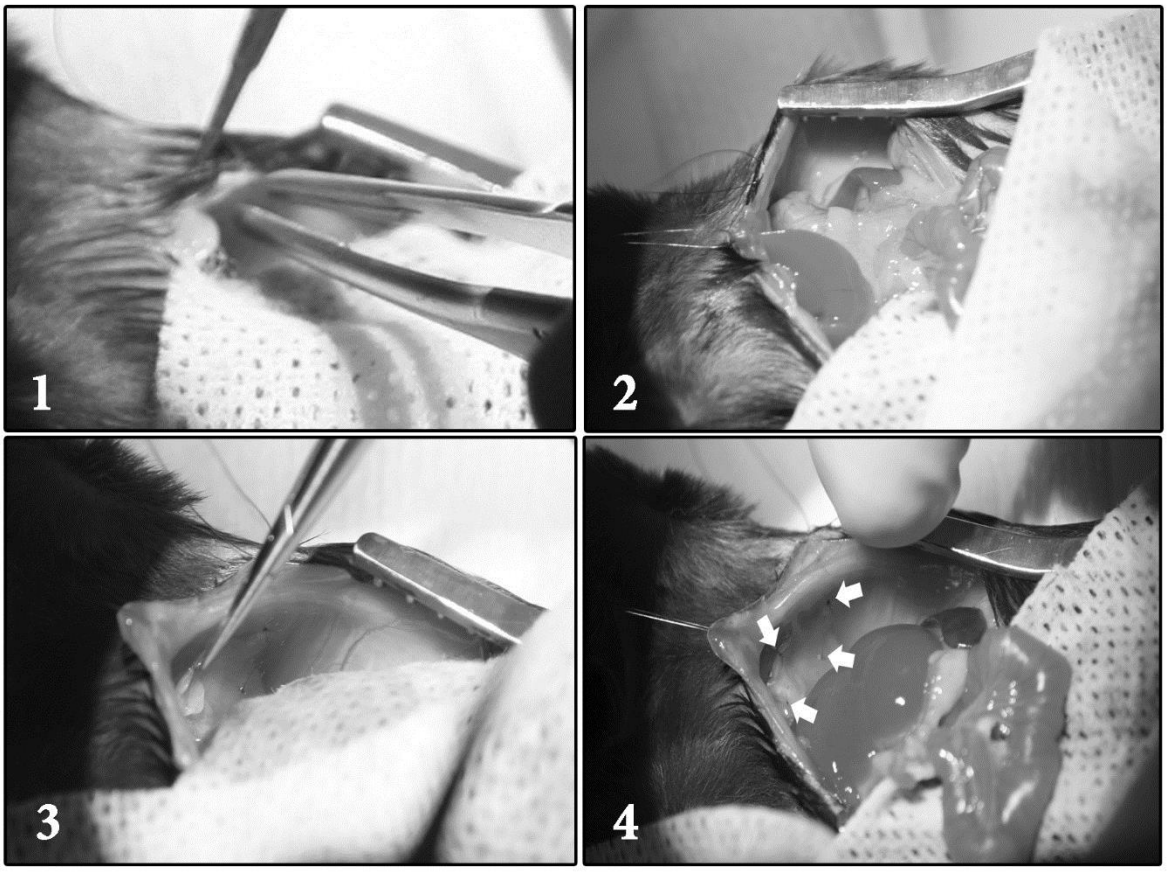

Figure 3.3 Schematic representation of surgical procedure performed during orthotropic implantation in mice

In a procumbent position, abdominal cavity was exposed and (1) rib cage was sutured on the xiphoidal process to improve area of surgery; (2) abdominal organs are pulled away to allow (3) positioning of the patch (either mDD or PTFE), which is (4) implanted with sutures. Arrow=sutures.

3.11.3 Surgical model of diaphragmatic hernia and implantation

Since the creation of an opening in the diaphragm causes pneumothorax immediately, it was necessary to aid mice with ventilation (PY2 73-0043 HSE-HA MiniVent, Harvard Apparatus). This condition was kept from first anaesthetic phase to the full closure of the abdomen. Briefly, xiphoidal process and organs were moved away from the surgical area; with a micro scissor it was made at first a defect of roughly 3x2 mm in the first phase (pilot experiments), then the opening was set at around 66mm^{2}, on the left side of the diaphragm (operator right-hand side). Either PTFE or mDD were implanted to cover the defect, using a continuous closure with a non-absorbable Prolene 8/0 (Fig. 3.4). Organs were finally put back in place and abdominal cavity was closed. Afterwards, the animals were checked to ensure arousal within 10 minutes after surgery, they were moved back to their cages and monitored for activity, ability to drink and eat and for signs of bleeding or infection. Mice were euthanized by cervical dislocation at 15 and 30 days p.i. in the pilot setting, whereas for the experimental phase were set at 30 and 90 days p.i.

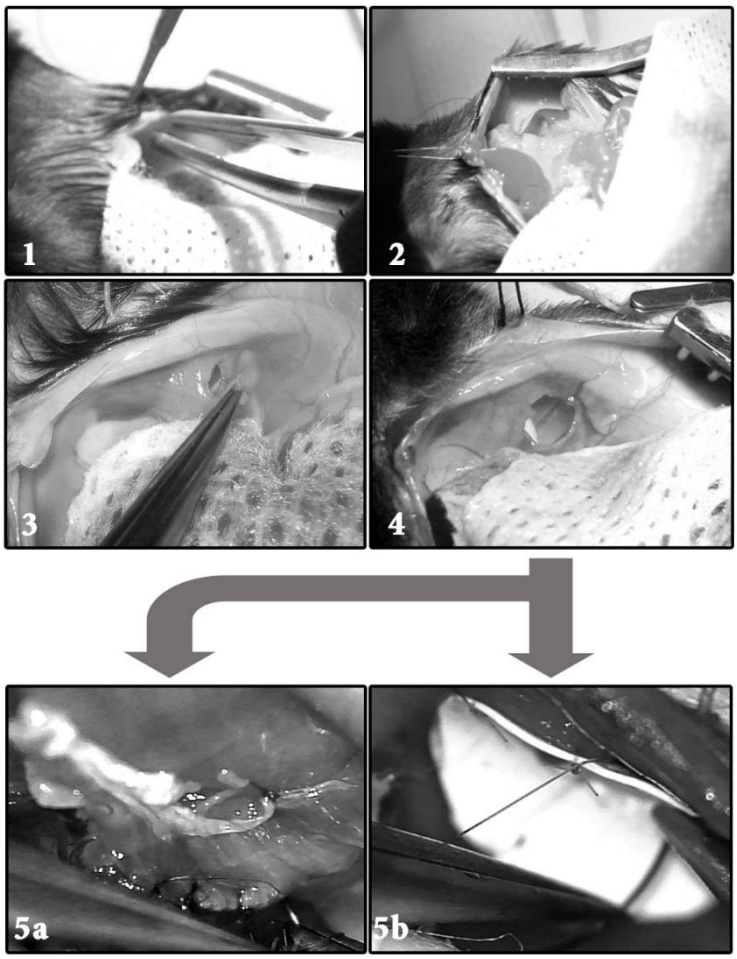

Figure 3.4: Schematic surgical procedure for the creation of the surgical CDH, followed by either mDD or PTFE closure.

Scheme of operation for the creation of the surgical model of CDH: 1) xyphoidal process was fixed, 2) freeing the surgical area allowing for careful organ dislodge to better expose the left side of the diaphragm; 3) defect was made using a micro scissor, in order to reproduce 4) a lateral opening, which then was closed with either 5a) mDD or 5b) PTFE.

3.12 Echography

After 30 days from the surgery, a thoracic echography was performed for all the animals, in order to evaluate their respiratory functions. Wt mice were analyzed as control. Thoracic and abdominal subcostal echography was performed using a high resolution echo machine with a 30 Mhz probe

(VEVO 2100 Visualsonics). Animals were chest shaved and anesthetized with 3% isoflurane, and temperature controlled anesthesia was maintained with 1.5% isoflurane. Two-dimensional cine loops and M-mode cine loops of right and left hemidiaphragms were recorded. Diaphragmatic excursion (as mm) was measured from M-mode cine loops of right and left hemidiaphragm. All mice were imaged by a single operator.

3.13 Haemoglobin (Hb) quantification

Drabkin's reagent lyses red blood cells and oxidizes all forms of Hb, with the exception of the minimally presentsulfhaemoglobin, to the stable HiCN form [163]. Samples used for quantification were homogenized and diluted 1 ⁄1000 with Drabkin's reagent(Sigma, USA) so that the final HiCN concen-tration fell within the range of the calibration curve(0–0Æ8g⁄l HiCN) produced using a HiCN standard calibrated to international standards (Sigma-Aldrich). After mixing, samples and standards were incubated at room temperature for 30 min and protected from light. Absorbance was read at 550 nm with Spectramax and the Hb concentration of each sample was calculated from the linear equation of the calibration curve.

3.14 Evans Blue injection

Evans Blue (Sigma, USA) was diluted to 0,5 % in 0.9 % NaCl solution. A total amount of 200 µl of the prepared solution was injected via tail vein and left diffusing in the bloodstream for 30 minutes, before animal euthanasia. To avoid loss of the dye, diaphragm muscles were fixed right after harvesting with 0.25% Glutaraldehyde (Sigma-Aldrich) in PBS.

3.15 Cell sources and culture

3.15 Mouse Satellite Cells

3.15.1.1 Isolation

SCs were isolated using a well-established method, by stripping of single muscle fibers dissociated from right and left EDL and SOL [164–166]. After enzymatic digestion with 0.2% (w/v) collagenase type I (Sigma-Aldrich), reconstituited in DMEM low-glucose (DMEM-LG), for 2 hours at 37°C. Then, muscles were transferred to a 100 mm plate containing 9 ml of plating medium [PL: DMEM-LG, 10% Horse Serum (HS, GIBCO-Invitrogen), 1% Penicillin/Streptomycin (P/S), 0.5% chicken embryo extract (CEE, SeraLab)] and gently stirred with the same medium using a micropipette to release single myofibers (1st dilution). Under phase contrast microscope, single fibers were carefully sucked up and counted while serially transferred to another 100 mm petri dish containing 8 ml of PL (2nd dilution). Fibers were transferred to a 50 ml Falcon tube and triturated 20 times using a 18 G needle mounted onto a 1 ml syringe to disengage SCs (stripping passage). The resulting cell suspension was filtered through 20 and 50 μm cell strainer and centrifuged at 2000 rpm for 5 minutes. Lastly, pellet was resuspended in cells growth medium.

3.15.1.2 Culture

Primary mSCs were plated freshly isolated in gelatin 1%-coated 35mm dishes resuspended in growth medium [GM; for mouse muscle cells mM-GM: DMEM high-glucose, 20% Fetal Bovine Serum (FBS, GIBCO-Invitrogen), 10% HS, 1% P/S, 0.5% CEE]. Cells were expanded and maintained at subconfluency (<60%) always on gelatin-coated dishes. Passages were performed using trypsin-EDTA 0.05% (Life Technologies, Invitrogen).

3.15.1.3 Differentiation

To evaluate differentiation, at passage 2 or 3 (p2-p3) of each preparation an aliquot of cells was plated at a density of 15000 cells/well of tissue culture 24-well plates. At least three wells for each preparation were prepared. Once cells reached a confluency over 90%, growth medium was changed to differentiating medium [mM-DM: DMEM high glucose, 2% HS, 1% P/S].

3.15.2 Mouse Diaphragm Fibroblasts

3.15.1.1 Isolation

Mouse diaphragms for mouse fibroblasts (mFbs) isolation were removed from the rib cage, minced to small pieces and rinsed in 10% Betadine® (Meda), which was then washed away with sterile PBS. Muscle was then minced again to obtain a slurry that was finally resuspended in 0.2% collagenase I. Digestion process was left to act for 2 hours at 37°C. Enzyme was blocked with blocking medium (BlM, composed of DMEM High glucose supplemented with 10% FBS and 2% P/S). Solution was filtered through a 70 and a 40 μm filters and centrifuged at 1200 rpm for 10 minutes.

3.15.1.2 Culture

Primary mFbs were plated freshly isolated in gelatin 1%-coated 35mm dishes resuspended in growth medium [F-GM: DMEM high-glucose, 20% FBS, 1% P/S, 0.5% CEE]. To enrich fibroblast population, medium was removed and changed after 1 hour. Attached cells were expanded and maintained at a confluency ≥80 %, always on gelatin-coated dishes. Passages were performed using trypsin-EDTA 0.05% (Life Technologies, Invitrogen).

3.15.3 Mouse cells from whole muscle digestion

3.15.3.1 Isolation

All the muscles were removed from the whole limb, being careful of removing fat and exceeding connective tissue, and rinsed in 10% Betadine® as previously described. Muscle was then minced to obtain a slurry that was finally resuspended in 0.2% collagenase I. Digestion process was left to act for 30 minutes at 37°C. Enzyme was blocked with BlM and solution was centrifuged at 1200 rpm for 10 minutes. Pellet was resuspended in 0.05% Trypsin for a second digestion process, that was carried out as the first for 30 minutes at 37°C. Enzyme was blocked again and solution was filtered through a 70 and a 40 μm filters. To remove red blood cells, solution was centrifuged at 1200 rpm for 10 minutes and pellet was resuspended in Red Blood Cells lysis buffer (Promega). After 3 minutes, buffer was blocked with the previously described medium. Solution then went through a last centrifuge at 1200 rpm for 10 minutes. This was an adaption of previous published protocols [167,168].

3.15.3.2 Culture

Primary whole digestion cell suspension was plated freshly isolated in gelatin 1%-coated 35mm dishes resuspended in mM-GM. Cells were expanded and maintained at subconfluency (<60%) always on gelatin-coated dishes. Passages were performed using trypsin-EDTA 0.05% (Life Technologies, Invitrogen)

3.15.3.3 Differentiation

To evaluate differentiation of the mixed population towards, at passage 2 or 3 (p2-p3) of each preparation an aliquot of cells was plated at a density of 15000 cells/well of tissue culture 24-well

plates. At least three wells for each preparation were prepared. Once cells reached a confluency over 90%, growth medium was changed to mM-DM.

3.15.4 Human Paediatric Muscle Precursos Cells and human muscle fibroblasts (phMPC and hFbs)

3.15.4.1 Isolation

Isolation of hpMPCs and hMFbs was carried out accordingly to the procedure recently published by Franzin et al. [169]. Briefly, muscle biopsies were firstly dissected into small pieces. After a rinse in 10% Betadine followed by 1X PBS wash, muscles were minced to a slurry. At this point, samples were alternatively resuspended in freezing medium [70% FBS, 20% dimethyl sulfoxide (DMSO,Sigma-Aldrich) and 10% DMEM high glucose] and frozen in liquid nitrogen for later digestion, or further processed as following. Slurry was incubated in 0.2% Collagenase I in a well of a 6-wells plate for 90 min at 37 °C. The enzymatic reaction was stopped by adding the BlM. The product of digestion was triturated with a serological pipette and centrifuged at 1200 g for 10 min. The pellet was resuspended with Trypsin-EDTA (0.05%, Gibco-Life Technologies) and and incubated in a well of a 6-wells plate for 60 min at 37 °C. The enzymatic reaction was stopped again with BlM. Suspension was homogenized using a serological pipette, filtered through 70 μm and 40 μm filters and centrifuged at 1200 g for 10 min. Red Blood cells were lysed as described above and suspension went through a last centrifuge at 1200 rpm for 10 minutes.

3.15.4.2 Culture

Primary cells mixtures were plated in a well of a 6-wells non tissue culture (nTC) plate in their growth medium [hM-GM; DMEM low glucose (Gibco-Life Technologies), 20% FBS, 10^{-6} M dexamethasone (Sigma-Aldrich), 10 ng/ml bFGF (R&D Systems), 10 μg/ml insulin (Humulin – Eli Lilly), 1% P/S].

The medium was changed after 72 hours. Cells were expanded and maintained at subconfluency (<70-80%) always on nTC dishes. Passages were performed using trypsin-EDTA 0.05%.
Specific separation among hpMPCs and hMFbs (to both clean first and enrich second) was done simply taking advantage of the higher proliferation rate and the faster attachment the latter have. Briefly, biopsies can result in a disproportion in the cell population towards the non-myogenic cells, which ca be noticed during the days before the first passage [169]. Whenever this was noticed, cells were immediately passaged to favour hMFbs growth over the myogenic cells.

3.15.4.3 Differentiation

Myogenic differentiation of h/pMPCs was evaluated at p3 and p5. Briefly, at least three wells of a 24-wells tissue culture (TC) plates at a density of 15000 cells/wells were prepared for each differentiation analysis. Once cells reached a confluency over 90%, growth medium was changed to human differentiating medium [hM-DM; AlphaMEM (Gibco-Life Technologies), 2% HS, 10 μg/ml insulin, 1% P/S].

3.15.5 Human Umbilical Vein Endothelial Cells (HUVECs)

HUVEC have been purchased at ProCell and have been cultured following manufacturer's instructions.

3.16 Immunocytochemistry

3.16.1 Proliferation and myogenic markers

To evaluate proliferation and expression of myogenic markers, at least 10 wells of a 96-wells plate at a density of 5000 cells/wells were prepared from each isolated sample, usually at p2 and p3 for mouse cells, and p3 and p5 for human cells. After 48 hours, cells were fixed in 4% PFA for 10 min at 4° C,

then rinsed in 1X PBS and permeabilized with 100 µl of 0.5% Triton X-100 in 1X PBS for 10 min at RT. Non-specific interactions were blocked with 100 µl of 5% HS- 5% Goat serum (GS, Gibco, Life technologies) in 1X PBS for 30 min at RT. Cells were then incubated with 60 µl of primary antibodies overnight (O/N) at 4°C. The day after, cells were washed twice with 1X PBS and incubated with 60 µl of labeled secondary antibodies for 1 hour at 37 °C. After double washing with 1X PBS, nuclei were counterstained with 60 µl of 1X HOECHST (Life Technologies) for 12 min at RT.

The following primary antibodies were used: rabbit anti-MyoD (Santa Cruz, dilution 1:50), mouse anti-MyoD1 (Dako dilution 1:100), rabbit anti-Myf5 (Santa Cruz, dilution 1:100), rabbit anti-Ki67 (Novus Biologicals, dilution 1:100), mouse anti-Pax7 (R&D Systems, dilution 1:50), mouse anti-TE-7 (Millipore, dilution 1:100), mouse anti-TCF-4 (Millipore, dilution 1:100), mouse anti-Vimentin (Sigma, dilution 1:100), rat anti-CD31 (Thermo Fisher, dilution 1:100). Secondary antibodies used were all purchased from Invitrogen, Alexa Fluor-conjugated according to host and needed fluorophore.

3.16.2 Differentiating cells

After 72h of differentiation, mouse or human cells were fixed in 4% PFA for 10 min at 4 °C, rinsed in 1X PBS and permeabilized with 250 µl of 0.5% Triton X-100 in 1X PBS for 10 min at RT. Non-specific interactions were blocked with 250 µl of 5%HS-% GS in 1X PBS for 30 min at RT. Cells were then incubated with 200 µl of primary antibodies for 1 hour at 37 °C. Antibody excess was washed away twice with 1X PBS and cells were incubated with 200 µl of labeled secondary antibodies for 1 hour at 37 °C. After double washing with 1X PBS, nuclei were counterstained with 200 µl of HOECHST 1Xfor 12 min at RT. The primary antibody used was mouse anti-MYHC (R&D System, dilution 1:100) and the secondary antibody was Alexa Fluor goat anti-mouse 594 (Life Technologies, dilution 1:200). To quantify myoblast fusion, the myogenic index (MI), defined as the number of nuclei residing in $MYHC^+$ cells containing three or more nuclei divided by the total number of nuclei, was calculated from 5 random fields of each sample.

3.17 Flow cytometry analyses

Cell surface antigen expression of cultivated cells was analysed after detachment by trypsin-EDTA treatment (passages 3 and 5). Briefly, cell suspensions were incubated with 5 µL of antibody for 20 min at 4 °C in the dark. After a wash step, the cells were resuspended in PBS 1X. Acquisition and analyses were performed using Accuri C6 flow cytometer (BD). The antibodies used were: FITC conjugated CD34 and PE conjugated CD56 for human cells, FITC conjugated Sca-1 and PE conjugated Synd-4 for mouse cells. 7-aminoactinomycinD (7AAD) was used to evaluate viability. All antibodies were purchased from BD Pharmigen.

3.18 Cell Seeding in vitro

3.18.1 Scaffold preparation

3.18.1.1 mDDs

All the mDDs were where cut as for the *in vivo* implants, by dividing the muscle in four parts. While scaffolds to be seeded were simply placed on the bottom of a well plate, the procedure for scaffolds to be injected required an additiona step, performed two wasy: 1) Sutures were applied to each corner to be fixed to a harbour (Harvard apparatus) in a 'flag' fashion or 2) Scaffolds were pinned in each corner to a customized semi-circular silicone support (Fig 3.5 B, C).

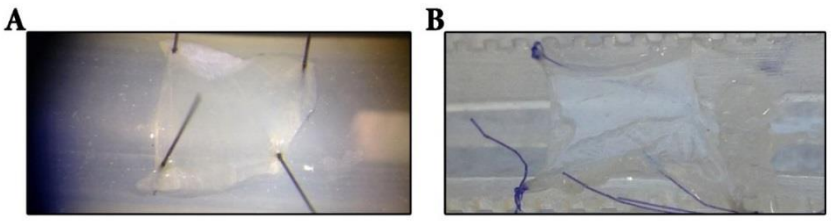

Fig. 3.5 mDDs mounted on the supports.

A) Sutured to the harbour B) Pinned on the semi-cylindrical support

3.18.1.2 rDDs

rDDs were cut to 1x1,2 cm patches. In this case, only one setting was used for seeding and culture. All scaffolds were prepared and mounted in the harbour as previously described for the mouse (Fig. 3.6).

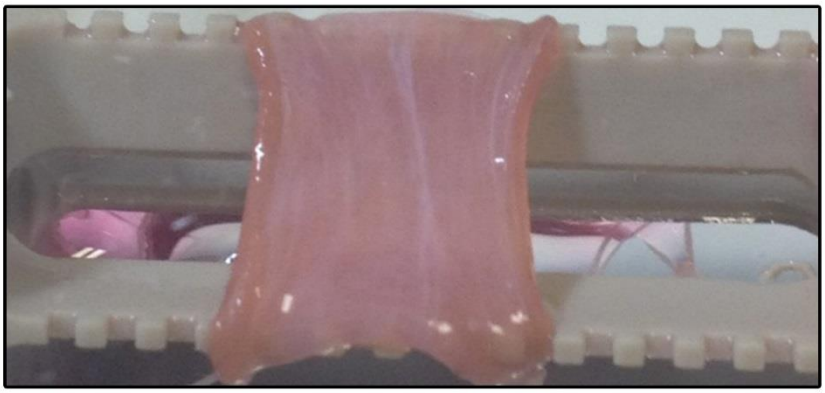

Fig. 3.6 rDDs mounted on the harbour supports (After culture)

3.18.2 Cells preparation

Cells (either of human or murine origin) were detached from culture using trypsin-EDTA 0.05%. Enzyme was blocked with their growth medium and suspension was centrifuged at 1200 rpm for 10 minutes. Cell pellet was then resuspended with an adequate volume to enable an accurate cell count. Once quantity of cells was determined, suspension was aliquoted and processed to obtain a concentration of 500000 cells/12 µl (for each quarter patch of scaffold to be seeded) or 700000 to 1000000 cells/12 µl (for each emidiaphragm or rDD patch to be seeded). For mSCs-mFbs preparation in particular, to avoid fibroblast overcoming the other cells, the latter were resuspended in mM-GM instead of F-GM, then a total of cells was achieved maintaining the proportion of 20% mFBs and 80% mSCs by mixing the two suspensions. Cells were resuspended either in Platelet gel derived supernatant (PGS), in their own growth medium or, for mSCs-mFbs, in mM-GM.

3.18.3 Seeding technique

A 50 µl Hamilton® syringe (705RN) with a 33G needle was used to performe multiple injection in the scaffold. Briefly, cells were aspirated in the syringe and serial injection were made trying to obtain a homogenous cell distribution to whole scaffold surface (Fig. 3.7, 3-4). Procedure was carried using a stereomicroscope (set to 4x to 6x) and was repeated for each scaffold to be seeded.

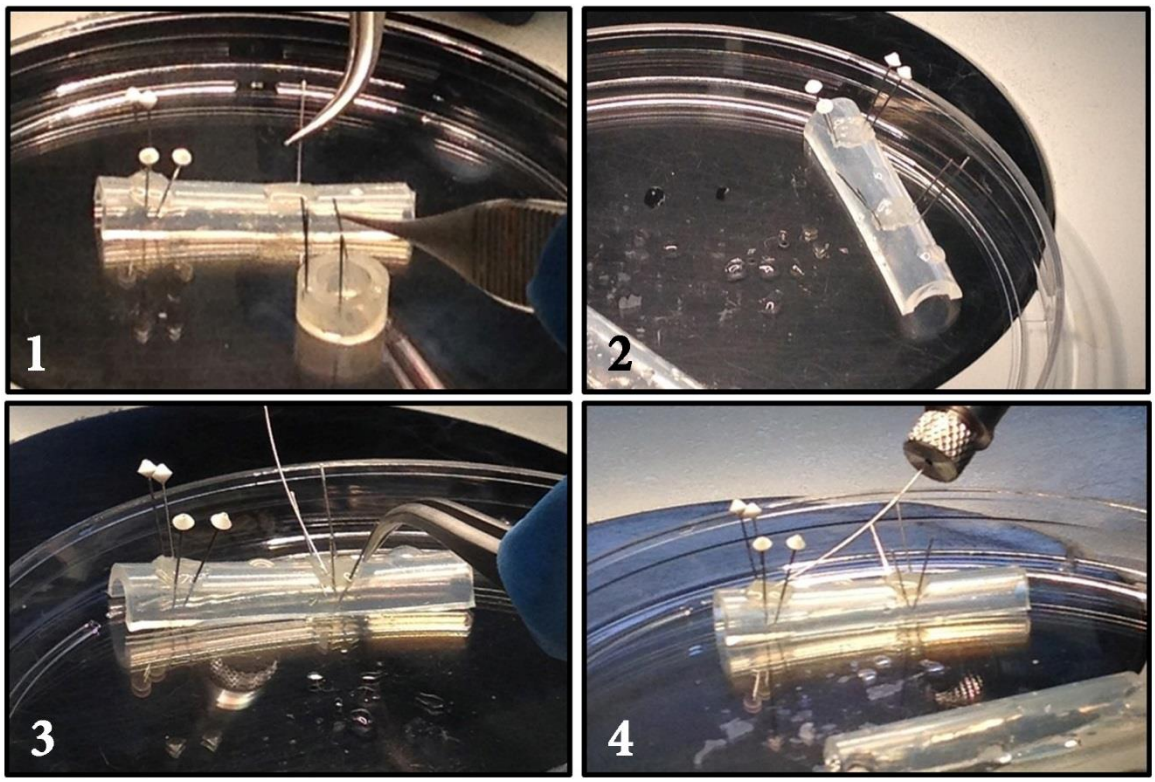

Fig. 3.7 Schematic representation of the procedure performed on mDDs from pinning on semi cylindrical tubes to injection

3.18.4 Culture conditions

Seeded scaffold were transferred to a well of a 6 well plated (if mounted on the semi-circular silicone support) or to a T175 flask (if mounted on the harbour) (Fig 3.8, 3.9).

After half an hour, enough growth medium to ensure full immersion of the scaffold was added (Usually 6 ml/well, 40 ml/flask). For all the conditions, after 4 days of culture in GM, medium was changed to induce the differentiation program. Medium (either GM or DM) was changed every 48 hours of culture condition. For each culture the time point was set at 7 days after injection.

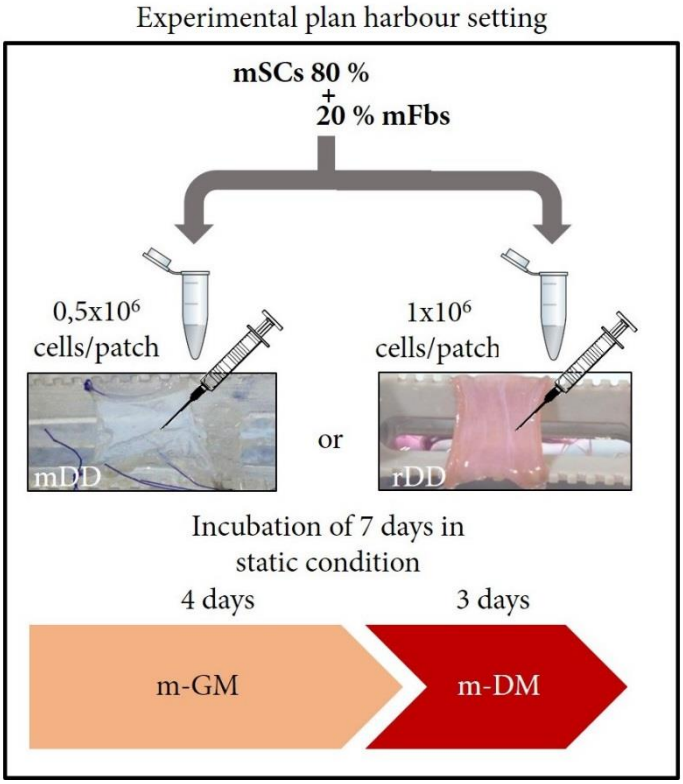

Figure 3.8 Experimental plan for settings on harbour

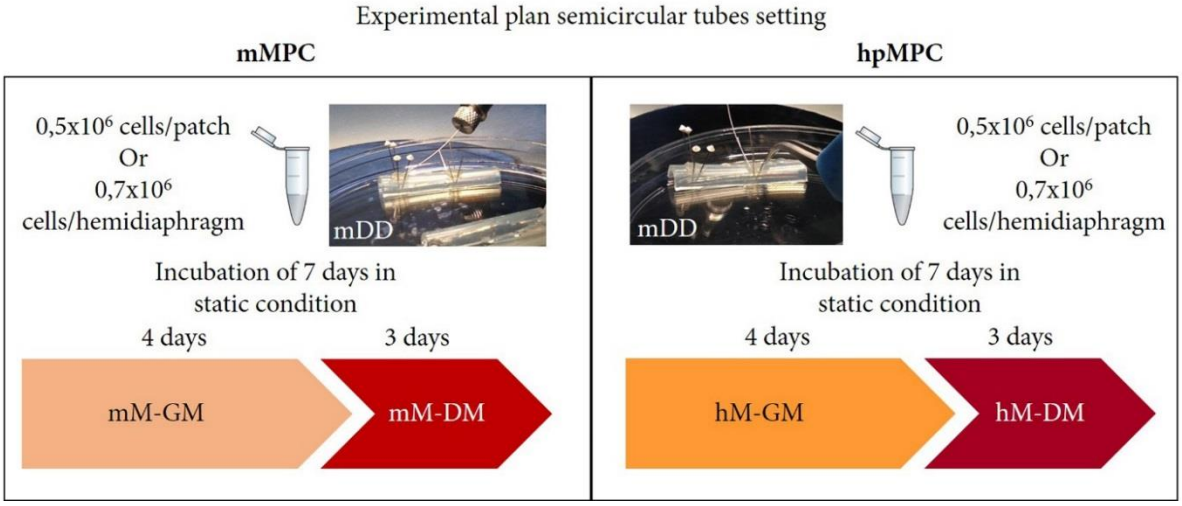

Figure 3.9 Experimental plan for setting on semicircular tubes

3.19 Plateled gel derived supernatant

PGS was obtained from the exudate of solidifying platelet gel [170]. Briefly, Plateled gel suspension was activated by adding Batroxobin supplemented with Ca in a proportion 5,9:1 in a Eppendorf conical tube. After 10 to 15 minute platelet gel was solidified and started to release an exudate. This exudate was then collected as supernatant by centrifuging the whole suspension.

3.20 Histology

3.20.1 Sample preparation

Samples intended for histology analyses were fixed with 4% paraformaldehyde (PFA) (Sigma-Aldrich) for 20 min. (mDDs) or 1 hour (rDDs) at 4 °C. Then, were dehydrated through an increasing sucrose (Sigma-Aldrich) gradient (10%, 15% and 30%); the first two steps were performed for 1h each, while samples were left in the last overnight (O/N). Lastly, the day after were frozen enclosed in the embedding medium O.C.T. (Kaltek), by immersion in pre-cooled (*via* liquid N_2) 2-MetylButane

(Sigma-Aldrich). The frozen tissues were sectioned with a cryostat (Leica CM1520) in sheets of 6-9 μm.

3.20.2 Histochemistry

3.20.2.1 Haematoxylin and eosin stain

Haematoxylin and eosin stain was done using Haematoxylin Eosin (HE) kit for rapid frozen section (Bio-Optica, UK).

Sections were rapidly re-hydrated with an inversed alcohol gradient and rinsed in distilled water. Then, they were put in reagent A (Harris haematoxylin) for 45 seconds and then rinsed in tap water. They were dipped in Buffer solution (prepared with reagent B) and rinsed again in tap water. Slides were put in reagent C (Eosin) for 30 seconds and dehydrated by dipping first in ethanol 95%, then in absolute ethanol and at the end in xylene; all dehydration steps were done twice. Sections were then mounted in organic mounting medium (Bio-Optica, UK).

3.20.2.2Masson's trichrome stain

Masson's trichrome (MT) is a staining procedure based on four different reagents: Weigert's iron haematoxylin for nuclei, picric acid for erythrocytes, a mixture of acid dyes (acid fuchsin-"ponceau de xylidine") for cytoplasm and aniline blue for connective tissue.

MT stain was done using Masson trichrome with aniline blue kit (Bio-Optica, UK). After a rapid re-hydration with descending alcohol gradient and distilled water, 3 drops of Weigert's iron haematoxylin A solution plus 3 drops of Weigert's iron haematoxylin B solution were put on each section and left act for 12 minutes. Without washing, 5 drops of reagent C (Picric acid) were left to act 4 minutes on the sections. Slides were then rinsed in distilled water and incubated 4 minutes with 5 drops of reagent D (Ponceau's fuchsin) and rinsed again in distilled water. Subsequently, 5 drops of

the reagent E were left on each section for 10 minutes, and without wash, 5 drops of the reagent F were left to act for 1 minute. After a final washing step in distilled water, section were dehydrated rapidly through ascending alcohols, stopping 1 minute in the last absolute ethanol. Sections were then cleared in xylene and mounted with organic mounting medium (Bio-Optica, UK).

3.20.2.3 Alcian blue stain

In Alcian blue (AB) stain, a sodium tetraborate solution transforms the dye into Monastral blue pigment, which is insoluble and can therefore be further manipulated without spreading in the tissue (Alcian blue-PAS). Alcian blue reacts with polyanions whose components are sulphuric and carboxylic radicals (phosphate radicals of nucleic acids do not react). As result, acid mucins only are stained. In particular, at pH 1 Alcian blue stains strongly sulphured mucins only, at pH 2.5 ionizes most acid mucins.

AB stain was done using Alcian blue pH 2.5 kit (Bio-Optica, UK). After a rapid re-hydration with descending alcohol gradient and distilled water, 10 drops of reagent A (Alcian blue pH 2.5) were left to act for 30 minutes on each section. Without wash, 10 drops of reagent B (sodium tetraborate) were put on each section and left to act 10 minutes. After a rinse in distilled water, section were incubated 10 minutes with 10 drops of reagent C (carmalum). After a final washing step in distilled water, section were dehydrated rapidly through ascending alcohols, stopping 1 minute in the last absolute ethanol. Sections were then cleared in xylene and mounted with organic mounting medium (Bio-Optica, UK).

3.20.2.4 Elastic Van Gieson stain

The Elastic Van Gieson stain (eVG) is based on the affinity towards elastic fibers displayed by resorcin fuchsin, a precipitate resulting from a reaction between resorcin and basic fuchsin and ferric chloride. Since this is not an absolutely specific method, other structures such as collagen and basal membranes

might be stained. Therefore it is essential to differentiate carefully in order to obtain a selective marked staining of elastic fibers. Counterstaining with Van Gieson trichromic stain makes it possible to differentiate collagen from connectivum showing nuclei at the same time.

eVG stain was made using Weigert Van Gieson for elastic fibers and connectivum (long method) (Bio-Optica, UK). After a rapid re-hydration with descending alcohol gradient and distilled water, 10 drops of reagent A (Periodic acid) were left to act for 10 minutes on each section. Slides were then rinsed in distilled water and incubated overnight in reagent B (Weigert's solution). After a rinse in distilled water, section were incubated 10 minutes with 10 drops of reagent C (acid differentiation buffer) and then rinsed again in distilled water. Subsequently, 3 drops of reagent D (Weigert's iron haematoxylin - A solution) plus 3 drops of reagent E (Weigert's iron haematoxylin - B solution) were put on each section and left act for 12 minutes. Sections were then washed in distilled water until colour turned dark blue-black and incubated in reagent F (Van Gieson's Picrofuchsin) for 45 seconds. After a final washing step in distilled water, section were dehydrate rapidly through ascending alcohols, stopping 1 minute in the last absolute ethanol. Sections were then cleared in xylene and mounted with organic mounting medium (Bio-Optica, UK).

3.21 Immunofluorescence

Sections were rehydrated and permeabilized with 0.5% Triton X-100 (Fluxa) in 1X PBS for 10 minutes at RT. Reagent was washed away in 1X PBS for 5 minutes twice, then nonspecific sites were saturated with 5% HS-5% GS in 1X PBS for 30 minutes. An adding step in mouse serum (Sigma-Aldrich, dilution 1:10) in 1X PBS or in Mouse-on-Mouse kit (M.O.M., Vector) for 30 minutes at RT was performed each time a primary antibody made in mouse was used in mouse tissue. Straight afterwards the samples were then incubated with primary antibody. Next, washing step with 1X PBS was performed twice, then slides were incubated with secondary antibody for 1 hour at 37 °C. After the last washing step with 1X PBS, slides were mounted and nuclei were counterstained with fluorescent mounting medium [(100 ng/ml 4',6-diamidino-2-phenylindole (DAPI) (Sigma-Aldrich)]. In table 2.1

were listed the antibodies and the tested conditions. Secondary antibodies used were all purchased from Invitrogen, Alexa Fluor-conjugated according to host and needed fluorophore. Full antibody list, hosts, brand and dilution are listed in the appendix Table A.1.

3.22 Vessel size analysis

Eight images per group (FD, transplanted after 7 days and 15 days) were analysed to examine the difference in vessel dimension. To this aim, for each image the perimeter and the area of each vessel (labelled with αSMA) were calculated using Fiji [171] or Imago 1 (Mayachitra). Next, their proportion was analytically obtained by means of the fractal dimension index.
(FRAC;
http://www.umass.edu/landeco/research/fragstats/documents/Metrics/Shape%20Metrics/Metrics/P9%20-%20FRAC.htm)

3.23 Microscopes and imaging system

Phase-contrast images were collected using an inverted microscope (Olympus IX71). Immunofluorescence analyses were performed using a fluorescence inverted microscope (Leica DMI6000B) or a confocal microscope (Zeiss LSM 710).

3.24 RNA extraction and PCR analyses

3.24.1 Extraction and Real-time PCR (qPCR)

After tissue or cell samples homogenation RNA has been extracted using TRizol reagent (Life Technologies) following manifacturer's instruction until acqueous phase isolation, then RNeasy Plus

Mini kit (QIAGEN GmbH) has been used starting from the addition of a volume of 70% ethanol following the supplier's instructions. RNA has been quantified with a ND-2000 spectrophotometer and 1 mg has been retrotranscripted with SuperScript II and related products (all from Life Technologies) in a 20 µl reaction. Real-time PCR reactions were performed using a LightCycler II (Roche, Monza, Italy). Reactions have been carried out in triplicate using 4 ml of FASTSTART SYBR GREEN MASTER (Roche) and 2 µl of primers mix FW + REV (final concentration, 300/300 nM) in a final volume of 20 µl. Serial dilutions of a positive control sample have been used to create a standard curve for the relative quantification. The amount of each mRNA has been normalized for the content in b2-microglobulin. Primer sequences used for mouse genes were the ones published in Piccoli et. Al [104], whereas the human genes are listed in *Appendix A* (table A.2)

3.24.2 Gel electrophoresis

The PCR products were analysed using 1.2% agarose gel (agarose 1.44g and 5µL ethidium bromide in 120mL Tris-Borate-EDTA buffer (0.5%)). Electrophoresis was performed for 60mins (120V).

3.25 Counts and measurements

Image based counts and measurements were performed with Fiji [171] or alternatively with Imago 1 (Mayachitra). For each analysis, at least five random pictures were used for data output. All graphs displayed were produced with GraphPad software 5 or 6.

3.26 Statistical analyses

Statistical analyses were performed with GraphPad software 5. The data were presented as mean ± S.E.M.. Differences between data groups were evaluated for significance either using the unpaired Student's t-test or one-way ANOVA. P-values indicated on figures are * = $p < 0.05$; ** = $p < 0.01$; *** = $p < 0.001$; **** = $p < 0.0001$.

Chapter 4 : Characterization of diaphragm derived acellular scaffold

4.1 Introduction

4.1.1 Scaffold concept in TE

In the specific context of TE, the scaffold is a structure able to support and promote survival, growth and terminal differentiation of seeded cells, with the aim of achieving the most efficient graft to repair or substitute a specific tissue or organ. Among the general attributes a scaffold must fulfil, of extreme importance are scaffold's ability to:

- modulate the immunogenic response from the host (biocompatibility), .
- integrate in the host in a time that permits sufficient cellular growth and tissue recover whilst not producing harmful degradation products (biodegradability or functional integration).
- support tissue growth through mechanical properties such that remodeling phase of tissue repair is allowed and tissue physiology is restored (Stiffness, porosity).

More specifically, as in nature the scaffolding structure of tissues and organ is the extracellular matrix (ECM), other scaffold attributes are usually determined according to the specific organ ECM properties. These, include mediation of cell adhesion via integrin receptors, proliferation and differentiation by the means of signaling molecules (growth factors, cytokines), as well as positive influence on cell survival [147,172–174]. Many studies were done to evaluate different materials for tissue engineering, and to date these have been traditionally divided into naturally-derived, synthetic and natural acellular scaffolds.

4.1.2 Tissues ad organs ECM

Providing structural, mechanical and biological support to our cells, the ECM is a complex three-dimensional organization of proteins and polysaccharides. Everything but an inert support structure, the ECM significantly determines cell phenotype and function *in vivo*, providing signals for a wide range of processes, thereby influencing cell survival, proliferation, migration, differentiation, morphology, secretory profile, metabolism, and other specialized activities [175–179]. This influence is though a dynamic reciprocity, as ECM is formed by its resident cells secretion products. These, usually undergo self-assembly and interact with other ECM components, resulting in a highly organized architecture in which both small immobilized molecules and structural macromolecules are responsible for tissue-type specific extracellular architecture . Structurally, macromolecules are distinguished in two main classes: fibrous proteins (including collagens and elastin) and glycoproteins (including fibronectin, proteoglycans (PGs) and laminin)[180] [181].

Precisely, collagen represents more than 90% of dry weight of the ECM, being its most abundant protein in mammalians. So far, 28 different types were discovered, each with characteristic properties and functions, nevertheless the most frequent is type I collagen. In nature, collagen is often associated with glycoproteins, elastin, laminin and can bind growth factors, generating a particular three-dimensional pattern.

Second for abundance, there is Fibronectin, a dimeric molecule present in both soluble and bound isoforms. This molecule is rich in the Arg-Gly-Asp (RGD) motif, a sequence known to mediate cell adhesion through the binding to integrins. It is found especially in the ECM of submucosal structure, basement membranes and interstitial tissues [182,183]

Chondroitin sulfates A and B, heparin, heparan sulfate and hyaluronic acid are instead some of the glycosaminoglycans present in the ECM. These, are of extreme importance for the dynamic reciprocity, as they represent the main reservoir of bound growth factors and cytokines [184–187], favor water retention and contribute to the gel properties of the ECM, therefore influencing tissue stiffness [41,178,188–191].

Depending on the body needs, composition and proportion of ECM molecules varies continuously, orchestrated not only by secretion of more structural molecules, but also by the activity of proteases able to cleave and digest structural proteins, f.eg Metalloproteases (MMP) [192–194]. These, in addition to the contribution to the remodeling of the matrix itself, can be considered also effectors of the dynamic reciprocity. Indeed, besides the stored cytokines and chemokines, remodeling processes lead to the release of small bioactive peptides, referred to as Matrikines [195,196].

As a correct regulation of the processes involving the ECM is critical in many biological processes, for example during development, homeostasis, and wound healing, is no surprise that alterations of its architecture and of dynamic reciprocity with resident cells can result in disease progression in many organ systems [197,198]. Non-functional, chronic or excessive fibrosis are some of the most common causes of tissue damage, in which the progressive remodeling of the ECM disrupts function and prevents regeneration [199,200]

Skeletal and cardiac muscle are perfect examples of ECM primary role in tissue function and disease. Mutations in the gene encoding the skeletal muscle ECM proteins, such as laminin alpha-2 or Dystrophin, lead to severe muscular dystrophy, which is due to an inability of muscle fibers to efficiently mechanically couple with the ECM [201]. Also, muscle stem cells (SCs) are defined by their unique anatomical niche, which is closely interconnected with surrounding ECM [33,202]. In the heart, scarring of the infarcted area, due to the necrosis of cardiomyocytes concomitantly with proliferation of myofibroblasts, results in loss of function of the organ [203,204]

4.1.3 Naturally derived scaffolds

These are usually composed of natural macromolecules, either alone or combined with other materials, which can be functionalized to form a three-dimensional support. Biocompatibility due to natural derivation results in low immunogenicity of these molecules, some of which are also able to mediate cellular responses through binding sites for cytokines [186,205,206]. Other advantages of these scaffolds are mainly due to the possibility of customization and therefore functionalization of the scaffolds. Changing molecule ratio and crosslinking material, for example, it is possible to alter

mechanical properties, porosity, fiber orientation, degradability [139,207]. Also, multiple ECM elements can be combined. For example, in vascular tissue engineering, which is one of the most studied and advanced fields, a tubular scaffold containing both collagen and elastin was produced, which was able to allow smooth muscle cells orientatation in line with its fibers [208].

4.1.4 Synthetic scaffolds

Use of synthetic materials is common practice in other areas of medicine, hence possible applications for tissue engineering purposes was a foreseeable consequence. Polyesters [poly-L-lactic acid (PLLA), poly glycolic acid (PGA) and poly(D,L-lactic-co-glycolic acid) (PLGA)] are used as sutures or as orthopedic fixatives (pins, rods and screws) [209]. To date, polyesters have been widely used to produce porous scaffolds as well. As for the abovementioned materials, adjusting various properties of the scaffold including crystallinity, molecular weight and porosity, it is possible to control scaffold properties, for example degradation rate [210,211]. Among scaffold modifications, we have:

- the addition of motifs such as RGD, to improve cell adhesion,
- the inclusion of growth factors (either by supplementation of the soluble factors or by adding the cell-binding epitopes [212]
- modification of mechanical properties (i.e. porosity), to positively affect both cell motility and vascularization [213].

Although clinical use supports biocompatibility of some synthetic materials, there could be problems during degradation into small particles or due to toxicity associated with acidic degradation. Other materials including poly-lactones, polyurethanes and poly-anhydrides, were used in many others different studies [214,215].

The road to reproduce a structure as complex as the ECM is still long though, and so far, advantages of synthetic material relies mostly on their production and reproducibility.

4.1.5 ECM as a biologic scaffold

While in some cases (i.e. skin wound or abdominal wall defect) the use of TE constructs made of naturally derived and synthetic material are sufficient, when it comes to organ failure, size and the three-dimensional architecture become essential, revealing the limits of those types of construct. The maintenance of a structure as similar as possible to the original, as well as the unique molecule reservoir derived from the one present in the native ECM, make in turn acellular scaffolds an attractive option for TE applications. The idea behind the use of such supports, was that to take advantage of the organs that could potentially be used for transplantation, without the material that could give rise to rejection. Indeed, without xenogeneic cellular components, it is possible to avoid inflammatory responses and immune-mediated rejection triggered by surface antigenic epitopes and by genetic material as well. Moreover, if the three-dimensional structural complexity and functional molecules within the leftover ECM can be preserved, regeneration processes could be efficiently induced.

With this hypothesis in mind, depending on soft or hard tissue, many were the organs tested using this approach and, so far, many have demonstrated efficacy in the repair of numerous soft tissues, including urinary bladder [216], esophagus [217], liver [218], lung [219], and trachea [220]. These numerous studies have shown the ability of these scaffolds to alter the default wound healing response when implanted in a site of injury [90,102,104,221]. In fact, it was confirmed that natural derivation of scaffold components allows a rapid degradation while undergoing constructive remodeling, rather than following default fibrotic scarring pathways, also probably through the release of matricriptic molecules [196,222,223]. Moreover, even though immune cells are always highly localized at site of implantation, acellular ECM did not seem to induce an immune rejecetion so far [224–226].

In general, several factors and mechanisms can influence the host response to a biologic scaffold, including the methods to decellularize the tissue and the source tissue itself. Adequate removal of cell antigens, for example, strictly depends on decellularization efficiency, which in turn as described is a key parameter to minimize adverse inflammatory response that would result in poor remodeling outcome. [123,227]. Being our organs so different one from the other, chosen protocol will necessarily

require optimization to suit specific application. To this aim, many decellularization protocols (which will further discussed in *4.1.5.1*) were developed, resulting in different degrees of tissue structure preservation whilst removing cells [228,229]

To conclude, meshes composed of natural allogeneic or xenogeneic extracellular matrix (ECM) have already reached the clinic , and are at present commercialized and used as an alternative to abrogate the foreign body response, prevent infection, and minimize or avoid excessive fibrosis [96,230].

4.1.5.1 Decellularization protocols

As discussed above, decellularization is a procedure that, starting from human/animal organs or tissues, aims at removing all the cellular antigens whilst providing a three-dimensional structure, molecular composition and biomechanical properties resembling those of the original tissue. In order to respect these parameters the best, characteristics of the specific tissue, such as its size, cellularity, density and thickness are always taken in account each time a protocol is designed. In particular, treatments can be summarized in physical, enzymatic and chemical, according to the reagent or the method used. These however, due to each different action, are often used in combination in order to enhance decellularization, for example disrupt cell membranes to expose cell content (physical or chemical), degrade nuclear material (chemical or enzymatic) and remove the remnant components from the matrix (physical). Common examples of physical methods are mechanical agitation, freeze/thaw cycles, pressure, electroporation and sonication. The enzymes usually employed can be trypsin, collagenases or endo/exonucleases. Lastly, chemicals used range through many possibilities: alkaline/acid or hypotonic/hypertonic solutions, chelating agents such as ethylene diamine tetraacetic acid (EDTA) or ethylene glycol tetraacetic acid (EGTA), detergents such as the nonionic Triton X-100, the ionic sodium dodecyl sulfate (SDS) and sodium deoxycholate (SDC) or the zwitterionic CHAPS, Sulfobetaine-10 and -16 or tributyl phosphate (TBP) [228,231].
Treatments are essentially applied two ways though: when possible, the whole organ is exposed by perfusion via the principal vascular tree (i.e. femoral artery for the hindlimb), alternatively it is

exposed by immersion, usually in agitation to allow a better distribution of reagents. The first was proven to be an efficient method to deliver decellularizing agents to the cells, removing debris from the tissue as well. When applied to decellularize organs such as the heart [81], the lungs [82;83], the liver [84], it was efficient enough to remove almost completely cellular material while preserving the three-dimensional structure. The second method, can act efficiently more when tissues are little or with a hardly accessible vasculature (i.e. small organs from small animals, thin sections of a specific tissue). From the cell removal point of view, a decellularization protocol is considered efficient when the following conditions are met: i) leftover dsDNA is less than 50 ng per mg of ECM (dry weight), ii) this DNA is represented by fragments under 200 bp, iii) Nuclear staining or Ematoxylin and Eosin (H&E) confirm absence of integer nuclei [232]. Furthermore, since the aim of the protocol is also ultrastructure preservation, it is necessary to evaluate whether the composition and biomechanical properties of the ECM are close to the physiological. This is usually done by the means of scanning electron microscopy (SEM) or transmission electron microscopy (TEM), histological colorations specific for the recognition of ECM structures (H&E, Masson's trichrome, Elastic Van Gieson, Alcian Blue) and protein quantifications. Protein composition of the ECM in particular, can be quantified either using quantification kits, which usually take advantage of spectrophotometric detection of bound/unbound dye to a specific component (i.e. Collagen, GAG, Elastin) or, as described more recently, by mass spectrometry (ref su questo). Mechanical properties are instead usually assessed through loading/unloading experiments, evaluating the stiffness/elasticity of the sample. Comparison of each analysis result to the corresponding value of original tissue, it is possible to select which decellularization protocol is the best for the tissue of interest [229,232].

4.1.6 Scaffold storage

Other than the properties so far described for a scaffold, next step to ease and increase clinical use requires two additional features: i) the possibility of a reproducible and easy production and ii) the guarantee it will maintain its characteristics for a considerable ‘shelf life’, thereby making it suitable for commercialization [233]. For example, the leading sellers of bone (INFUSE® - Medtronic, USA)

and skin (Apligraf® - Organogenesis, USA) substitutes have a shelf life of 2 years and 15 days respectively, a considerable difference.

Since decellularized scaffold take advantage of the complex interconnection and composition that collagen, elastin fibers, proteoglycans and glycoproteins have, as well as growth factors reservoir [234], it is necessary to appropriately preserve of these components and their intermolecular connections. Failing in this may significantly affect the behaviour of scaffolds *in vivo*. Unfortunately, thus far, complexity of ECM translated into complexity of choice when considering which could be the most appropriate storage methodology [235,236].

As for many laboratory uses, to freeze the moment by storing at sub-zero temperatures has long been applied as a methodology to preserve cells and tissues for extended periods of time. As a matter of fact, it has been shown that storage of decellularized tissue at an elevated temperature or humidity is detrimental for tissue structure and stability [236,237]. Liquid nitrogen instead, with - 196 °C, does not allow for any chemical reactions to take place, as energy levels are extremely low. [with the only deterioration suggested to occur being due to DNA damage by background radiation [238,239] check]. This procedure however isn't free of dangers for the tissue, as it may be damaged during the freezing stage, either if the process occurs too slowly (i.e. solution and mechanical effects) or too rapidly (i.e. ice formation and osmotic rupture) [240]. Introduction of cryoprotective agents [241], led to a considerable change in methodologies. Dimethyl sulphoxide (DMSO), originally a cell-permeating agent, can stabilize proteins, the plasma membrane and reduce the rates of ice nucleation and crystal growth [240]. Indeed, it is the currently broadly used standard agent to control cells and allografts freezing DMSO [242,243], flanked often by isopropanol or isopenthane, two other reagents with slow cooling rates. However, concerns about osmotic damages can be ignored as decellularize scaffolds are cell-free. Indeed, so far it has been demonstrated that freezing and thawing had no effect in the mechanical characteristics of decellularized lungs [235].

Considered a compromise between room temperature and freezing, storage of samples at 4 °C in a solution supplemented with antibiotic/antimycotic (i.e. Penicillin-Streptomycin) is now a condition

that cannot be kept for more than two or three months after sample preparation, as structure and angiogenic potential of the tissue was demonstrated to negatively change throughout time [244]. Moreover, in a recent study, it was underlined the need for a sufficiently intact ECM to allow cell survival and proliferation, as well as suggesting that fragile cells might be more sensitive to changes caused by mid-long term (3 and 6 months) storage at 4°C (225 Bonenfant 2013).

Freeze-drying (i.e. FD) instead is a dehydration process used to preserve bio-materials. Briefly, after freezing, water is removed by sublimation through lowering the pressure (primary drying), followed by desorption of the unfrozen water (secondary drying).[245][245][245][245][245][245][245][245] This methodology should reduce any physic-chemical change, and it is easily reversed by water immersion [246].

4.2 Results

4.2.1 Development of mDD scaffold

Diaphragm muscle were harvested from B6 mice as described, and immersed along with the rib cage into each DET reagent. First thing, it was assessed the number of expositions to the treatment, referred to as 'cycles', necessary to achieve complete decellularization. Based on previous literature (conconi 2009), number of cycle essayed was from 1 to 4. Macroscopically, tissue reflected the decrease of cellular components throughout the cycles, becoming clearer and clearer (Fig. 4.1 A).

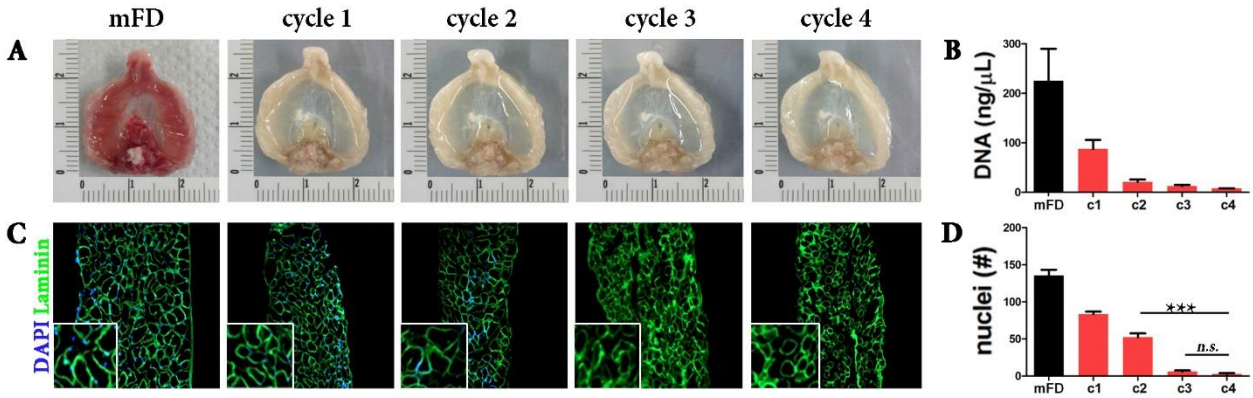

Figure 4.1 – Mouse diaphragm decellularization efficiency (Adapted from figure 1 in Piccoli et al.)

A)Macroscopic images prior and following one to four cycles of decellularization; B) DNA quantification c=cycle; C) nuclear (DAPI) and structural (laminin) staining of samples from one to four cycles; D) Nuclei quantification from at least 5 random field per tissue sample (n=3)

DNA measurement reflected macroscopic appearance of diaphragm, with an almost complete removal of DNA achieved as early as cycle 3 (Fig.4.1 B; mFD: 225.5±91.2; c1: 87.5±26.1; c2: 21±7.1; c3: 12.5±3.5; c4: 8±0.2 ng/µL), with no significant difference between 3 and 4 cycles (Fig. 4.1 B). Moreover, IF for laminin counterstained with DAPI, performed on sections from samples stopped after each cycle, allowed both to confirm the absence of cellular material (# of nuclei/field) (Fig. 4.1 C) and appreciate the maintenance of architecture (laminin structural integrity), after 3 cycles of DET (Fig. 4.1 B). Excessive exposition to decellularization reagents may result in loss of similarity with original tissue, so the less the tissue is exposed while achieving removal of nuclear antigens, the better. Hence, as similar results were achieved with 3 and 4 cycles, it was decided to set first as ideal number of DET.

4.2.1.1 Characterization of mDD

To assess the effects of DET, further characterizing the structure of the obtained mDDs, both the histological appearance and the main ECM components were evaluated. In particular, latter were first

estimated taking advantage of chemical histological colorations and then quantified using specific kits. HE, a standard methodology to evaluate histological appearance of a tissue, revealed the close similarity of mDDs with the tissue of origin (Fig. 4.2 A). Remarkably, the fibers structure was only devoid of the side nuclei, while the whole syncytium (pink cytoplasm) seemed to be still present. This was confirmed also by measuring the thickness of both, which resulted in no significance between the two conditions (Fig. 4.2 B), underlining the integrity of the structure. MT is another standard histological coloration, aimed at highlighting the connective tissue by the means of collagen (blue). Along with MT, other two standard colorations are AB, aimed at highlighting GAGs, and elastic eVG stain, which marks elastic fibers. Histologically, collagens (Fig. 4.2 C), GAGs (4.2 E) and elastin (Fig. 4.2 G) staining exhibited their preservation after 3 cycles of DET. However, while the quantification of collagen (Fig. 4.2 D) and elastin (Fig. 4.2 H) displayed no significant decrease in mDD compared to mFD, sGAG seemed to be partially lost after 3 DETs (Fig. 4.2 F; mFD: 0.57±0.05; c3: 0.30±0.13 µg/mg wet tissue).

Next, to evaluate whether similarity to FD architecture could result in similar mechanical properties or reflected sGAG loss, characterization moved on assessment of mDDs' stiffness and elastic modulus. Loading-unloading experiments (Fig. 4.3 A) to measure tensile strength and stress-strain curve, displayed a decreased stiffness (Fig. 4.3 B) along with a decreased elastic modulus (Fig. 4.3 C) in mDD, but in both cases difference compared to FD was not significant.

Through electron microscopy, it is possible to reach magnifications much higher than optical microscopy. By the means of scanning electron microscopy (SEM), it was looked deeply in the appearance of mDDs. High magnification images confirmed elimination of nuclei and allowed to better appreciate the integrity of tissue microarchitecture, which 3D arrangement was maintained alongside conservation of myofibers structure (Fig. 4.4). Interestingly, although similar to FD in these two aspects, mDDs displayed a more loosened ECM network (Fig 4.4, mDD), which may account for the flexibility displayed with mechanical testing (Fig. 4.4).

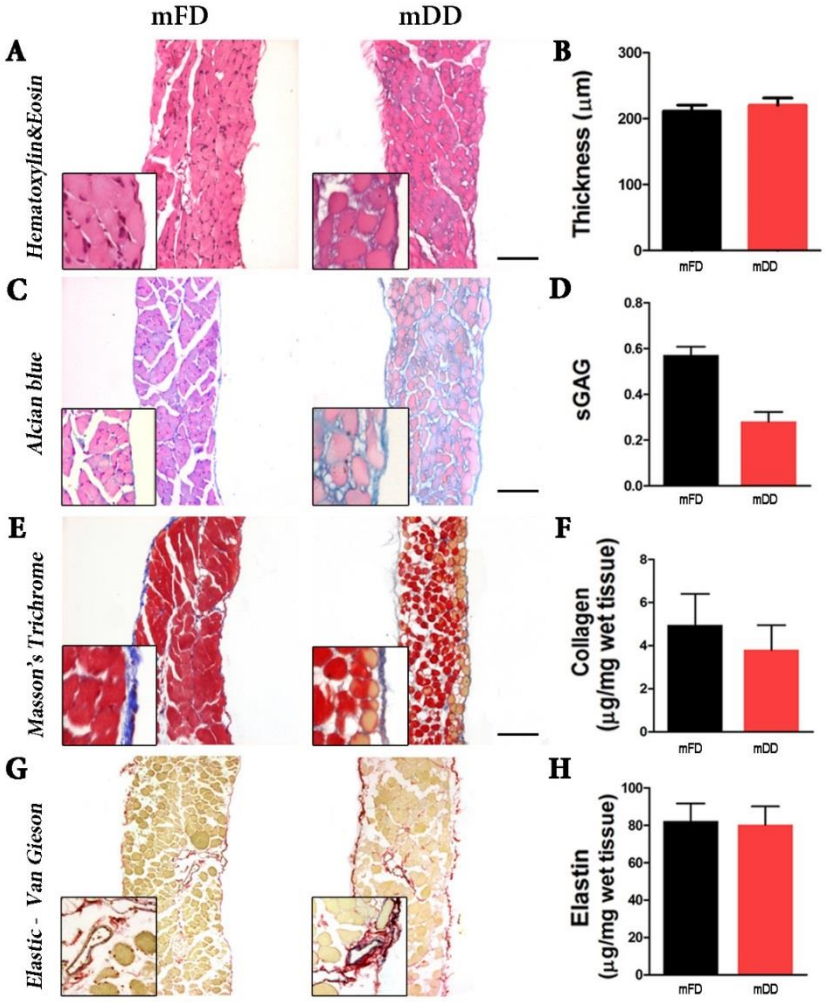

Figure 4.2. – Scaffold structure preservation compared to a mFD

A) HE staining on FD and mDD; B) Thickness measure quantified from HE; C) MT aimed at highlighting collagen fibers; D) Collagen quantified in FD and mDD samples; E) AB GAG stain; F) sGAG quantified in FD and mDD samples; G) eVG stain of elastic fibers; H) Elastin quantified in FD and mDD samples.

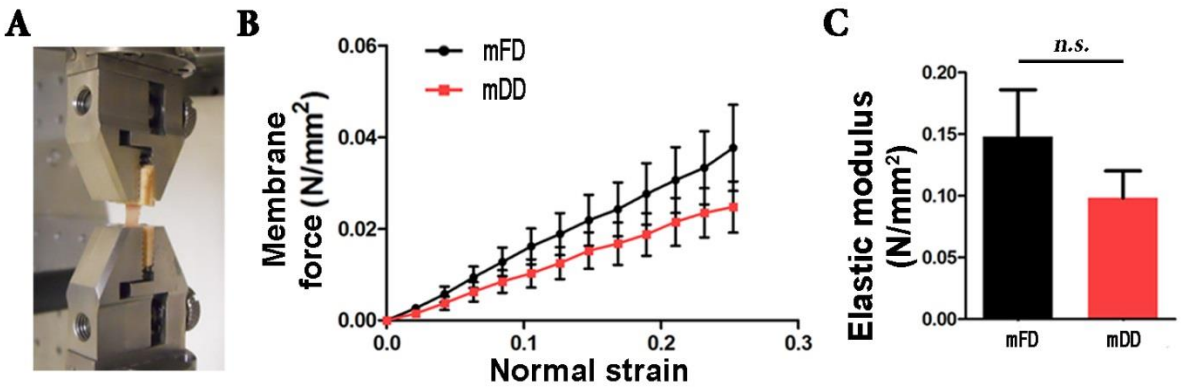

Figure 4.3 - Biomechanical characteristics and their relationship to components of the extracellular matrix

A) Exemplification of loading setting; B) Stiffness measure of FD and mDD compared C) Flexibility (elastic modulus) of mFD and mDDs

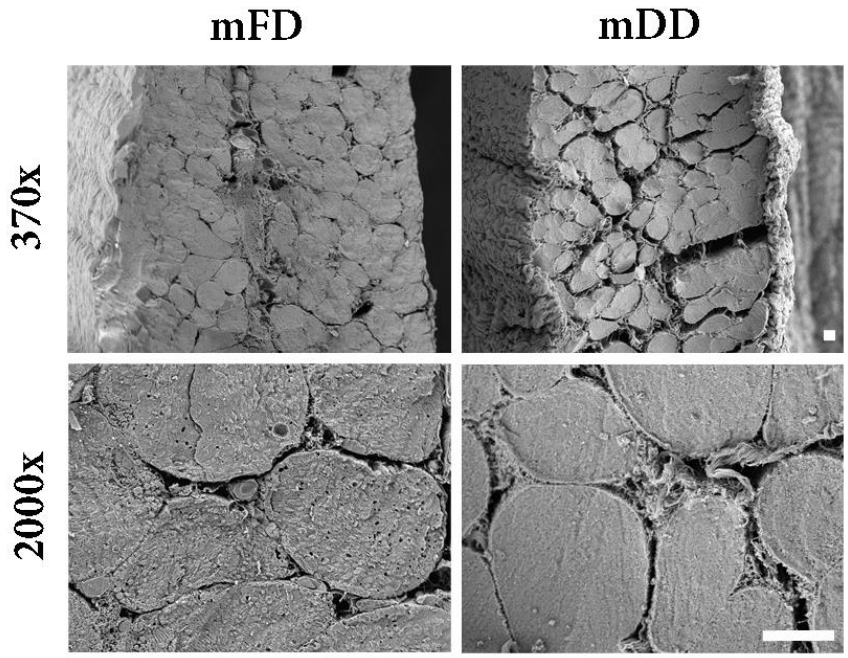

Figure 4.4 - Electron microscopy of mFD and mDD

SEM performed allow to appreciate ultrastructure similarities between mFD and mDD. Scalebar=100 μm

4.2.2 In vivo evaluation of mDD-host interactions

To reach a level II (defined by the United States Department of Health and Human services as 'Non-randomized controlled trial') in the characterization and validation of mDD as candidate for clinical applications, biological effects of mDDs were assessed by the means of orthotropic implantations in healthy diaphragms. As further step, a model of atrophy (HAS-*Cre*, $Smn^{F7/F7}$) was used. Outcomes of the implantation were then analyzed 4, 7, 15, 30 and 90 days after surgery (n≥4 for each condition and for mFD healthy or diseased controls).

Surgical procedure was carried as described in *3.11.2.*

4.2.2.1 Healthy environment

At the time of harvest, mDDs could still be distinguished from the surrounding native tissue after 4, 7 and 15 days, whereas for any further time point, the area of graft was marked only by the sutures, which during surgery were used non-absorbable for this purpose (Fig.4.5 B). Notably, throughout the time points was observed an increasing level of liver adhesion to the implanted area, which was in line with common concerns after implantations on the diaphragm (27[BrouwerKatrienM;DaamenWillekeF;ReijnenDaphne;VerstegenRuudH;LammersGerwen;HafmansTheoG;WismansRonnieG;vanKuppeveltToinH;Wijnen2013].,). However, even if it was left alone to protect the samples to be analyzed histologically or with IF (Fig. 4.5 C), liver could be detached easily using particular care, therefore it was removed in all the other samples. Hence, in any case this affected the results obtained nor introduced other types of variability.

Histological colorations (HE, MT) allowed appreciating the extent of remodeling that occurred during time, both in native diaphragm and mDD patch (Fig. 4.5 D, F). Stimulation of native tissue was such that it grew significantly in thickness between 4 and 15 days p.i., to then return to basal levels afterwards (Fig.4.5 E). This transitory modification was in line with reabsorption of the foreign tissue, which naturally occurs in a healthy environment. Indeed, while being gradually both invaded and remodeled by resident cells, patch thickness started decreasing significantly as early as 7 days, to be

almost completely disappeared after 90 days (Fig. 4.5 D, F, G). IF for Ki67 confirmed active state and proliferation of migrated cells, as soon after implant number of +ve cells increased significantly (Fig. 4.5 H, I 4 days). As for native thickness, this process reverted towards physiological state during time (Fig. 4.5 I, 90 days).

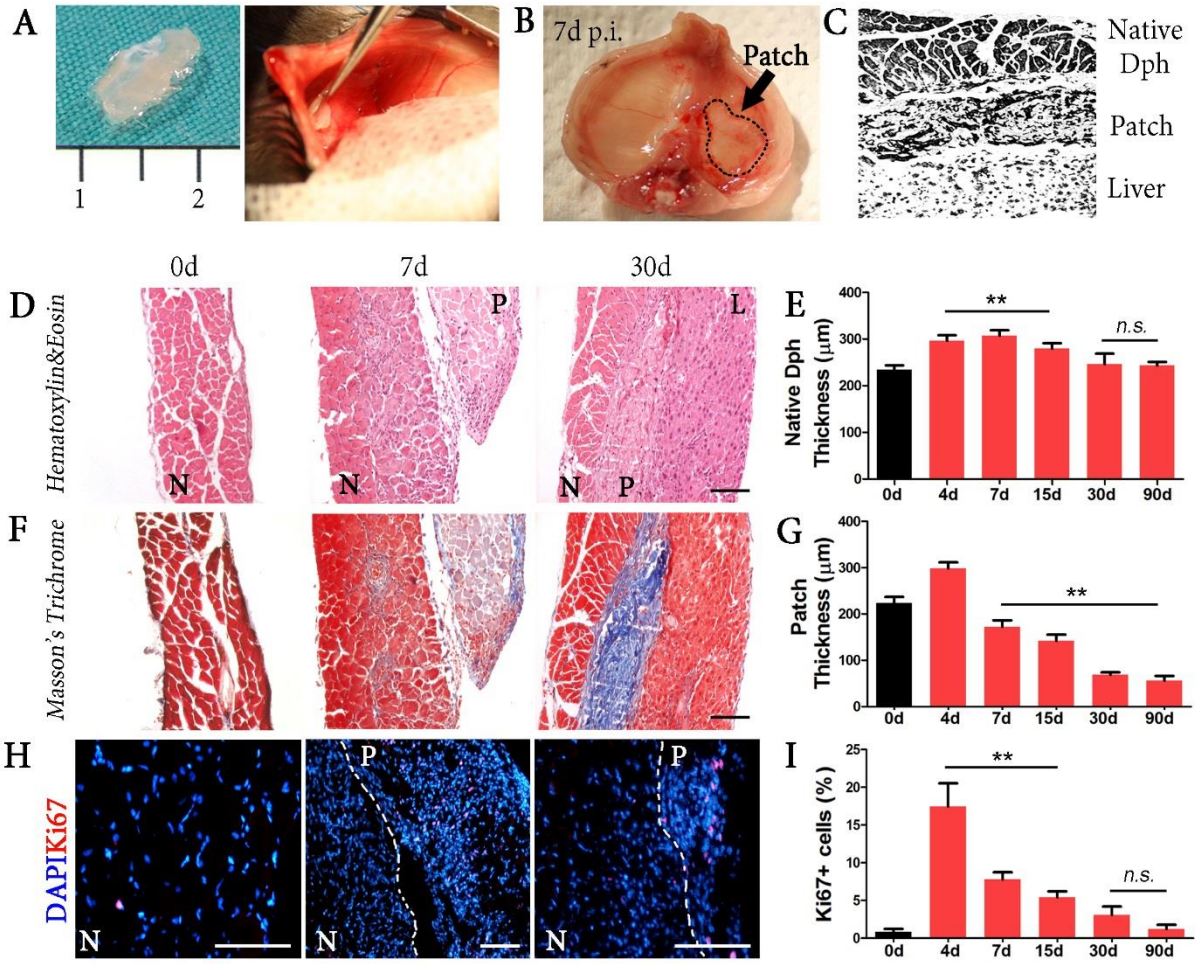

Figure 4.5 (Adapted from figure 2 of Piccoli et al 2015)

Macroscopic appearance and host-scaffold behavior (A) mDD patch before and after implantation; (B) Diaphragm harvested 7 days p.i.; (C) Scheme of samples assembly p.i.; (D, F) HE and MT performed on samples 0, 7, 30 and 90 days p.i; (E) Host diaphragm thickness progression throughout all the time points; (G) mDD reabsorption throughout time; (H–I) IF and quantification of proliferating $Ki67^{+}$ cells. Native Dph = host diaphragm, N = native tissue, P = patch, L = liver. **p < .01; n.s. = not significant by ANOVA and Student t-test. Scale bar = 100 μm

As thickening of the native diaphragm did not reflected cross sectional area (CSA), it was supposed that mDD implantation elicited rather a hyperplasic than a hypertrophic effect (Fig.4.6 A, B). Indeed, growth seemed to derive from newly formed fibers, as revealed by embryonic myosin heavy chain (Myh3) positive fibers in the native diaphragm, located in the region close to the patch at the earliest time points (Fig.4.6 E,F). This was confirmed also by the peak of Myh3 gene expression rate after 4 days, compared to physiological levels, thus emphasizing the triggering effect of applied acellular matrix (Fig. 4.6 I). As further validation, center nucleated fibers were clearly present throughout all the time points (Fig. 4.6 A). Interestingly, the expression of the myogenic precursor marker Myf5 was detectable only between day 7 and 30 p.i.. In this case, +ve cells were located mostly in the acellular matrix until the latter time point, indicating that the massive activation and proliferation of SCs occurred earlier was turned off (Fig.4.6 C, D). Analogously to Myh3, activation of myogenic population was also supported by the levels of gene expression of both Myf5 and Myogenin, between 4 and 15 days after treatment. In general, the decrease towards physiological levels found in all analyses was in line with the hypothesized switching off the regenerating process.

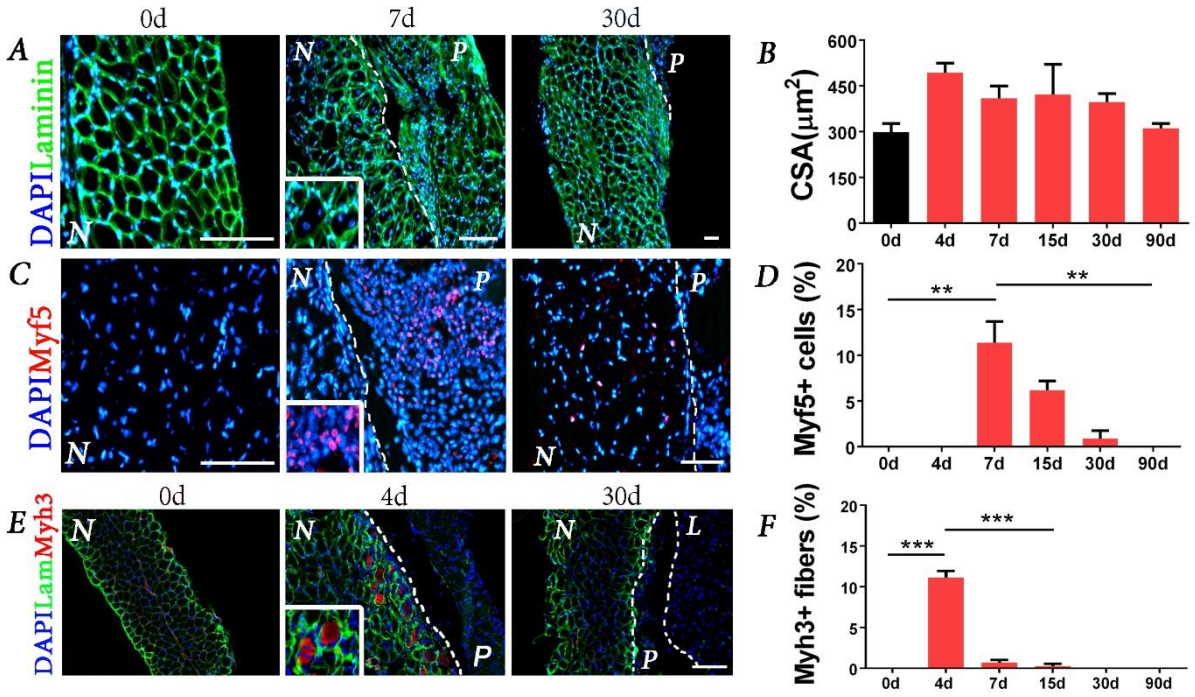

Figure 4.6 (Adapted from figure 3 and supplementary figure 1 in Piccoli et al 2015)

Myogenic effect on host cells. (A) Exemplification of host diaphragm growth response displayed by laminin IF; (B) Quantification of fiber cross sectional area measured at all time points; (C, E) Exemplification of host myogenic response displayed by IF; (D, F) count (% of cells) of $Myf5^{+}$ cells and $Myh3^{+}$ fibers through the time points; (G-I) qPCR displaying expression of *Myf55*,*Myogenin* and *Myh3* at all time points. CSA=Cross sectional area, N = native tissue, P = patch, L = liver. **p < .01; ***p < .001 by ANOVA and Student t-test; scalebar = 100 μm.

Coherently with other studies on decellularized matrices, mDD implantation was associated with a significantly increased presence of CD3 and CD4 expressing cells, particularly within the fraction of FoxP3+ cells. Myogenic cells likewise, both of the cell types followed a timing-dependent trend, peaking at 7 days p.i. to then lower in numbers until basal level was reached (Fig. 4.7 A, B, C). Alongside, cells of the innate immunity were found inside the mDD, as well as in the neighbouring area (CD68+ cells; Fig. 4.7 F). Notably, after an initial balance in the polarization state, these cells shifted towards an M2 fate over the M1, as shown by Arginase I expression, both at protein and gene level (Fig. 4.7 D-I). This data was corroborated by the calculated M1:M2 ratio (Fig. 4.7 G, J).

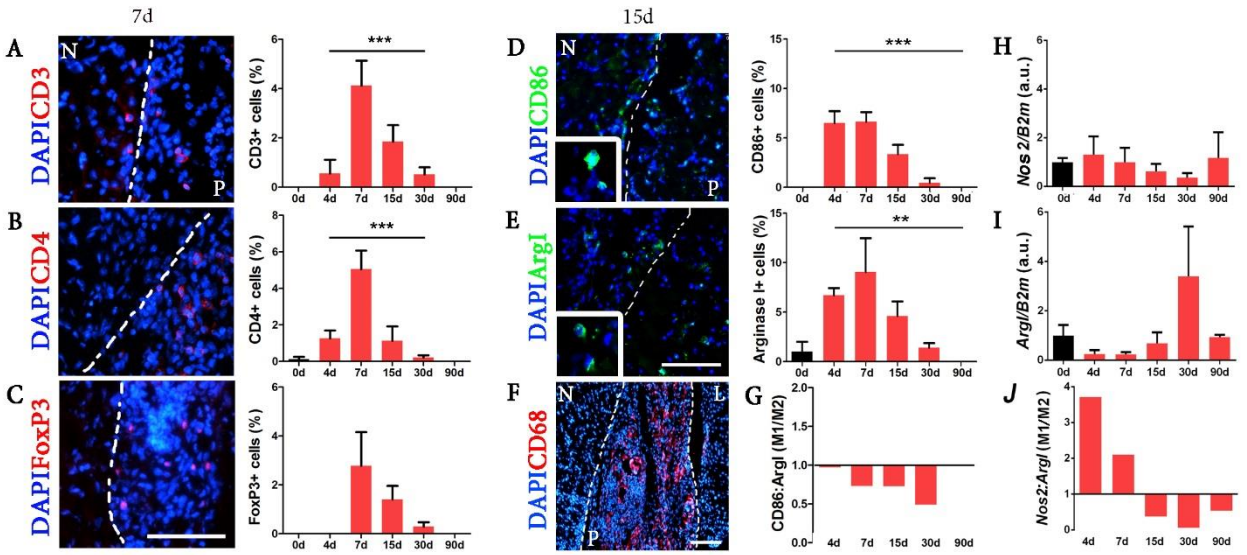

Figure 4.7 (Adapted from figure 4 in Piccoli et al. 2015)

Innate and adaptive immune response (A–C) Representative IF (7 days p.i.) and quantification of $CD3^+$, $CD4^+$ and $FoxP3^+$ through time; (D–E) IF and quantification of $CD86^+$ (M1) and Arginase I^+ (M2) macrophages; (F) IF for pan-macrophages CD68; (G) Ratio between M1/M2 polarized macrophages calculated on the basis of CD86/ArgI expression; (H–I) Gene expression of Nos2 (M1) and Arginase I (M2) in treated diaphragms throughout the time points. B2m was used as housekeeping gene; (J) Ratio between Nos2/ArgI expression. N = native tissue, P = patch, L = liver. **p < .01; ***p < .001; n.s. = not significant by ANOVA test. Scalebar = 100 μm.

4.2.2.2 Diseased environment

Given the outcomes of the implantation in a healthy environment, the next step was to confirm the anti-inflammation and pro-regenerative effects also in a diseased environment. Histological analyses showed comparable cell invasion and matrix remodeling as in healthy mice (Fig. 4.8 A), however, unlike previous results, overall thickness of atrophic diaphragm gradually increased during the time points, to a measure close to a normal mouse diaphragm (Fig. 4.8 B). In addition, stimulatory effect seemed delayed and, in the analyzed interval, did not resulted in a reestablishment of basal level.

Kinetics of patch reabsorption were comparable to healthy implant instead (Fig. 4.8 C, D). Combination of a healthy-derived mDD with the atrophic diaphragm also resulted in an amelioration of the rib cage as well as both lung morphology and area, 30 days p.i., endorsing the idea of mDD acting as a support rather than representing a burden (Fig. 4.8 E, F). Nevertheless, since deformation of the chest is a consequence of the atrophy and not of a pulmonary dysfunction, it was not surprising to see any difference in pulmonary volume compared to an untreated animal. Mechanical tests performed on implanted diaphragms unveiled an amelioration in the flexibility as well. Indeed, while after 30 days after implantation the tissue had a deformation ability comparable to native condition, elastic modulus decreased significantly ($P<0.05$, Fig. 4.8 F). Moreover, internal comparison of treated side with non-treated side of same diaphragm (i.e. contralateral side, CL) 90 days after implantation, highlighted that thickening of implanted area was due to hyperplasia (Fig. 4.8 G, Fiber/Width), as in case of healthy diaphragm.

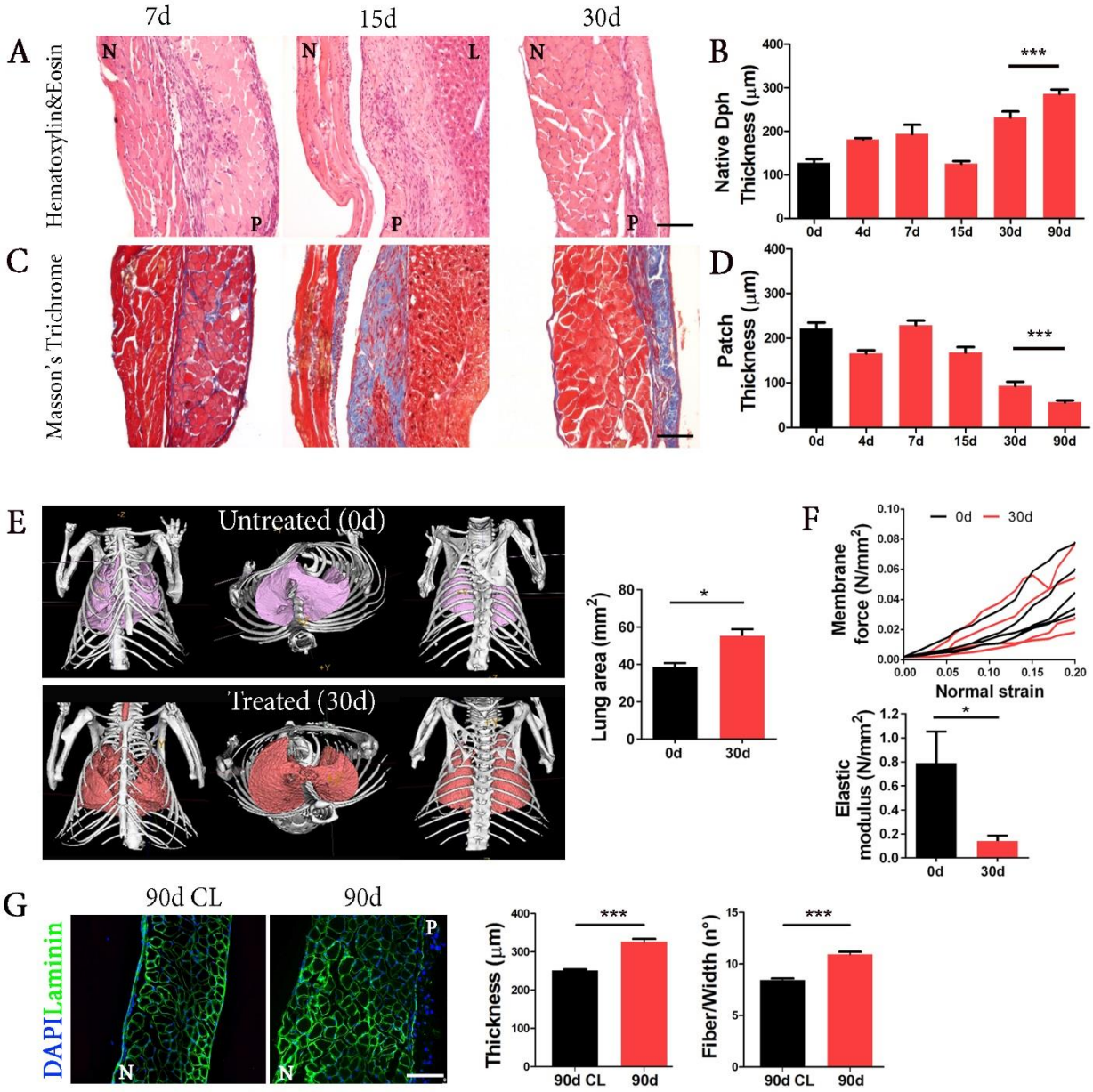

Figure 4.8 (Adapted from figure 5 of Piccoli M. et al)

Atrophic implantation outcomes. (A, C) Histological appearance of treated diaphragms 7, 15, 30 and 90 days p.i.; (B, D). Atrophic diaphragm growth in thickness and mDD reabsorption through all the time points; (E, F) CT scan and lung area of baseline atrophic condition (0d) and treated 30 days p.i. ; (G) Mechanical properties of baseline atrophic condition (0d) and treated atrophic diaphragms 30 days p.i. ; (H) Confirmation of topical hyperplasia effect by comparison of mDD treated and non-treated contralateral (CL) side 90d p.i. by the means of thickness and fibers number. N = native tissue, P = patch, L = liver. *p < .05; ***p < .001 by Student t-test; scalebar = 100 µm.

As expected, overall CSA of stimulated diaphragm was not significantly different to the atrophic basal condition (Fig. 4.9 A). However, the higher distribution between small and mid-size fibers at the early time points (Fig. 4.9 B) reflected the up-regulation of Myh3 both at gene and protein expression, mimicking the situation found in healthy mice implantations (Fig. 4.9 C). Confirming our hypothesis of a delayed but prolonged effect, cell activation and proliferation was lower but lasted longer than previous experiments. Indeed, Ki67+ cells presence was significantly higher until 90 days post-implantation (Fig. 4.9 D). Expression of MyoD (as alernative marker for myogenic precursors) trended similarly, with enhanced number of ve+ cells after 4 days, decreasing through time but still lasting after 90 days (Fig. 4.9 G). Interestingly, mRNA levels of Myogenin behaved differently, decreasing to level even lower than basal condition, a situation that may reflect the amelioration of defected muscle though, as mDD stimulation might have supplied to the continue demand for regeneration this model has (Fig. 4.9 H). Another feature of this model is a basal inflammatory state, which may be the cause of the slightly different response seen when comparing healthy and diseased macrophage polarization. Indeed, unlike in healthy environment, CD86+ (M1) macrophages were already detectable in untreated diaphragms (Fig. 4.9 E, DAPI-CD86). Additionally, as displayed by gene expression, after an initial effect, macrophage shift towards the M2 polarization (quantified by the means of ArgI) seemed to require more time to take place (Fig. 4.9 F). This behavior added up to the one seen for the other measures, strengthening the hypothesis of still a pro-regenerative and anti-inflammation effect of the implanted mDD, just delayed but lasting longer compared to healthy state.

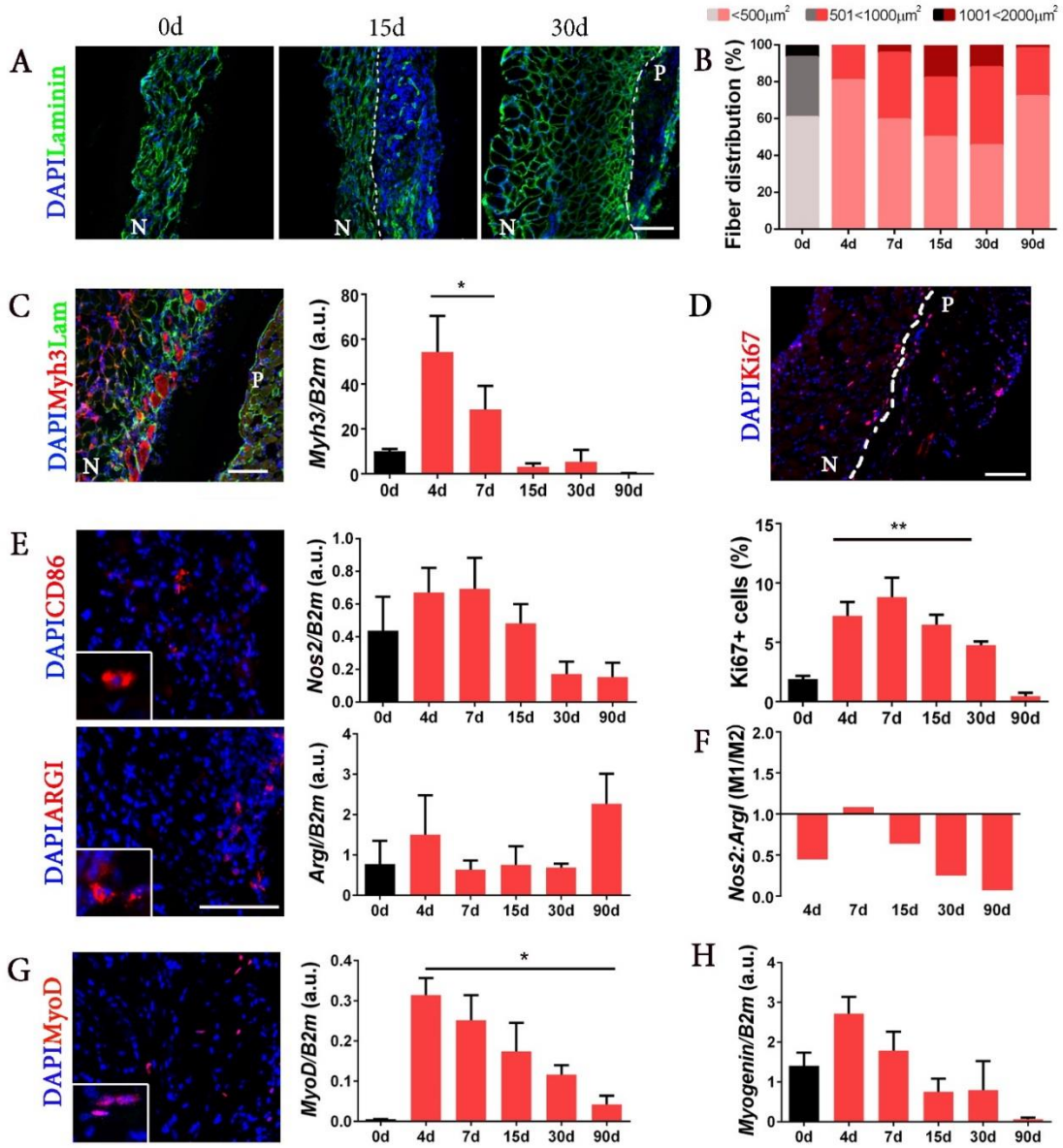

Figure 4.9 (Adapted from figure 6 of Piccoli M. et al)

Cellular response upon implantation in the atrophic diaphragm. (A) Exemplification of muscle appearance *via* IF for Laminin; (B) Fiber CSA distribution during pre (0d) and p.i. (4-90d); (C) Representative IF (4 days) and quantification of *Myh3* expression at all time points; (D, E) Representative IF (7 days) and quantification of proliferating Ki67^{+} cells; (F) IF and qPCR of M1 (CD86 and *Nos2*) and M2 (*Arginase I*) polarization state at the different time points; (G) Ratio between M1/M2 macrophages, on the basis of *Nos2*/*ArgI* expression; (H) IF and qPCR of MyoD^{+} precursor cells at all time points. (I) qPCR quantification of *Myogenin* through time points; B2m was used as housekeeping gene. N = native tissue, P = patch, L = liver. *p < .05; **p < .01 by ANOVA test; scalebar = 100 μm.

4.2.3 Development of a rDD scaffold

Diaphragm muscle were harvested from New Zealand rabbits as described, along with the surrounding rib cage, then washed in PBS 1X before beginning of DET. Likewise mDDs, it was necessary to first determine the number of cycles needed to achieve complete decellularization. Based on number of cycle set for the mouse, this time 5 to 8 cycles were tested. Interestingly, progression of decellularization mirrored what saw in mice both macroscopically (Fig. 4.10 A) and microscopically. Indeed, leftover DNA amount trended similarly, with a significant decrease as early as 5 cycles, which apparently stabilized after the 6^{th} (Fig 4.11 C, E; rFD: 150.6 ± 12.78; cycle 5: 84.61 ± 4.325; cycle 6: 34.12 ± 5.661; cycle 7: 26.40 ± 1.243; cycle 8: 17.05 ± 5.699 ng/µL). Moreover, the appearance of laminin-DAPI IF, confirmed the tendency seen before: the maintenance of structural integrity whilst obtaining cell removal through cycles of DET (Fig. 4.11 B, D). Notably, albeit DNA quantification of 6 cycles resulted no significantly different to 7 and 8, presence of DAPI stained nuclear material could still be detected by IF. Considering this, besides the notion of reducing the number of cycles to the best balance between decellularization and structure preservation, the cycles chosen for further analyses were 7.

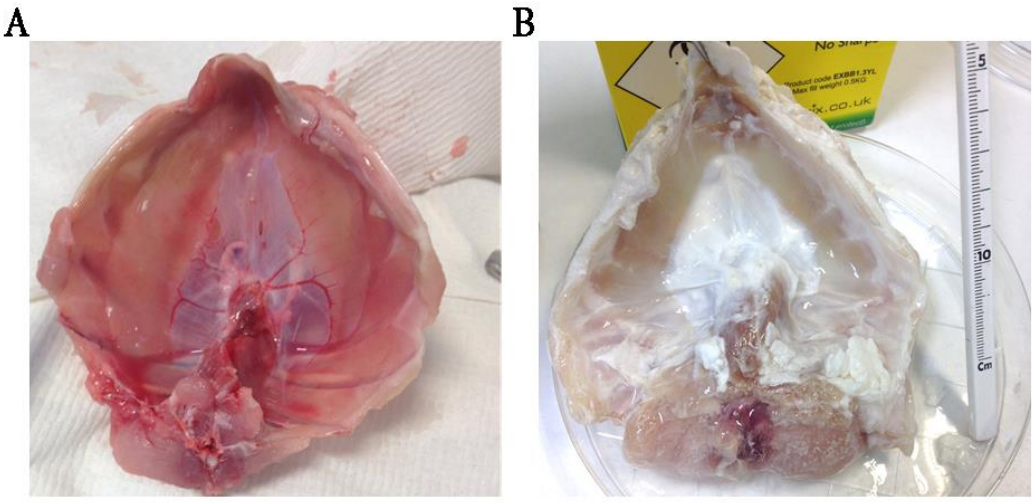

Figure 4.10 - Decellularization of rabbit diaphragm

Macroscopic images prior (A) and following (B) seven cycles cycles of decellularization.

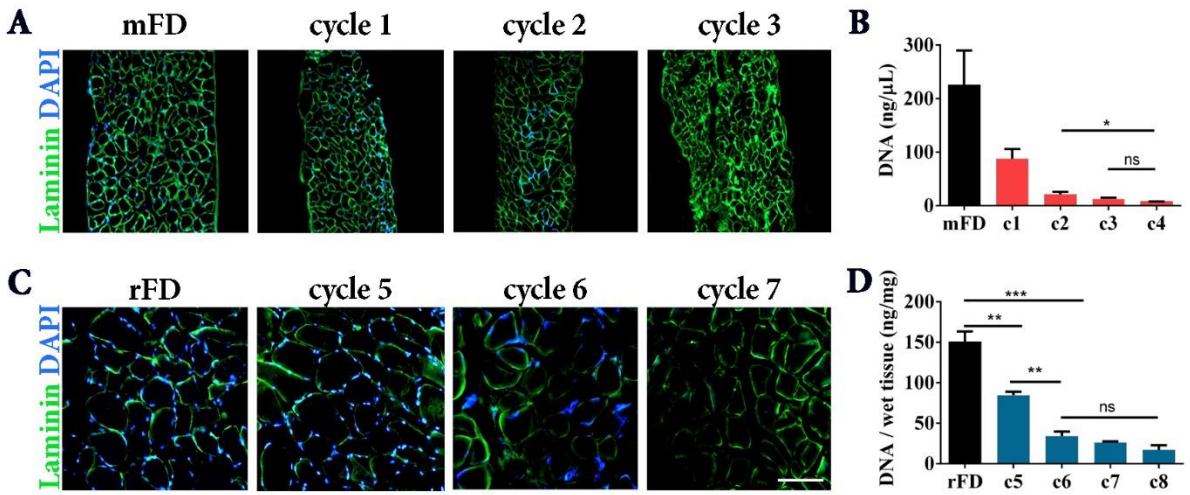

Figure 4.11 – Comparison between mouse and rabbit decellularization

Progression of rabbit diaphragm decellularization went coherently to mouse result. A, C) IF of tissues decellularized through DET cycles to discriminate remaining $DAPI^{+}$ nuclei from tissue structure (laminin); C, D) DNA quantification (c=cycle); scalebar=100 µ

4.2.3.1 Characterization of decellularized structure.

Also for rDDs, HE proved the high level of similarity DET allows to obtain, even after 7 cycles of treatment. (ipotetica Fig. 4.12 A). About the ECM components, although only macroscopically, MT coloration the maintenance of the connective tissue of the scaffold (Fig. 4.12 B). In line with the other two histological colorations, GAG marked by AB appeared preserved (Fig. 4.12 C). Based on results with mDDs, it was expected a variation only for sGAG, therefore these were the only ECM components that were effectively quantified thus far. However, surprisingly, the quantity of sGAG in the rDDs seemed to be more concentrated (Fig. 4.12 D; rFD: 2.584 ± 0.4508; rDD: 7.029 ± 1.219). Tissue architecture preservation was evaluated using SEM, which as for the mDDs allowed to appreciate the decellularization (hollow round pockets on fibers side) and the tissue similarity to the rFD not exposed to DET (Fig. 4.13.

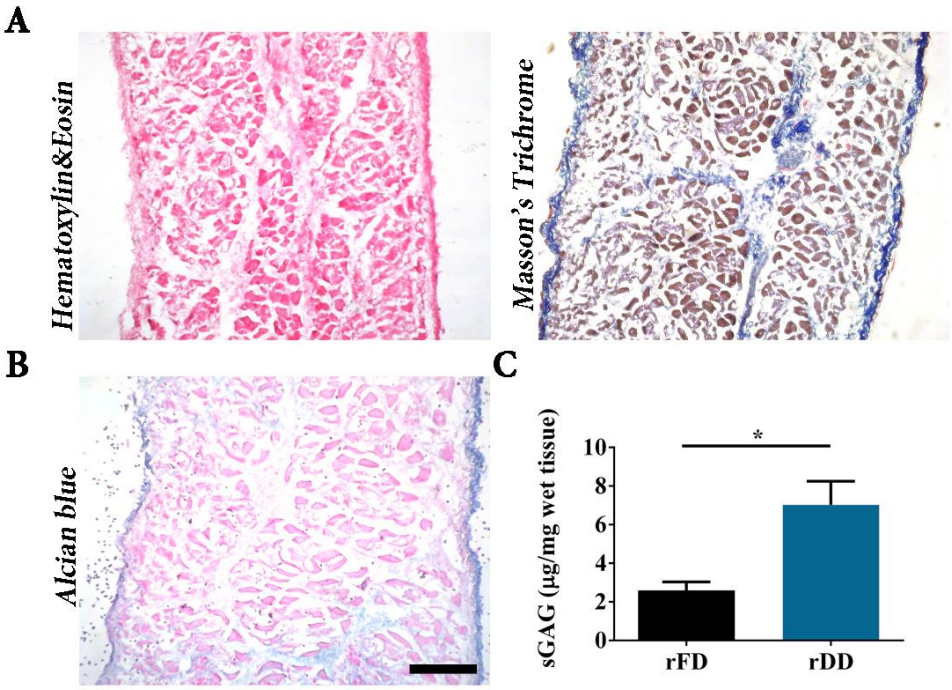

Figure 4.12- rDD structure compared to FD rabbit diaphragm.

Oveview developed rDD ECM. A) H-E staining and: Masson's Trichrome of developed rDD; B) Alcian blue for sGAG and C) quantification of the ECM component (rFD=2.584±0.45, rDD=7.029±1.219 µg/mg wet tissue) Scale=200µm

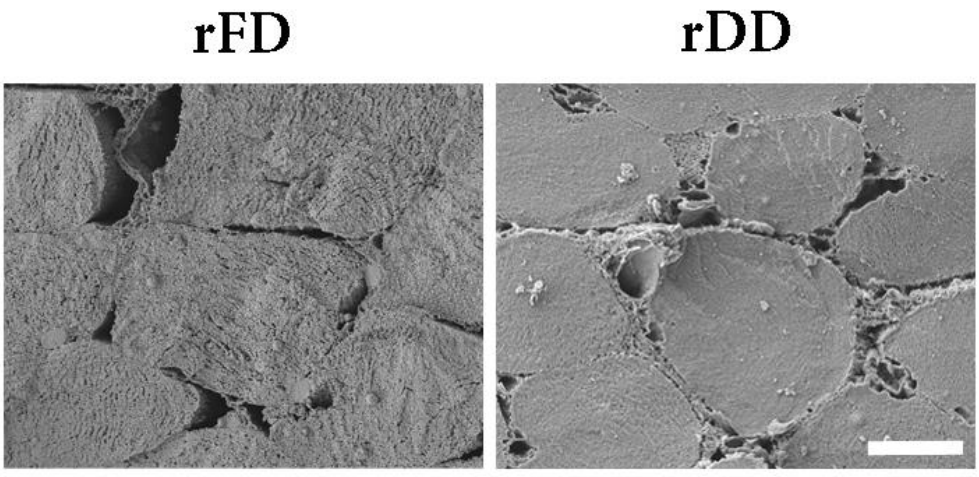

Figure 4.13 - Electron microscopy of mFD and mDD

SEM performed allow to appreciate ultrastructure similarities between mFD and mDD. Scalebar=100 µm

4.3 Discussion

4.3.1 Scaffold development

Advances achieved thus far in the field of TE permitted to translate into clinic some of the promises held since it arising from regenerative medicine. Indeed, at least from the scaffolding point of view, several products, from both xeno and allogeneic origin, were already commercialized [123] while others, both alone or cell seeded, are actually in clinical use (bladder, urethra and trachea[220,247,248]). This however, was a level reached only by simple structure organs/tissue. In this respect, organs with a higher modular complexity, such as the heart, lung, and liver [249–251], are still undergoing pre-clinical studies, as well as skeletal muscle [50,151]. In particular, even though the structure and the features of the latter have been broadly studied [27], the reproduction of such complex organization still represent one of the major challenges when trying to develop a functional skeletal muscle, though just recently, steps forward this aim were done [56,91]. In general, as the muscle has a well-known innate regeneration potential [47], the need of implantation/transplantation over a simple repair is determined by the size and kind of the muscle defect, thus influencing SMTE priorities. Indeed, the higher demand is represented by VML (or even by amputation as the ultimate aim), thus most of the studies focus on the repair of large volumes of muscle [252]. Following in line are defects such as abdominal wall and diaphragmatic hernia, which instead require a wider surface and a thinner width, depending on the type of defect [114,253]. In both cases, the easier the construct is obtained the better, thus further influencing the main elements in TE: cellular component and scaffold [12]. With this aim, starting with a structure that closely resembles the original tissue, passed from option to reality quite quickly, as soon as decellularization of organs and tissues was achieved [254].

To date, advantages of these type of scaffolds are established, and have been used in both experimental SMTE approaches and in clinical settings [50]. However, as mentioned above, only few studies have focused on the creation of a muscle-derived decellularized scaffold for implantation/transplantation of flat muscle, and, so far, none from the mouse.

Considering this, it was firstly evaluated the possibility to obtain a decellularized scaffold derived from mouse diaphragm, taking advantage of its pre-structured flat organization. By further adapting the established protocol developed by Meezan et al. [161], which was readapted by [109], it was possible to achieve complete removal of cellular material whilst maintaining a structure close to the original. Indeed, i) amount of residual DNA reduced by 95%, ii) length of this leftover material lower than 200bp along with iii) the absence of visible DAPI stained nuclei, after 3 cycles of DET, were in line with the proposed criteria for a successful decellularization [232]. Consequently, these were considered the ideal number of cycles for a complete depletion of antigens, which quantiy/presence is known to be one of the features influencing outcomes *in vivo* [227]. Ultrastructural and histological analyses, by the means of SEM and histological colorations, confirmed that 3 cycles of DET could yield a scaffold with an architecture closely resembling a healthy mouse diaphragm. To further confirm that ECM composition was not only preserved macroscopically, but also proportionally, the main components of the scaffolding structure were quantified. Both collagen and elastin sustained the treatment quite well, whereas sGAG proportion diminished. This however, is a feature common to the organs and tissues decellularized via DET. SEM on the other hand allowed to appreciate in detail the similarity between the muscle before and after treatment, with only a difference in tightness of ECM, which may be the consequence of both GAG loss. This in turn may have reflected on mechanical properties, since the scaffold had a slightly higher flexibility and lower stiffness, which anyway did not resulted significantly different. Mechanical properties, particularly in the muscle, were highlighted during the last decade as features of extreme importance, able to significantly impact on cell behaviour [178,255,256], hence the similarity found was a highly desirable outcome as well.

4.3.2 *In vivo* behaviour

TE efforts are aimed at the delivery of a construct, which finally results in both integration and restoration of functionality, by the means of constructive remodelling. In this respect, it is necessary to validate at pre-clinical level not only the cellular component features, but also the behaviour of each scaffold, upon implantation in a viable recipient. Moreover, among the in vivo levels of evidence, the one validated in large animals is the closer to clinical application, while usually testing in small animals represent the level before. Considering this, going by steps after first level of evidence *in vitro*, decellularized matrices (mDDs) were implanted *in vivo*, first in a healthy environment, then, to further validate results seen with the first setting, in an atrophic mouse model.

*Healthy environment.*In line with previous results [90,118], mDDs presence led to changes in the recipient muscle, as a result of a well-known cascade of events ranging from absorption to ECM remodelling, driven mainly by the modulatory effects on the immune system these types of scaffold were demonstrated to have [221]. Precisely, mDD was able to induce a local shift in the balance between macrophage polarization state through time, from M1 towards M2, a population that is commonly associated to pro-regenerative events [257]. Moreover, transitory hyperplasia observed in the recipient muscle (restored to normal thickness after 90 days), as result of the stimuli on muscle stem and progenitor cells, was a clear sign of the ECM influence more from the regeneration side rather than simply representing a foreign body burdening the muscle. Indeed, across the timepoint CSA of the fibers did not increase, while amount of fibers present increased, excluding a compensatory hypertrophy [122]. These data were further confirmed by the presence of Myh3+ (a marker of neo fibers [258], mostly at the interface with the implanted mDD. During time, as expected from biological scaffolds [55,259], mDDs were increasingly remodelled and reabsorbed, displaying another desirable feature (bio-degradability). This however, must be carefully tested, because a reabsorption occurring too rapidly can lead to an insufficient stimulation, in case of large defect.

The cellular response raised by the scaffold attracted a remarkable percentage of invading cells, a feature known to biological scaffolds, which are able to release upon remodelling, factors that can attract recipient cells [223,260]. This, was highlighted by muscle specific marker Myf5, which could

be detected in the interval between 7 and 30 days after surgery . These were stimulated not only to grow and migrate into the mDD, but also to further differentiate and fuse into myotubes, which merged generating young, new fibers. Nevertheless, the main population found in the transplanted scaffold was represented by immune cells. This was no surprise, since it is well established that innate immunity cells, followed by adaptive immunity cells, are the population that is firstly recruited to the implantation site, whatever its composition [226,261]. During muscle regeneration, interaction between immune cells and myogenic cells was more than once proven to be essential, as impairment or depletion of the first, resulted in uneffective regeneration processes [123]. Precisely, inflammation is indeed one of the steps necessary for regeneration [47,262]. Considering this, correct manipulation of these interactions can lead to enhancement of muscle regeneration. Indeed, macrophages display a broad spectrum of phenotypes which are easily inducible in non-polarized cells, by the means of either molecular [263] or topographic cues [264], thus making possible to deploy the balance between inflammation and regeneration. In the mDD-implanted context, both IF and molecular biology analyses confirmed the shift rapidly induced by the scaffold, which seemed to favour the polarization towards M2 (pro-regenerative) as early as 4 days after surgery. Interestingly, the cells of the adaptive immunity, which as expected displayed a timely related migration after monocytes, underlined the lack of cytotoxicity by presence of type 2 T lymphocytes [265].

Diseased environment Any muscle specific disease leading to an impaired functionality of the muscle, namely myopathy, can extend from the peripheral to internal, thus affecting the diaphragm as well. This, as well as diaphragm specific diseases such as congenital diaphragmatic hernias, results in an additional significant impairment of life quality, or, in worst cases, to death. With the outcomes of a healthy environment in mind, it was decided to test the behaviour of both scaffold and recipient in a diseased context, to evaluate whether the scaffold could lead to an improved condition of the diaphragm, by triggering a comparable regeneration response. Precisely, the model chosen was a SMA mimicking model, the HSA-*Cre*, $Smn^{F7/F7}$, which displays an atrophic phenotype due to the SMN depletion restricted solely to skeletal muscles.

Remarkably, the hypothesized positive effects were macroscopically visible 30 days after surgery, as CT scan performed on these animals displayed that an amelioration of both the chest anatomy and lung area occurred. Additionally, improvements the mechanical properties were detected, as elastic modulus of diseased diaphragm improved to a value similar to the calculated in healthy mice.

This mouse model is characterized by a chronic inflammatory condition, which is consequence of the constant attempts the muscle does to revert the atrophy induced by depletion of SMN [266]. Hence, it was surprising to see that mDD effects, despite basal polarization towards M1 derived from the abovementioned situation, were such that could induce a polarization toward M2 also in this setting. Indeed, the proportion between Nos2 and Arginase I gene expression favoured the second. Moreover, the amount of adaptive immune CD4+FoxP3+ cells seemed even increased compared to what seen before, suggesting higher transplant acceptance [267].

Healthy environment likewise, the implantation of mDD elicited a hyperplasic response, which resulted in an increase in thickness of the recipient diaphragm. However, although similar the effect did not seemed transient, but appeared to be increasing through the analysed interval instead (0-90 days). Indeed, at the further time point, measured thickness reached the range of a normal diaphragm. Hyperplasic response, was confirmed by the mean of myogenic precursor commitment (MyoD protein and mRNA) and maturation (Myh3 protein and mRNA). While precursors detection trended coherently with the thickness measure, being still detectable after 90 days, formation of fibers peaked 4 days after surgery, to then decrease under basal level. This data however has not to be considered negative, since as described, the muscle of these mice is subdued to a chronic degeneration-regeneration (depicted by the basal level of mRNA in the control). Actually, on the contrary the absence of newly forming fibers could be a supplementary clue of the recipient muscle amelioration. Previous studies already demonstrated the presence of products derived from ECM remodelling, which used to condition culture medium, are able to elicit a M2-like polarization in macrophages *in vitro* [268]. Although yet not completely defined, an obvious consequence of the huge variety and difference intra and inter organs that were decellularized thus far, it is known that the ECM is physiologically a reservoir of cytokines and products resulting from its degradation during remodelling. Nonetheless, several works, including the present study (*chapter 5*), tried to quantify or

define which of the reservoir molecules remains within the scaffold after decellularization . What was certainly confirmed is that the DET, allowed the yield of a biochemically active scaffold, effective enough to stimulate multiple responses, directed towards the constructive remodelling, both in a healthy and diseased environment. Moreover, it seemed that in the atrophic model, the mDD scaffold was able to supply to the recipient muscle sustained regeneration demand, whereas being not necessary in the healthy muscle, latter simply tended to normal conditions.

Interestingly, there may be a correlation between the transitory or prolonged effects, hinted by expression of the myogenic marker Myf5 and MyoD: it appeared that a mutual exclusion of Myf5 over MyoD occurred in the healthy, whereas the contrary happened in the SMA model. Hence, while indicating that between the two models the myogenic pathway was activated differently, the comparable result (i.e. local hickening due to muscle fibers generation) supported the concept of these two transcription factors compensating one another during development, but maintaining simultaneously distinct and specific functions [269].

Though not fitting the typical definition of TE, the elicited effects observed in both scaffold-only settings, make this, as well as other decellularized matrices obtained via DET, a potential tool for several applications. These, can vary from the simple analysis of cell-ECM behaviour *in vitro*, a potentially useful tool when applied in the cancer research [270,271], to cell delivery, promoting the regeneration in small defects or ultimately the creation of a functional muscle construct. Moreover, although not being a cellular therapy, thereby not being able to restore any genetic effect, decellularized matrices may hold promises also as candidates for muscle diseases as a temporary treatment.

4.3.3 Preliminary characterization of rabbit-derived scaffold

Next step in pre-clinical evaluation, as described in the previous section, is to test the sample material (either cells or scaffold) in large animals, which can be rabbit, dogs, or non-human primates (ref?). With this aim, it was chose to test the smallest of large animal, the rabbit, thus deciding to develop an autologous decellularized scaffold, since the mDD could not cover the size gap. In this case, it is

important to underline that a decellularized scaffold, derived from rabbit diaphragm using a DET, was already developed and tested *in vivo* [55,109]. Nevertheless, in any case a complete characterization of the scaffold was displayed, nor there were further attempts.

Rabbit diaphragms underwent the same testing performed for the mouse, in order to set the best condition to develop a rabbit decellularized diaphragm (rDD) scaffold. Again, the re-adapted DET was applied, but being the tissue bigger than the previously tested, number of cycles was increased accordingly. Efficiency in depleting cells from cycle 5 to 8 were analysed, pursuing the best condition to meet the previous quoted criteria, necessary for a biomaterial to be considered as adequate [232]. Once ideal number of cycle was set, rDDs thus derived were characterized by the means of structural integrity, via both histological coloration and SEM. Outcome of the analyses allowed to determine 7 DET cycles as the election methodology to obtain a rDD successfully. This can be considered a step further in the development of an autologous tissue, aimed at the repair of flat muscle defect, even of large size, considered the surface of the rabbit diaphragm. Additionally, as adaption of the protocol resulted in a proportional result, further scaling up of the protocol can be considered possible, making more steps toward clinical approval and use.

Chapter 5 Angiogenetic properties of diaphragm derived acellular matrix

5.1 Introduction

5.1.1 Vasculogenesis and angiogenesis

Besides diploblastic animals, which develop only from ecto and endoderm, all other animals have a mesoderm as well (triploblastic), developing throughout the evolution more and more complex organs. Among these, vertebrates (as well as some invertebrates), developed a way to transport nutrient and oxygen to the whole body, namely the cardiovascular system. Crucial for the life and growth of the living being, it is indeed the first functional organ to form within the developing vertebrate embryo. The cardiovascular system comprises i) the heart (cardio), pumping ii) the blood to the whole body via iii) the blood vessels (vascular system). These are then further distinguished between venous and arterial circulatory network [272].

The formation of a new blood vessel from a primitive stem cell is called 'vasculogenesis'. During development, a endothelial cells (EC) form epithelial tubes from a luminized rudimentary vascular meshwork, which is then remodeled into specialized subtypes (including arteries, veins, lymphatics and capillaries),organizes through pruning and anastomotic growth, to finally become stabilized through the recruitment of mural cells. While embryo is growing, vascular system expands concomitantly by sprouting and proliferating from the pre exhisting network, to guarantee an adequate supply of nutrients and oxygen. This second type of vessel formation, which after the embryo development becomes the main process to form new blood vessels, takes the name of 'angiogenesis'. Moreover, pivotal role of this system is also due to molecular interactions with the others, as it is known to participate in regulation of tissue morphogenesis as well [273]. For these processes to occur, an extremely fine orchestration is required, therefore the amount of signaling pathways that act to coordinate the establishment and maintenance of the vascular system is not surprising [274,275].

Considering this plethora of fine-tuned interactions, any perturbation of any of these nodes can have an impact on the entire circuit, leading to a failure of normal embryo development, or, in the live born, several types of diseases.

5.1.1.1 Stimuli driving angiogenesis

Circumstances that lead to angiogenesis are various, but can be generally summarized as four different environmental origins: i) developmental (after embryo vasculogenesis), ii) exercise-induced, iii) tissue repair and iv) tumour growth. [276,277]. Although these four have commonalities and divergences in the angiogenesis milieus and the resultant vascular networks, whichever the cause the tissue signals to the existing vasculature that there is a need for new blood vessels. This trigger is usually a distress situation, resulting from mechanical, metabolic or hypoxic stimuli [278], sensed primarily by the endothelium. Examples of such are chronic hypoxia due to abnormal tissue growth (tumour), vascular occlusion (tissue repair) or increased metabolic rates (exercise-induction). Indeed, during exercise, muscle contractions lead to increased shear stress in the microcirculation (by deforming vascular bed) and to increased mechanical strain in the muscle fibres themselves, both events known to induce the release of pro-angiogenic factors [279]. Following are summarized the thus far established angiogenesis stimuli.

Blood flow Linked to angiogenesis since long, it was demonstrated that blood velocity regulates both capillary growth and regression. While trying to model vasculature physics, its network structure was linked to tissue oxygenation as well. Rise of new technologies allowed the study of blood flow with computational models with increasing accuracy, recognizing the many different parameters of the microcirculation (diameter, flow rate, shear stress and ultimately oxygen exchange), which influence plasticity and remodeling (i.e. angiogenesis, adaption of vessel wall) of the vascular system. To summarize, type of angiogenic response can be dictated by the flow, usually with the aim to maximize oxygen delivery [280].

Hypoxia Besides reduction of blood flow, namely *ischaemia*, alterations in oxygen supply to the tissues can be also due to other causes. For example, respiratory dysfunctions or diseases involving red blood

cell (anaemia) can result in hypoxic condition [281]. Effectors of angiogenesis mediated by hypoxia are usually molecules able to activate or regulate pathways cascades, ultimately resulting in blood vessel growth. Two well-known examples are nitric oxide (NO) and hypoxia-inducible transcription factors (HIFs). The first, requires oxygen to be produced by NO synthases (eNOS, nNOS, iNOS), which then acts as inhibitory feedback to avoid excessive consumption. This balance was postulated to be connected to the Fahraeus effect, which in turn result most significant in the vessels that usually give rise to new sprouts (diameter <30 lm) [282]. NO was also shown to be involved in tumour growth and metastasis, as it promotes both vascular permeability and EC proliferation and migration [283]. Increased shear stress also promotes nitric oxide production, as seen with skeletal muscle contraction, highlighting a commonality between chemical and mechanical pathways for sprouting angiogenesis [284]. HIFs are in turn stabilized by decrease of oxygen tension, and can then act as transcription factors for vascular endothelial growth factor (VEGF) and its receptors (VEGFRs), which are the principal actors in pro-angiogenic molecular mechanisms. Among the isoforms of HIFs, the best studied is HIF-1, which is structured in an oxygen-sensitive subunit, HIF-1a, and a constitutively active subunit HIF-1b/ARNT. While oxygen induces degradation of HIF-1a, hypoxia allows HIF- 1a to remain stable. This allows translocation in the nucleus and binding to HIF-1b, then further binding to hypoxia response elements in VEGF and VEGFR genes [285].

Inflammation Occurring both during tissue healing and tumour growth, it is well established that the innate immunity cells, including macrophages, monocytes and progenitor cells, produce factors which mediate the growth of new blood vessels [286]. While the wound healing is a process that naturally feedbacks to restore normal quantity of immune cells and factors in the tissue, tumour progression often results in reiteration of the stimulation. . Many were the studies in this field as well, trying to recapitulate and understand both successful or unsuccessful wound repair[287], also confirming linkage between different stimuli.

Molecular pathways activated by these conditions, were largely studied and can be examined in depth elsewhere [274,288,289].

5.1.2 Vasculature significancy in TE

Due to the crucial role that blood supply has for the functionality and the normal physiology of human body, the ability to stimulate and control angiogenesis has a significant impact for a wide range of clinical applications. In TE in particular, the aim is the successful repair of a variety of damaged or diseased organs, which in turn rely on survival and integration of the implant. Hence, among other features, the angiogenesis potential and in the correct anastomization of the grafted compound are essential. Since TE arose, approaches aiming at stimulating the host vasculature were several, but they can be summarized in three types: i) in situ vascularization, ii) cell-mediated angiogenesis and iii) pre vascularization. These are further described in the following subsections.

5.1.2.1 In situ vascularization

Not a complete TE approach compared to other two, *in situ* vascularization aims at stimulating angiogenesis in the host by using cell-free naturally-derived or synthetic scaffolds, functionalized to a bioactive state by adding proteins known to be involved in angiogenesis (i.e. growth factors or chemotactic molecules). To this aim, acellular scaffolds could be a step in front of the others, since their unique reservoir of molecules can enhance the angiogenesis stimuli. However, to date simplicity of the approach reflected on the outcomes: although it was found in different studies a certain degree of growth of blood vessels in the scaffold and/or in the surrounding area, relying on the hosts cells solely resulted in a limitation in case of less porous materials or depending on the size of the defect. Hence, this approach is more indicated to assay angiogeneic potentiality of a scaffold ore in case of small defects. [290]

5.1.2.2 Cell-mediated angiogenesis

Angiogenesis can be achieved by combining the previous approach (or each type of scaffold in general) with a cell population able either to differentiate into blood vessels or to stimulate angiogenesis in a paracrine fashion. This cell-mediated angiogenesis is an *in situ* approach as well, with the addition of cells to the scaffold occurring concomitantly or right before the implant. An example of cell population broadly used and well known to have many paracrine effects are MSCs, which in many occasions proven a good choice for graft survival and tissue vascularization [291]. While resulting in better outcomes, compared to the ones obtained using a scaffold-only approach, this approach might still have limitation connected to nature of the defect. If the defect is such that purpose of implantation is helping regeneration through also boosting of pro angiogeneic stimuli (f.eg. skin wound, small or mid-size ulcers), then this approach may be sufficient. Else, in case of transplantation of large portions of tissues or whole organs, the time required for vascularization of the construct, even if boosted, might not be sufficient.

5.1.2.3 Pre-vascularization

Lastly, there is the creation of a functional vascular network before implantation, namely pre-vascularization. The hypothesis behind this approach is corroborated by current surgical approaches both in case of orthotropic (normal transplant) and heterotopic (i.e. a body part to be kept vital) implant. Indeed, both surgical and implant-induced anastomosis of the host with the pre-existing vasculature of the organ/body part allows the tissue to rapidly introduce nutrients and oxygen, permitting its survival. Several approaches can be used to obtain a pre-vascularized construct, but all require cells able to recreate angiogenesis in vitro, usually ECs (i.e. human umbilical vein endothelial cells, HUVECs) or progenitors able to differentiate into this and other vascular populations. Elected cells can be then scaffold directed, using for example a pre patterned structure [292], or by self-assembly, stimulated via pro-angiogenic molecules [213]. On top of these, angiogenesis enhancement or other biological aspects of the construct (i.e. formation of muscular tissue) can be pursued by

adding another cell population (i.e. MSCs or Myoblasts respectively) [92]. While representing the methodology closest to the concept and the aims of TE, ideal to apply in case of substitution of entire organs or large portion of tissue, results this way are still far from flawlessness. Although were many the developed approaches, the time required to form a pre-existing vasculature, the mechanisms to be controlled or the subsequent correct anastomosis with the host, are just some of the many aspects that must be further analyzed.

5.1.3 Default response after implant involves angiogenesis

The implantation of a foreign device of any type, from synthetic or acellular biomaterials to even living tissue constructs, result always in its interactions with native cells, immunological and inflammatory responses. Host immune response can also be exacerbated or elicited if additional injury is caused (i.e. surgical implantation). In general, the events following implantation of anything that does not belong originally to the body, are reunited under the name of foreign body response (or reaction, FBR) [293]. The understanding of how the components of TE construct interact at the site of implantation (i.e. molecular mechanisms; structural or mechanical stimuli) is essential to make eventual modifications towards increased efficiency of the approach. Indeed, ultimate approach would be the one not only avoiding any adverse effects of the host response, but also harnessing FBR and enhancing host tissue regeneration. The FBR takes place as a well-known sequence of events, which are following briefly described.

i) The implanted biomaterial is rapidly covered with proteins from the surrounding tissue and blood (i.e. Factor XII, complement C3, IgG, fibronectin), namely the Vroman effect [294]. ii) Concomitantly, local distressed cells of the host release signals, which add up to recruit granulocytes (also known as polymorphonuclear leukocytes PMNs). These cells then secrete factors to recruit and activate other immune cells (i.e. monocyte chemoattractant protein 1, MCP-1; interleukin 8, IL-8) and release degranulation products (i.e. proteolytic enzymes and ROS). iii) Site of implantation becomes infiltrated with other inflammatory cells, mainly monocytes that differentiate into macrophages and further polarize towards pro (M1) or anti-inflammatory types (M2) (ref su

macrophages?). Before polarizing, macrophages usually secrete inflammatory cytokines (i.e. tumor necrosis factor-a, TNF-a; interleukin-6, IL-6), and again MCP-1, to induce further recruit immune cells. It is important to underline that to date a link between material properties and polarization of macrophages has been established, as these cells will either predominantly express one of the two states depending on the implanted device. iv) Whether of M1 or M2 type, factors released by macrophages are critical to the formation of granulation tissue, which is formed by recruited fibroblasts, secreting and forming new ECM, and newly formed blood vessels. Indeed, unbalance between the two types can result in the impairment of the regeneration process. For example, if secreted factors stimulate excessively fibroblast recruitment or collagen deposition, the regeneration will shift to fibrosis [295,296]. Moreover, a biomaterial difficult to degrade, often lead to formation of foreign body giant cells (FBGCs), which can secrete ROS, proteases or acids, resulting in highly degradative environment. Thus, these cells are often used as marker of unsuccessful outcome. v) As last step in the cascade of events of FBR, dendritic cells (DCs) can be activated by pattern recognition receptor (PRR) engagement with the released or digested material. These in turn, as antigen presenting cells (APCs), are able to activate cytotoxic T-cells and promote helper T cell responses (Th1, Th2, Th17, or Treg)

Together with resident cells, recruited cells of the immune system are responsible for removing foreign material, resorbing cell debris and necrotic tissue and to a significant extent for the initiation of angiogenesis and extracellular matrix deposition. Although mechanisms of these latter roles are still being defined, it is clear that immune cells play a critical role in regulating wound healing, particularly in controlling neovascularization, as demonstrated in several studies [261]. However, as currently cause-effect has yet to be demonstrated, knowledge on the topic has not gone beyond the correlation with M1/M2 paradigm. Because angiogenesis is as complex as it is our immune system, both being not completely understood, it is clear that further investigation is needed.

To conclude, on top of the features that directly involve both vascularization and angiogenetic stimuli driven by the TE construct, it is worth taking in account the FRB machinery as well. Aiming at this, acellular matrix scaffold represent ideal candidates, proven to both retain pro-angiogenetic properties and to be able to immune modulate host response [105,221,297]

5.2 Results

5.2.1 Diaphragm-derived decellularized matrix retains angiogenic potential

Patches cut from decellularized diaphragm, positive and negative controls were and placed on the CAM, an established in vivo system to evaluate angiogenesis towards or inside a specimen. After placement, samples and controls were analyzed daily under a stereomicroscope. Diaphragm matrices were found to be adherent to the CAM, which vessels started to surround the samples, growing towards the tissues just after 24h. At day 7 after implantation, matrices were completely wrapped by the CAM and the vessels were organized in a network surrounding the tissue samples (Fig. 5.1 A). Vessel growth, by the means of number of blood vessels converging towards the specimen, was quantified after 7 days in a blinded fashion. The number of allantoic vessels converging towards the acellular matrices was increased significantly ($P < 0.05$), compared to both negative and positive controls at the same time-point (Fig. 5.1 B).

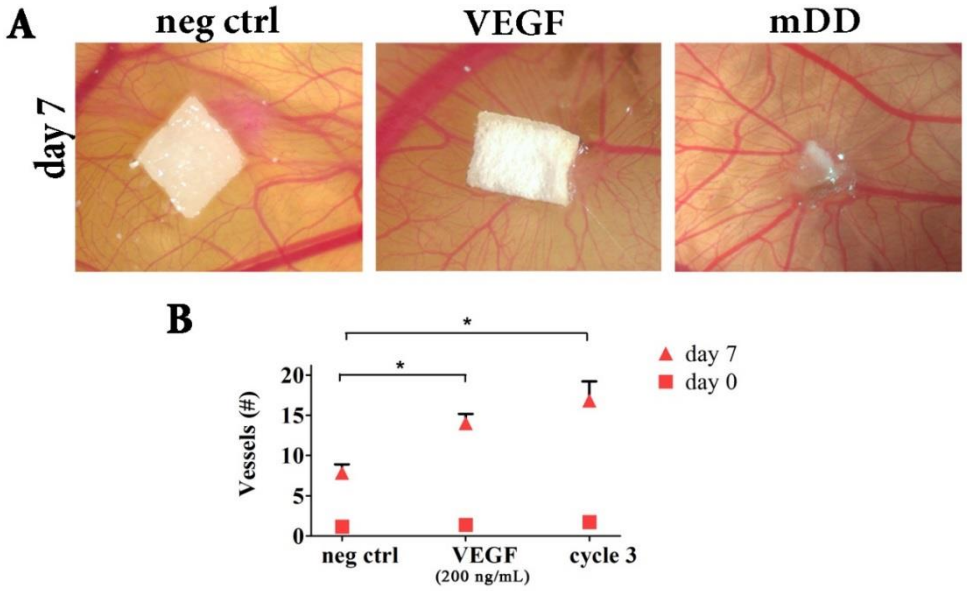

Figure 5.1 CAM assay performed on fertilized eggs outcomes

Representation of CAM assay. A) Appearance of samples after 7 days placed onto the chorioallantoic membrane; B) Quantification of the vessels converging or contacting the sample as result of a blinded count.

To both confirm results saw in CAM assay and to verify whether the matrix retained anything connected to the pro-angiogenic potential displayed, an array of 53 proteins involved in mouse angiogenesis was used. As in the membranes developed after western blot (WB), each spot intensity correlates with protein amount. The presence of several spots (Fig5.2 A), even though all reduced at different rates, revealed that most of the analysed proteins were still present in the decellularized tissue, from specific angiogeneic cytokines (i.e. VEGF or Angiopoietins) to matrikines or enzymes necessary for endothelialisation (as Endothelin or metalloproteases) (Fig.5.2 B). Next, the levels of four cytokines considered important for both angiogenesis and skeletal muscle were quantified via ELISA tests. Besides EGF (1.292 ± 0.216 pg/mg in healthy diaphragm), the amount of the other three cytokines could be measured also in the decellularized tissue. VEGF was reduced from 0.580 ± 0.06 pg/mg in mFD to 0.068 ± 0.02 pg/mg in the decellularised scaffold, SDF-1 was reduced from 2.432 ± 0.204 pg/mg in mFD to 0.642 ± 0.13 pg/mg in the decellularised scaffold and HGF was reduced from 1.939 ± 0.02 pg/mg in mFD to 0.003 ± 0.0001 pg/mg in the decellularised scaffold (Fig. 5.3 A-D).

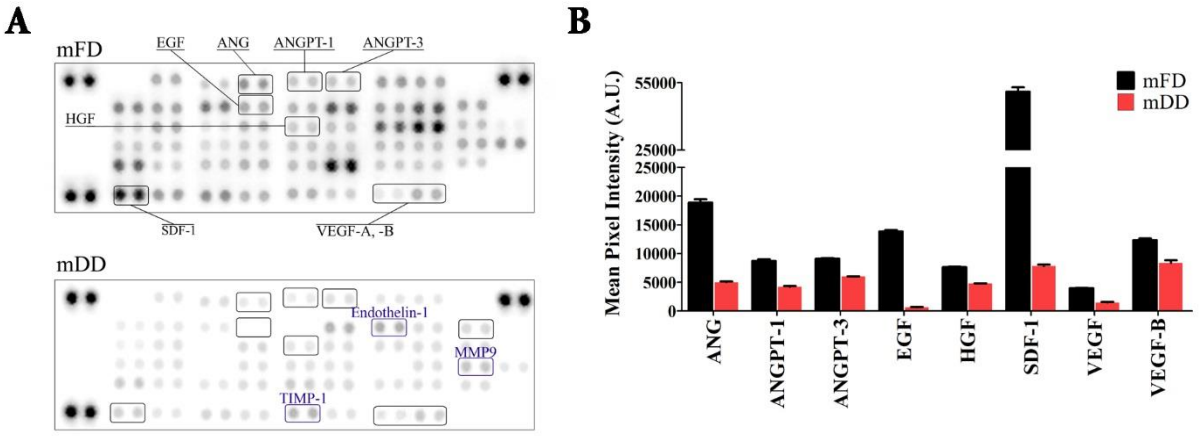

Figure 5.2 Proteome mouse angiogenesis array

Preservation of several proteins after DET. A) Membrane spots developed from mFD and mDD samples, underlining the preservation of proteins important for the ECM-Angiogenesis interaction; B) Pixel intensity of the highlighted spots (from mFD in A) compared to mDD. EGF=Epidermal growth factor, HGF=Hepatocyte growth factor, SDF-1=Stromal derived factor 1, ANG=Angiogenin, ANGPT-1 and -

3=Angiopoietin-1 and 3, VEGF-A,-B= Vascular endothelial growth factor-A and B, TIMP-1=Tissue inhibitor of metalloproteases 1, MMP9=Metalloprotease 9.

Although ELISA is usually considered a method more accurate, principle of protein array is basically the same, just different in the development phase. It was then hypothesized that, accounting for the lack of detection of EFG in the mDD samples, could be just the different antibody type.

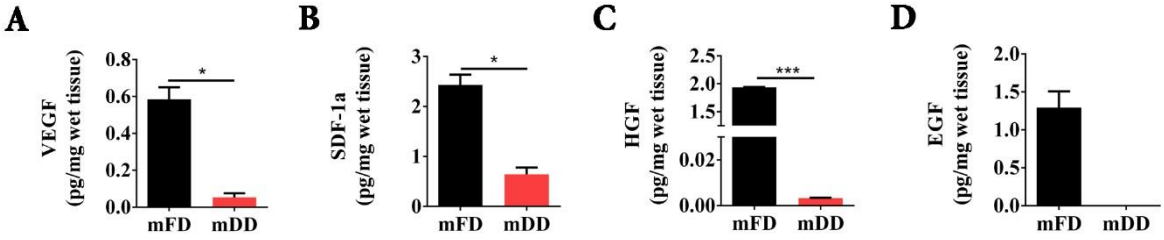

Figure 5.3 ELISA quantification of four cytokines involved in both muscle repair and angiogenesis.

Quantification performed on patches of mDD and equal amount of mFD. A-D) VEGF, SDF-1, HGF and EGF leftover in mDD compared to mFD.

5.2.2 Cell-scaffold interaction

ECM patches implanted in the subcutaneous space on the back of GFP+ mice could still be well distinguished both after 7 and 15 days and, in line with CAM assay results, appeared vascularized (Fig.5.4 A). Immunofluoresce performed on the excised samples revealed the presence of SMA+ vessels of different appereance at the earliest timepoint, while after 15 days majority of the individuated vessels had a similar shape (Fig.5.4 C). The amount of haemoglobin quantified on the harvested patches (mettere valori), corroborated the previous data on functional graft vascularization (Fig. 5.4 B).

As it is known that DET allows a vessels integrity such that they can be still detected via immunolabeling of SMA (Fig 5.5 A), it was not surprising to find abovementioned structures in the

scaffolds after 7 days, while as expected they were not detected after 15 days. In the earliest time point SMA+ vessels were found to be contacted and seemed to be repopulated by host cells. Confirming that these structures could be recognized by endothelial cells, HUVECs seeded on top of the decellularized matrix had migrated towards the pre-existing vessels after 48h (Fig5.5 B).

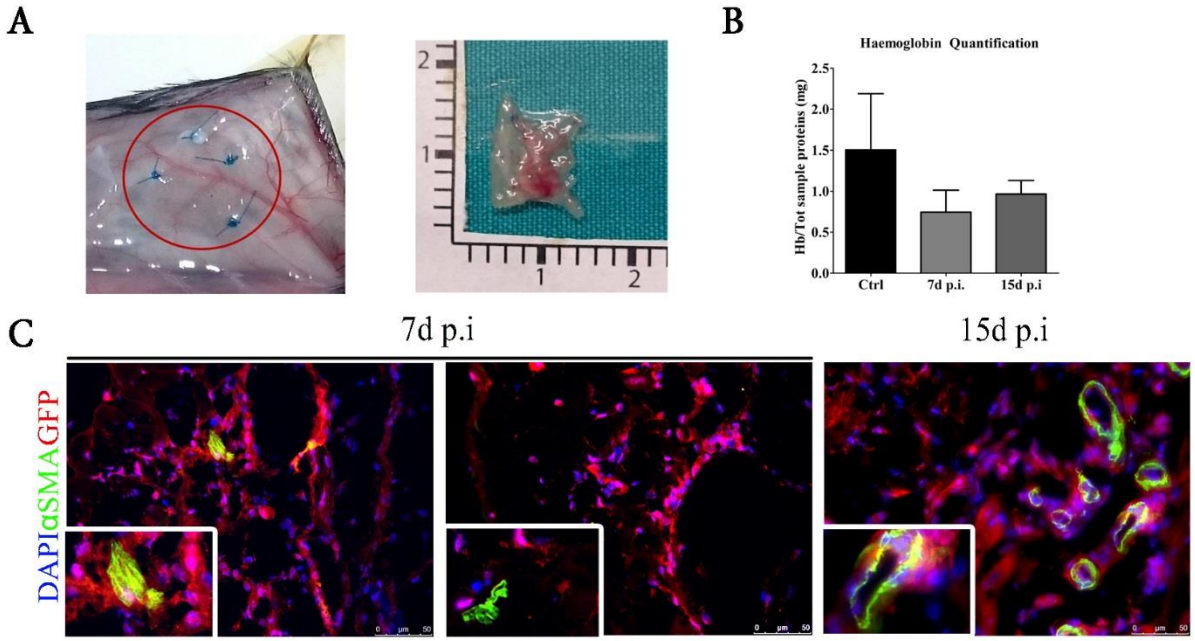

Figure 5.4 Subcutaneous transplant outcomes

SC implants in GFP mice reproduced what seen in CAM A) Macroscopic appearance pre and p.i. ; B) Haemoglobin quantification of explanted mDDs compared to a skin control; C) IF performed on explanted mDD to evaluate GFP^+ cells interaction in the mDD 7 and 15 p.i.

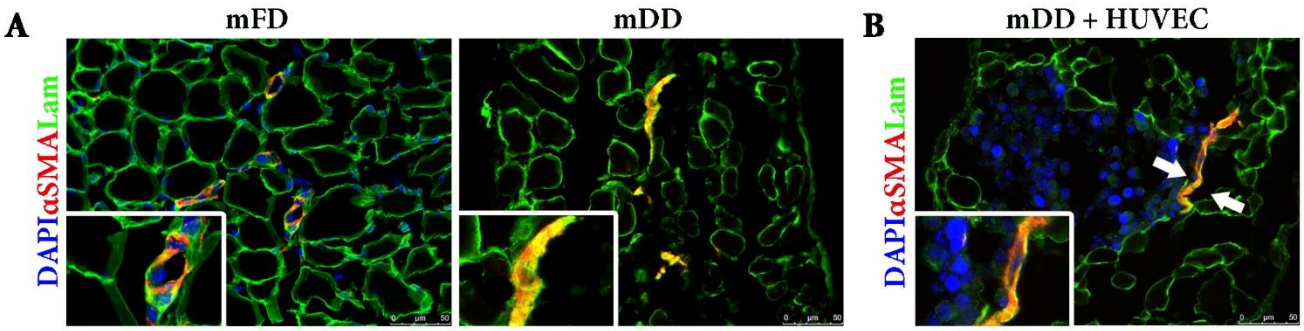

Figure 5.5 Vessels preserve their *tunica media* and can be recognized by HUVEC

SMA^+ vessels but DAPI or GFP^- saw in SC implants are the mFD vessel preserved after DET. A) Comparison of vessel in mFD and after decellularization performed via SMA-Lam IF; B) Seeded HUVECs could be found after 48h to be in contact with the vessels, as depicted with SMA-Lam IF.

5.2.3 Angiogenetic response to orthotropic transplantation of decellularized matrix vs PTFE

Given the data obtained with the previous experiments, a further step to evaluate its angiogenic properties was done by performing an orthotropic implantation (as seen in chapter 4).

Histological analysis revealed the profound difference between a biological and a synthetic material: while the acellular patch experienced remodelling coherently to the outcome seen during the previous characterization. the PTFE was surrounded by a capsule of cellularized extracellular matrix (thick at the beginning then thin after 15 days). Interestingly, after 15 days the PTFE-implanted diaphragm looked as an healthy muscle, whereas the effects of the decellularized scaffold implants still seemed to persist (fig.5.6).

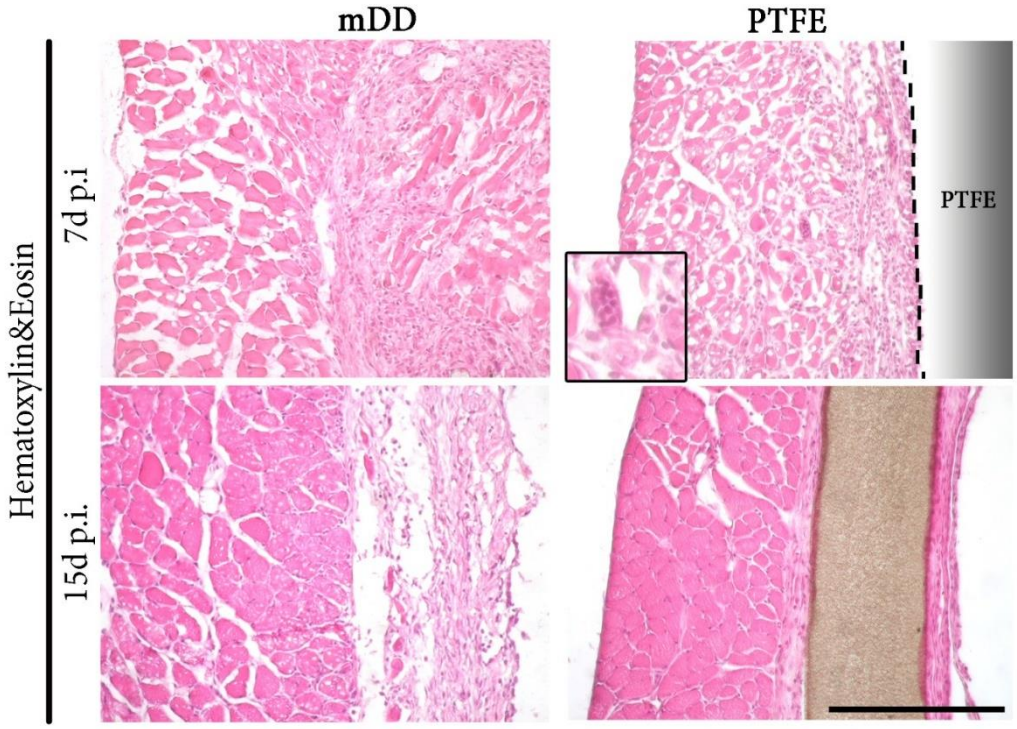

Figure 5.6 Comparison between mDD and PTFE implants

With HE stain is possible to appreciate differences between the two implants; While mDD elicits a response resulting in the growth of the muscle, PTFE rapidly provokes an FBR reaction (tipically associated with foreign body giant cells, inset), which turns to a stable sustained management of the foreign body.

CD31+ cells, detected via IF, were found to have migrated in the applied scaffold as other cells from the host (fig.5.7 A). Their percentage increased significantly ($P<0.0001$) in number after 7 days p.i., compared to the quantity in the mFD (fig.5.7 A, mDD). Although these cells could be detected also in the capsule surrounding the PTFE, their number was not significantly different than a basal condition (Fig. 5.7.A, mDD). The co-staining of SMA and vWF in the lumen was both considered an indication of functional vessel and used to measure size and shape distribution of the vessels afterwards. In transplanted matrix distribution was between small and mid-size vessels 7 days p.i. (from 2.0 to 1.75, and from 1.75 to 1.55 respectively), then after 15 days resembled a baseline condition (vessels also from 1.55 to lower values) Fig. 5.7 D, mDD). On the contrary, at the interface between PTFE and hosts diaphragm, vessels had a distribution similar to native condition 7 days p.i., to then display a grouping in the middle size vessels at the later time point (Fig.5.7 D, PTFE).

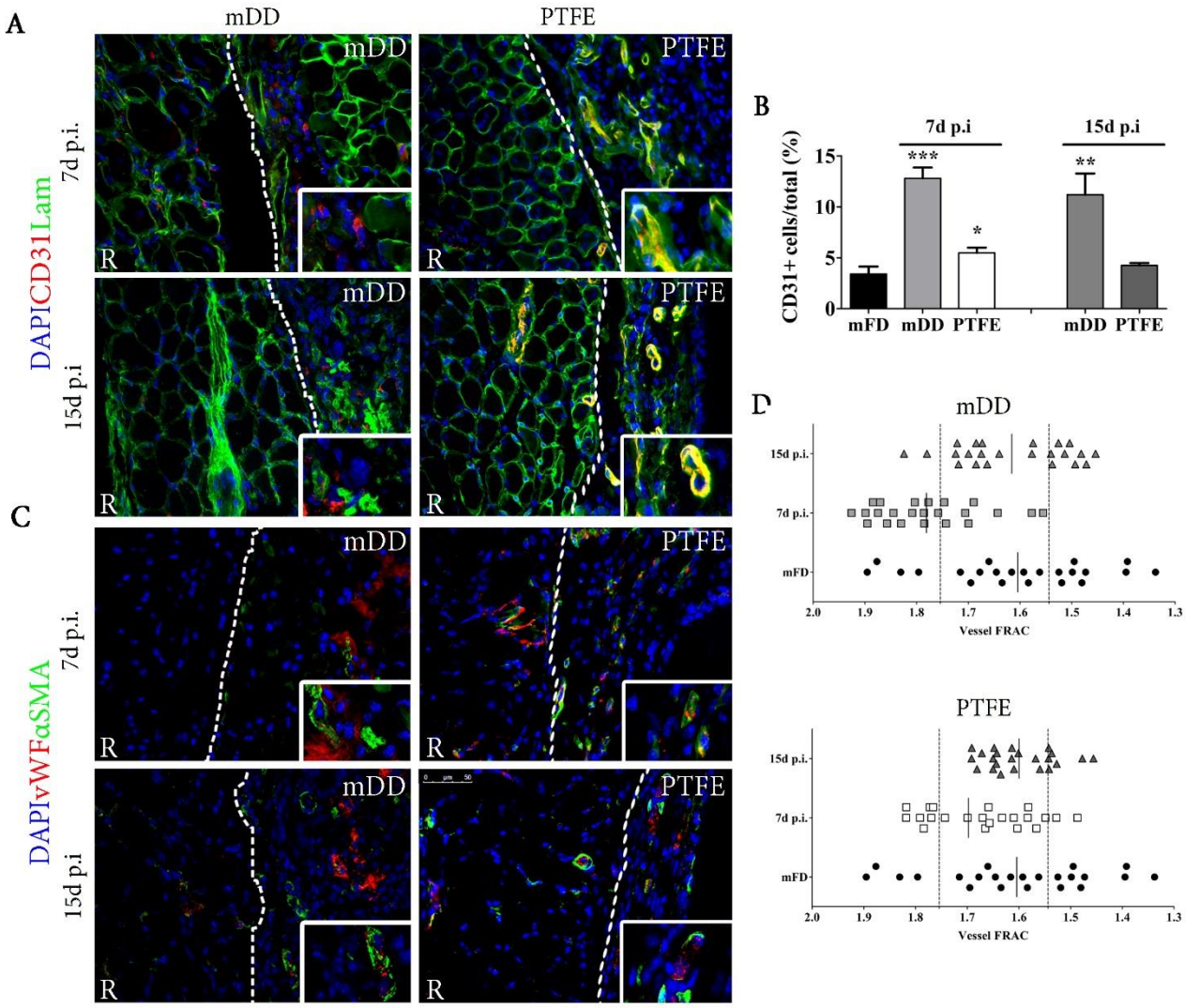

Figure 5.7 Comparison of angiogenetic response of the host implanted with either mDD or PTFE

The angiogenetic response was analysed both at cell level and at vessels appearance level. A) IF to detect CD31-Lam in both mDD and PTFE implanted animals at the two time points; B) +ve cell were counted and compared to a baseline mFD; C) Detection of functional vessels, along with the size and shape, *via* vWF and SMA IF both in mDD and PTFE implanted animals at the two time points; D) Distribution of the vessels found in the two implanted areas, displayed in comparison with mFD. R=Recipient, *p <0.05**p <0.01; ***p <0.001

While in PTFE implants it was assumed that all the vessels branched from the host *via* angiogenesis only, then expecting in all vessels co-staining for SMA and vWF, with the data from SC implantation in mind, it was evaluated the proportion among mDD original non-functional vessels and functional vessels. Evans Blue, an auto fluorescent dye (red spectrum) that cannot pass the endothelium wall

unless the vessel is not completely formed, was injected before the sacrifice of a subgroup among the animals implanted with mDD. The presence of complete and functional vessels in the scaffold was thus confirmed whenever the dye was found in the lumen of functional vessels.

Even though the non-functional vessels could still be found in the mDD 15 days p.i., number of double +ve vessels in the acellular matrix increased (Fig. 5.8). These findings were in line with the analysis of vessels shape.

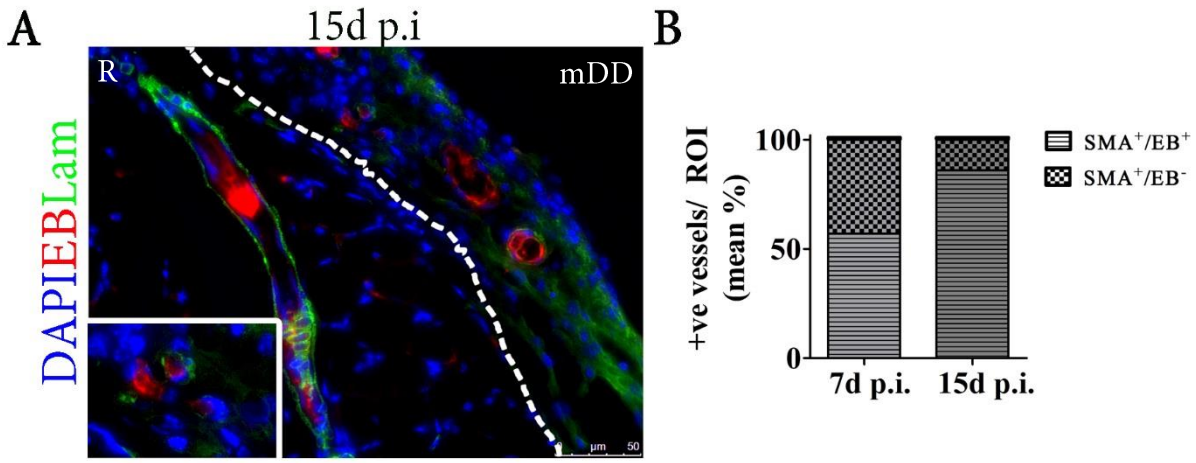

5.8 Evans blue dye detection in mDD implanted animals

Evans blue dye could be detected captured inside vessels, after immediated fixation of the sample. A) Exemplification of dye detection 15 days p.i. in a sample implanted with mDD; B) Proportion of functional and non-functional vessels through time, in mDD samples.

5.2.4 Molecular profiling of host-scaffold protein expression

The pattern displayed by PTFE vs mDD implants reflected the difference between the very natures of the two materials. To aid the observation, it was used an organization based on the best-known process in which each protein was involved (Fig. 5.9 full panel). Protein expression displayed an abrupt increase 7 days after surgery (Fig. 5.9, white bars) compared to mDDs (Fig. 5.9, light gray bars), supporting the rapid vessel constitution seen *via* IF. At the later time point, while more than half of the proteins in both cases trended towards the baseline (Fig. 5.9), other alternatively displayed an

inverse expression, by decreasing, increasing or unchanging in respect to the other sample and each previous time point. (Fig. 5.9). To aid data interpretation, proteins were plotted under four different categories, according to the function or involvement in angiogenesis.

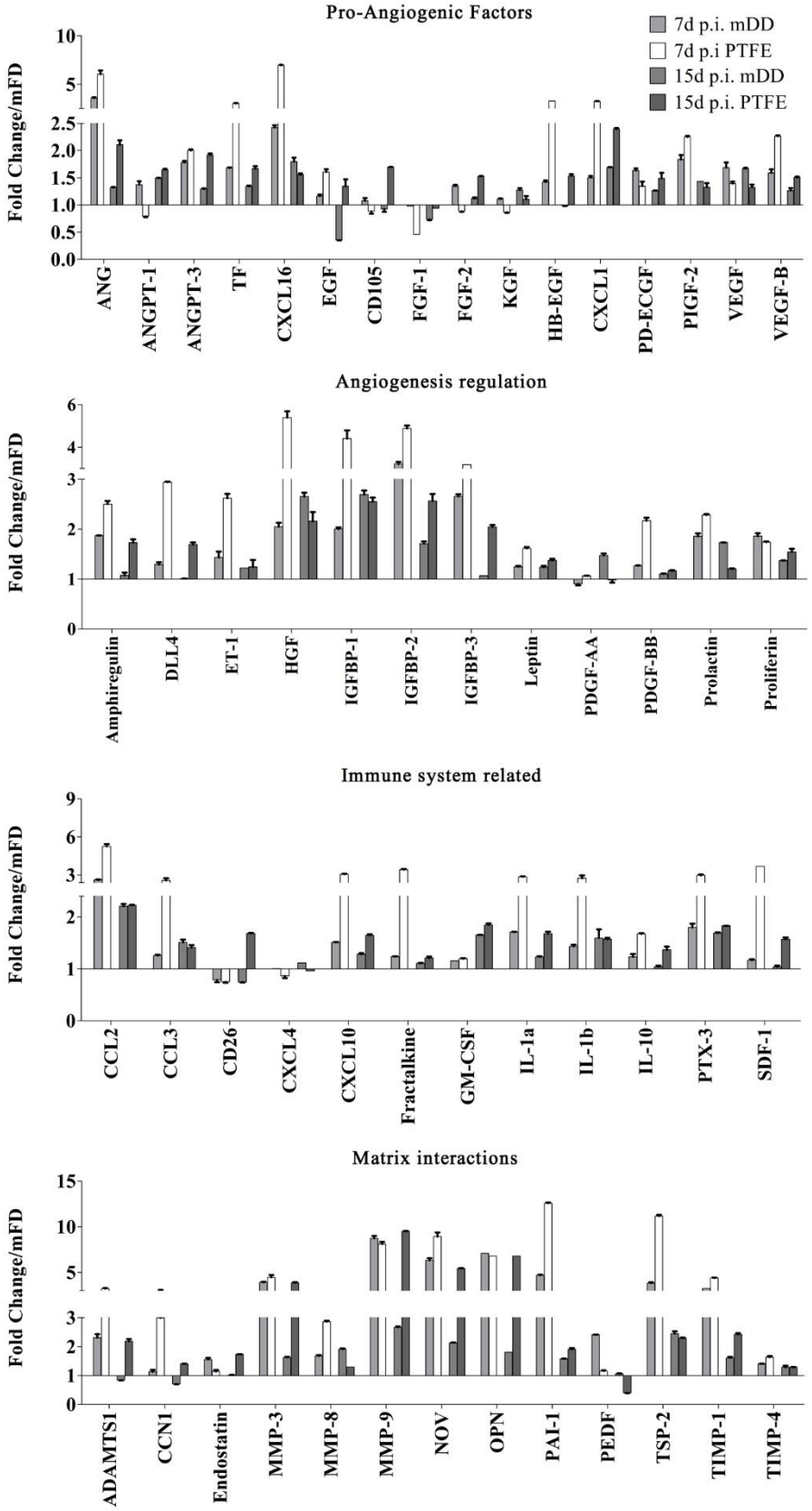

Figure 5.9 Molecular profiling of mDD or PTFE driven response in recipient diaphragm

5.3 Discussion

Among the many feature required to fit as election material for TE approaches (ref scaffold requirements), the ability to attract vessels from the host, while modulating its response towards a pro regenerative and constructive environment, is crucial. This ability, namely angiogenetic potential, is essential since in the body, cell survival, tissue physiology and normal functionality rely almost entirely on blood supply [273]. Throughout the past years, a variety of methods to induce angiogenesis has been tried, evaluating angiogenesis potential and angiogenetic pathways (state of the art). Being such an interdisciplinary field, the approaches TE intended focus on each of the components of the one defined as 'TE triad': i) cells, ii) scaffold and iii) molecules. Consequently, the many options derived from each, rapidly multiply when choice takes in account tissues or organs innate regenerating potential, as well as their complexity. Fortunately, from the cellular side, other disciplinary fields come to help in characterizing and determining angiogenetic potential of each population, for example for either cellular biology or translational medicine [298]. Cell component alike, molecules involved in angiogenesis are object of study, for example in system biology [278] or molecular biology [274]. On the contrary, scaffold components still have quite an extended gap to cover, since advances in technology year by year add up potential candidates to be evaluated [299,300]. Synthetic scaffold, for instance, to date can be customized to allow soluble factors loading, which can be then released with a preconfigured and measurable level of release , or can be patterned to allow growth of structures which will self-assembly into vessel-like tubular units [301]. Whenever the aim is, for example to enhance a natural angiogenetic response, to elicit angiogenesis, or to constitute modular pre-vascularized units, starting from a synthetic or naturally-derived scaffold, will require to take in account the original, natural design, thus accordingly to the specific organ ECM properties. In this respect, again, the possibility to skip this tailoring passage, by starting directly from a scaffold closely resembling the tissue of origin came in help, could be the right choice.

As several studies demonstrated, scaffold derived from decellularized tissue inherit not only the structure, but also the unique reservoir of the original tissue, thus eliciting different responses, when

compared to other material. This potentiality, made these scaffold the most attractive TE-based alternative to supply the extensive demand for organ transplant [159]

The developed mDD demonstrated to be particularly similar to the original tissue, and provoked several pro-regenerative effects (*chapter 4*) that were consistent (or perhaps even better) in comparison with other decellularized tissue implants. Nevertheless, the angiogenetic potential of the scaffold remained undisclosed, thus it was decided to examine in depth whether this property was a feature of our scaffold or not.

4.3.1 Pro angiogenic factor are retained in the mDD

The ability to stimulate and control angiogenesis was firstly assessed via the well-known CAM assay [302], which takes advantage of the high vascularity of the chorioallantoic membrane, easily distinguished by making an opening on the eggshell. The specimen to be analysed is simply placed on top of the membrane and, if able to stimulate angiogenesis, will result in converging or additionally even penetrating vessels, depending on the potential and, of course, on the day after placement as well. Since, as described in *4.3.3*, the interference with a normal healthy system elicits a baseline angiogenesis, it is necessary to use an inert negative control, as well as a positive control to verify the results (usually represented by a porous material filled with pro-angiogenetic molecules, i.e. VEGF). When mDDs were placed onto the CAMs, vessels started to surround the tissues, displaying a directed growth as early as 24h after. At day 7, vessels attracted, organized in a network surrounding the tissues, were much higher compared to both negative and positive controls.

In the sections before, it was mentioned many times the existence of a molecule reservoir lying within the decellularized matrices. This hypothesis rose from the established role ECM has *in vivo*, which is known to interact with cells not only via mechanical signals [303], but acts also via release of the molecules attached to the ECM components or even derived from digestion of such (ref su ECM varie). This, was turned into a confirmation during time, disclosed by several studies describing the

effects derived from interaction between acellular matrices and cells both *in vitro*(ref) and *in vivo* (ref), the study herein likewise. In this respect, angiogenesis in no exception, as it is acknowledged that during this process, interaction with ECM and resulting signals, are of paramount significance [197,304]

Hence, consequently to the results seen with CAM assay, possible angiogenetic molecules within the developed decellularized matrix were investigated. By the means of a pre-patterned array, 53 molecules known to be involved in mouse angiogenesis processes, either directly or indirectly, were probed among the proteins extracted from mDD homogenization. Almost all of the spots in the membrane developed a signal, whereas the negative controls were undetectable, indicating that several of the molecules essayed were still present and measureable after decellularization. Comparison with the amount of proteins spotted in the membranes developed from a FD healthy diaphragm revealed that while for some a significant reduction occurred, for others the decrease was moderate (e.g. VEGFs, ANGPTs). Interestingly, the proportion of many proteins ECM-related was maintained as well (eg. MMP8,9 and TIMP-1).

The protein array data however, not being a direct quantification method, can be used only as comparison between two or more conditions, or simply to evaluate presence/absence of a proteinhapter 4 of interest. Considering this, it was decided to quantify *via* ELISA test two among the cytokines known to be important for angiogenesis, VEFG and EGF , one cytokine directly involved in both angiogenesis and skeletal muscle growth/repair, HGF [305], and a protein generally linked to many important processes (i.e. chemotaxis of immune cells), SDF-1 [306]. Unlike EGF, which was the only that could not be detected, the other factors, expectedly from the array results, experienced a significant decrease, but could still be quantified.

The confirmation of angiogenetic potential, derived not only from the mechanical effect induced by contact (in CAM), but most likely due also to factors demonstrated to be retained within the ECM of mDDs, has a significant impact on the abovementioned (*chapter 4*) applications for this scaffold. For TE in particular, adds up to the many features demonstrated, alleging this as an ideal component for

the delivery of cells or for tissue reconstruction. Moreover, since the presence of almost all of the array proteins, the similarity to the native reservoir (although reduced) was confirmed to be maintained. This can both allow for the scaffold to avoid the pre conditioning that usually other types of support undergo but also, in case the aim is to further enhance angiogenesis, to top up the matrix with a lower amount of chosen factor. In this respect, having quantified some of the cytokines most important for angiogenesis, could be the initial step for a tunable control of this process. This, for instance, might be the case for VEGF, since gradient of this molecule are known to regulate proliferation and sprouting process of ECs [307]

4.3.2 Scaffold-driven angiogenesis *in vivo*

Aiming at the completion of the characterization, we decided to further analyse the angiogenic potential *in vivo*. At first, it was used a common method to evaluate angiogenetic potential of both a cell population or a contruct, namely subcutaneous implant, which was considered as preliminary setting to confirm CAM assay results.
It was chose to use as recipient a GFP+ mouse, hypothesizing that this would have helped to mark and recognize the vessel forming host eventually formed. Implanted patches of mDDs where then analysed 7 days or 15 days after surgery. Moreover, explanted mDDs were used for Drabkin assay (ref da sigma datasheet), which is used to quantify haemoglobin, to confirm presence of functional vessels in the scaffold.

At both time point, GFP+/SMA+ vessels could be detected via IF, indicating a complete integration of hosts vasculature. Functionality of these vessels, was confirmed as the explanted tissue, subsequently to the application of Drabkin protocol, displayed at both time point the presence of haemoglobin and of blood flow consequently. Interestingly, while at 15 days the totality of vessels SMA+ in the scaffold where GFP+ as well, after 7 days from implantation displayed a dual situation instead, with vessels either SMA+/GFP- or SMA+/GFP+, hinting that not only our DET could have preserved the innermost (as intima was depleted) connective layer, but also the hollow structure of

media. Hence, taking a step back, SMA IF, performed hunting for SMA+ vessels in the mDDs, turned out positive, as such structure even though collapsed, could be detected indeed. Just to have a hint on whether these leftover vessels, on top of the overall ECM properties, could be recognized thus interacting with cells, HUVECs, a cell population known to be able to form capillary-like networks [308]were seeded on mDDs. Surprisingly, after 48h of interaction with the scaffold, cells seemed to have not only migrated toward vessels, but also to have arranged into their natural location.

After evaluating the effects of subcutaneous transplant, the next step was to proceed with the analysis of angiogenetic response in a setting that could better validate the scaffold properties for a clinical use, namely the orthotropic transplant in a healthy diaphragm. This, was the ultimate scenery chosen, hence it was in this model that angiogenetic potential and host response were assessed. Since the prolonged contact of any device, either synthetic or biological, result always in a FBR, which in turn activates angiogenesis during the cascade of events involved [261], it was decided to add a further control. On top of the diaphragm healthy condition, the implantation of PTFE, the gold-standard material used for such applications in clinical settings [155,309], hence the ideal material for a comparison with others [253], was added as FBR comparison condition. Again, time point of implants were 7 days (known as the peak of FBR), and 15 days (far enough to evaluate chronic responses). Outcome of mDD vs PTFE displayed an extremely marked difference in all the analysed aspects, some expected (i.e. a synthetic material cannot be remodelled), and unexpected

To start, histological analyses (colorations and IF) revealed in mDD implants a remodelling consistent with the previous results, both from cell migration (*chapter 4*) and angiogenesis potential (outlined above) points of view, whereas the PTFE seemed to have elicited an abrupt response, which after 15 days appeared to have stabilized. Precisely, recipient CD31+ cells could be detected in the ECM of the biological scaffold, as well as functional and leftover vessels, of which the latter decreased in time. The presence of functional vessel was detected two ways i) through staining for vWF, a protein belonging to both platelet and ECs secretome [310], thereby indicating the constitution of both epithelium and blood flow in SMA+/vWf+ vases and ii) by detection of the dye Evans Blue, a compound with a use

comparable to isodextran, in the vessels [311]. PTFE implants instead, while displaying the presence of CD31+ only inside functional vessels (detected this time only with the first method), appeared to have elicited angiogenesis more rapidly, but with a different aim. Indeed, distribution among the size of the vessels found in the two environmental settings, in the case of mDD after 15 days resembled a normal tissue, whereas the synthetic material at first seemed to recall a normal distribution, which later regressed. The possible explanation for this dissimilarity could be that the already exhibited pro-regenerative and immunomodulatory properties of the scaffold developed in the present study, resulted in a coherent angiogenetic response alongside. In contrast, the inert synthetic material, being not recognized as natural by the recipient, elicited the previously hypothesized baseline FBR. In both cases indeed, a response coherent to normal biological processes was stimulated [312]. While the latter was aimed at managing the intromission and restoring the normal physiology (as seen after 15 days), creating vessels aimed more at delivering host immune cells efficiently, rather than constituting a remodelled tissue, the mDD transplanted instead was recognized as tissue to be remodelled and reabsorbed, stimulating a regenerative angiogenesis, thus aimed at stable functional vessel, simultaneously.

The striking difference among the two situation was further confirmed with the same protein array used for angiogenesis protein detection (*4.3.1*). Indeed, the pattern displayed by PTFE implants reflected the hasty effect hypothesized, with an intense increase observed after 7 days, when compared to mDDs. Intriguingly, both patterns in most of the cases appear to trend similarly, by increasing or decreasing after 7 days, to then tend to baseline (healthy diaphragm), suggesting that, although with different aims, some extend of overlap had occurred in the responses.

The understanding of construct-host interactions is essential to avoid any adverse effect by both modulating FBR (i.e. graft vs host) and enhancing regeneration (i.e. functional integration). These two feature, were demonstrated to be directly interconnected, widening the aspects to look after while developing a TE approach. The mDD this way proved to be a promising material, adding to its list of desirable features, the pro-angiogenesis potential. Precisely, the ability to modulate the immune

system reflected on the FBR, which was driven towards a constructive remodeling, resulting in the induction of the myogenic program and ultimately into a restoration of normal condition (healthy environment) or amelioration on the way to it (atrophic model).
The proteins which displayed an inverse or different pattern compared to the PTFE, are involved in several aspect of angiogenesis, however, if taken together seem to endorse the hypothesized difference between the two mechanisms. Specifically, while in the case of mDD these mirror a coherent time course of events, leading to stability (turning off the responses and actualizing maintenance), the intensity of protein expression still found after 15 days from PTFE implantation support the idea of a chronic response elicited by the perpetuated contact with this non-absorbable material.

Since angiogenesis and its machinery are undeniably a complex topic, yet to be completely understood, it is of fundamental importance to deepen investigation on the interactions between the scaffold and the host, unveiling the specific players from both sides, either cellular, mechanical or molecular.

Chapter 6 : Diaphragm-derived decellularized scaffold as potential tool for CDH repair

6.1. Introduction

6.1.1 Diaphragm muscle

The diaphragm is the largest of the respiratory muscles; with a unique shape of a modified half-dome made of musculofibrous tissue, it separates the thoracic from the abdominal cavity. Formation of this muscle is made up by four embryologic components: the *septum transversum*, the pleuroperitoneal folds (PPFs, two in total), the cervical myotomes and the dorsal mesentery. During development, muscle precursors migrate from the dermomyotome of cervical somites following guidance cues provided by the somatopleure substructure, then localize in the pleuroperitoneal fold. Next, concomitantly with phrenic branch outgrowth, diaphragmatic myoblasts migrate from the fold and fuse to form muscle fibers, which then extend from i) the lateral aspect of the *septum transversum* to the body wall in the costal areas and ii) the esophageal mesentery to the dorsal aspects of the crural region. The tendinous central portion, namely the central tendon, derives instead from the *septum transversum*, which eventually becomes surrounded by the growing muscle fibers. Once fully developed, these are disposed concentrically from the central tendon to the rib cage, so boundaries of diaphragm muscular portion will be the lower sixth rib (bilaterally), the posterior xiphoid process, and the external and internal arcuate ligaments [313].

While several structures traverse the diaphragm, distinct apertures of the diaphragm are three, and exist to allow the passage of the aorta, esophagus, and *vena cava* from the thoracic to the abdominal cavity. The aortic aperture is the lowest and most posterior of the openings, lying under the median ligament at the level of the 11-12th thoracic *vertebrae*. The esophageal hiatus opens ventrally next to the aortic, but is fully surrounded by muscle and lies at the level of the 10th thoracic *vertebra.* Last and highest of the openings, *vena cava* crosses the diaphragm at level of the disk space between the 8th and 9th thoracic *vertebrae.* Arterial supply to the diaphragm comes from the right and left phrenic

arteries, the intercostal arteries, and the pericardiophrenic and musculophrenic branches of the internal thoracic arteries. Venous drainage instead occurs *via* the inferior *vena cava* and azygous vein on the right and the adrenal/renal and hemizygous veins on the left.

The diaphragm receives its unique neurological impulse from the phrenic nerve, which originates primarily from the 4th cervical ramus but also has contributions from the 3rd and 5th rami. It is important to remember that muscles in the diaphragm are striated though belong to the skeletal type, hence respiratory functions are not controlled by the involuntary nervous system (sympathetic and parasympathetic) (Fig. 6.1).

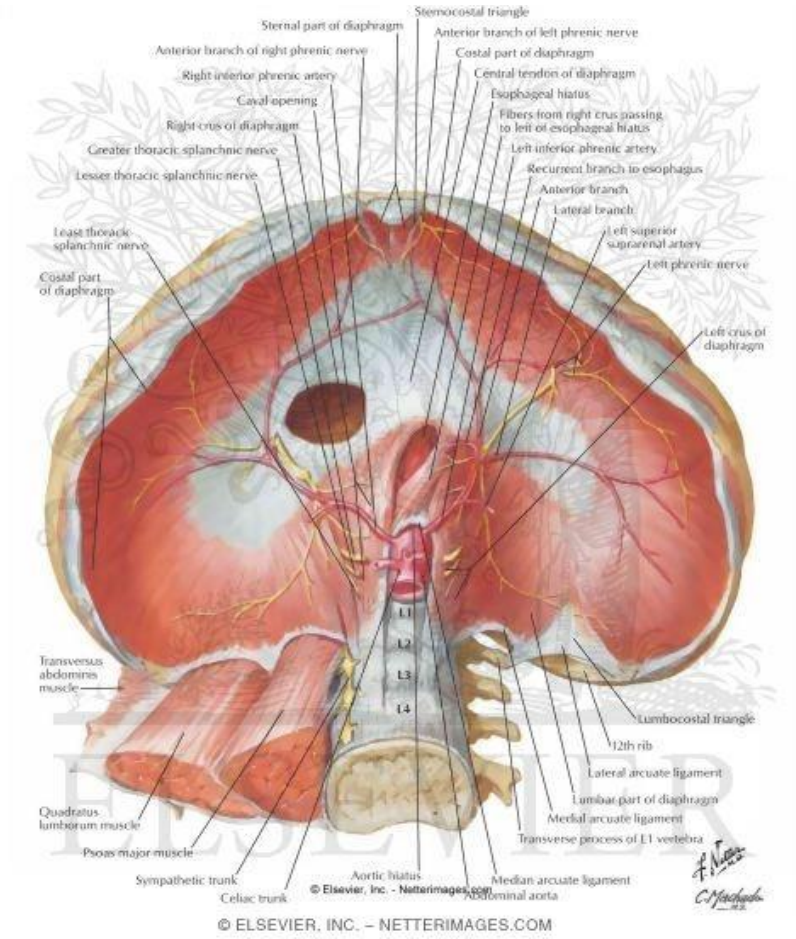

Figure 6.1: Overview of human diaphragm from abdominal side (from Atlas of Human Anatomy - 4th Edition. Author: Frank H. Netter).

Functional and histological analyses revealed that most of the diaphragm fibers are the type I (slow twitch, oxidative type). Indeed, the mean relative proportion of these was found to be about 50%, the remaining proportion being evenly divided into type IIa and IIb fibers (fast twitch, oxidative/glycolytic type and glycolytic type, respectively) [314]. As normal respiration is dependent on the diaphragm functionality. Contraction of the diaphragm has following functions: (i) decreasing intrapleural pressure, (ii) expanding the rib cage through its zone of apposition by generating positive intra-abdominal pressure, and (iii) expanding the rib cage using the abdomen as a fulcrum. Therefore, it is important to understand how different diseases and disorders result in diaphragm dysfunction [315].

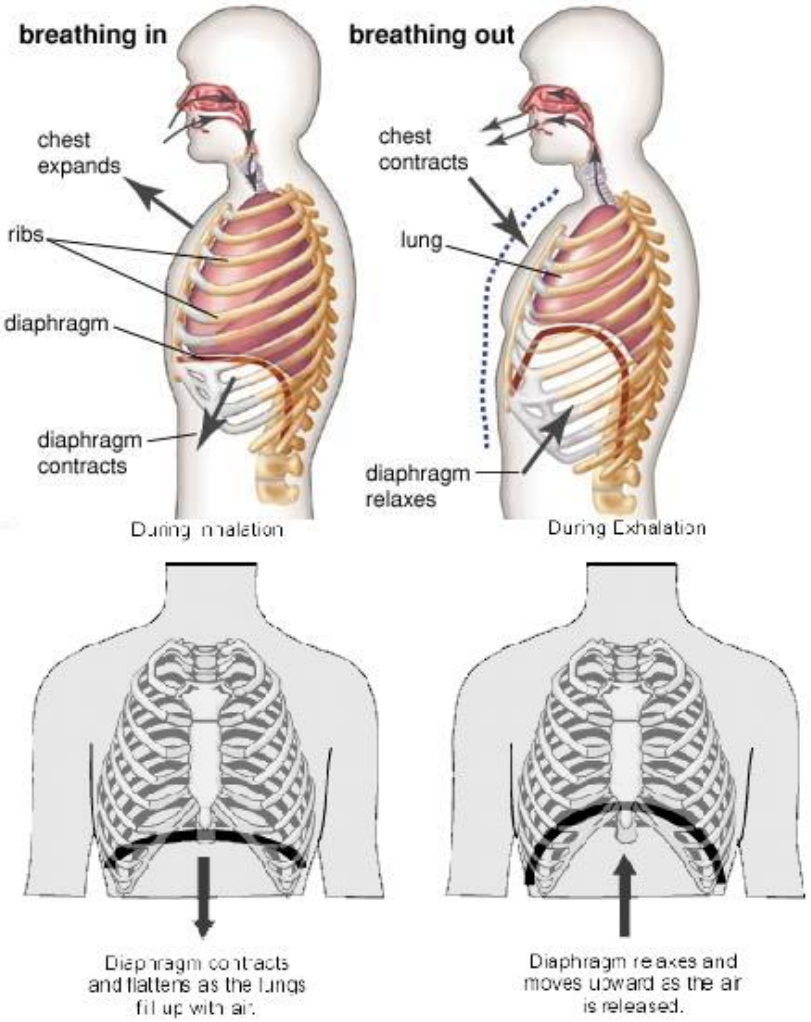

Figure 6.2 Diaphragm movements during respiration.

(From https://ellbond.files.wordpress.com/2012/10/untitled.png)

6.1.1.1 Disorders that can affect diaphragm

When normal activity of the diaphragm is disrupted, as result of any damage or defect, respiratory dysfunctions occur. Although our body is able to intrinsically compensate the decrease of diaphragmatic function, it cannot successfully restore compromised respiration resulting from a significantly lowered or absent excursion of the diaphragm. This inability to provide adequate negative intrathoracic pressure leads to decreased ventilation, which in turn lowers the amount of oxygen provided to the alveoli.

Diaphragm disorders are typically classified into two broad categories: congenital and acquired. The most common cause of acquired diaphragmatic disorders is trauma, which is usually a rupture that can occur secondary to both blunt and penetrating trauma. Examples of the latter are motor vehicle accidents and direct perforation through gunshot or stab wounds. For blunt trauma instead, several theories have been postulated regarding the mechanism of rupture, including shearing of a stretched membrane, avulsion of the diaphragm from its points of attachment, and sudden force transmission through viscera acting as a viscous fluid. Conversely, congenital defects take place due to genetic disorders that affect the development or the correct function of the diaphragm. Congenital diaphragmatic hernia (CDH) is an example of disease that occurs when the muscular entities of the diaphragm do not develop normally, usually resulting in displacement of abdominal components into the thorax [3]. Specific origin and different type of CDH will be further discussed in *4.2*. In general, any myophathy involving the skeletal muscles results in the decrease of muscular development and function of the diaphragm, as i.e. result of atrophy or dystrophy.

The most known and common myopathies are dystrophies, such as Duchenne's muscular dystrophy (DMD) and Myotonic Dystrophy 1 and 2 (DM1, DM2), followed by atrophies, for example spinal muscular atrophy (SMA). Although genetics behind each disorder are heterogeneous, usually outcome result in similar effects. For example, in DMD the main symptom is muscle weakness associated with muscle wasting and the voluntary muscles being first affected. Symptoms and signs classically associated with DM1 are generally mild and involve the smooth muscle (including gastro-intestinal symptoms), hypersomnia (daytime sleepiness), muscle wasting, dysphagia, and respiratory

insufficiency. In SMA, symptoms vary depending on the disorder type, the stage of the disease and individual factors, and may include: areflexia, marked hypotonia of muscles, difficulty in achieving developmental milestones, difficulty sitting/standing/walking, respiratory distress, bell-shaped torso (caused by using only abdominal muscles for respiration), and fasciculation (twitching) of the tongue. Several animal models have been made to investigate which genes could be responsible of each pathology or to evaluate clinical approaches to ameliorate the condition of affected individuals. For example, mdx is a mouse model that lacks dystrophin, which absence is known to be one of the reasons of insurgence of the DMD [316]. Instead, in HSA-Cre,SmnF7/F7 mouse model, the absence of the protein Smn mirrors the lack of the same protein that causes SMA in human, resulting in an atrophy of the muscles [266].

Since the diaphragm belongs to the skeletal musculature, as soon as progression of the disease extends to it, affected individuals exhibit breathing difficulties that can ultimately result in death. Indeed, most common cause of death, next to heart failure, is respiratory insufficiency.

6.1.2 Congenital diaphragmatic hernia

Any event that interferes with the integrity of diaphragm structure, leading to an opening through which abdominal organs can herniate into the thoracic cavity, is categorized as diaphragmatic hernia. If the opening is caused by incomplete development due to a genetic disorder, it takes the name of congenital diaphragmatic hernia (CDH), otherwise it is generally registered as traumatic or acquired. With an incidence lower than 1 in 2500 live births, CDH accounts for 8% of birth defects and 1-2% of infant mortality [317].

Location where the incomplete closure of the diaphragm occurs can be different (figura difetti) and each type of hernia is categorized accordingly. When the defect is present posterolaterally (either side), it is called Bochdalek hernia (70-75% of the cases). Alternatively, 23-28% of the cases are represented by Morgagni hernia, located ventrally close to the sternum, while remaining 2-7% is just described as central hernia (Fig. 6.3) . The size of defect in Bochdalek hernias is described by the CDH study group classification from A to D accordingly [155], determining the severity of the symptomps

(Fig. 6.3, inset). Associated mortality rates rise with the severity of the defect or concomitant malformations (i.e. 2% in A, 61% in D), because the bigger the opening, the more it is accompanied by herniation of the stomach, intestines, liver, and/or spleen into the chest cavity (Georgescu), with topical decrease in lung performance consequently. Although majority of this types of hernias originate on the left or right side (85% and almost 10% respectively), there is also the change to develop the defect bilaterally (5%) [318].

Lastly, in rare cases, fetus is missing almost a complete side of the diaphragm, which thus far is a condition resulting in no survival.

In general, the 40% of CDH cases are present concomitantly with other defects, for example congenital heart defects, which occurs in the 20% of CDH patients [309].

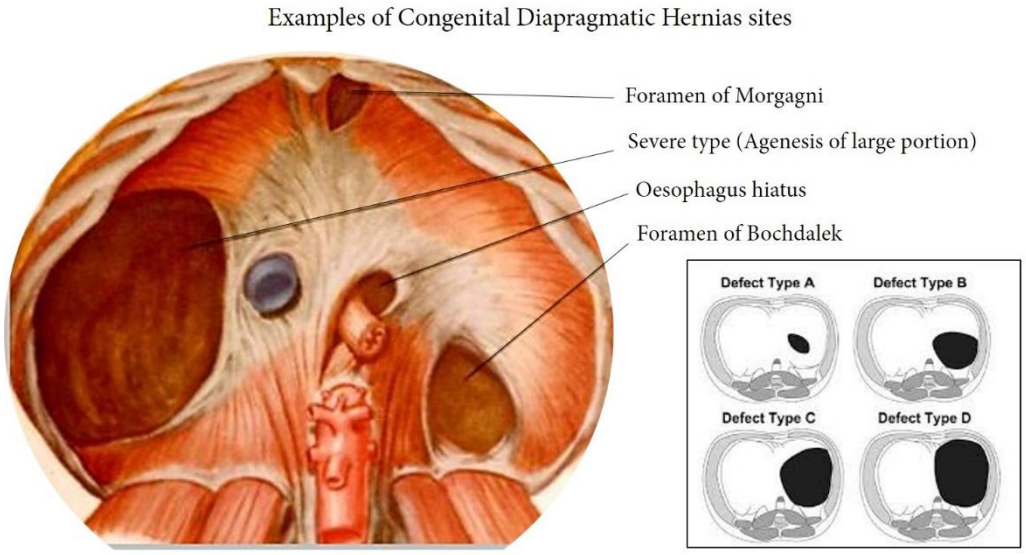

Figure 6.3 Types of congenital diaphragmatic hernias (inset, classification accordin CDH study group)

Adaption of

(http://www.learningradiology.com/lectures/chestlectures/Diseases%20of%20The%20Diaphragm2012/data/images/img15.jpg)

6.1.2.1 CDH Pathogenesis

Throughout the years, many were the hypothesized mechanism behind CDH, which pathogenesis thus far, remains poorly understood.

One of the oldest hypotheses was the existence of a link between retinoids and the devolpment of the defect. This was effectively demonstrated in rats, where variations of Vitamin A in dams' diet during gestation led to different incidence in the offspring. Indeed, lack of Vitamin A increased CDH insurgence to a frequency of 25-40% of live born pups, while restoring a normal diet during gestation decreased number of CDH cases (49 cate). More recently, significance of retinoic acid pathway was not only confirmed for diaphragm development, but also for organogenesis in general (91, 24 cate). Through the use of molecules able to interfere downstream or upstream the pathway, it was also possible to model the defect in animals. A well-known example is the nitrofen-induced rat model of CDH, which as name suggests take advantage inhibitory action of nitrofen on retinal dehydrogenase RALDH-2. In humans, risk of CDH development is thought to increase in association with smoke, alcohol, obesity, drugs and immunosuppressive mucophenylate mofetil as well [319].

Interestingly, there seems to be a connection also with multiple genetic disorders, as in the 10-35% of patients affected were found chromosomic alterations associated with other pathologies. Complete/mosaic aneuploidies, deletions or duplications are only some of the defects detected. For example, common in child affected by Morgagni hernia, is the aneuploidy cause of the Down's syndrome, the trisomy 21. Another example is the tetrasomy 12p, which is a copy number variation disease, known as Pallister-Killian syndrome [320]. A recent study, linked the expression of Gata4 to the development of CDH, as deletion of this gene led to formation of a lateral opening in the diaphragm. Surprisingly, this gene was expressed only by connective tissue cells of PFFs, but not by myogenic cells, revealing the significance of connective tissue during tissue morphogenesis (Merritt 2015). This work was in line with previous knowledge of 3-5% of CDH patients having the 8b23.1 deletion syndrome, which involves genes Sox7 and Gata4. In general, genomic characterization of CDH patients revealed that more than 20 genes have mutations, thus gene-disease correlation cannot be clarified yet.

6.1.2.2 Associated morbidity and causes of mortality

Mortality associated to CDH has to date a range varying from 42 to 68% of cases, mainly depending on size of the defect (58 cate). As described above, pulmonary distress due to the inadequate pressure of the thoracic cavity, caused both by the hole itself and by other organs herniation, results in hypoplasia or hypertension of lungs [309].

Herniated organs, not in their physiological location anymore, can be functionally impaired as well. Oesophageal reflux is one of the most common resulting additional defects (45 to 89% of CDH), which, concomitantly to other issue, often leads to poor growth with failure to thrive in the first year of life (58). Also, causes not directly connected with involved organs were reported. Delays in control of motility, neurodevelopmental and even language problems, on top of behavioural disorders, have a rate that varies between 12 and 77% of cases. These defects can probably be associated to alteration in oxygen supply caused by respiratory dysfunction, which negatively reflect on correct brain functions. Extracorporeal membrane oxygenation (ECMO), a current treatment for CDH, can represent a higher risk in this sense as well.

At least, obstruction of the organs don't belonging to thoracic cavity can impair correct muscoskeletal development of the thorax itself, resulting in deformities such as pectus deformities, asymmetry of chest wall or scoliosis. Moreover, use of non-elastic patches for hernia repair can increase incidence of these deformities [230]

6.1.2.3. Diagnosis

Since human diaphragm begins to develop at the third week of gestation, being complete by the eighth week, congenital defects take place quite soon. However, current prenatal diagnosis is possible in about 80% of cases. Abnormalities are usually detected via sonography or echocardiography, which allows to detect eventual heart dysfunctions as well. Furthermore, magnetic resonance imaging (MRI) is the election methodology to detect herniated organs. Alternatively, diaphragmatic hernia can be

detected indirectly by the means of the impairment caused in lung development. Methods used with this aim are MRI lung volumetry or expected lung head ratio (O/E LHR).

If for some reason CDH remains undetected until birth, it is still possible to evaluate whether is present by checking newborn symptoms, such as respiratory or feeding problems, then confirming suspects with chest radiography [321].

6.1.2.4. Current treatments

Approaches to CDH are currently focused on facing the issues resulting from the defect two ways: i) intervening on the lung located on the side of the opening to help its correct development and/or ii) close the gap using prosthetic meshes.

Fetal endoluminal tracheal occlusion (FETO) is a technique developed aiming at i). However, its use is not evenly approved hence to date is applied only in cases of high risk for the patient.

High-frequency oscillatory ventilation (HFOV), to prevent trauma or extracorporeal membrane oxygenation (ECMO), which uses a heart-lung artificial machinery to purify the blood from dioxide carbon and to oxygenate it, are other methods to help lung recovery and increase survival rate . However, ECMO, which is a very invasive technique, has not proven significant survival benefits yet.

As alternative therapies, molecular intervention via the local delivery of specific molecules that could help lung development and growth were tested. Two examples of these approaches were nitric oxide (iNO) and sildenafil: while the former was unsuccessful to the point that patients continued to need ECMO, with any decrease in mortality, the latter showed some successes, functioning as a pulmonary vasodilator [309,321]

Surgical closure of the gap via thoracotomy or laparotomy is currently the standard procedure for hernia repair, concomitantly with the restoration of the original location of the herniated organs. Closure approach depends on size and position of the opening, with a 60 to 70% of cases resolved with primary suture repair (small defects). In cases where size of hernia is too extended to allow the abovementioned technique, surgeons will need a prosthetic or naturally-derived mesh. Examples of

natural meshes are autologous tissues such as abdominal/thoracic muscle flaps, free fascia lata grafts or, more recently, xenogeneic acellular matrices [158], while prosthetic materials can be polypropylene meshes, reinforced silastic sheets (made of silicone) and combinations of PTFE (named often by its commercial name Goretex®) alone or with other materials. Although the latter was registered to be the material currently used most frequently (81% of cases), it is not free of disadvantages and limitations [23]. Being an inert material, on one hand it has an elevated durability, but on the other is non-functional and does not comply patient growth. Moreover, although as foreign body it triggers neovascularization and fibrosis, patient tissue does actually not grow within the graft (Meyer 2015). At last, its lack of compliance due to inadequate stiffness, compared to diaphragm elasticity and fluidity, is associated with spinal/thoracic/abdominal wall deformities, as well as detachment of the patch resulting in recurrence of herniation [322,323].

Other possible complications that may rise after surgical treatment are associated with adhesions, infections and short bowel obstruction.

All these drawbacks have encouraged the development of biologic and cell-based engineered constructs, opening the way to regenerative medicine and tissue engineering approaches.

6.1.3 Clinical and pre-clinical evidence for TE-based solutions for CDH

Thus far, eight patients affected by different diaphragm defects were treated using an acellular matrices either from human acellular dermis (HADM), porcine acellular dermis (PADM) or a fetal bovine dermal mesh (FBDM). It is important to underline that these were all traumatic defects hence outcomes do not and cannot fully reflect those in paediatric patients. Cases and follow up outcomes are summarized in table 5.1.

Choice of biological meshes was done due to the results acellular matrix had thus far. It was felt that synthetic meshes would have been a high risk for infection, adhesion and eventual recurrence, whereas biological properties were demonstrated to be more compliant, less adhesiogenic and to have vascular ingrowth stimulating cell turnover and proper remodeling.

Indeed, with the aim of supporting clinical scaling of TE applications for CDH repair, several prospective animal models and several repair approaches have been studied. However, as described in the previous chapter, besides the effective TE approaches summarized in table 2, the other approaches were more focused on evaluating outcomes using different types of repair patches by means of scaffold-only transplantations [230,253,323,324].

Ideally, right after prenatal diagnosis of a diaphragmatic defect, patient cells (or other non-immunogenic but myogenic cell sources) would be cultured and combined with autologous or xenogeneic acellular tissue readily available for surgical correction after birth.

Although by then, PTFE stand still as gold standard for CDH closure, it is foreseeable that further diaphragmatic engineering will find its way into clinics.

6.2 Results

6.2.1 Experimental design and pilot implants

As it was never tried in mice, the surgical model of CDH needed to be accurately designed and standardized. With this aim, pilot experiments were performed in order to create a hole (which at first was of approximately 3x2 mm) in the left side of the diaphragm of B6 mice, mimicking the type A Bochdalek hernia phenotype. Patches of mDD (prepared as in chapter 3) were tailored to fit the opening then used to cover the defect. Alternatively, implantation of PTFE patches of same size were considered the control treatment. Sacrifice was done after 15 days (mDD implantation only) and after 30 days (for both conditions). Number of animals used, along with overall survival rates, are summarized in table 5.1.

Table 6.1|Pilot experiments implants

Set of implants	Animals/scaffold implanted	Survival percentage	starting weight (g)	Harvest (days p.i.)
#1	3 mDD	33,3%	<20	15
#2	2 mDD and 1 PTFE	66,7%	<22 and <30	30

At all conditions, after both time points, implanted material stayed in place, managing to keep the defect covered (Fig 6.4). As expected, mDD patches were distinguishable from the surrounding tissue only for the sutures, whereas PTFE, being non-absorbable, was visible but partially covered by a layer of host tissue (Fig. 6.4, 30d p.i. PTFE, red circle). Liver was found in adherence.

To evaluate inflammatory state and structural integrity altogether, double IF directed against laminin and CD11b (a pan-macrophage marker) was performed on the samples. Remarkably, while 15 days post mDD implantation several inflammatory cells (CD11b+ cells) were present at the site of injury, with the scaffold being rapidly digested, remodelled and surrounded by small fibers (indicating regeneration, Fig. 6.5, CD11b-Lam IF), after 30 days both the defect and mDD patch were completely absent. Importantly, unlike PTFE implants, which were still injured and filled with immune cells, the muscle seemed to be still regenerating, as a strong indication of scaffold pro-regenerating properties (Fig. 6.5).

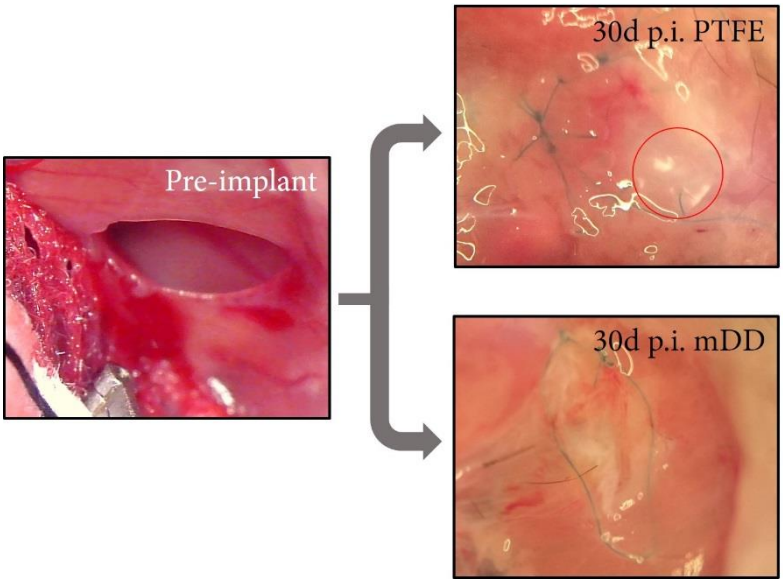

Fig 6.4 Macroscopic appearance of either PTFE or mDD 30d p.i.

Continuous stitch helped the detection of the implanted materials; While 30 d p.i. PTFE was trapped in the recipient FBR capsule, with some end still visible (red circle), 30d p.i. mDD was undistinguishable from host tissue.

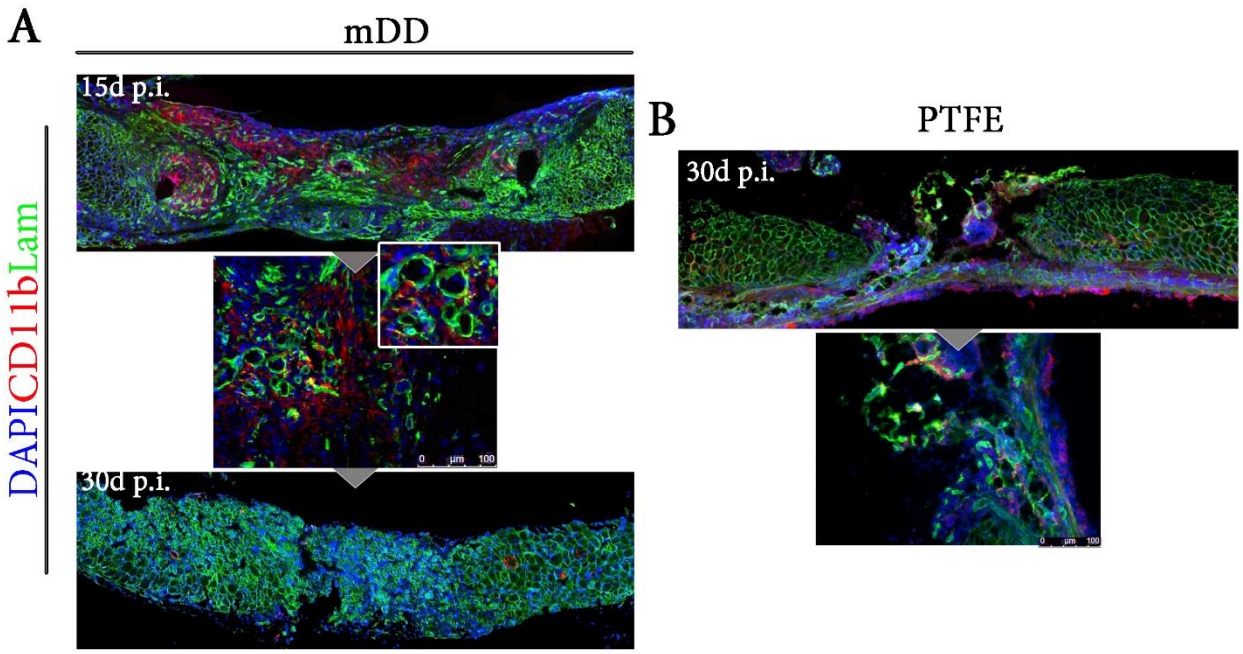

Fig 6.5 Comparison of the immune response and closure attempt by mDD vs PTFE

Closure repair efficiency of mDD vs PTFE; A) 15 days p.i. the opening could be distinguished but displayed a high number of new forming fibers (inset), which resulted in gap closure 30 days p.i. ,whereas B) in PTFE implants the defect was still present.

While these preliminary experiments proven useful for the standardization of the procedure, as well as displaying host response upon implantation, it was felt that a type A defect was not really reproducing the clinical condition usually requiring mesh implantation, often non syngeneic. Consequently, not only the testing was shifted to an allogeneic implantation (B6 derived mDDs on BALB/c recipients), but also a larger defect was set (approximately 66 mm^2). Lastly, as it was hypothesized that to appreciate regeneration of a more severe defect, more time would be needed, time points were prolonged from 15 to 30 and from 30 to 90 days respectively. The experiments performed after this pivotal set were then considered as experimental phase. Below are summarized the experiments performed thus far , as well as reported body weight before/after implant (at time of the harvest).

Table 6.2| Summary of CDH experiments

Set of implants	Animals/scaffold implanted	Survival percentage	starting weight (g)	final weight (g)	Harvest (days p.i.)
#3	2 mDD	100,0%	23	24	30
			25	28	90
#4	2 PTFE	100,0%	28	32	30
			28	41	90
#5	1 mDD	100,0%	31	38	90
#6	1 mDD	100,0%	31	28	30
#7	2 mDD	100,0%	26	28	30
			27	28	90
#8	2 mDD	50,0%	30	34	30
			36	N/A	
#9	2 PTFE	0,0%	N/A	N/A	N/A
#10	1 PTFE	100,0%	26	28	30
#11	1 mDD		32	34	
#12	2 PTFE	100,0%	36	37	90
			28	24	
#13	2 PTFE	50,0%	24	28	30
			N/A	N/A	90
#14	2 PTFE	50,0%	27	23	30
			N/A	N/A	90
#15	2 mDD	50,0%	28	Ongoing	90
			N7A	N/A	

6.2.2 mDD vs PTFE implantation in CDH surgery model

A total of 20 mice underwent surgical creation of defect, which was covered with either mDD patch or PTFE patch straight after. The overall survival percentage was averagely 71,4% (higher than in pilot experiments). Of the remaining 28% deceased, only one mouse did not survive further than 10 days after surgery, whereas the other animals mortality was registered within 48 hours, probably due to poor recovery after the surgical procedures.

6.2.2.1 Macroscopic appereance, diaphragm excursion and histological outcomes

Symptomatology of mice during time, along with the appearance of recipient diaphragms at moment of harvest, confirmed that no host vs graft reaction occurred, thus confirming the non-immunogenicity of both materials. Thirty days after surgery, animals underwent a chest echography (n=X). BALB/c mice, used as untreated controls, allowed estimating the excursion of the left hemi-diaphragm to a mean 1.26 ± 0.01 mm during normal breathing. 30 days p.i., while PTFE mice displayed and excursion of the treated side of 0.67 ± 0.23 mm, mDD-implanted diaphragm ranged 0.63 ± 0.12 mm, significantly lower than the control, but not to the synthetic mesh treated mice (Fig. 6.6 D). At the later time point instead, echography displayed a significant increase in the mDD-implanted animals (0.80 ± 0.03 mm), while also the excursion of PTFE-implanted increased, but to a rate which was 143% of the baseline control.

Macroscopically, mDD seemed to have well integrated with host diaphragm, without displaying any sign of detachment or re-herniation, whereas PTFE was not as efficient. Indeed, while in all cases liver adhesion occurred, in _ implants done with PTFE it manage to herniate into the thoracic side as well (Fig. 6.6 A, PTFE, dark gray circle)). More importantly, as displayed in chapter 4, blood vessels extended also in the mDD, while due to its composition, PTFE could not be invaded nor integrated with the host. Implants harvested at the later time point, did not display any particular macroscopic difference: the mDD implant was still distinguishable only by the sutures, whereas PTFE was still covered by a dense layer of connective tissue. Remarkably, while the excursion with the first seemed to be ameliorating after 90 days, the latter had negatively influenced the diaphragm of the recipient, as the excursion was springing from one to the other side, probably due to the stiffness of the PTFE (Fig. 6.6 B).

Histological analysis confirmed the different action the two types of materials did. The implanted mDDs underwent high remodelling, and were found almost completely digested. Indeed, thickness of mDDs was averagely 104.4 ± 19.68 μm in the middle part; significantly lower ($P < 0.0001$) than a mFD (234.63 ± 9.24 μm), to further decrease, as found in the later time point (38,44 ± 2,217 μm). Despite this, as seen macroscopically, the defect was not present anymore (Fig. 6.6, C, mDD. Being

inert, PTFE was unchanged after all time points (around 170 µm). In particular, HE stain confirmed the previous seen migration of the host cells, which will be described deeper in the next section. MT stain instead revealed the fibrosis occurred in both samples. Precisely, implanted PTFE was surrounded by a dense fibrotic capsule while host diaphragm on the sides looked scarred, whereas on the contrary, although some extent of fibrosis was detected at the edges, most of the connective tissue marked by the coloration was the leftover mDD in the defected area (Fig. 6.6, MT, blue areas). These results were in line with the remodelling seen in *Chapter 3*.

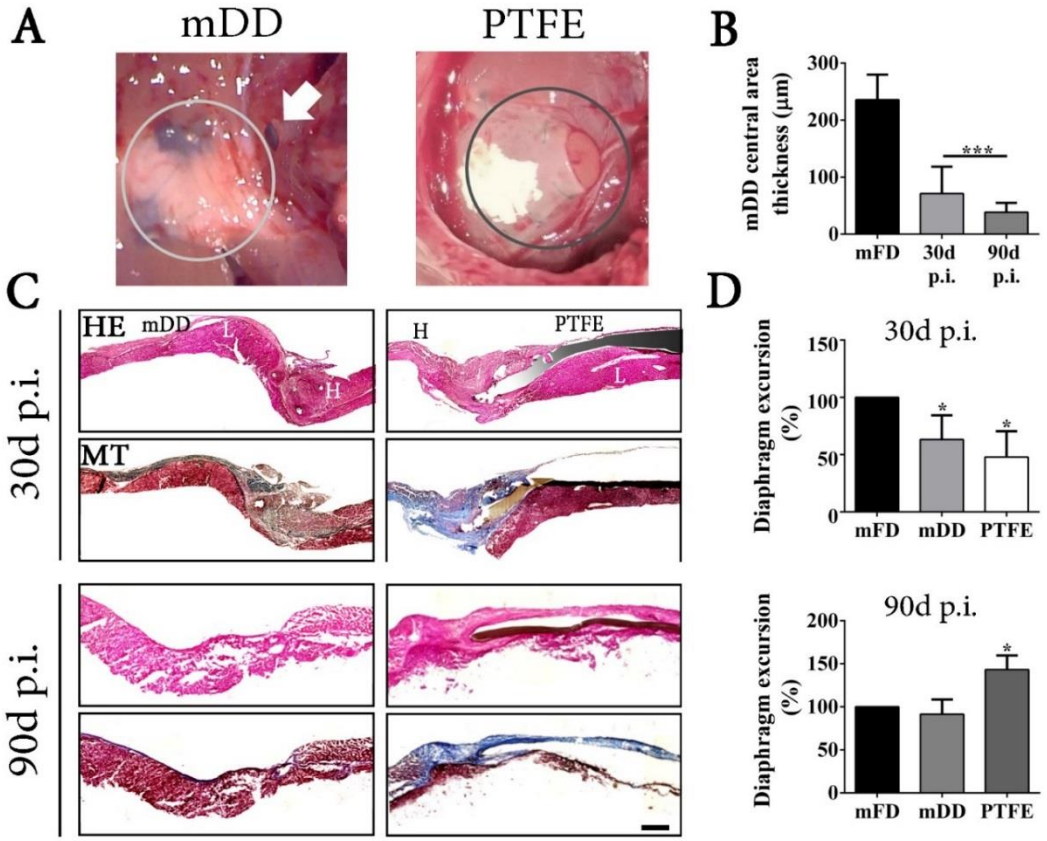

Figure 6.6 Macroscopic appearance and first measurements of mDD vs PTFE implant.

Outcomes after 30 days and 90 days from implant. A) Macroscopically, while mDD was well integrated with recipient muscle (mDD, light gray circle), PTFE displayed recurrence of the hernia (dark gray circle); B) TO confirm integration, it was evaluated level of remodelling in the central area; C) overview of the defected area covered with either mDD or PTFE, through time; D) diaphragm excursion was measured *via* echography. Arrow=Oesophagus hiatus, H=Host, L=Liver. Scalebar=100 µm.

6.2.2.3 Cellular response upon implantation

In the interval between 30 and 90 days, besides MyoD, which appeared to be slightly increased, the other analysed markers decreased. Interestingly, while displaying this trend, the proportion between PTFE and mDDs seemed to be maintained (Fig. 6.7). To be more detailed, the amount of Ki67+ cells was still not significant among the two conditions, as it was in the earliest time point (Fig. 6.7, B, D, both ns in Ki67). On the inflammatory side, CD68+ cells were more abundant in the PTFE implant than in the mDD, but then again the statistical difference from 30 to 90 days was kept (Fig. 6.7 B, D, both $p < 0.05$ in CD68). Last (thus far), MyoD was evaluated to determine the myogenic population response specifically. In this case, it was detectable in the mDD implants (Fig. 6.7 A, B, MyoD), whereas in the PTFE-implanted diaphragm it was very difficult. Hence it was thought of using another way to evaluate the effects of both scaffolds on such population, namely the qPCR.

All the result, calculated as fold change over the housekeeping gene β2 microglobulin (B2m), in any case, resulted significant among samples nor time points, since thus far only one set of samples was analyzed. Despite this, although only at transcriptional level, qPCR allowed to detect several myogenic markers, as well as providing a hint of the effects yielded by the implants. These, are summarized below.

Myf5. Expression was found to be lower than all other samples in both time points after PTFE implant, whereas mDD-implanted diaphragms had a comparable expression through time, slightly inferior than control (Fig. 6.7, A).

MyoD. The condition displayed at transcriptional level mirrored the issues experienced while trying to detect MyoD at protein level via IF. Indeed, control and equally PTFE-implanted samples expression levels were much lower than the ones measured for the mDDs (Fig. 6.7, B).

Myogenin. As seen for *MyoD*, the synthetic material did not seemed to have elicited an increased transcription of this gene. On the contrary, it appeared that the biological scaffold had much higher effect in this respect (Fig. 6.7 C).

Myh3 and *MyHC*. These early (the first) and late (the latter) differentiating markers had a different expression pattern. Apparently indeed, there has not been any change in mature fibers amount (Fig. 6.7, E), which were probably still in the early generation phase, as depicted by *Myh3* expression. Moreover, besides the marked difference among PTFE-implanted and mDD-implanted samples, in the first case young fibers seemed to decrease through time, whereas in the second levels behaved contrarily (Fig. 6.7 D).

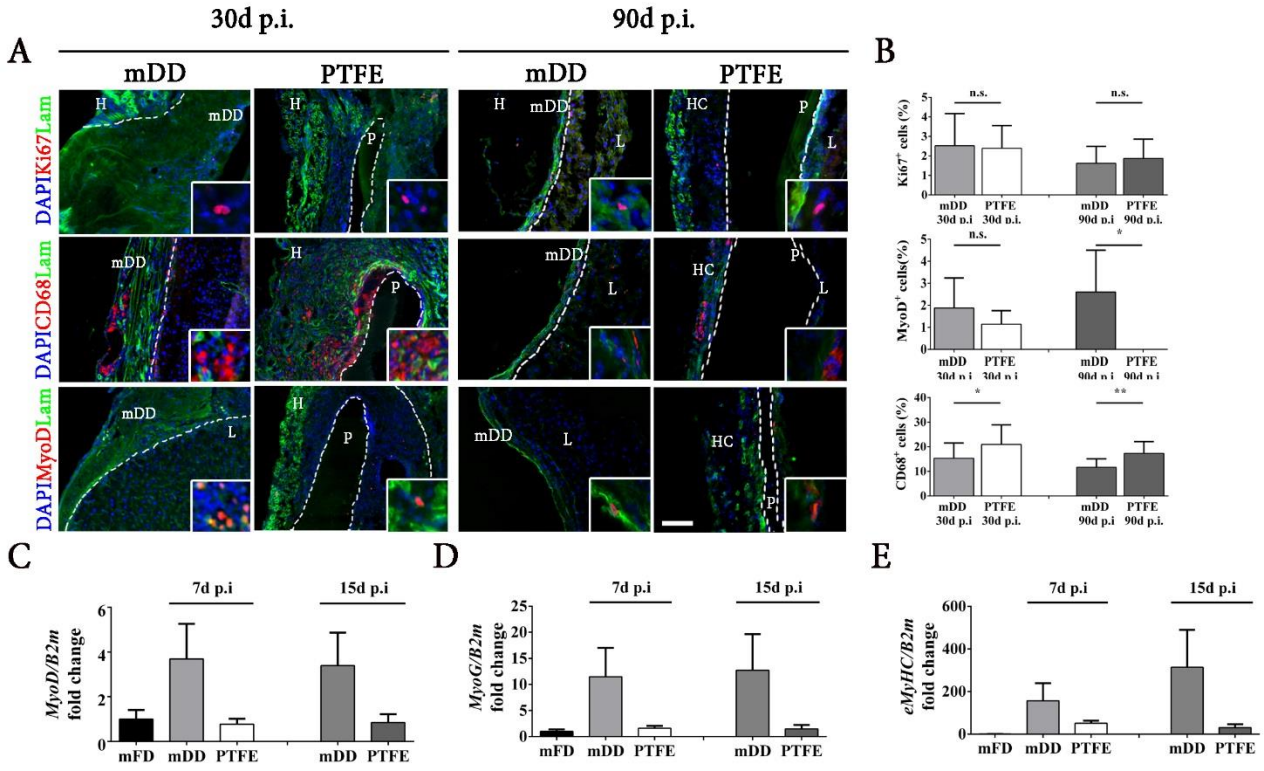

Fig. 6.7 Overview of cellular response in the implanted diaphragms

The response of the host was evaluated both at protein and at mRNA expression level. A) Comparison betwenn mDD and PTFE at both time point, for the proliferation marker Ki67, the pan-macrophage CD68 and the myogenic marker MyoD; B) respective quantification of each marker stained with IF; C) qPCR for MyoD , D) Myogenin and E) eMYHC (Myh3) genes. H=host, L=liver, HC=Host capsule. Scalebar=100µm

6.2.3 Autologous excised tissue as sham

The transplantation of vital autologous tissue excised either from the same animal undergoing surgery (autograft) or from another donor (allograft), was hypothesized or done by different groups, as control of the ideal TE construct to be delivered. In our case, an allograft was performed. The portion of a vital and healthy diaphragm from a syngeneic donor, matching the size of recipient defect, were excised and implanted to cover the defect. As this was recently done, thus far only histological coloration of the samples was performed.

6.3 Discussion

The high mortality still associated to CDH, along with the lack of a treatment to be considered ultimate, displayed by levels of recurrence in the patients managing to survive (ref Llosty2014, Leeuwen 2014), accounts for the increasing pursuit of the ideal strategy for a stable and positive outcome. The mortality rates, as well as the recurrence, increase accordingly to the type of defect, which in turn determines the degree of herniation into the chest cavity (Georgescu), which result in decreased lung performance accordingly. While approaches to repair the defect were tried also prenatally (ref), even evaluating to avoid lung hypoplasia *via* cell therapy in utero (IUT, [325]), the approach to date most frequently employed is surgical closure of the defect. These, range from primary closure or muscle flap auto transplant, i.e. for small defects, from the implantation of a synthetic inert material for mild to severe cases [154,230]. However, the composition of synthetic meshes often represent a double-edged sword, as on one hand, their non-absorbable structure allows a long-term preservation, on the other though, especially in large defects, their rigidity can lead to outcomes such as hernia recurrence (due to tearing) or even structural deformities [24,230]
Regenerative medicine, and subsequently TE, were born while trying to overcome, among other clinical issues, the problems related to the use of synthetic materials. Ever since, several approaches were studied, by applying the elements of this interdisciplinary field either alone [323] or combined

[116]. Amid these, the several features displayed by decellularized tissues allowed not only for translation of such into clinical trials, among which some also aimed at hernia repair, but also for their commercialization to large-scale distribution [232]

Previously to the present work, a mouse diaphragm was successfully turned into an ECM devoid of cells, then, the resulting decellularized scaffold, was characterized confirming not only its similarity to the original tissue but also its potentiality as therapeutic tool, under several points of view (Immunity, myogenicity, angiogenetic potential). Next in line towards clinical application of a decellularized diaphragm-derived scaffold, there is the validation in the environmental setting reproducing the defect meant to repair. With this aim, it was developed the first mouse model of surgical model of diaphragmatic hernia [319]. This model was subsequently used in a syngeneic environment to evaluate the decellularized diaphragm as potential tool for the repair of this defect compared to the material to date most commonly used (PTFE, [253]).

As expected, mortality rates of the animals were not due to a graft vs host rejection (further confirming absence of foreign cellular antigens), but mainly because of a poor recovery after surgical procedure. This is indeed a quite invasive procedure, reason why the surgeons are always pursuing for the best procedure also from this point of view [21,326]. Among animals that arrived to analyses endpoint, only one did not experienced weight gain, hence it was further confirmed that poor outcomes were not related to rejection. The particular differences between excursion of mDD and PTFE implanted diaphragms during breathing, measured *via* echography, may have different explanations, one per implant type, according to each material properties, and one physiological, which adds up to the other two. Starting from the physiology, the phrenic nerve might have been cut during surgery, thus removing the motor control of the defected area, resulting in a slower recovery not yet occurred after 30 days; in CDH this nerve instead finds, during development, other ways around [318]. The result seen at both time points with PTFE could be due to the stiffness of this material. Indeed, its lack of compliance may have caused its springing from one to the other side: every time the force applied by the action of breathing surpasses the yield point, PTFE experience a

plastic deformation, flicking towards the direction of inhalation/exhalation with a consequent higher force, thus resulting in a wider range. On the contrary, while at first the thickness and flexibility of the mDD may impair the fluidity of the breathing movements, the constructive remodelling occurred after 90 days, along with the thinner hence more compliant dimension of the patch, allow for an ameliorated movement. As suggested before, both implant type could have started from a further impaired situation, whether a portion of the phrenic nerve is excised. In general, focusing on the response gave by the mDD, the outcome was quite positive considering the excursion recovery experience, along with the lack of recurrence, since one of the scaffold alone concerns is that reabsorption might be too quick, thereby impairing a full recovery.

Coherently with previously reported outcomes of diaphragm implantation, liver was adherent to the implant area and, only in defects closed with PTFE, it was observed recurrence (as well in line with previous reports) [323], precisely by liver herniation. Moreover, again, lack of compliance cause by the stiffness of the synthetic patch, resulted in some cases in chest deformity due to the strain induced on the rib cage. Expectations on the appearance of the two implants at the harvest were fulfilled, with PTFE having the capsule seen 7 and 15 days after implant (chapter 4) whereas not being able to distinguish mDD from the recipient tissue.

Unlike previous experiments though, the starting condition of the muscle was an injury, hence microscopically, the regeneration environmental setting was quite different. Nevertheless, as introduced before while explaining diaphragm excursion, non-defected implant likewise the mDD experienced an elevated remodelling, becoming thinner during time, a normal consequence of *in vivo* remodelling kinetics seen with [259]. This time however, evaluation of the fibrotic response was more difficult, because the leftover ECM, as well as the FBR capsule, are mostly constituted by collagen fibers, thus markedly staining blue when performing MT coloration. Even so, if considering only the two ends of the defect, mDD-implanted diaphragm experienced much less fibrosis than the PTFE-treated. Additionally, histological coloration also displayed the better outcome of mDD, since higher number of blood vessels, again in the ends of the defect treated with the decellularized scaffold, along with small, regenerating fibers, could be found. This difference, could be the result of a less focused

response in the PTFE implants, which forces to restore the physiological condition are divided into both trying to repair the defect while continuously engaging a foreign non-absorbable material through FBR [312,327]. On the contrary, besides the previously demonstrated angiogenetic potential (*Chapter 4*) of mDD over the inert material, the other scaffold features collaborate and guide the host to a constructive response [104,221,328]. This was hypothesized and partially confirmed, also in the present study, to be happening via the molecules released during that very same constructive remodelling [223].

The cell response detected via IF, from one hand was in line with the result accounting for the healthy environment published by Piccoli et. al, , on the other, the molecular biology performed, underlined important aspects differently occurring, of the myogenic response specifically. Precisely, 30 days post-implantation, the amount of proliferating cells was less than 5% in both of the implants (coherent with the published data), whereas the amount of immune cells detected was prominent among the cell types (while in Piccoli et al. trended to baseline before this time point), but however significantly different between PTFE-implants, which displayed the higher amount. The myogenic response was studied in depth also this time, nevertheless, the qPCR results, being two completely different experimental sets, despite using the same type of control (healthy diaphragm) cannot be compared to the results seen before. As additional difference, both Myf5 and MyoD appeared to be active in both implants.In any case, since as depicted i) this environment sets differently from before (injury vs healthy) and ii) there is already an internal control treatment (mDD vs PTFE), this issues cannot be considered limiting.

Quite the opposite, comparison between PTFE and mDD allowed to appreciate the beneficial effects elicited by the latter, as well as being the right setting for testing aimed at clinical treatment of CDH [253]. For instance, all the myogenic markers analysed, which represent different differentiation phases, from activated progenitor (Myf5+ overlapping MyoD+) through myoblasts committed to fusion (MyoD+ overlapping Myogenin) until young formed fibers (Myh3) [329] , were more expressed in mDD implants. Moreover, while the early phase were stable, the maturing markers increased over time, whereas the PTFE situation stayed still for all.

Despite these outcomes, which in comparison to PTFE confirm the potentialities of decellularized diaphragm as repair alternative to CDH, the defect size of this model sets between the types A and B Bochdalek hernias. As consequence, although true that the double-edged sword of the neonatal setting (growth distress on scaffold vs higher staminal potential of recipient cell) was not took in account, we do not know whether the scaffold only approach would be enough. Indeed, the host cells alone, even if supported and instructed by the decellularized ECM, could not be sufficient to reach a functional remodelling/recovery complete enough to be considered adequate for clinical use in larger defects (types C and D) without additional help [155].

Therefore, as well as in general, there is space for improvement, for example aiming at the completion of the TE approach, by adding cells, signals or both. This, which was already tried in other models [154], could represent the right improvement in this model as well, leading to the delivery of a functional portion of muscle, able to better integrate with the edges of the defects, resulting in the restoration of a normal condition. With this in mind, the next step of experiments took place: to test the effects of allotransplant, as control of best condition [116,118,330] and the development of a recellularization approach, further discussed in the next chapter, aiming at re-vitalizing the muscle.

Chapter 7 : Evaluation of a recellularization approach

7.1 Introduction

7.1.1 Cells in TE

As described in chapter 1, to fall correctly under the definition of TE, the cellular component must be added to chosen scaffolding structure. Thus, not only the correct scaffold, but also the choice of an appropriate cell source is key for a successful approach. On top of the compatibility that cells must have, that translates in the ability of avoiding host's rejection, desirable features are high potency, proliferation and differentiation potential, while being non-tumorigenic. Cell sources are introduced below.

7.1.1.1 Embryonic stem cells

Originating from the ICM, Embryonic stem cells (ESCs) are the cell population deriving the three primary germ layers: ectoderm, endoderm, and mesoderm. Thus, this cell population can be defined as pluripotent as is able to expand into the majority of cellular lines except the extra-embryonic tissues only, which originate in the trophoblast that surrounds the ICM [331].
Due to the nature of their origin, hindrance towards clinical use of this cell population lies mainly on ethical and immunogenicity concerns. In fact, while tumorigenic potential could be avoided by terminal differentiation into the desired lineage (loss of pluripotency), increasing expression of Major Histocompatibility Complex class I (MHC-I) is observed upon commitment of these cells [332].
Hence, even though in an allogeneic context immunogenicity would be less compared to whole organ transplantation, some form of immunosuppression would still be required.

7.1.1.2 Induced pluripotent stem cells

Based on the idea that genetic material of a somatic cell is not lost upon differentiation, but lies inactivated and intact (40), Takahashi & Yamanaka selected 24 genes that had been associated with maintenance of pluripotency in ESCs and retrovirally transduced them onto mouse embryonic fibroblasts. Then, after obtaining colonies with ESC-like properties, each gene was removed one by one to assess whether there could have been one or more necessary and sufficient to induce reprogramming. After a huge screening, four were the factors found: Oct3-4, Sox2, c-Myc and Klf4 [333]. Cells resulting from transfection of only these four factor were termed induced pluripotent stem cells (iPSCs), as they exhibited ESC-like characteristics in the sense of morphology, proliferation and could form teratomas upon implantation as well.

After scaling to human origin, immunogenicity and ethical issues associated with hESCs were overcome. Indeed, since human iPSCs can be developed from an autologous biopsy, allogeneic immunogenicity is not a problem [334]. Still, the tumorigenicity associated to pluripotency remains a concern. Indeed, although these cells can be re-differentiated to different lineages, they were found to maintain a sort of memory from the somatic lineage they were derived [335]. Thus, iPSCs are currently being further investigated and have not scaled up to clinical applications yet.

7.1.1.3 Adult stem cells

In some tissues, cells turnover occurs normally, due to the presence of undifferentiated cells able to activate, proliferate and differentiate, without exhausting their reservoir (i.e. intestinal epithelium; skin). In other cases, a particular cell population is activated upon injury, with the aim of differentiating and restoring normal tissue physiology (i.e. skeletal muscle). As they are found in the adult, are able to self-renew and usually reside in a defined niche, they are generally defined Adult stem cells (ASCs). According to potency, they are usually broadly divided in [336]:

(i) Mesenchymal stem cells (MSCs). They are found in bone marrow, adipose tissue and likely in other tissues, in close connection to the vascular bed.
(ii) Progenitor cells as the organ-specific stem cells that have either a multipotent or unipotent role in organ regeneration [for example muscle Satellite cells (SCs), Mesoangioblasts (MABs)].

Many were the studies involving the application of ASCs, but most of them focused on the use of haemapoietic stem cells (HSCs) and MSCs, which have already found application in clinic for both allogeneic (55) and autologous (54) transplantation (59-63). While mostly on the cellular therapy side, a specific TE approach involving MSCs was already applied in clinic as well [220].

7.1.1.4 Amniotic fluid stem cells

With the aim of verifying the existence of a pluripotent cell population in the amniotic fluid, which was expressing Oct4 both at the transcriptional and protein level (79), de Coppi et al. not only confirmed the previous report, but also demonstrated that these cells were able to generate clonal cell lines. Remarkably, they seemed capable of differentiating into lineages representative of all three embryonic germ layers [337]. Named amniotic fluid stem cells (AFSCs) due to their origin, these cells are characterized by the expression of the surface antigen c-kit (CD117), the type III tyrosine kinase receptor of the stem cell factor.

AFSCs can be isolated from the amniotic fluid of humans and rodents and, once isolated, they can be expanded in feeder layer-free, serum-rich conditions without evidence of spontaneous differentiation *in vitro*.
While almost all clonal human AFSC lines express Oct4 and NANOG, which are markers of pluripotency, they do not form tumours when injected into severe combined immunodeficient (SCID) mice.

Interestingly, upon primary and secondary transplantation in mice, AFSCs display a multilineage hematopoietic potential [338]. In the presence of lung injury, AFSCs not only exhibited tissue engraftment, but also expressed specific alveolar and bronchiolar epithelial markers.
More recently, AFSCs were shown to integrate and ameliorate both a mouse model of necrotic intestinal injury [339] and a mouse model of spinal muscular atrophy [266].

7.1.2 Candidates specifically for SMTE

Throughout the years, several cells types were found to reside in the skeletal muscle, revealing different potential and role in physiological and repair processes of this tissue. Among these more than a progenitor cell was discovered to be able to take a myogenic fate and to differentiate into skeletal muscle, both in vitro and in vivo [340] Nevertheless, after all these years the population considered the main progenitor stem cell, responsible of the majority of the homeostasis of this tissue, are the Satellite cells (SCs) [341].
Besides resident progenitor cells, which as seen are categorized as ASCs, multipotent or pluripotent stem cells able to differentiate towards the mesodermal lineage, particularly into paraxial mesoderm, represent attractive candidates for SMTE.
Depending on the need, different approaches may be chosen, thus influencing choice of the cell population as well. Indeed, whether the aim is to repair a portion of the muscle or to re-create a whole muscle itself, ASCs may be preferred over pluripotent stem cells or vice versa. For example, the use of a population that can differentiate just into skeletal muscle could be considered sufficient to repair a damaged muscle, grafting functional skeletal units whilst leaving the subsequent muscle tissue growth, innervation and vascularization to the host's cells. Nevertheless, as many SMTE approaches displayed, outcome of the implantation varies significantly depending on scaffold properties as well (see table 1.1), making thus far unclear which cell population is the best.
Conversely, when considering the substitution of large portion of tissue, things become more complicated hence making unfeasible the use of just a type of ASC. Since is necessary to give the graft the adequate support to guarantee its survival and functionality, it is not possible to think of just

transplanting muscle units, but instead must be delivered a construct as complete as possible to rapidly integrate with the host. To this aim, cells able to differentiate into one or more germinal layers represent and advantage, because due to their potential, it could be possible to reproduce the development of the tissue with just one cell source, thereby ideally obtaining a construct closely resembling the natural counterpart. Alternatively, the combination of two or more progenitor cells could be used, prioritizing the structures that can help construct survival and integration. Actually, this second option was the only one already applied, with the first still being investigated, due to the time that manipulation and differentiation of pluripotent stem cells requires. In these approaches, cells to be combined were: i) a muscular progenitor population, to constitute the main component of the tissue, ii) an endothelial progenitor cell with known ability to form vascular networks in vitro and iii) cells able to interact and secrete ECM, namely fibroblasts.

In general, when considering which should be the right candidate, on top of the abovementioned desirable features for cells to be used in TE approaches (*section 7.1.1*) , cells should not only be able to reproduce mature skeletal muscle, but also it is highly desirable to reconstitute the natural SCs reservoir of the muscle. Furthermore, the more they can be expanded in vitro whilst maintaining these features, the better.

Cells used or considered for SMTE are summarized below.

7.1.2.1 SCs

Being the endogenous organ-specific adult stem cell population, prone to myogenic differentiation and specialized in muscle growth and repair, SCs show several advantages over other cell sources. Not only as resident they can be harvested from muscle biopsies, but also unique expression of the marker Pax7 makes possible to purify such population [342]. Their natural commitment towards the formation of skeletal muscle eliminates the manipulation that other cells may require to obtain progenitor cells with same potency, avoiding concerns about possible de-differentiation or tumour formation. However, this represents a sort of double edged sword, because in vitro expansion often leads to spontaneous differentiation, with loss of proliferative potential and stemness. Overcoming

this issue is not impossible though: as this has been linked to loss of contact with their natural niche, it could be sufficient to reproduce the same environment of the ECM in vivo. By this mean, growth of these cells in the right environment (i.e. acellular matrix derived from muscle) in vitro, or delivery in vivo taking advantage of the natural mechanisms that occur during muscle regeneration were tried. Although a degree of muscle growth and regeneration was found, these studies underlined the limits that using a single cell population represents, reflecting the complexity of the processes involved. Indeed, SCs interact with many other cells populations, which are known to help and improve muscle regeneration [47,343]

7.1.2.1 Muscle precursor cells

A step forward in the myogenic commitment, muscle precursor cells (MPCs) are commonly referred to as Myoblasts. Although not as stem as SCs, these cells display the same myogenic potential, and where shown to be able to restore their pool as well. Myoblasts can be considered the effectors of muscle repair, as they are the cells that, further differentiating into myocytes, will form new skeletal muscle. These cells are easily harvested and expanded from rodent and human muscle biopsy as well, in which can be further selected mainly through the specific marker CD56. One of the advantages of using myoblasts is that they and are naturally more numerous than SCs, which represent only the 4-5% of the whole muscle population [344]. Unlike their population of origin, there is also a commercial version of an immortalized line both for mouse (C2C12) and for rat (L6), which therefore can be ideally expanded endlessly, obtaining high numbers of cells. On one hand, this represents a great advantage when considering that one of the major limitations in TE is the number of cells, but on the other hand, their usage is limited in animal models, as the use of such cells cannot be translated to clinic. Another disadvantage of cell lines is that while being well characterized, they do not really reflect natural variety.

Though these cell lines are still used also in SMTE approaches, it would be preferable to use primary cells.

7.1.2.3 Other myogenic ASCs

Though as mentioned before SCs and MPCs are still the population of main interest when considering cells for SMTE, one of the main limitations to their usage is the low survival rate displayed in vivo [150]. as well as low migratory capacity. After many years of studies focused on skeletal muscle physiology, it is now largely accepted that other stem cells participate, at least to some extent, to its development and regeneration [345,346]. While displaying a multipotent profile, many of these cells are able of to differentiate into myogenic cells (upon certain conditions) and to migrate to (or at?) the site of muscular injury, thus representing a potential alternative to SCs and MPCs. Listed following are the worth-mentioning populations.

CD133+ progenitors cells: Already considered in a cellular therapy approach for muscular dystrophy, these cells displayed higher regenerative potential when compared to myoblasts. Moreover, the adhesion markers expressed right after isolation reflect their migratory potential. Limit to the use of these cells is due to their low number in the muscle [347].

Muscle derived stem cells (MDSCs): Can be considered an extremely enriched sub-population of muscle progenitor cells, which are isolated from muscle biopsied after many pre-plating passages, based on their late adherence when cultured. As CD133+ cells, comparison with myoblasts revealed a more favourable outcome for MDSCs upon transplantation.

PW1+ interstitial cells (PICs): Multipotential progenitor able to give rise to smooth, skeletal muscle and to fibroadipose cells, PICs were found to be involved in muscle repair through TNFα/caspase signalling. Though Pax7- while quiescent, upon injury they can express this marker and assume a myogenic fate [348]

SK-34: Another interstitial population, these cells express CD34 and Sca-1, but do not express myogenic specific markers nor CD45. These cells were found to be multipotential, as upon transplantation, they were able to differentiate into muscular, vascular and neural glia cells [349].

Mesoangioblasts (MABs): So called due to their vessel-associated location and to their mesenchymal differentiating potential, MABs already reached the pre-clinical large animal level, with promising results. Another advantage of these cells is the high migratory potential [91].

Myogenic Endothelial Cells (MECs): As the name suggests, MECs express both myogenic and endothelial specific markers, i.e. Pax7, CD56 (humans), CD144 and CD34. Moreover, they display osteogenic and chondrogenic differentiation potential. Human MECs were used in a SCID model of cardiotoxin injury, revealing a more efficient muscle repair compared to myoblasts.

Pericytes: These cells became more interesting as, recently, were found to be closely involved in the regulation of vessel formation. In vivo, they are mural cells found in micro-vessels in close contact with both endothelial cells and basal lamina. Pericytes have great plasticity, emerging as a heterogeneous population able to differentiate into smooth muscle cells, adipocytes, osteoblasts, chondrocytes and myoblasts. Not only, as for MECs, transplantation in the cardiotoxin-injured muscle of SCID mice led to positive outcomes, but later it was also demonstrated that pericytes contribute to muscle growth and satellite cells pool [350].

7.1.2.4 ESCs and iPSCs

Since ESCs and iPSCs can differentiate into the three germ layers, to direct their fate into a specific one or even more precisely into a particular cell lineage, an accurate and complicated management of their genetic program is required. Thus far, while generation of functioning muscle cells has been achieved by forcing the expression of muscle specific transcription factors (such as Myod1, Pax3 and Pax7), these strategies usually yield a population which reflects poor control and reproducibility, as percentages of the target cell population varies. Among these, there was also a study using differentiated ESCs to restore a cardiotoxin-injured muscle [351], which on one hand displayed no de differentiation nor teratoma formation whilst regenerating the muscle and even the SCs, on the other did not documented the efficiency nor the degree of differentiation of the cells. Lately, alternative approaches taking advantage of molecules able to modulate signalling pathways to induce a paraxial mesoderm fate. Although efficiency and precision in the determination of the fate was increased, length and complexity of the protocol still makes cost and feasibility for clinical translation a limit [352]

7.1.2.6 MSCs

Due to their well-known multipotency, mesenchymal stem cells (MSCs) have also been considered as potential source; moreover, they can be isolated from several adult tissues. Free from ethical issues compared to ESCs, their myogenic potential has been already elucidated in several studies [353]. Another advantage of these cells, is that they have been proved to have an immunomodulatory effect as well, hence they adhere to the non immunogenic criteria transplanted cells must have, helping the regeneration of the muscle. As summarized in table 1, so far MSCs were tested combined with autologous acellular muscle in a VML and in a CDH model [115,116], but while representing an improvement compared to other constructs, the outcome of the implantation still resulted in limited regeneration.

7.1.2.7 AFSCs

Recently, AFSCs were tested in a model of spinal muscular atrophy (SMA), in which these cells were able to both integrate in the muscle during its regeneration and to replenish the SCs niche [266]. Others, differentiated human AFSCs into myogenic cells by either taking advantage of a combination small molecule/myogenic environment or by directly forcing the expression of the gene MYOD by lentiviral transfection [354]. In general, AFSCs proven to have immunomodulatory properties as well, thus making these cells a potential candidate not only for SMTE but also for many other regenerative medicine applications [355].

7.1.3 Methods to combine cells and constructs in SMTE

It is necessary to keep in mind that although possible to implant a scaffold alone, either artificially functionalized or not, thereby relying on endogenous cell population for the cellularization and remodelling, this approach cannot really be considered a TE approach. In SMTE as well, the

combination of the cellular component and the scaffold, must be done beforehand. In the past decade, the techniques tested for scaffold cellularization were many, but can be summarized as follows:

- Incorporation of the cells in a liquid form of the scaffolding material, which is then stimulated to solidify [91]
- Plating the cells in particular mechanic condition, thereby ensuring the self-assembly of autologous secreted ECM [87]
- Seeding of the cells on top of the scaffold, trying to take advantage of either their innate ability of migrating into the 3D structure, or of the scaffold porosity [116]
- Lately, on top of injecting the cells in the muscular tissue, it cells were also perfused. This however was possible just because the vascular tree was left intact, as a whole limb was decellularized via incannulation [92].

In general, the choice of which method to use aiming at re-creating a tissue as efficiently as possible, not only depends on cell source, but also on scaffold properties. Indeed, if the scaffold is an acellular matrix derived from native tissue, 'only' seeding/injecting or perfusing the cells is possible. This however does not necessarily represents a limit, because as said the starting structure already closely resembles the originals'. Next, once determined the method to combine cells with the scaffold, of extreme importance is the choice of growth condition of the construct. Indeed, to guarantee cell survival, proliferation and differentiation in the scaffold, is the necessary condition in order to build an organ or a tissue in vitro, or to stimulate its regeneration in vivo. To achieve this, the construct can be i) grown controlling and recreating the ideal environment artificially or ii) implanted in vivo right after combining cells and scaffold, thus taking advantage of the stimuli and nutrients delivered by the host tissue [220]. While in case of in vivo implant choices are limited to the location in which the construct will grow (excluding direct orthotropic delivery of the construct, usually a highly vascularized area), in vitro growth gives rise to a variety of conditions that can be applied. In detail, culture condition can be static or dynamic. In both cases, it is possible to control cells fate accordingly to differentiation protocols of given population (i.e. exposing the construct to cytokines, small molecules or through the variation of nutrients in the medium), but dynamic condition adds variables that can enhance efficiency of cell integration via mechanical and/or electrical stimulation as well.

Hence, static condition can be carried out normally, using same culture condition of cell lines, whereas dynamic condition will require a machinery allowing a further control of the environmental condition, namely a bioreactor. Ideally, bioreactors can enhance construct cellularization and allow the growth of larger portions of tissue to even entire organs, allowing the delivery of a more complete construct.

7.1.3.1 Platelet Gel to support cellularization and graft remodeling

While recreating the ideal conditions for cell growth, survival and differentiation through the abovementioned conditions, it is also possible to add to scaffold or to cell preparation molecules and nutrients that can boost and help the preliminary phases of cellularization and, in vivo, constructive remodelling. To this aim, a potential candidate is represented by platelet gel (PG), a gelatin-like substance obtaine by activating platelet rich plasma (PRP) took from cord or pheripheral blood, with either human thrombin or batroxobin, supplemented with calcium gluconate [356] PG is known to be rich in several growth factors, previously contained in the platelet granules, as PDGF, TGFbeta1, HGF, basic FGF and VEGF, thereby allow the delivery of a multiple set of factors with a single preparation. Another advantage of PG is that it has been already employed to improve tissue repair in orthopedic, oral maxillofacial, dermatological surgery , and muscle injuries, hence is already clinically approved. Moreover, although PRP was not considered immunogenic so far, it is possible to reduce risks by concentrating the factors released through a series of centrifugations, as most of these remain in the supernatant fraction of PG (SPG). Therefore, both PG or SPG can be used for cell delivery. For SMTE interests in particular, not only it has been demonstrated that PRP favors the proliferation of hMPCs whilst maintaining either stemness and differentiation abilities, but it is also considered an useful tool to modulate regeneration and fibrotic response in the muscle [357,358].

7.2 Results

7.2.1 Development of a methodology aimed at scaffold recellularization

7.2.1.1 Cell delivery method development

Considering the width of the diaphragm, two methodologies were tested: i) to seed on top or ii) to inject the cells into the decellularized tissue. As the most limiting condition, set up of the methodology was performed on mDDs only, whereas rDDs were used only once protocol was set. Moreover, for simplicity only one cell population (mSCs) was used. Outcomes of the two procedures are described below.

Seeding on top. A common methodology used aiming at recellularization, in our case was not as efficient. Although allowing in most cases survival of the cells, these were found stuck on top of the tissue, thus not being able to integrate nor migrate into the scaffold (Fig. 7.1 A). This though might be due to the known low migratory ability of the used cells (ref), supported as well by recent studies (ref ghost fibers).

Injection of cells. Unlike seeding, which does not require any particular tool, while developing this method thinness of the scaffold had to be taken in account designing this method, because a piercing material too big would have certainly damaged the tissue excessively. With this aim, 27, 29G syringe were firstly tested, but it was immediately felt that they were not suitable. Secondly, 31G needle insulin syringes and the pulled tip of a Pasteur pipette (which were comparable in size) were tested (Fig. 7.1 B). However, since another parameter to consider was the tool that could ease the procedure the most, the Pasteur pipette was discarded, as it required a complicated setting (operator had to suck and blow from a tube connected through a filter to the pipette, while holding the pipette as well). The 31G syringe, similarly to the other insulin syringes, had a piercing surface that was considered too damaging. The last tool tested was a 33G Hamilton syringe. This was the final tool chosen, as it was both easy to handle and allowed to pierce the scaffolds within their size, without causing damages big as the whole width (Fig. 7.1 C).

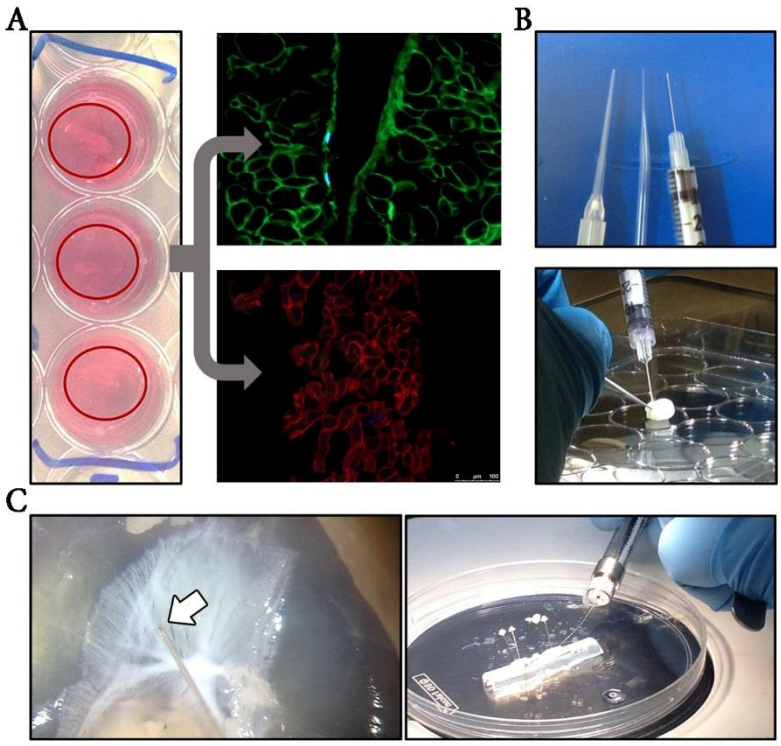

Fig 7.1 Schematic representation of method development.

The use of the 33G came up after several tests. A) Simple seeding efficiency was not successful, and cells did not seem to stay attached to the scaffold; B) It was then thought of an injection, from left to right: a tip for gel loading, a head of a glass pipette molded with fire and a 31G needle; C) Microscopic appearance of a 33G needle compared to a mDD on the right, while left is a final procedure step.

7.2.1.2 Culture condition evaluation

Considering the importance of the culture conditions (as described in the general introduction), several settings were tested alongside delivery method. These, were decided accordingly, then further enhanced considering the nature of the scaffold (muscle). Culture conditions, described below, kept all 7 days during the method development.

mDD patches on the bottom of a well plate. Scaffold patches were simply placed on the bottom of a 24w plate, then covered with culture medium. This condition was only used for seeding experiments (Fig. 7.2A; Fig. 7.1 for outcomes).

mDD as whole in a well plate. Tried with either seeding or injection, taking advantage of the support that the rib cage naturally gives to the diaphragm. Whole mDDs were covered with medium as for the previous condition (Fig. 7.2 B). Although on one hand an ideal condition due to the perfect matching measure fitting a 24plate well and to the position maintained thanks to the rib cage, on the other this setting made size matter. Indeed, the amount of medium needed was much higher that the quantity required in the previous setting, moreover, the second thought was that also cell number required and/or consequently time needed for repopulation had to (or would have, considering time) increase.

Harbor structure. A prototype system designed by Harvard Apparatus, this was tested only in the injection setting. Although originally intended to be used in a bioreactor, it was used in static culture instead, placed on the bottom of a 75 cm^2 flask, then covered with medium (Fig. 7.2 C, right). This support was particularly interesting because, besides the potential use in a bioreactor, the mounting setting represented also a form of tensile stimulus (Fig. 7.2 C, left). The harbor was used with mDDs and in the preliminary experiments with rDDs.

Semicircular silicon support. Tested in both seeding and injection. The semicircular shape reproduced in a way the dome shape of the diaphragm, while the silicon allowed a firm fixation of the specimen to the support (necessary to ease injection) using pins. Moreover, by pinning the tissue in a tense fashion, the semicircular shape of the support could reproduce the dome shape of the diaphragm. Length was set to fit a well of a 6well plate, which was used for culture (Fig 7.2 D). This condition was tested only with mDD.

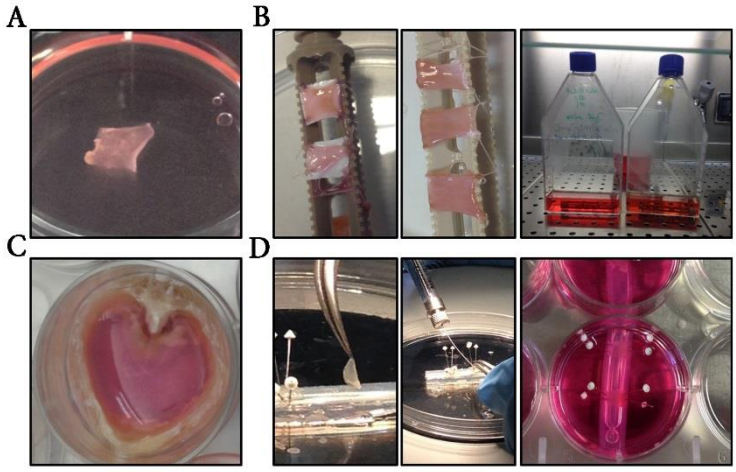

Figure 7.2 Different culture condition used for DDs

Culture condition varied according to the method. A) Seeded scaffold were placed on the bottom of a well, B) harbour served for both injected mDDs and RDDs; C) It was tried the culture maintaining the rib cage as if it were a well; D) last, the best setting so far was the use of semi cylindrical tubes.

7.2.2 Characterization of selected cells

Cells to be tested in recellularization experiments, isolated and cultured as described in 1.9, were characterized beforehand. Features of each is described below.

7.2.2.1 mSCs

Isolated mSCs could be expanded avoiding the contamination of other cell types, as depicted by the rounded (typical of stem cells) or spindle shape (Fig. 7.3, A), by using an well-known protocol aimed at 'stripping' the SCs from the isolated fibers (ref Luca, Anna, original? Guarda tesi). Cells were expressing as expected, Pax7 as well as expression of other myogenic markers such as MyoD (Fig. 7.3, B). As control of myogenesis, differentiation was induced. IF to detect MyHC displayed the formation of several myotubes (Fig. 7.3, C).

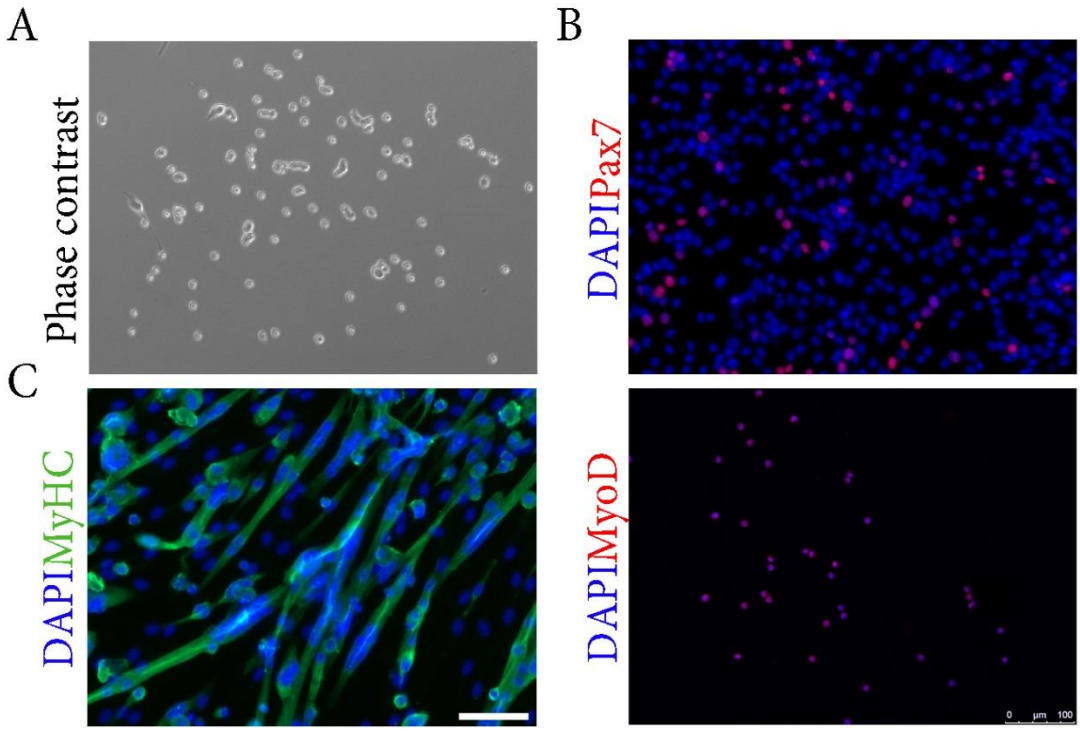

Fig. 7.3 Schematic representation of mSCs used

Isolated SCs display the typical A) round shape, express B) myogenic markers Pax 7 and MyoD (stem and early myogenic respectively) and can differentiate upon stimulation, forming C) myotubes $MyHC^{+}$. Scale=100um

7.2.2.2 mFbs

Fibroblast could be easily expanded and in short was first the predominant, then the only population present in culture, upon isolation from a mFD (ref anna u). Several Ki67+ cells were found while in culture, confirming proliferation state of cells before injection (Fig. 7..4, A). For mFbs, unfortunately, thus far the recognition relies mostly on morphology of the cells, however, to underline the typical fibroblast shape, a staining for Vimentin was performed (Fig. 7.4)

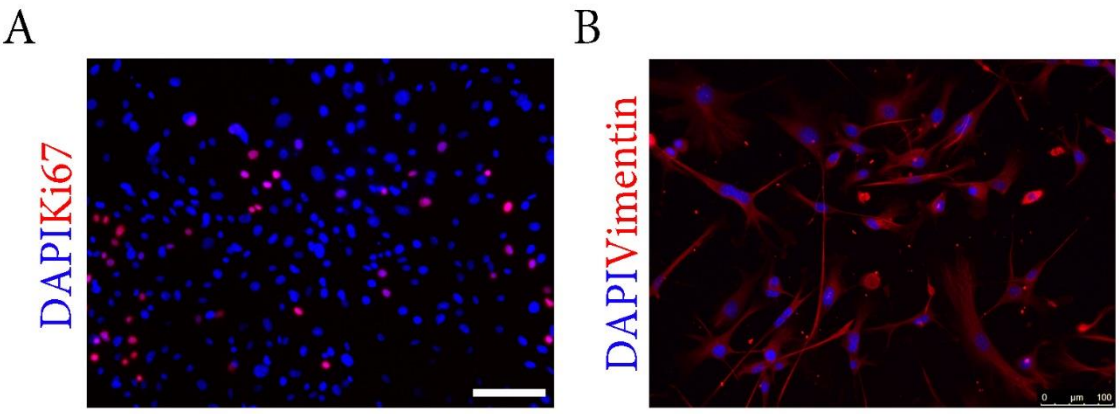

7.4 Exemplification of cultured mFbs.

The high proliferative state typical of these cells was coherent in these cultures as well. A) $Ki67^{+}$ cells; B) Recognition of fibroblast shape by staining of Vimentin.

7.2.2.3 mMPCs and mFbs resulting from whole muscle digestion

Cell isolated by digesting the whole muscle were less easier to expand without interferences resulting from the mFbs intrinsic higher resistance and proliferative state, compared to other populations, which are usually decrease in number through passages (i.e. mSCs) or even disappear after first (i.e. Neural cells, Immune cells) or second passage (i.e. ECs) if kept in altogether. Nevertheless, though starting from a fair variety of cell types (Fig. 7.5, Phase contrast) our culture condition resulted in a good balance between mMPCs and mFbs at early passages (Fig. 7.5). This, was also confirmed by different morphology highlighted by Vimentin IF (Fig. 7.5).

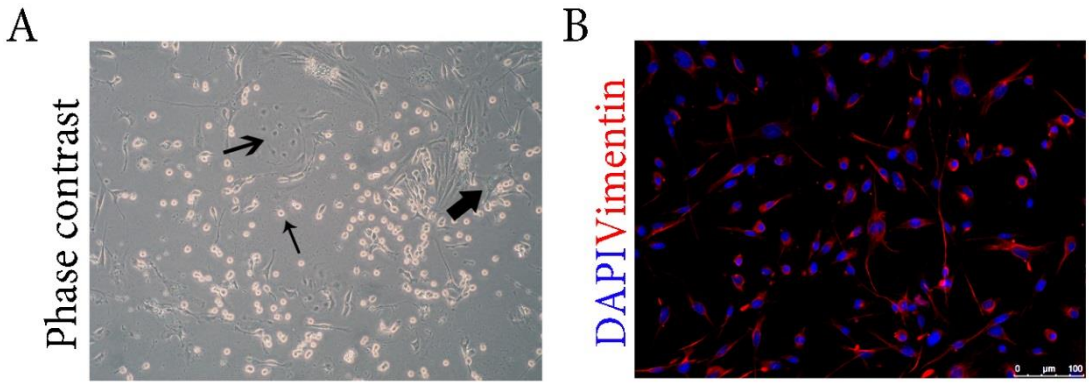

Fig. 7.5 Cells variety isolated by whole muscle digestion.

Unlike single fiber isolation, by isolating the cells from the whole muscle the variability is higher. A) Primary culture (p0) has, besides muscle cells (thin arrow), also other cell types like ECs (medium arrow) and Fbs (thick arrow); B) after the first passages this variety is usually lost and only mMPCs and mFbs persist.

The amount of Ki67+ cells was high, indicating that cells were comfortably growing (Fig. 7.6, Ki67). Myogenic marker expression allowed appreciating the variety among mMPCs, which could be found still in a stem-like state (Fig. 7.6, Pax7) or as myoblasts (Fig. 7.6, MyoD). By inducing differentiation, it was possible to evaluate differentiation potential as well, which was detected as MyHC+ myocytes/myotubes (Fig. 7.6, MyHC)

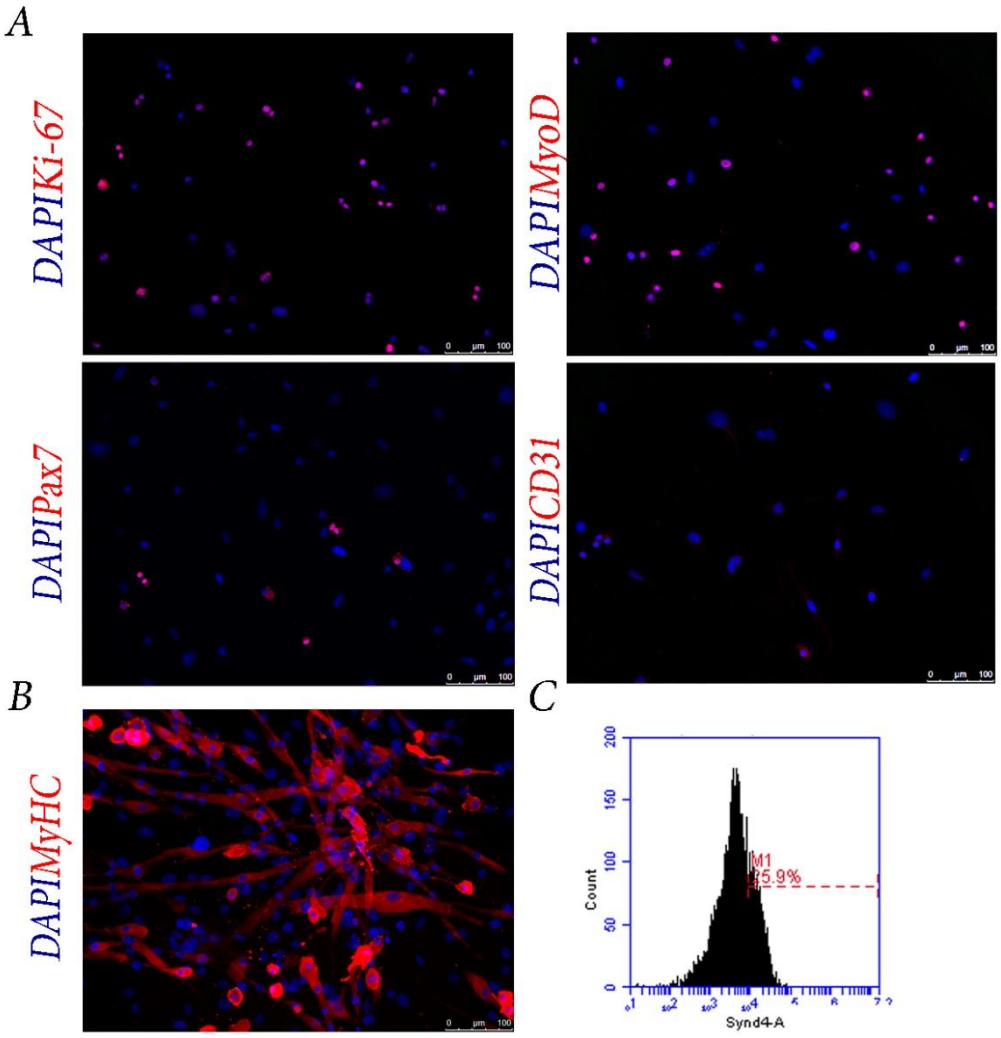

Fig 7.6 Exemplification of proliferation and profile of the whole muscle population.

Despite the variety displayed, cells become with time more and more myogenic. A) There seem to be a good balance between proliferation (Ki67) and quiescence or early state (Pax7 and MyoD), before p2 is still possible to find cells which are not myogenic or fbs (CD31); Cells able able to readily differentiate (MyHC); C) proportion of Syndecan-4 cells by Flow cytometry (marker of satellite cells). Synd4=Syndecan-4

7.2.2.4 phMPCs

While at first it was thought of using adult biopsies , the higher potentiality in the paediatric ages make the biopsies more interesting, although much less frequent. The protocol recently published

(ref Franzin C et al. 2015), allowed to isolate MPCs from human paediatric biopsies as well as from adult muscle. Donor age and biopsies number are summarized in table 7.1.

Table 7.1| Summary of paediatric biopsies used for cell seeding

Donor	Birth date	Sex
1	2008	M
2	2002	F
3	2009	F
4	2011	M
5	2014	M
6	2000	F
7	1998	M

As human, percentage of muscle precursor cells could be easily evaluated by CD56 flow cytometry (FC), as indicator of efficient isolation and expansion of myogenic cells (Fig.7.7 A; from an average of 92.17 ± 5.41% at p3 to a 87.8 ± 1.4% at p5). In general, both isolation and expansion were considered successful whenever the phMPCs reached or surpassed the 80% of cells. Doubling time, calculated in order to evaluate the proliferation abilities throughout passages, reflected the youth origin of these cells (mean 22.65 ± 2.089 at p3, 25.10 ± 3.57 at p5 and 22.44 ± 1.22 at p8, expressed in h, Fig. 7.7 B). Expression of Ki67 was used as additional proliferation index (Fig. 7.7, D). Same as the other cell populations, myogenicity assessed via the muscle-specific markers (PAX7, MYF5 and MYOD), in order to both confirm FC analyses and evaluate distribution among the myogenic lineage, was consistent with the previous result (considering probable transitory double positive cells) at equivalent passage (Fig. 7.7 D). Overall, $KI67^{+}$ cells were 52.62 ± 4.52%, $PAX7^{+}$ cells were 21.50 ± 2.26%, $MYF5^{+}$ cells were 64.02 ± 2.51% and $MYOD^{+}$ cells were 52.68 ± 3.08%. The percentage of myogenic cells seen with FC was further confirmed by the almost complementary proportion of fibroblast (mean 22.50 ± 3.34% of cells, Fig. 7.7 C), which was measured through IF against TE-7, a recently discovered human fibroblast specific marker (Fig. 7.7, D, TE-7).

Lastly, this percentage of non-myogenic cells was not an impairment, since the maintenance of a good differentiation capacity of the myogenic cells. MyCH+ myotubes, could be formed indeed efficiently, confirming potentiality of these cells (Fig. 7.7, D, MyHC).

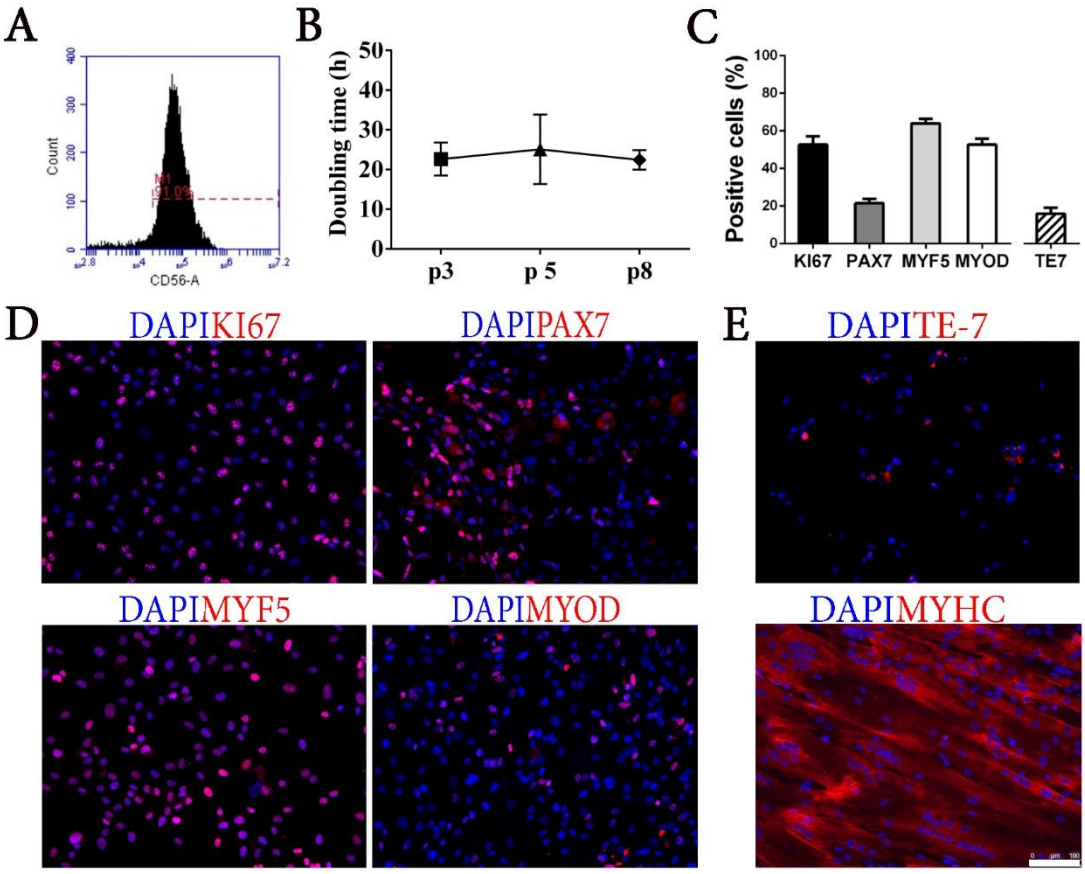

Figure 7.7. Human MPCs characterization.

Characterization panel for phMPCs. A) Histogram representing the percentage of $CD56^{+}$ cells (p5); B) doubling time (hours) of human MPCs; C) quantification of KI67+, PAX7+, MYF5+, MYOD+ and TE7+ cells; D) IF performed at p5 for KI67, PAX7, MYF5 and MYOD D) IF performed at p5 for TE7 upper panel and MyHC down below. Scale bar:=100 μm

7.2.2.4 hMFbs

As for mFbs, it was possible to obtain a pure culture of hMFbs every time the isolation procedure yielded a low number of CD56+ cells, simply expanding the culture. As less limiting population, it was cultured in the same medium as phMPCs, which did not seem to affect hMFbs healthy state (Fig. 7.8).

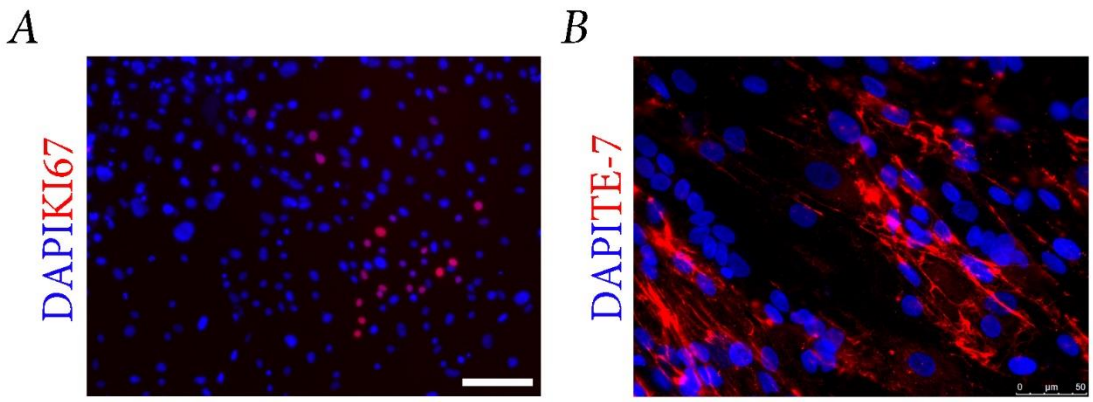

Figure 7.8 Exemplification of hFbs cultured in hM-GM

7.2.3 Evaluation of mDD recellularization

Among the tested settings, the two elected methodologies were: i) Injection in the scaffold mounted in the harbor and ii) injection in the scaffold fixed to the semicircular tube. Also, while among the different cell populations chosen, only mSCs co-injected with mFbs were used with the first method, for the second were preferred mMPC or hpMPC, since the isolation was more practical.

7.2.3.1 Injection with mSCs and mFbs

Various degrees of cellularity were observed in the different samples analyzed, but in all cases, most of the surface was colonized, whereas the inner part was less homogeneously populated (Fig. 7.9). Interestingly, cells still proliferating although in differentiating condition, were detected more on the surface (Fig. 7.9 A, Ki67). The ones expressing less committed myogenic markers (Fig. 7.9 A, MyoD), as well as differentiating (Fig. 7.9 A, MyHC), were instead found across all the populated areas. The disproportion between proliferating and differentiating cells, was however expectable from cells growing in differentiating condition (Fig. 7.9 B, Ki67 and MyHC on graph). Notably, it did not seem that particular interactions occurred among cells and the surrounding fibers, which appeared in close contact more likely due to the deposition done with the injection, preferring to grow and secrete laminin on their own, or growing on the surface, rather than a real attachment or integration (Fig. 7.9, Arrows).

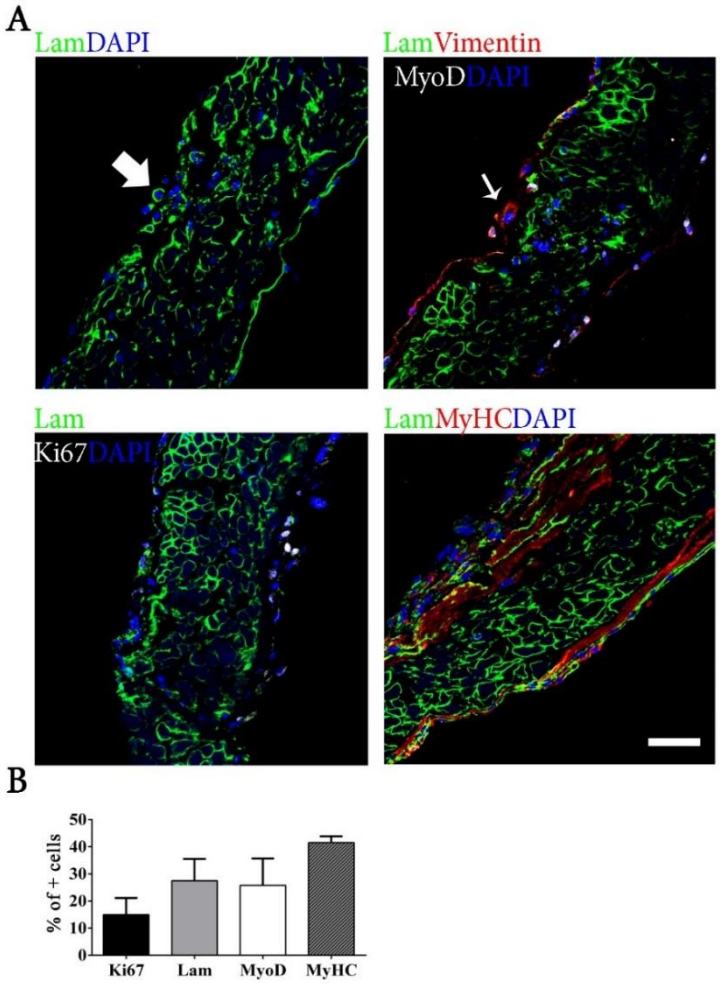

Figure 7.9 Summary of outcomes co-injecting mSC and mFbs grown separately.

Compared to seeding only, injection and harbour growth system led to much better results. A) Cells deposit laminin (thick arrow), express marker such as MyoD, proliferate and cooperate with fibroblasts (thin arrow), finally growing into layers of $MyHC^{+}$ cells. B) Quantification of markers detected *via* IF Ki67 14,96 ± 2,756, Lam 27,54 ± 3,572, MyoD 41,53 ± 1,328, MyHC 25,75 ± 4,973. Scalebar=100µm

7.2.3.2 Preliminary results of injection with mMPCs on semi cylindrical tubes

Consistent with the results seen with the co-injection, the use of a single population originally mixed but with a similar type of cells (mSCs, mMyoblasts and mFbs) leaded to a comparable distribution in the injected mDDs. Actually, proportion between surface and inner part of the scaffold looked better, as cells seemed more evenly distributed (Fig. 7.10). Not surprisingly, the amount of proliferating cells was coherent with the differentiating conditions sustained during culture (Fig. 7.10, A, Ki67). On the contrary, the distribution along the myogenic commitment span was shifted towards the differentiation (Fig. 7.10, B).

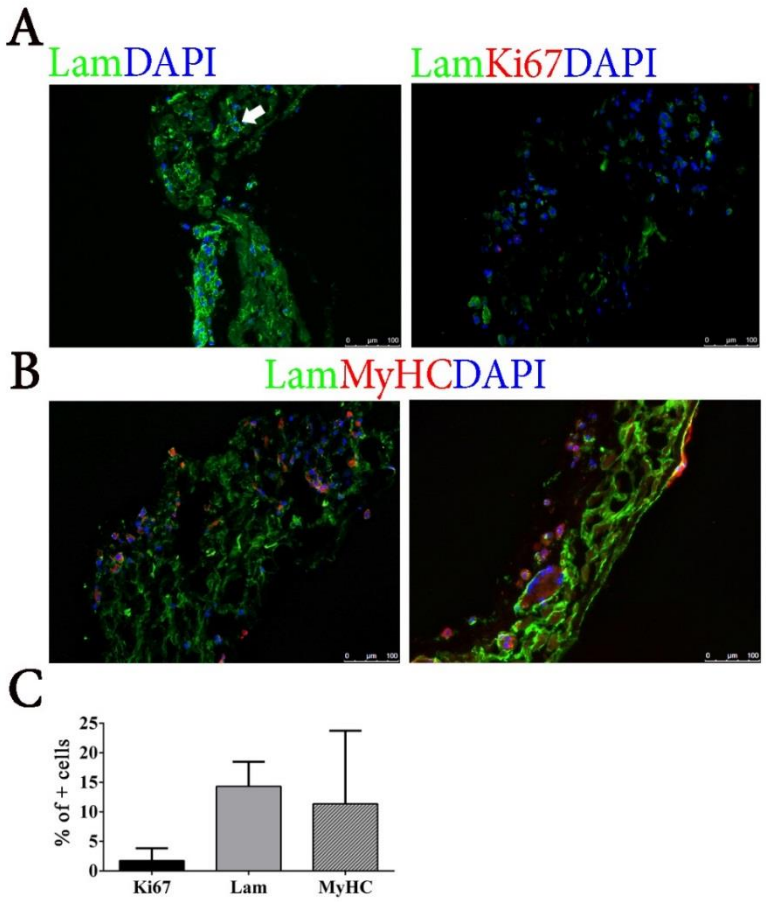

Fig 7.10 Summary of preliminary results with mMPCs

Results staring already with a combination of myogenic and a little of non-myogenic cells seem to reproduce what seen with the co-injection. A) Also in this case cells depositing laminin on their own were found (arrow); cells were found to be Desmin positive, as expected from myogenic cells, while the proliferating cells (Ki67) were low as expected, being in differentiation; B) Remarkably, mononucleated and mature myotubes could be found; C) Quantification of markers in this set of experiments.

7.2.3.3 Injection with phMPCs

Presence of cells was successfully detectable also after injection of phMPCs (Fig. 7.11), which seemed to have distributed more homogeneously. Same as mMPCs, on the surface of the scaffold cells started

to group and tended to grow in layers, where the scaffold seemed more remodeled. Proliferation detected were in line as well (Fig. 7.11 A, KI67). The amount of PAX7 expressing cells instead, despite the differentiating condition of culture, could be resulting from the paediatric origin of these (Fig. 7.11, A, PAX7. Later myogenic markers (Fig. 7.11 A, MYF5) was considerably low, whereas SAA, a marker of late differentiation, was found at a percentage (Fig. 7.11 A, SAA) that could match the different between quiescent and differentiated cells, as well as the proliferating (considering the presence of cell in an intermediate state).

Last, another additional analysis step was performed by molecular biology. The following preliminary results were aimed at further assessing the expression of specific myogenic genes in injected mDDs. The housekeeping *β2-microglobulin* was used as marker of basal expression for comparisons. Both early (Fig.6.20, MYOD) and late (Fig. 6.20, MYHC) genes were expressed in all loaded samples, endorsing the results previously obtained, remarkably, it was also possible to detect expression of *Dystrophin*, whereas differently, the other common myogenic marker MYF5 (Fig. 7.11, A, MYF5) was detected only in the cultured cells control.

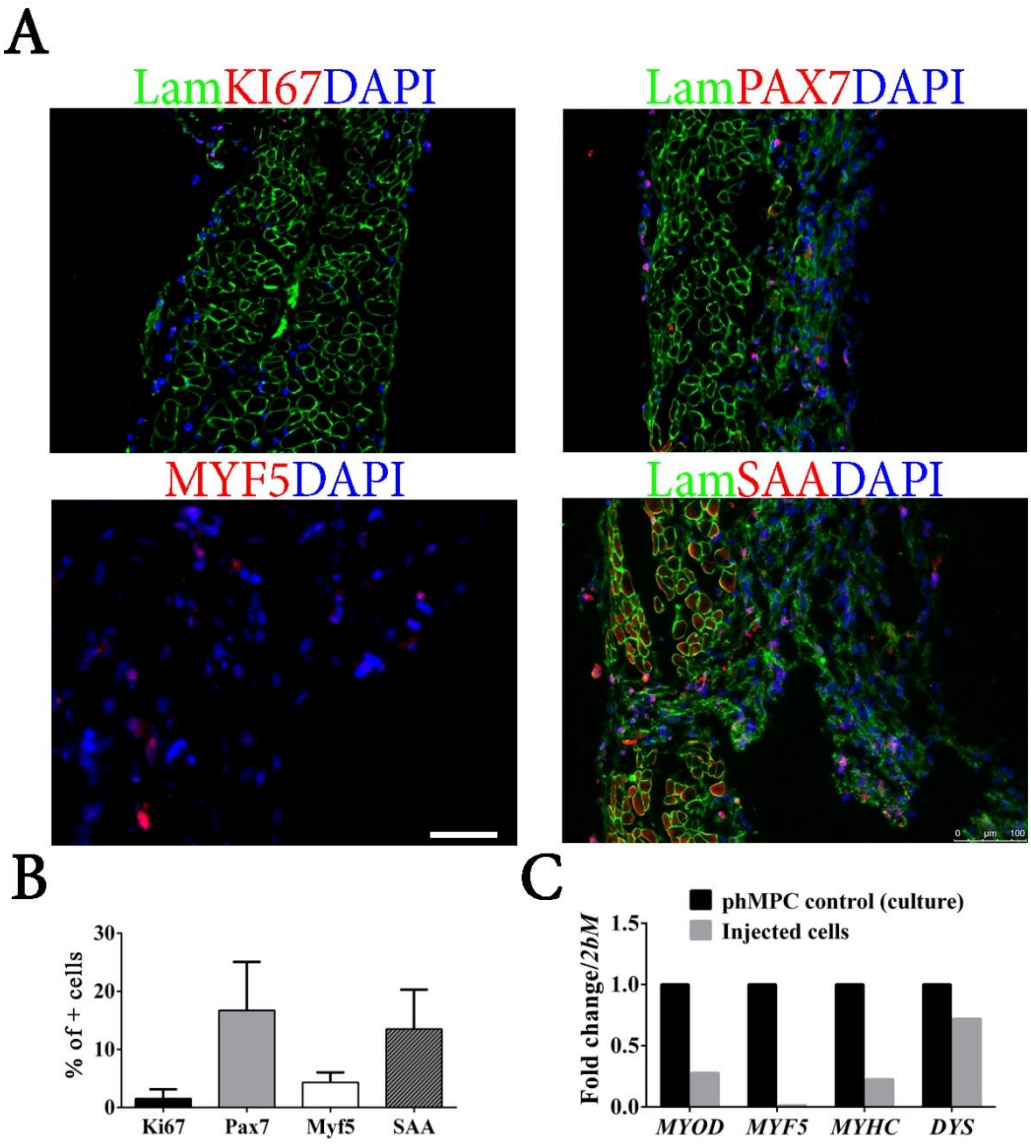

Figure 7.11 Overview of phMPC injection outcomes

phMPC are an attractive choice, both able to maintain stemness and to differentiate. A) Proliferating cells were low also in this experimental set (Ki67), but the amount of cells PAX7^{+}, along with the committed marker MYF5 and SAA are coherent, indicating that proliferation phase had ended; B) Quantification of the markers detected via IF; C) qPCR of myogenic markers

7.2.3 Preliminary recellularization test with rDD scaffold

Efficiency of cell injection was higher than the observed with mDDs, more likely because of both larger surface and width of rDDs, as demonstrated by distribution both inside and outside the scaffolds (Fig. 7.12). Interestingly, while on the surface cells reproduced the layered organization seen in mDDs, in the inner part the majority positioned either circularly around pre-existing fibers (Fig. 7.12, thick arrow) or in a circular fashion as well, but forming clusters in the interstitial space in-between (Fig 7.12, thin arrow). In both cases, new laminin seemed to have been secreted and deposited, since some cluster were formed by a multinucleated laminin envelope. Another interesting feature of injected cells was the expression pattern of laminin and vimentin. Indeed, it seemed that in most cases expression of these two proteins was mutually exclusive (Fig. 7.12, laminin-vimentin). Expression of myogenic specific markers, such as Pax7 and Myogenin, indicated the differentiation state of mSCs as both still progenitors (Fig. 7.12, Pax7+ cells) and committed (data not shown)

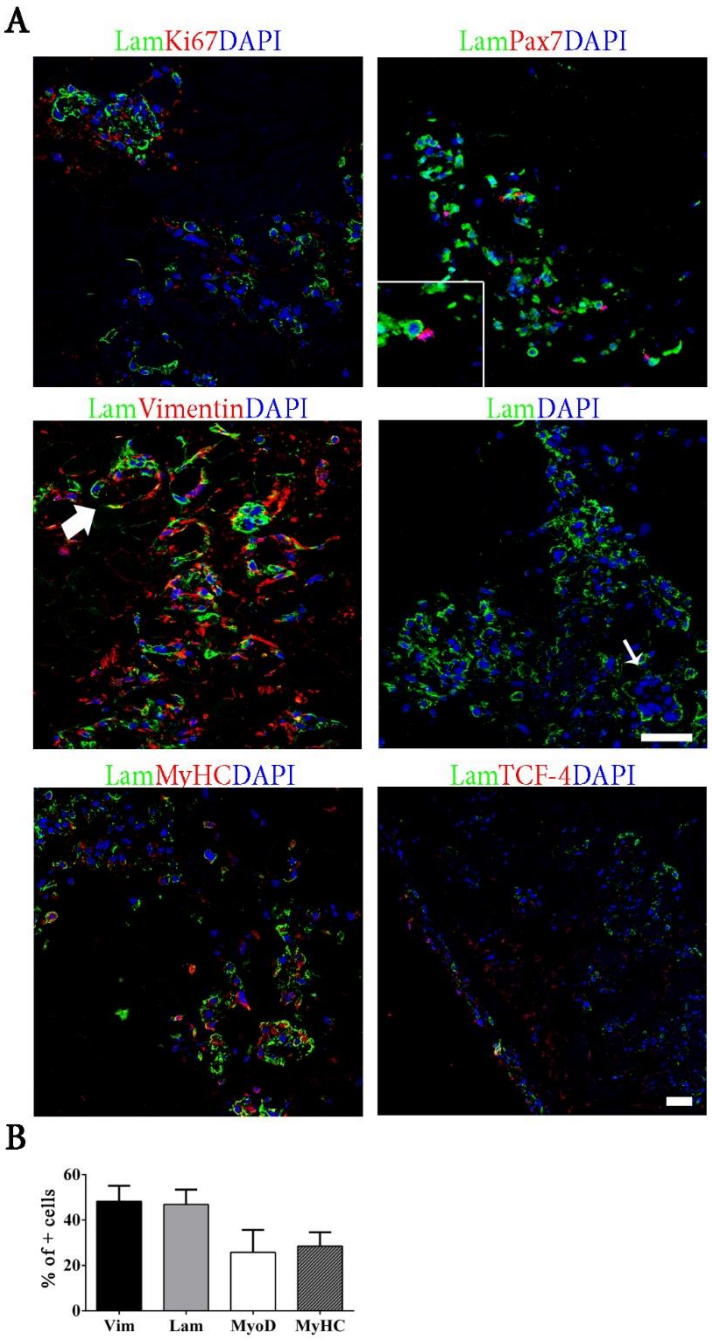

Figure 7.12 Overview of preliminary result obtained *via* rDD injection

Behaviour in rDD scaffold was much different to what seen with mDD. A) Similarly to hpMPC, myogenic program appears to be shifter either on the quiescent (Pax7) or committed program (MyHC), due also to the culture not favouring proliferation (Ki67) for the last three days; Intriguingly, there is a mutual expression of Vimentin (Lam-Vimentin), but more important the distribution of the cells resemble more the native state, forming cluster around fibers (thick arrow) or themselves (thin arrow), probably creating new fibers (MyHC). B) Quantification of markers expressed in the samples

7.3 Discussion

Despite the encouraging effects that the mDD demonstrated in healthy, atrophic and CDH setting, the scaffold-only approach must be considered limited, compared to a fully developed TE approach. Indeed, regeneration seen with CDH model, from one hand endorses the idea of this scaffold as ideal, from the other rises doubts concerning the time required to constitute a functional recovery, even more if considering larger defects. Indeed, it was demonstrated, although in a VML setting, that when a defect is too extended, the acellular matrix alone do not seem sufficient [25].
Hence, aiming at the delivery of a more complete construct, which can further help the recipient cells, it was evaluated in several studied the addition of the two other components of TE triad to the scaffold: the cells, as well as the signals. Precisely, if using a customizable synthetic or naturally derived structures, cells can i) be combined simultaneously to polymerization of the material, thus enveloping the cells within [56], or ii) by seeding the cells in a custom pre patterned structure, which occurently can also be made porous [50]. On the contrary, delivery of a complete construct starting from an acellular matrix represents a new setting, which was just recently dealt with, to date only partially disclosed consequently [87,92]. For this reason, starting almost from the scratch, it was necessary at first to determine the method to combine cells to both mDD and rDD scaffods.

It was decided to develop the method starting from the mouse, because of both the advantages and limitations of the size. From one hand, considering the little dimension of the mDD patches, it was though affordable using less cell; from the other, feasibility in such thin structure was thought to reflect doable use in larger tissues (i.e. rDD). Nevertheless, the thinness of the mouse diaphragm, which at first was considered a feature helping the scaffold repopulation, was instead just a challenging issue. In fact, the seeding only approach, firstly tried hypothesizing that low muscle cells migration would have not been a problem in such little width, was ineffective, made impossible also by the connective barrier on both sides of the diaphragm . Reason for not deepening seeding was that requiring more manipulation, it was felt to be more interesting to test another condition, so an alternative method was evaluated consequently.

Aiming at releasing the cells inside the structure, it was thought of injection as a good way to deliver the cells into the scaffold, however, at the same time the limits seen previously reflected on the choice of the tool used for injection. Indeed, among these, the one set as best (the Hamilton syringe with 33G needle), was the one with the smallest piercing volume. The decision not to decrease any further the dimension of the needle (34-36G), was due to the distress that being pushed through a small diameter may cause to the cells (as for example in flow cytometry, ref su morte o stress su cell). To both increase efficiency and ease the procedure, DDs were put in a tense environment: in a flag fashion on a harbour or pinned on a semi-cylindrical support. The two conditions, helped the angle used to inject, as well as making the scaffold easy to handle, and were subsequently used as advantageous culture condition as well. Indeed, the very same tension helping the procedure, is a type of mechanical directional stress known to help myogenic cells (along with other types) alignment and consequent differentiation. Moreover, these supports can be further customized to fit in a bioreactor, thus adding features that can help the constitution of a complete graft, for example electrical stimulation, another known physical induction of alignment and differentiation [39] .

Once conditions of these methods were set, it was proceeded with testing of different cell populations, cell-scaffold interaction (i.e. survival and differentiation), and scaffold permissiveness to be repopulated. Being this the case of a skeletal muscle-derived scaffold, SCs and MPCs were considered an obvious candidate, although known to not migrate extensively within muscle, an issue thought to be possibly overcome by multiple, homogenous injections. Indeed, mSCs were the cells used during the development of the method. Moreover, as this could be considered an autologous setting, was thought to be the ideal test field to evaluate eventual re-vitalization of the scaffold.

Culture condition with mSCs co-injected with mFbs, mMPCs and hMPCs were kept for 7 days, trying to balance proliferation phase with differentiation phase, by changing the medium from a growth sustaining to a differentiating in the middle. Due to the (although slightly) higher complexity of culturing mSCs and mFbs separately, the injection of mMPCs and hMPCs was preferred

subsequently. Moreover, since the first experiments with rDDs were done during a year of exchange-experience in London, as well as using a support that could just be found there, in Padua it was not possible to reproduce rabbit experiments.

In the mDDs the three different cell population were able to survive, while displaying both still proliferation phase (although 4 days since put in differentiation medium) as well as myogenic markers. Precisely, while markers accounting for differentiation (Myf5, MyoD)(56,62,97 cate) and fiber maturation (Myh3) (1 cate) could be detected, some extent of Pax7+ cells were found as well and interestingly, low in the mouse cells, but considerably high in the human. This however, as marker of stemness of muscle cells may be human resulting from the paediatric origin of the human cells, which are much higher than in an adult [27,359].
In general, mDD permitted for the cells to survive, not inhibiting proliferation nor differentiation. Moreover, the proportion between cells and non-myogenic cells in the cells seeded, appeared to be maintained, resulting in a positive collaboration, when compared to a single population injection. It must be taken in account though, that in order to add the signal component to the approach, the delivery of the cells was performed in a suspension of PGS, which is known to be filled in growth factors [170] , hence the effects observed were enhanced to an yet unknown extent.

On the contrary, preliminary results in the rDD attained with injection of mSCs and mFbs, displayed both how the larger surface/width resulted in a higher efficiency and, since in a PGS-less setting, the particular interaction/influence in this environment. Although still requiring optimization, as the area of the scaffold was not homogeneously populated, in those where the cells were present both proliferation and differentiation where displayed. Intriguingly, the appearance of cell disposition displayed an additional feature, compared to mDD. While the layered organization seen on the surface of the mouse scaffolds was observed also in the rabbit, in the inner part most of the cells seemed to have differentiated, deposited new laminin and either positioned in an ordered fashion around fibers or, alternatively, forming cell clusters enveloped in laminin where the space between

fibers was enough. On this last result in particular, would be interesting whether the mFbs digested the fibers to lead the way towards the reconstitution of new, young fibers [41,346].

Despite these results, in particular the one of rDD, it appear that cells act on their own, stimulated to grow by the scaffold, but forced to look for space and engaged in digesting the pre-existing fibers, rather than becoming part of them. Recently, Webster et al demonstrated how, naturally, during muscle repair the cells are strictly allocated, with no sign of migration through the neighbouring barriers [360]. Although not considering other cell populations than SCs, this may be an explanation of what seen *in vitro*. Hence, whether the maintenance of the fibers is positive or not, has yet to be clarified. On one hand, the hollow fiber was depicted as a binary-like structure, guiding cells, on the other tough, it could be an idea to functionalize the fiber to direct the cells to home and subsequently fuse in it, as it happens with the dead ends of a broken fiber, during regeneration [29], a process a little further in the regeneration time span.
This, could be tested taking inspiration from the exactly the regeneration mechanism, by trying to reproduce between the cells and the scaffold, what happens in nature. Since the molecules involved in muscle fusion, as well as the mechanism behind , were uncovered though the past years in several studies, this opens a whole new chapter in the potential approach to attain a revitalized muscle [189,361].

Until then, the method developed, meant as both delivery of cells and culture system setting, represents a good platform to further evaluate cell-scaffold behaviour, scaffold effects and even cell-cell interaction (as seen with CM experiments) due to the resemblance to the natural tissue. This latter feature, additionally, could be the testing of the ideal test field to essay each cell population to obtain a complete skeletal muscle construct [340].

Chapter 8 : Conclusions

The present study, developed during my PhD, has been aimed at obtaining decellularized matrices from mouse and rabbit diaphragm that preserve architectural organization similar to the original tissue while being devoid of cellular antigens. Following, the mouse diaphragm-derived scaffold effects were characterized in vivo under three different circumstances: a healthy environment, an atrophic model and a surgical model of CDH. Lastly, it was developed a method in vitro to both focus on cell-scaffold interaction and che rappresentasse un metodo per valutare il comportamento delle cellule in un ambiente che somiglia alla matrice in vivo.

8.1 Chapter 4 conclusions

The work in this chapter shows that an acellular natural matrix can be obtained via DET from both mouse and rabbit, avoiding the disruption of structural and mechanical characteristics of the native tissue. Outcomes of implantation *in vivo*, although only temporary and topical, disclosed the potential of using decellularization-derived scaffolds for TE and even maybe non-TE applications. Indeed, the effect naturally achieved (no modification nor customization was applied to matrices after decellularization) with the scaffold, particularly in the HSA-*Cre*, $Smn^{F7/F7}$ mouse model, from the immunomodulatory-guided effects to the local thickening, strongly indicate the pro-regenerative potential of such material, which even produced a strong improvement in the anatomy of the chest.
The findings described in this chapter, led to a publication that was submitted and published in September 2015 [104].

8.2 Chapter 5 conclusions

The work presented in this chapter indicates that the previously developed acellular ECM have pro-angiogenetic potential, which in part derives from the reservoir of molecules preserved after decellularization. In line with the features observed in chapter 3, upon implantation the scaffold was able to steer the host response towards a constructive response over a chronic response, effect that was appreciated also in comparison with the implantation of a synthetic inert material (PTFE). With this chapter, the characterization of this mouse diaphragm-derived decellularized as scaffold can be considered complete, thus allowing to move on to the next steps of the scaling-up stairway.

8.3 Chapter 6 conclusions

In summary, this chapter developed around the testing of mDD as potential tool for the repair of CDHs. This potential was validated by comparison with PTFE, the election material actually used for surgical closure of defects in the diaphragm, which not only elicited in some cases adverse effects (re-herniation, chest deformity), but also was in general less effective in inducing muscle growth.
Being though defective hernias even more severe than the model used, the enhancement of the scaffold alone with the other elements of the TE triad (cells and signals) needs to be considered.

8.4 Chapter 7 conclusions

The method developed allows to efficiently deliver cell into the DDs developed previously, thus representing a good candidate for further settings, aimed at evaluating different cell types, as well as scaffold-cell interactions and cell-cell interaction, as hinted by the CM experiments. Results in the rDDs particularly underlined the significance of testing environments closer to the actual clinical situation, as well as the resulting effects of having a structure easier to be handled and repopulated.

8.5 Areas of future work/future directions

8.5.1 Decellularization

Combination of the most appropriate scaffold, along with correct choice of the cells, is a fundamental requirement for successful regenerative medicine.

The results seen in both chapter 4 and 5, have added the decellularized diaphragm from mouse to the previous list of appropriate scaffold, while re-proposing the rabbit. Indeed, adapting the protocol used for mDD to fit the different size of the latter, decellularized diaphragms from rabbit were efficiently achieved as well. However, while this protocol yields a structural similarity whilst removing cells only by immersion, there is still space for improvement. Indeed, recently rat diaphragm-derived scaffolds were achieved by Gubareva et al. *via* incannulation [116], a well-known procedure that can lead to same results [250,297], by also preserving the vasculature, a feature that can become useful for several applications, from the perfusion seeding [92]to a quicker anastomosis. This way, it is foreseeable in near future the further scaling up of this treatment to obtain DDs from even larger animals.

8.5.2 Applications for mDDs

Although being from small animal, resulting in applications only at pre-clinical level, mDD represents an optimal tool for any proof of concept studies. Some examples could be the evaluation of cell-ECM interactions in an autologous setting or even the constitution of a mix of environmental cues aimed at driving a specific differentiation from a multipotent state [362].

Another application could be the comparison with another biomaterial either as standard or to evaluate other aspects *in vivo*. As example, this last possibility, along with the increasing significance of mechanotransductional interactions during the last years [255], led to the thought that there was still space left for maneuver in the the evaluation of the properties of mDD and of its interaction *in vivo*. As consequence, preliminary studies, in which we introduced two decellularized materials starting from two tissues with a completely different stiffness (skin and intestine) compared to the

diaphragm, are underway. These two were prepared the same way as the mDDs, made acellular *via* 3 cycles of DET (Fig. 8.1). As result, we had two tissues with mechanical properties such that diaphragm scaffold stiffness set in-between (data not shown). The implant *in vivo* of a stiffer (skin) and a more flexible scaffold (intestine), led to responses which reflected the opposite mechanical properties. Indeed, while skin led to a faster response (Fig. 8.2 A), the one raised by intestine seemed to be taking place delayed (Fig. 8.2 B).

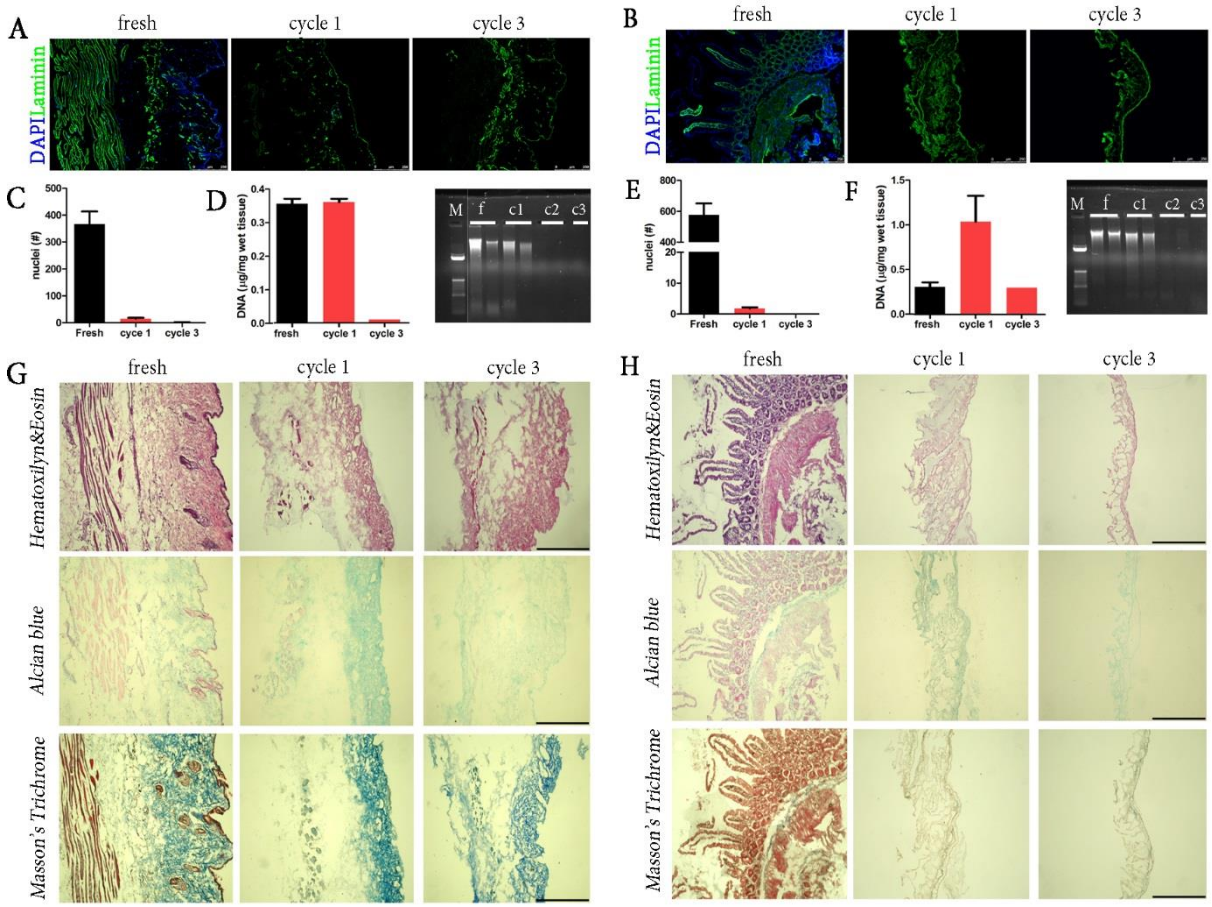

Figure 8.1 Overview of skin and intestine decellularization.

Decellularized skin and intestine were prepared via 3 cycles of DET. A, B) Laminin IF counterstained with DAPI to evaluate nuclear content leftover in skin and intestine scaffolds compared to original tissues; C, E) Nuclei count for DAPI content in skin and intestine compared with the derived scaffolds ; D, F) quantification of extracted DNA from fresh and decellularized skin and intestine; G, H) Panel of histologies performed on skin and intestine.

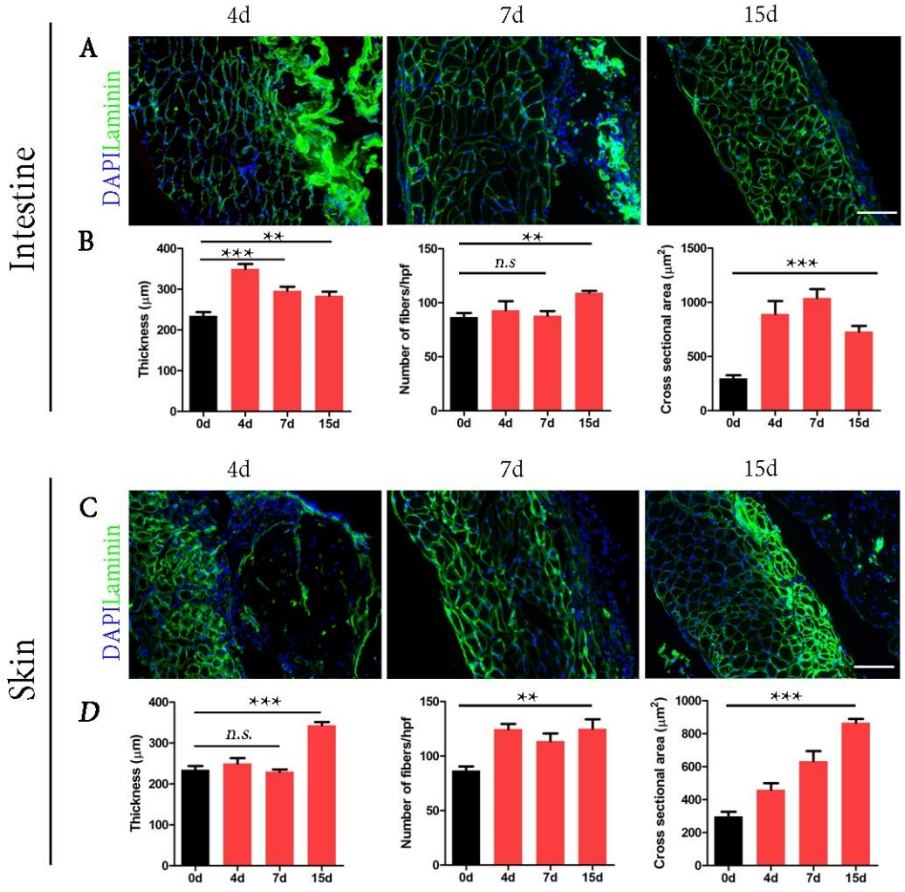

Figure 8.2 Preliminary evaluation of recipient diaphragm behaviour with different scaffolds

Different scaffolds elicited different responses. A, C) appearance of scaffold (right) and host diaphragm (left) upon implantation; B, D) Variation of diaphragm thickness and response resulting from the implant of decellularized skin (stiffer) or intestine (softer).

8.5.3 Applications for rDDs

On top of the aforementioned potential applications, rabbit diaphragm can result in a scaling up of the proposed analyses, and potentially represents, since considered a large animal, a candidate for paediatric clinical trials. Indeed, according to the defect to close, a rabbit hemi-diaphragm could be

an appropriate solution for CDH closure in the newborn [363]. Thus, in the next future, a deeper characterization of the rDD will be performed, and will likely be tested *in vivo* as well.

8.5.2 *In vitro* applications of the methodology

The methodology and culture settings developed, supported by the results seen in chapter 7, can be considered a valid tool through which apply the uses proposed for the DDs. Indeed, it can provide an easy setting to evaluate cell-scaffold interactions, subsequent effects and cell-cell interactions, since the delivery in an ECM, although devoid of cells, might mimic the natural scenery. This could be the example of trying to test or reproduce *in vitro* what seen recently with the concept of ghost fibers (ref), by simply essaying in comparison a scaffold like the DET-derived, in which fibers are complete, or a scaffold in which fibers are hollow but still structured (ref muscolo via SDS, è stato pubblicato qualcosa?). Thus, comparison is also another application of this tool, which can be used to both evaluate whether a scaffold is prone to repopulation as well as the right environmental combination, while looking for the best scaffold candidate and conditions to yield the best muscle-like construct.
Following this trail, seeing the efficiency yielded by the co-presence of Fbs with MPCs, preliminary experiments were designed and performed to assess whether the effect between cells could be paracrine or not. Additionally, being these cells interacting with a scaffold, the experimental plan (Fig. 8.3) was tailored to evaluate its influence. Following preliminary results were obtained using mDDs only. For these experimental set up it was decided to use human cells.

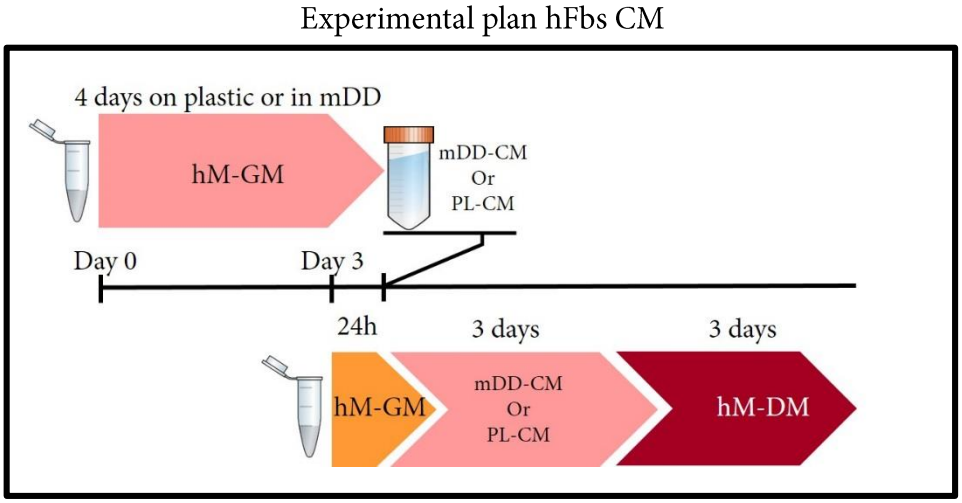

Fig. 8.3 Experimental design

Fibroblasts cultured both on plastic (PL) or scaffold (mDD), were growing normally after 4 days of culture (Fig. 8.4). Remarkably, while distribution of the cells in the control and CM-PL condition was consistent with all the previous results, in the culture exposed to CM-mDD cells where found clustering, displaying late proliferation markers and a better organized structure as well (Fig. 8.4).

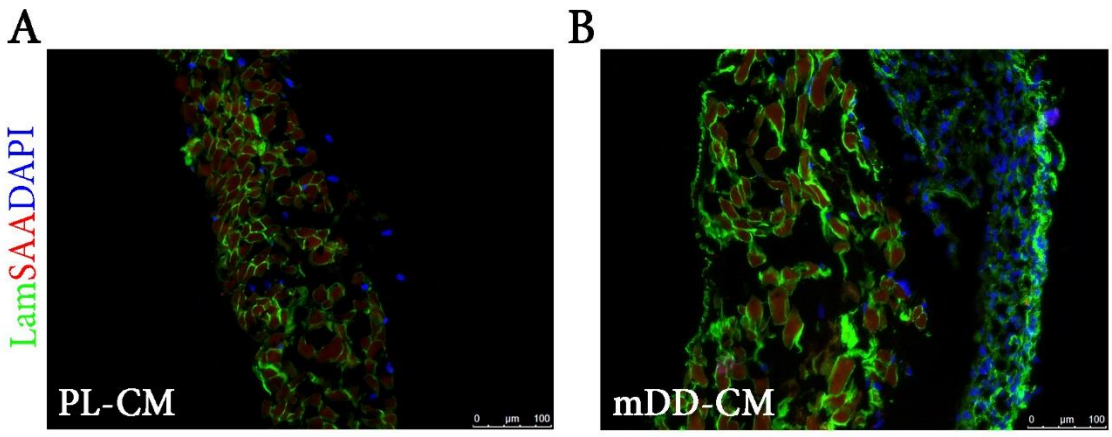

Fig. 8.4 The striking difference between the two culture condition.

These results, which will be further investigated in future, seem to both endorse the present study results of mDD stimulation (seen in *chapter 4-7*) and previous studies on paracrine influence of fibroblasts enhancing myogenic cell differentiation in a paracrine fashion, either mechanically activated, as studied by Hicks et al. [364] or under normal conditions [365].

8.5.3 *In vivo* applications resulting from methodology

As introduced in the previous section, the methodology can be used to evaluate and then set the best conditions: i) from the cell side, ii) the scaffold side, iii) the molecules side and lastly but as important iv) environmental side, to deliver a construct for muscle substitution, in case of DDs, particularly for the clinical management an treatment of CDHs. An example of the third was for instance the CM-mDDs driven amelioration of mMPCs differentiation.
Hence, the methodology can represent a valid benchmark aimed at reproducing what is indeed the ultimate aim of SMTE. Moreover, if the ideal parameters will be set, it could represent a step of the pre-implantation phase, aiding the preparation of the final construct to delivery

Appendix A: Antibody and primer tables

Table A.1| List of antibodies

Antibody	Host	Brand	Dilution
Alpha Sarcomeric Actin	Mouse	Sigma	1:100
Arg1	Rabbit	Abcam	1:100
CD11b	Rat	Abcam	1:100
CD3	Rabbit	Abcam	1:100
CD31	Rat	Invitrogen	1:100
CD4	Rabbit	Abcam	1:100
CD68	Rat	Abcam	1:100
CD86	Rabbit	Abcam	1:100
eMYHC (Myh3)	Mouse	Santa Cruz	1:100
FoxP3	Rabbit	Abcam	1:100
GFP-AlexaFluor 594	.	Life technologies	1:150
Ki67	Rabbit	Abcam	1:100
Laminin	Rabbit	Sigma	1:200
Laminin	Rat	Sigma	1:100
Myf5	Rabbit	Santa Cruz	1:50
MyHC	Mouse	R&D systems	1:100
MyoD	Rabbit	Santa Cruz	1:20
MyoD1	Mouse	Dako	1:80
Pax7	Mouse	R&D systems	1:100
TCF-4	Mouse	Millipore	1:100
TE-7	Mouse	Millipore	1:100
Vimentin	Mouse	Abcam	1:100
vWF	Rabbit	Dako	1:200
αSMA	Mouse	Abcam	1:100

Table A.2 | List of human primers

Gene	Primers	T (°C)	Product length (bp)
MYF5	FW: CCACCTCCAACTGCTCTGAT RV: AGGTGATCCGGTCCACTATG	60	171
MYOD	FW: CAGCCCGCGCTCCAACTGCT RV: TTCCCGGGCCTGGGTTCGCT	62	126
MYHC	FW: CAGCCTGGAGCAGCTGTGCAT RV: TGCCCATAGGCTTCTCGATGAGCTC	58	176
DYSTR	FW: TCATCTGCTGCTGTGGTTATCTCCT RV: ACTTCCTCTTCACTGGCTGAGTGG	56	194
beta2M	FW: CAACTTCAATGTCGGATGGATG RV: GCTGTGCTCGCGCTACTCT	60	161

Appendix B: Publications and Presentations

Publications

1. Improvement of diaphragmatic performance through orthotopic application of decellularized extracellular matrix patch – M. Piccoli, L. Urbani, **M.E. Alvarez-Fallas**, C. Franzin, A. Dedja, E. Bertin, G. Zuccolotto, A. Rosato, P. Pavan, N. Elvassore, P. De Coppi and M. Pozzobon. Biomaterials, 2015

- The Human Pancreas as a Source of Protolerogenic Extracellular Matrix Scaffold for a New-generation Bioartificial Endocrine Pancreas. A Peloso, L Urbani, P Cravedi, R Katari, P Maghsoudlou, **ME Alvarez Fallas**, V Sordi, A Citro, C Purroy, G Niu, JP McQuilling, S Sittadjody, AC Farney, SS Iskandar, J Rogers, RJ Stratta, EC Opara, L Piemonti, C Furdui, S Soker, P De Coppi and G Orlando. Annals of Surgery, 2015.

Conference abstracts

- A decellularized matrix as tissue engineering approach for remodeling diseased diaphragm of HSA-Cre, Smn F7/F7mouse model – L. Urbani, M. Piccoli, M. E. Alvarez Fallas, A. Dedja, E. Magrofuoco, J. Fishman, N. Elvassore, C. Franzin, M. Pozzobon, P. De Coppi.
Presented at EUPSA 2013 and ISSCR 2013

- Acellular skeletal muscle matrix ameliorates atrophic diaphragm – M. Piccoli, L. Urbani, M.E. Alvarez Fallas, A. Dedja, C. Franzin, P. De Coppi, M. Pozzobon.
Presented at TERMIS EU 2014

- Muscle acellular matrix prootes diaphragm remodelling and regeneration through m2 macrophage polarization – L. Urbani, M. Piccoli, M. E. Alvarez Fallas, A. Dedja, C. Franzin, M. Pozzobon, P. De Coppi.
Presented at EMBO 2014

- Tissue engineering approach with acellular matrix supports affected diaphragm of an atrophic mouse moel with activation of resident cells - L. Urbani, M. Piccoli, M. E. Alvarez Fallas, A. Dedja, E. Magrofuoco, N. Elvassore, C. Franzin, M. Pozzobon, P. De Coppi.
Presented at Perinatal Medicine 2014

- Tissue engineered skeletal muscle produced in vitro with natural extracellular matrix and muscle precursor cells for in vivo regeneration - - A. Urciuolo, F. Scottoni, S. Loukogeorgakis, R. R. Wong, P. Maghsoudlou, M. E. Alvarez Fallas, A. Gjinovci, S. Eaton, P. De Coppi, L. Urbani
Presented at EUPSA 2015

- Bioreactor 3d tissue culture for the development of an artificial oesophagus for congenital atresia - L. Urbani, C. Camilli, C. Crowley, F. Scottoni, M. E. Alvarez Fallas, A. Urciuolo, R. R. Wong, P. Maghsoudlou, G. Cossu, M. Lowdell, P. De Coppi.
Presented at EUPSA 2015

- Efficient muscle regeneration potential of human muscle precursor cells expanded in hypoxia – M. Pozzobon, C. Franzin, M. Piccoli, M. E. Alvarez Fallas, V. Parazzi, L. Urbani, C. Biz, L. Lazzari, P. De Coppi.

Presented at ISSCR 2015

- Angiogenic potential of diaphragm derived acellular matrix obtained using detergent enzymatic treatment - M. E. Alvarez Fallas, L. Urbani, M. Piccoli, C. Franzin, E. Bertin, C. Trevisan, M. Pozzobon.
Presented at TERMIS 2015

- Development of an Artificial Oesophagus Engineered with Mesoangioblasts in a Peristaltic 3d Dynamic Culture - L. Urbani, C. Camilli, C. Crowley, F. Scottoni, M. E. Alvarez Fallas, A. Urciuolo, R. R. Wong, P. Maghsoudlou, G. Cossu, M. Lowdell, P. De Coppi.
Presented at TERMIS 2015

- Reconstruction of Gut Muscle Layer: Mesoangioblasts' Delivery Optimization in Decellularised Scaffolds - L. Urbani, C. Camilli, F. Scottoni, C. Crowley, E.Hannon. A. Urciuolo, M. E. Alvarez Fallas, R. R. Wong, P. Maghsoudlou, G. Cossu, P. De Coppi
Presented at TERMIS 2015

- Acellular Muscular Tissue and Muscle Precursor Cells for In Vivo Regeneration - A. Urciuolo, F. Scottoni, S. Loukogeorgakis, R. R. Wong, P. Maghsoudlou, M. E. Alvarez Fallas, A. Gjinovci, S. Eaton, P. De Coppi, L. Urbani.
Presented at TERMIS 2015

Bibliography

[1] Y.-G. Yang, M. Sykes, Xenotransplantation: current status and a perspective on the future., Nat. Rev. Immunol. 7 (2007) 519–31. doi:10.1038/nri2099.

[2] C.J. Phelps, C. Koike, T.D. Vaught, J. Boone, K.D. Wells, S.-H. Chen, et al., Production of alpha 1,3-galactosyltransferase-deficient pigs., Science. 299 (2003) 411–414. doi:10.1126/science.1078942.

[3] T. Fujimura, Y. Takahagi, T. Shigehisa, H. Nagashima, S. Miyagawa, R. Shirakura, et al., Production of alpha 1,3-galactosyltransferase gene-deficient pigs by somatic cell nuclear transfer: A novel selection method for gal alpha 1,3-gal antigen-deficient cells, Mol. Reprod. Dev. 75 (2008) 1372–1378. doi:10.1002/mrd.20890.

[4] K. Yamada, K. Yazawa, A. Shimizu, T. Iwanaga, Y. Hisashi, M. Nuhn, et al., Marked prolongation of porcine renal xenograft survival in baboons through the use of alpha1,3-galactosyltransferase gene-knockout donors and the cotransplantation of vascularized thymic tissue., Nat. Med. 11 (2005) 32–4. doi:10.1038/nm1172.

[5] K. Kuwaki, Y.-L. Tseng, F.J.M.F. Dor, A. Shimizu, S.L. Houser, T.M. Sanderson, et al., Heart transplantation in baboons using alpha1,3-galactosyltransferase gene-knockout pigs as donors: initial experience., Nat. Med. 11 (2005) 29–31. doi:10.1038/nm1171.

[6] J.L. Platt, Acute vascular rejection., Transplant. Proc. 32 (2000) 839–40.

[7] B. Ekser, D.K.C. Cooper, Overcoming the barriers to xenotransplantation: prospects for the future., Expert Rev. Clin. Immunol. 6 (2010) 219–30.

[8] V. Tisato, E. Cozzi, Xenotransplantation: An overview of the field, Methods Mol. Biol. 885 (2012) 1–16. doi:10.1007/978-1-61779-845-0_1.

[9] L. Spitz, Oesophageal atresia., Orphanet J. Rare Dis. 2 (2007) 24. doi:10.1186/1750-1172-2-24.

[10] L. Spitz, E. Kiely, A. Pierro, A. Coran, A. Hamza, D. Lund, Gastric Transposition in Children - A 21-Year Experience, in: J. Pediatr. Surg., 2004: pp. 276–281. doi:10.1016/j.jpedsurg.2003.11.032.

[11] S.P. Loukogeorgakis, A. Pierro, Replacement surgery for esophageal atresia., Eur. J. Pediatr. Surg. 23 (2013) 182–90. doi:10.1055/s-0033-1347915.

[12] R. Langer, J. Vacanti, Tissue engineering, Science (80-.). 260 (1993) 920–926. doi:10.1126/science.8493529.

[13] C. a Sewry, C. Jimenez-Mallebrera, F. Muntoni, Congenital myopathies., Curr. Opin. Neurol. 21 (2008) 569–75. doi:10.1097/WCO.0b013e32830f93c7.

[14] H.R. Champion, R.F. Bellamy, C.P. Roberts, A. Leppaniemi, A profile of combat injury., J. Trauma. 54 (2003) S13–S19. doi:10.1097/01.TA.0000057151.02906.27.

[15] A.R. Kumar, N.S. Grewal, T.L. Chung, J.P. Bradley, Lessons from the modern battlefield: successful upper extremity injury reconstruction in the subacute period., J. Trauma. 67 (2009) 752–757. doi:10.1097/TA.0b013e3181808115.

[16] R.P. Luck, S. Verbin, Rhabdomyolysis, Pediatr. Emerg. Care. 24 (2008) 262–268. doi:10.1097/PEC.0b013e31816bc7b7.

[17] B.F. Grogan, J.R. Hsu, Volumetric muscle loss., J. Am. Acad. Orthop. Surg. 19 Suppl 1 (2011) S35–S37.

[18] L. Clauser, C. Curioni, S. Spanio, The use of the temporalis muscle flap in facial and craniofacial reconstructive surgery. A review of 182 cases, J. Cranio-Maxillo-Facial Surg. 23 (1995) 203–214. doi:10.1016/S1010-5182(05)80209-4.

[19] B. Celiköz, M. Sengezer, S. Işik, M. Türegün, M. Deveci, H. Duman, et al., Subacute reconstruction of lower leg and foot defects due to high velocity-high energy injuries caused by gunshots, missiles, and land mines., Microsurgery. 25 (2005) 3–14; discussion 15. doi:10.1002/micr.20049.

[20] K. a Barrie, S.P. Steinmann, A.Y. Shin, R.J. Spinner, A.T. Bishop, Gracilis free muscle transfer for restoration of function after complete brachial plexus avulsion., Neurosurg. Focus. 16 (2004) E8. doi:10.3171/foc.2004.16.5.9.

[21] S.L. Lee, N.D. Poulos, S.K. Greenholz, Staged reconstruction of large congenital diaphragmatic defects with synthetic patch followed by reverse latissimus dorsi muscle, J Pediatr Surg. 37 (2002) 367–370. doi:DOI 10.1053/jpsu.2002.30837.

[22] W.P. Adams Jr., A.H. Lipschitz, M. Ansari, J.M. Kenkel, R.J. Rohrich, Functional donor site morbidity following latissimus dorsi muscle flap transfer, Ann Plast Surg. 53 (2004) 6–11.

doi:DOI 10.1097/01.sap.0000106430.56501.b5.

[23] a. J. Wood, M.J. Cozad, D. a. Grant, a. M. Ostdiek, S.L. Bachman, S. a. Grant, Materials characterization and histological analysis of explanted polypropylene, PTFE, and PET hernia meshes from an individual patient, J. Mater. Sci. Mater. Med. 24 (2013) 1113–1122. doi:10.1007/s10856-013-4872-y.

[24] E.J. Grethel, R.A. Cortes, A.J. Wagner, M.S. Clifton, H. Lee, D.L. Farmer, et al., Prosthetic patches for congenital diaphragmatic hernia repair: Surgisis vs Gore-Tex., J. Pediatr. Surg. 41 (2006) 29–33; discussion 29–33. doi:10.1016/j.jpedsurg.2005.10.005.

[25] K. Garg, C.L. Ward, C.R. Rathbone, B.T. Corona, Transplantation of devitalized muscle scaffolds is insufficient for appreciable de novo muscle fiber regeneration after volumetric muscle loss injury, Cell Tissue Res. 358 (2014) 857–873. doi:10.1007/s00441-014-2006-6.

[26] L.M.R. Ferreira, E.M. Floriddia, G. Quadrato, S. Di Giovanni, Neural regeneration: Lessons from regenerating and non-regenerating systems, Mol. Neurobiol. 46 (2012) 227–241. doi:10.1007/s12035-012-8290-9.

[27] S. Ciciliot, S. Schiaffino, Regeneration of mammalian skeletal muscle. Basic mechanisms and clinical implications., Curr. Pharm. Des. 16 (2010) 906–914. doi:10.2174/138161210790883453.

[28] J. De Souza, C. Gottfried, Muscle injury: review of experimental models., J. Electromyogr. Kinesiol. 23 (2013) 1253–60. doi:10.1016/j.jelekin.2013.07.009.

[29] T.A. Järvinen, M. Järvinen, H. Kalimo, Regeneration of injured skeletal muscle after the injury., Muscles. Ligaments Tendons J. 3 (2013) 337–45. doi:10.11138/mltj/2013.3.4.337.

[30] J.G. Tidball, K. Dorshkind, M. Wehling-Henricks, Shared signaling systems in myeloid cell-mediated muscle regeneration., Development. 141 (2014) 1184–96. doi:10.1242/dev.098285.

[31] D. Alexander, Satellite Cell of Skeletal Muscle Fibers, J. Biophys. Biochem. Cytol. 9 (1961) 493–495. doi:10.1083/jcb.9.2.493.

[32] J. von Maltzahn, A.E. Jones, R.J. Parks, M. a Rudnicki, Pax7 is critical for the normal function of satellite cells in adult skeletal muscle., Proc. Natl. Acad. Sci. U. S. A. 110 (2013) 16474–9. doi:10.1073/pnas.1307680110.

[33] A. Pasut, A.E. Jones, M. a Rudnicki, Isolation and culture of individual myofibers and their satellite cells from adult skeletal muscle., J. Vis. Exp. (2013) e50074. doi:10.3791/50074.

[34] N.L. Estrella, C. a. Desjardins, S.E. Nocco, A.L. Clark, Y. Maksimenko, F.J. Naya, MEF2 Transcription Factors Regulate Distinct Gene Programs in Mammalian Skeletal Muscle Differentiation, J. Biol. Chem. 290 (2015) 1256–1268. doi:10.1074/jbc.M114.589838.

[35] T. Braun, M. Gautel, Transcriptional mechanisms regulating skeletal muscle differentiation, growth and homeostasis, Nat. Rev. Mol. Cell Biol. 12 (2011) 349–361. doi:10.1038/nrm3118.

[36] S.B.P. CHARGE, Cellular and Molecular Regulation of Muscle Regeneration, Physiol. Rev. 84 (2004) 209–238. doi:10.1152/physrev.00019.2003.

[37] W. Lin, R.W. Burgess, B. Dominguez, S.L. Pfaff, J.R. Sanes, K.F. Lee, Distinct roles of nerve and muscle in postsynaptic differentiation of the neuromuscular synapse., Nature. 410 (2001) 1057–1064. doi:10.1038/35074025.

[38] Y. Shwartz, E. Blitz, E. Zelzer, One load to rule them all: Mechanical control of the musculoskeletal system in development and aging, Differentiation. 86 (2013) 104–111. doi:10.1016/j.diff.2013.07.003.

[39] K. Cole, T. Miller, Mechanical and Electrical Stimulation Device for the Creation of a Functional Unit of Human Skeletal Muscle in Vitro, (2015).

[40] S. Ahadian, S. Ostrovidov, V. Hosseini, H. Kaji, M. Ramalingam, H. Bae, et al., Electrical stimulation as a biomimicry tool for regulating muscle cell behavior., Organogenesis. 9 (2013) 87–92. doi:10.4161/org.25121.

[41] J.J. Tomasek, G. Gabbiani, B. Hinz, C. Chaponnier, R. a Brown, Myofibroblasts and mechano-regulation of connective tissue remodelling., Nat. Rev. Mol. Cell Biol. 3 (2002) 349–63. doi:10.1038/nrm809.

[42] V. Dhawan, I.F. Lytle, D.E. Dow, Y.-C. Huang, D.L. Brown, Neurotization improves contractile forces of tissue-engineered skeletal muscle., Tissue Eng. 13 (2007) 2813–2821. doi:10.1089/ten.2007.0003.

[43] S. Chen, T. Nakamoto, N. Kawazoe, G. Chen, Engineering multi-layered skeletal muscle tissue by using 3D microgrooved collagen scaffolds, Biomaterials. 73 (2015) 23–31.

doi:10.1016/j.biomaterials.2015.09.010.

[44] S. Levenberg, J. Rouwkema, M. Macdonald, E.S. Garfein, D.S. Kohane, D.C. Darland, et al., Engineering vascularized skeletal muscle tissue, Nat. Biotechnol. 23 (2005) 879–884. doi:10.1038/nbt1109.

[45] J.S. Choi, S.J. Lee, G.J. Christ, A. Atala, J.J. Yoo, The influence of electrospun aligned poly(ε-caprolactone)/collagen nanofiber meshes on the formation of self-aligned skeletal muscle myotubes, Biomaterials. 29 (2008) 2899–2906. doi:10.1016/j.biomaterials.2008.03.031.

[46] F.S. Kamelger, R. Marksteiner, E. Margreiter, G. Klima, G. Wechselberger, S. Hering, et al., A comparative study of three different biomaterials in the engineering of skeletal muscle using a rat animal model, Biomaterials. 25 (2004) 1649–1655. doi:10.1016/S0142-9612(03)00520-9.

[47] L.C. Ceafalan, B.O. Popescu, M.E. Hinescu, Cellular players in skeletal muscle regeneration., Biomed Res. Int. 2014 (2014) 957014. doi:10.1155/2014/957014.

[48] C.S. Cheng, B.N. Davis, L. Madden, N. Bursac, G. a Truskey, Physiology and metabolism of tissue-engineered skeletal muscle., Exp. Biol. Med. (Maywood). (2014) 1203–1214. doi:10.1177/1535370214538589.

[49] J. Huard, Y. Li, F.H. Fu, Muscle injuries and repair: current trends in research., J. Bone Joint Surg. Am. 84-A (2002) 822–832.

[50] G. Cittadella Vigodarzere, S. Mantero, Skeletal muscle tissue engineering: strategies for volumetric constructs, Front. Physiol. 5 (2014) 1–13. doi:10.3389/fphys.2014.00362.

[51] J.M. Grasman, M.J. Zayas, R.L. Page, G.D. Pins, Biomimetic scaffolds for regeneration of volumetric muscle loss in skeletal muscle injuries, Acta Biomater. 25 (2015) 2–15. doi:10.1016/j.actbio.2015.07.038.

[52] H. Egusa, M. Kobayashi, T. Matsumoto, J.-I. Sasaki, S. Uraguchi, H. Yatani, Application of cyclic strain for accelerated skeletal myogenic differentiation of mouse bone marrow-derived mesenchymal stromal cells with cell alignment., Tissue Eng. Part A. 19 (2013) 770–82. doi:10.1089/ten.TEA.2012.0164.

[53] R. Shah, J.C. Knowles, N.P. Hunt, M.P. Lewis, Development of a novel smart scaffold for human skeletal muscle regeneration, J. Tissue Eng. Regen. Med. (2013) n/a–n/a.

doi:10.1002/term.1780.

[54] S. Siegel, K. Noblett, J. Mangel, T. Giebling, S.E. Sutherland, E.T. Bird, Results of a prospective, randomized , multicenter study evaluating sacral neuromodulation with Interstim therapy compared to standard medical therapy at 6 monts in subjects with mild symptoms of overactive bladder, Neurourol. Urodyn. 34 (2015) 224–230. doi:10.1002/nau.

[55] M.T. Conconi, S. Bellini, D. Teoli, P. de Coppi, D. Ribatti, B. Nico, et al., *In vitro* and *in vivo* evaluation of acellular diaphragmatic matrices seeded with muscle precursors cells and coated with VEGF silica gels to repair muscle defect of the diaphragm, J. Biomed. Mater. Res. Part A. 89A (2009) 304–316. doi:10.1002/jbm.a.31982.

[56] L. Madden, M. Juhas, W.E. Kraus, G.A. Truskey, N. Bursac, Bioengineered human myobundles mimic clinical responses of skeletal muscle to drugs, Elife. 4 (2015) 1–14. doi:10.7554/eLife.04885.

[57] X. Qi, Z. Shan, Y. Ji, V. Guerra, J.C. Alexander, B.K. Ormerod, et al., Supplementary Methods, 2000 (2014).

[58] L. Wang, J. Shansky, H. Vandenburgh, Induced formation and maturation of acetylcholine receptor clusters in a defined 3D bio-artificial muscle., Mol. Neurobiol. 48 (2013) 397–403. doi:10.1007/s12035-013-8412-z.

[59] M.T. Wolf, C.L. Dearth, S.B. Sonnenberg, E.G. Loboa, S.F. Badylak, Naturally derived and synthetic scaffolds for skeletal muscle reconstruction, Adv. Drug Deliv. Rev. 84 (2015) 208–221. doi:10.1016/j.addr.2014.08.011.

[60] E. Serena, M. Flaibani, S. Carnio, L. Boldrin, L. Vitiello, P. De Coppi, et al., Electrophysiologic stimulation improves myogenic potential of muscle precursor cells grown in a 3D collagen scaffold, 30 (2008).

[61] P.B. Van Wachem, J.A. Plantinga, M.J.B. Wissink, R. Beernink, A.A. Poot, G.H.M. Engbers, et al., In vivo biocompatibility of carbodiimide-crosslinked collagen matrices : Effects of crosslink density , heparin immobilization , and bFGF loading, (2000) 9–11.

[62] S. Kin, A. Hagiwara, Y. Nakase, Y. Kuriu, S. Nakashima, T. Yoshikawa, et al., Regeneration of Skeletal Muscle Using In Situ Tissue Engineering on an Acellular Collagen Sponge Scaffold in

a Rabbit Model, ASAIO J. 53 (2007) 506–513. doi:10.1097/MAT.0b013e3180d09d81.

[63] S.P. Frey, H. Jansen, M.J. Raschke, R.H. Meffert, S. Ochman, VEGF improves skeletal muscle regeneration after acute trauma and reconstruction of the limb in a rabbit model., Clin. Orthop. Relat. Res. 470 (2012) 3607–3614. doi:10.1007/s11999-012-2456-7.

[64] Y.-C. Huang, R.G. Dennis, L. Larkin, K. Baar, Rapid formation of functional muscle in vitro using fibrin gels., J. Appl. Physiol. 98 (2005) 706–13. doi:10.1152/japplphysiol.00273.2004.

[65] D. Gholobova, L. Decroix, V. Van Muylder, L. Desender, M. Gerard, G. Carpentier, et al., Endothelial Network Formation Within Human Tissue-Engineered Skeletal Muscle, Tissue Eng. Part A. 21 (2015) 150901071945000. doi:10.1089/ten.tea.2015.0093.

[66] B. Kalman, C. Monge, a. Bigot, V. Mouly, C. Picart, T. Boudou, Engineering human 3D micromuscles with co-culture of fibroblasts and myoblasts, Comput. Methods Biomech. Biomed. Engin. 5842 (2015) 1–2. doi:10.1080/10255842.2015.1069557.

[67] Y. Li, C.T. Poon, M. Li, T.J. Lu, B. Pingguan-Murphy, F. Xu, Chinese-Noodle-Inspired Muscle Myofiber Fabrication, Adv. Funct. Mater. (2015) n/a–n/a. doi:10.1002/adfm.201502018.

[68] A.S. Salimath, A.J. García, Biofunctional hydrogels for skeletal muscle constructs, J. Tissue Eng. Regen. Med. 24 (2014) n/a–n/a. doi:10.1002/term.1881.

[69] H. Takahashi, T. Shimizu, M. Nakayama, M. Yamato, T. Okano, The use of anisotropic cell sheets to control orientation during the self-organization of 3D muscle tissue, Biomaterials. 34 (2013) 7372–7380. doi:10.1016/j.biomaterials.2013.06.033.

[70] Y. Morimoto, M. Kato-Negishi, H. Onoe, S. Takeuchi, Three-dimensional neuron–muscle constructs with neuromuscular junctions, Biomaterials. 34 (2013) 9413–9419. doi:10.1016/j.biomaterials.2013.08.062.

[71] S.S. Nunes, J.W. Miklas, J. Liu, R. Aschar-Sobbi, Y. Xiao, B. Zhang, et al., Biowire: a platform for maturation of human pluripotent stem cell–derived cardiomyocytes, Nat. Methods. 10 (2013) 781–787. doi:10.1038/nmeth.2524.

[72] I.E. Palamà, S. D'Amone, A.M.L. Coluccia, G. Gigli, Micropatterned polyelectrolyte nanofilms promote alignment and myogenic differentiation of C2C12 cells in standard growth media., Biotechnol. Bioeng. 110 (2013) 586–96. doi:10.1002/bit.24626.

[73] C. Snyman, K.P. Goetsch, K.H. Myburgh, C.U. Niesler, Simple silicone chamber system for in vitro three-dimensional skeletal muscle tissue formation., Front. Physiol. 4 (2013) 349. doi:10.3389/fphys.2013.00349.

[74] W. Bian, M. Juhas, T.W. Pfeiler, N. Bursac, Local Tissue Geometry Determines Contractile Force Generation of Engineered Muscle Networks, Tissue Eng. Part A. 18 (2012) 957–967. doi:10.1089/ten.tea.2011.0313.

[75] C. Monge, K. Ren, K. Berton, R. Guillot, D. Peyrade, C. Picart, Engineering Muscle Tissues on Microstructured Polyelectrolyte Multilayer Films, Tissue Eng. Part A. 18 (2012) 1664–1676. doi:10.1089/ten.tea.2012.0079.

[76] A.P. Sharples, D.J. Player, N.R.W. Martin, V. Mudera, C.E. Stewart, M.P. Lewis, Modelling in vivo skeletal muscle ageing in vitro using three-dimensional bioengineered constructs, Aging Cell. 11 (2012) 986–995. doi:10.1111/j.1474-9726.2012.00869.x.

[77] M.R. Weist, M.S. Wellington, J.E. Bermudez, T.Y. Kostrominova, C.L. Mendias, E.M. Arruda, et al., TGF-β1 enhances contractility in engineered skeletal muscle., J. Tissue Eng. Regen. Med. 7 (2013) 562–71. doi:10.1002/term.551.

[78] E.D.F. Ker, A.S. Nain, L.E. Weiss, J. Wang, J. Suhan, C.H. Amon, et al., Bioprinting of growth factors onto aligned sub-micron fibrous scaffolds for simultaneous control of cell differentiation and alignment, Biomaterials. 32 (2011) 8097–8107. doi:10.1016/j.biomaterials.2011.07.025.

[79] M. Li, C.E. Dickinson, E.B. Finkelstein, C.M. Neville, C. a. Sundback, The Role of Fibroblasts in Self-Assembled Skeletal Muscle, Tissue Eng. Part A. 17 (2011) 2641–2650. doi:10.1089/ten.tea.2010.0700.

[80] C.P. Pennisi, C.G. Olesen, M. de Zee, J. Rasmussen, V. Zachar, Uniaxial Cyclic Strain Drives Assembly and Differentiation of Skeletal Myocytes, Tissue Eng. Part A. 17 (2011) 2543–2550. doi:10.1089/ten.tea.2011.0089.

[81] D.W.J. van der Schaft, A.C.C. van Spreeuwel, H.C. van Assen, F.P.T. Baaijens, Mechanoregulation of Vascularization in Aligned Tissue-Engineered Muscle: A Role for Vascular Endothelial Growth Factor, Tissue Eng. Part A. 17 (2011) 2857–2865.

doi:10.1089/ten.tea.2011.0214.

[82] M.T. Lam, Y.-C. Huang, R.K. Birla, S. Takayama, Microfeature guided skeletal muscle tissue engineering for highly organized 3-dimensional free-standing constructs, Biomaterials. 30 (2009) 1150–1155. doi:10.1016/j.biomaterials.2008.11.014.

[83] S. a. Riboldi, N. Sadr, L. Pigini, P. Neuenschwander, M. Simonet, P. Mognol, et al., Skeletal myogenesis on highly orientated microfibrous polyesterurethane scaffolds, J. Biomed. Mater. Res. - Part A. 84 (2008) 1094–1101. doi:10.1002/jbm.a.31534.

[84] A.J. Engler, Myotubes differentiate optimally on substrates with tissue-like stiffness: pathological implications for soft or stiff microenvironments, J. Cell Biol. 166 (2004) 877–887. doi:10.1083/jcb.200405004.

[85] M.K. Dennis, A.S. Field, R. Burai, C. Ramesh, K. Whitney, C.G. Bologa, et al., NIH Public Access, 127 (2012) 358–366. doi:10.1016/j.jsbmb.2011.07.002.Identification.

[86] R.G. Dennis, P.E. Kosnik, Excitability and isometric contractile properties of mammalian skeletal muscle constructs engineered in vitro., In Vitro Cell. Dev. Biol. Anim. 36 (2000) 327–335. doi:10.1290/1071-2690(2000)036<0327:EAICPO>2.0.CO;2.

[87] S. Carosio, L. Barberi, E. Rizzuto, C. Nicoletti, Z. Del Prete, A. Musarò, Generation of eX vivo-vascularized Muscle Engineered Tissue (X-MET)., Sci. Rep. 3 (2013) 1420. doi:10.1038/srep01420.

[88] J. Kof, K. Kaufman-francis, S. Yulia, A.P. Daria, A. Landesberg, J. Kof, et al., Correction for Koffler et al., Improved vascular organization enhances functional integration of engineered skeletal muscle grafts, Proc. Natl. Acad. Sci. 109 (2012) 1353. doi:10.1073/pnas.1120303109.

[89] M. Juhas, G.C. Engelmayr, A.N. Fontanella, G.M. Palmer, N. Bursac, Biomimetic engineered muscle with capacity for vascular integration and functional maturation in vivo, Proc. Natl. Acad. Sci. 111 (2014) 5508–5513. doi:10.1073/pnas.1402723111.

[90] B.T. Corona, X. Wu, C.L. Ward, J.S. McDaniel, C.R. Rathbone, T.J. Walters, The promotion of a functional fibrosis in skeletal muscle with volumetric muscle loss injury following the transplantation of muscle-ECM, Biomaterials. 34 (2013) 3324–3335. doi:10.1016/j.biomaterials.2013.01.061.

[91] C. Fuoco, R. Rizzi, A. Biondo, E. Longa, A. Mascaro, K. Shapira-, et al., In vivo generation of a mature and functional artificial skeletal muscle, (2015) 1–13.

[92] B.J. Jank, L. Xiong, P.T. Moser, J.P. Guyette, X. Ren, C.L. Cetrulo, et al., Engineered composite tissue as a bioartificial limb graft, Biomaterials. 61 (2015) 246–256. doi:10.1016/j.biomaterials.2015.04.051.

[93] K.W. VanDusen, B.C. Syverud, M.L. Williams, J.D. Lee, L.M. Larkin, Engineered skeletal muscle units for repair of volumetric muscle loss in the tibialis anterior muscle of a rat., Tissue Eng. Part A. 20 (2014) 2920–30. doi:10.1089/ten.TEA.2014.0060.

[94] G.H. Borschel, D.E. Dow, R.G. Dennis, D.L. Brown, Tissue-engineered axially vascularized contractile skeletal muscle., Plast. Reconstr. Surg. 117 (2006) 2235–42. doi:10.1097/01.prs.0000224295.54073.49.

[95] M.A. Brady, M.P. Lewis, V. Mudera, Synergy between myogenic and non-myogenic cells in a 3D tissue-engineered craniofacial skeletal muscle construct, J. Tissue Eng. Regen. Med. 2 (2008) 408–417. doi:10.1002/term.

[96] J.E. Valentin, N.J. Turner, T.W. Gilbert, S.F. Badylak, Functional skeletal muscle formation with a biologic scaffold, Biomaterials. 31 (2010) 7475–7484. doi:10.1016/j.biomaterials.2010.06.039.

[97] A.K. Saxena, J. Marler, M. Benvenuto, G.H. Willital, J.P. Vacanti, Skeletal muscle tissue engineering using isolated myoblasts on synthetic biodegradable polymers: preliminary studies., Tissue Eng. 5 (1999) 525–32. http://www.ncbi.nlm.nih.gov/pubmed/10611544.

[98] a K. Saxena, G.H. Willital, J.P. Vacanti, Vascularized three-dimensional skeletal muscle tissue-engineering., Biomed. Mater. Eng. 11 (2001) 275–281.

[99] Y.M. Ju, A. Atala, J.J. Yoo, S.J. Lee, In situ regeneration of skeletal muscle tissue through host cell recruitment, Acta Biomater. 10 (2014) 4332–4339. doi:10.1016/j.actbio.2014.06.022.

[100] Y. Shandalov, D. Egozi, J. Koffler, D. Dado-Rosenfeld, D. Ben-Shimol, A. Freiman, et al., An engineered muscle flap for reconstruction of large soft tissue defects, Proc. Natl. Acad. Sci. 111 (2014) 6010–6015. doi:10.1073/pnas.1402679111.

[101] A. Lesman, J. Koffler, R. Atlas, Y.J. Blinder, Z. Kam, S. Levenberg, Engineering vessel-like

networks within multicellular fibrin-based constructs, Biomaterials. 32 (2011) 7856–7869. doi:10.1016/j.biomaterials.2011.07.003.

[102] B. Perniconi, A. Costa, P. Aulino, L. Teodori, S. Adamo, D. Coletti, The pro-myogenic environment provided by whole organ scale acellular scaffolds from skeletal muscle, Biomaterials. 32 (2011) 7870–7882. doi:10.1016/j.biomaterials.2011.07.016.

[103] B. Perniconi, D. Coletti, P. Aulino, A. Costa, P. Aprile, L. Santacroce, et al., Muscle acellular scaffold as a biomaterial: effects on C2C12 cell differentiation and interaction with the murine host environment., Front. Physiol. 5 (2014) 354. doi:10.3389/fphys.2014.00354.

[104] M. Piccoli, L. Urbani, M.E. Alvarez-Fallas, C. Franzin, A. Dedja, E. Bertin, et al., Improvement of diaphragmatic performance through orthotopic application of decellularized extracellular matrix patch, Biomaterials. 74 (2016) 245–255. doi:10.1016/j.biomaterials.2015.10.005.

[105] B.N. Brown, J.E. Valentin, A.M. Stewart-Akers, G.P. McCabe, S.F. Badylak, Macrophage phenotype and remodeling outcomes in response to biologic scaffolds with and without a cellular component, Biomaterials. 30 (2009) 1482–1491. doi:10.1016/j.biomaterials.2008.11.040.

[106] E.K. Merritt, D.W. Hammers, M. Tierney, L.J. Suggs, T.J. Walters, R.P. Farrar, Functional assessment of skeletal muscle regeneration utilizing homologous extracellular matrix as scaffolding., Tissue Eng. Part A. 16 (2010) 1395–1405. doi:10.1089/ten.tea.2009.0226.

[107] X.K. Chen, T.J. Walters, Muscle-derived decellularised extracellular matrix improves functional recovery in a rat latissimus dorsi muscle defect model, J. Plast. Reconstr. Aesthetic Surg. 66 (2013) 1750–1758. doi:10.1016/j.bjps.2013.07.037.

[108] S.A. Hurd, N.M. Bhatti, A.M. Walker, B.M. Kasukonis, J.C. Wolchok, Development of a biological scaffold engineered using the extracellular matrix secreted by skeletal muscle cells, Biomaterials. 49 (2015) 9–17. doi:10.1016/j.biomaterials.2015.01.027.

[109] G. P., C. M., R. Lo Piccolo, Z. G., S. R., P. P., Experimental abdominal wall defect repaired with acellular matrix, Pediatr. Surg. Int. 18 (2002) 327–331. doi:10.1007/s00383-002-0849-5.

[110] T. Ayele, A.B.Z. Zuki, B.M.A. Noorjahan, M.M. Noordin, Tissue engineering approach to repair abdominal wall defects using cell-seeded bovine tunica vaginalis in a rabbit model, J.

Mater. Sci. Mater. Med. 21 (2010) 1721–1730. doi:10.1007/s10856-010-4007-7.

[111] A. Porzionato, M. Sfriso, A. Pontini, V. Macchi, L. Petrelli, P. Pavan, et al., Decellularized Human Skeletal Muscle as Biologic Scaffold for Reconstructive Surgery, Int. J. Mol. Sci. 16 (2015) 14808–14831. doi:10.3390/ijms160714808.

[112] M. Marzaro, M.T. Conconi, L. Perin, S. Giuliani, P. Gamba, P. De Coppi, et al., Autologous satellite cell seeding improves in vivo biocompatibility of homologous muscle acellular matrix implants., Int. J. Mol. Med. 10 (2002) 177–82. http://www.ncbi.nlm.nih.gov/pubmed/12119555.

[113] M.T. Conconi, P. De Coppi, S. Bellini, G. Zara, M. Sabatti, M. Marzaro, et al., Homologous muscle acellular matrix seeded with autologous myoblasts as a tissue-engineering approach to abdominal wall-defect repair, Biomaterials. 26 (2005) 2567–2574. doi:10.1016/j.biomaterials.2004.07.035.

[114] P. De Coppi, S. Bellini, M.T. Conconi, M. Sabatti, E. Simonato, P.G. Gamba, et al., Myoblast-acellular skeletal muscle matrix constructs guarantee a long-term repair of experimental full-thickness abdominal wall defects, Tissue Eng. 12 (2006) 1929–1936. doi:10.1089/ten.2006.12.1929.

[115] E.K. Merritt, M. V Cannon, D.W. Hammers, L.N. Le, R. Gokhale, A. Sarathy, et al., Repair of traumatic skeletal muscle injury with bone-marrow-derived mesenchymal stem cells seeded on extracellular matrix., Tissue Eng. Part A. 16 (2010) 2871–2881. doi:10.1089/ten.tea.2009.0826.

[116] E.A. Gubareva, S. Sjöqvist, I. V Gilevich, A.S. Sotnichenko, E. V Kuevda, M.L. Lim, et al., Orthotopic transplantation of a tissue engineered diaphragm in rats, Biomaterials. 77 (2016) 320–335. doi:10.1016/j.biomaterials.2015.11.020.

[117] B.M. Sicari, V. Agrawal, B.F. Siu, C.J. Medberry, C.L. Dearth, N.J. Turner, et al., A Murine Model of Volumetric Muscle Loss and a Regenerative Medicine Approach for Tissue Replacement, Tissue Eng. Part A. 18 (2012) 1941–1948. doi:10.1089/ten.tea.2012.0475.

[118] B.M. Sicari, J.P. Rubin, C.L. Dearth, M.T. Wolf, F. Ambrosio, M. Boninger, et al., An acellular biologic scaffold promotes skeletal muscle formation in mice and humans with volumetric

muscle loss., Sci. Transl. Med. 6 (2014) 234ra58. doi:10.1126/scitranslmed.3008085.

[119] J. Song, P. Hornsby, M. Stanley, K.R. AbdelFattah, S.E. Wolf, Porcine urinary bladder extracellular matrix activates skeletal myogenesis in mouse muscle cryoinjury, J. Regen. Med. Tissue Eng. 3 (2014) 3. doi:10.7243/2050-1218-3-3.

[120] J. Ma, S. Sahoo, A.R. Baker, K.A. Derwin, Investigating muscle regeneration with a dermis/small intestinal submucosa scaffold in a rat full-thickness abdominal wall defect model., J. Biomed. Mater. Res. B. Appl. Biomater. (2014). doi:10.1002/jbm.b.33166.

[121] B.T. Corona, C.L. Ward, H.B. Baker, T.J. Walters, G.J. Christ, Implantation of *In Vitro* Tissue Engineered Muscle Repair Constructs and Bladder Acellular Matrices Partially Restore *In Vivo* Skeletal Muscle Function in a Rat Model of Volumetric Muscle Loss Injury, Tissue Eng. Part A. 20 (2013) 131219054609007. doi:10.1089/ten.tea.2012.0761.

[122] J.E. Valentin, A.M. Stewart-akers, D. Ph, T.W. Gilbert, D. Ph, S.F. Badylak, et al., Macrophage Participation in the Degradation and Remodeling of Extracellular Matrix Scaffolds, 15 (2009).

[123] B.N. Brown, R. Londono, S. Tottey, L. Zhang, K. a. Kukla, M.T. Wolf, et al., Macrophage phenotype as a predictor of constructive remodeling following the implantation of biologically derived surgical mesh materials, Acta Biomater. 8 (2012) 978–987. doi:10.1016/j.actbio.2011.11.031.

[124] A. Aurora, J.L. Roe, B.T. Corona, T.J. Walters, An acellular biologic scaffold does not regenerate appreciable de novo muscle tissue in rat models of volumetric muscle loss injury, Biomaterials. 67 (2015) 393–407. doi:10.1016/j.biomaterials.2015.07.040.

[125] M.T. Wolf, K.A. Daly, J.E. Reing, S.F. Badylak, Biologic scaffold composed of skeletal muscle extracellular matrix, Biomaterials. 33 (2012) 2916–2925. doi:10.1016/j.biomaterials.2011.12.055.

[126] L. Wang, J.A. Johnson, D.W. Chang, Q. Zhang, Decellularized musculofascial extracellular matrix for tissue engineering, Biomaterials. 34 (2013) 2641–2654. doi:10.1016/j.biomaterials.2012.12.048.

[127] N.J. Turner, A.J. Yates, D.J. Weber, I.R. Qureshi, D.B. Stolz, T.W. Gilbert, et al., Xenogeneic extracellular matrix as an inductive scaffold for regeneration of a functioning

musculotendinous junction., Tissue Eng. Part A. 16 (2010) 3309–3317. doi:10.1089/ten.tea.2010.0169.

[128] V.J. Mase, J.R. Hsu, S.E. Wolf, J.C. Wenke, D.G. Baer, J. Owens, et al., Clinical application of an acellular biologic scaffold for surgical repair of a large, traumatic quadriceps femoris muscle defect., Orthopedics. 33 (2010) 511. doi:10.3928/01477447-20100526-24.

[129] M. a Machingal, B.T. Corona, T.J. Walters, V. Kesireddy, C.N. Koval, A. Dannahower, et al., A tissue-engineered muscle repair construct for functional restoration of an irrecoverable muscle injury in a murine model., Tissue Eng. Part A. 17 (2011) 2291–2303. doi:10.1089/ten.tea.2010.0682.

[130] B.T. Corona, M.A. Machingal, T. Criswell, M. Vadhavkar, A.C. Dannahower, C. Bergman, et al., Further development of a tissue engineered muscle repair construct in vitro for enhanced functional recovery following implantation in vivo in a murine model of volumetric muscle loss injury., Tissue Eng. Part A. 18 (2012) 1213–28. doi:10.1089/ten.TEA.2011.0614.

[131] M.T. Wolf, K. a. Daly, E.P. Brennan-Pierce, S. a. Johnson, C. a. Carruthers, A. D'Amore, et al., A hydrogel derived from decellularized dermal extracellular matrix, Biomaterials. 33 (2012) 7028–7038. doi:10.1016/j.biomaterials.2012.06.051.

[132] S. Farnebo, C. Woon, Design and Characterization of an Injectable Tendon Hydrogel: A Scaffold for Guided Tissue Regeneration in the Musculoskeletal System, Tissue …. (2013) 1–46. doi:10.1089/ten.TEA.2013.0207.

[133] B.T. Corona, K. Garg, C.L. Ward, J.S. McDaniel, T.J. Walters, C.R. Rathbone, Autologous minced muscle grafts: a tissue engineering therapy for the volumetric loss of skeletal muscle., Am. J. Physiol. Cell Physiol. 305 (2013) C761–75. doi:10.1152/ajpcell.00189.2013.

[134] C.L. Ward, L. Ji, B.T. Corona, An Autologous Muscle Tissue Expansion Approach for the Treatment of Volumetric Muscle Loss, Biores. Open Access. 4 (2015) 198–208. doi:10.1089/biores.2015.0009.

[135] E. Hill, T. Boontheekul, D.J. Mooney, Regulating activation of transplanted cells controls tissue regeneration., Proc. Natl. Acad. Sci. U. S. A. 103 (2006) 2494–2499. doi:10.1073/pnas.0506004103.

[136] C. Borselli, H. Storrie, F. Benesch-Lee, D. Shvartsman, C. Cezar, J.W. Lichtman, et al., Functional muscle regeneration with combined delivery of angiogenesis and myogenesis factors, Proc. Natl. Acad. Sci. 107 (2010) 3287–3292. doi:10.1073/pnas.0903875106.

[137] X.-W. Du, H.-L. Wu, Y.-F. Zhu, J.-B. Hu, F. Jin, R.-P. Lv, et al., Experimental study of therapy of bone marrow mesenchymal stem cells or muscle-like cells/calcium alginate composite gel for the treatment of stress urinary incontinence., Neurourol. Urodyn. 32 (2013) 281–6. doi:10.1002/nau.22291.

[138] C. Borselli, C.A. Cezar, D. Shvartsman, H.H. Vandenburgh, D.J. Mooney, The role of multifunctional delivery scaffold in the ability of cultured myoblasts to promote muscle regeneration, Biomaterials. 32 (2011) 8905–8914. doi:10.1016/j.biomaterials.2011.08.019.

[139] L. Wang, L. Cao, J. Shansky, Z. Wang, D. Mooney, H. Vandenburgh, Minimally Invasive Approach to the Repair of Injured Skeletal Muscle With a Shape-memory Scaffold, Mol. Ther. 22 (2014) 1441–1449. doi:10.1038/mt.2014.78.

[140] S. Kin, A. Hagiwara, Y. Nakase, Y. Kuriu, S. Nakashima, T. Yoshikawa, et al., Regeneration of Skeletal Muscle Using In Situ Tissue Engineering on an Acellular Collagen Sponge Scaffold in a Rabbit Model, ASAIO J. 53 (2007) 506–513. doi:10.1097/MAT.0b013e3180d09d81.

[141] V. Kroehne, I. Heschel, F. Schügner, D. Lasrich, J.W. Bartsch, H. Jockusch, Use of a novel collagen matrix with oriented pore structure for muscle cell differentiation in cell culture and in grafts, J. Cell. Mol. Med. 12 (2008) 1640–1648. doi:10.1111/j.1582-4934.2008.00238.x.

[142] S. Carnio, E. Serena, C.A. Rossi, P. De Coppi, N. Elvassore, L. Vitiello, Three-dimensional porous scaffold allows long-term wild-type cell delivery in dystrophic muscle, J. Tissue Eng. Regen. Med. 5 (2011) 1–10. doi:10.1002/term.282.

[143] K.-C. Kuo, R.-Z. Lin, H.-W. Tien, P.-Y. Wu, Y.-C. Li, J.M. Melero-Martin, et al., Bioengineering vascularized tissue constructs using an injectable cell-laden enzymatically crosslinked collagen hydrogel derived from dermal extracellular matrix, Acta Biomater. 27 (2015) 151–166. doi:10.1016/j.actbio.2015.09.002.

[144] P.B. van Wachem, L. a Brouwer, M.J. van Luyn, Absence of muscle regeneration after implantation of a collagen matrix seeded with myoblasts., Biomaterials. 20 (1999) 419–26.

doi:10.1016/S0142-9612(98)00185-9.

[145] J.P. Beier, J. Stern-Straeter, V.T. Foerster, U. Kneser, G.B. Stark, A.D. Bach, Tissue engineering of injectable muscle: three-dimensional myoblast-fibrin injection in the syngeneic rat animal model., Plast. Reconstr. Surg. 118 (2006) 1113–21; discussion 1122–4. doi:10.1097/01.prs.0000221007.97115.1d.

[146] R.L. Page, C. Malcuit, L. Vilner, I. Vojtic, S. Shaw, E. Hedblom, et al., Restoration of skeletal muscle defects with adult human cells delivered on fibrin microthreads., Tissue Eng. Part A. 17 (2011) 2629–40. doi:10.1089/ten.TEA.2011.0024.

[147] C. Gerard, M.A. Forest, G. Beauregard, D. Skuk, J.P. Tremblay, Fibrin Gel Improves the Survival of Transplanted Myoblasts, 21 (2012) 127–137.

[148] M.L. Williams, T.Y. Kostrominova, E.M. Arruda, L.M. Larkin, Effect of implantation on engineered skeletal muscle constructs, J. Tissue Eng. Regen. Med. 7 (2013) 434–442. doi:10.1002/term.537.

[149] T.L. Criswell, B.T. Corona, Z. Wang, Y. Zhou, G. Niu, Y. Xu, et al., The role of endothelial cells in myofiber differentiation and the vascularization and innervation of bioengineered muscle tissue in vivo, Biomaterials. 34 (2013) 140–149. doi:10.1016/j.biomaterials.2012.09.045.

[150] C.A. Rossi, M. Flaibani, B. Blaauw, M. Pozzobon, E. Figallo, C. Reggiani, et al., In vivo tissue engineering of functional skeletal muscle by freshly isolated satellite cells embedded in a photopolymerizable hydrogel., FASEB J. 25 (2011) 2296–2304. doi:10.1096/fj.10-174755.

[151] K. Garg, C.L. Ward, B.T. Corona, Asynchronous inflammation and myogenic cell migration limit muscle tissue regeneration mediated by acellular scaffolds, Inflamm. Cell Signal. (2014) 6–8. doi:10.14800/ics.530.

[152] F.S. Tedesco, A. Dellavalle, J. Diaz-Manera, G. Messina, G. Cossu, Repairing skeletal muscle: regenerative potential of skeletal muscle stem cells., J. Clin. Invest. 120 (2010) 11–9. doi:10.1172/JCI40373.

[153] F.S. Tedesco, G. Cossu, Stem cell therapies for muscle disorders, Curr. Opin. Neurol. 25 (2012) 597–603. doi:10.1097/WCO.0b013e328357f288.

[154] D.O. Fauza, Tissue engineering in congenital diaphragmatic hernia., Semin. Pediatr. Surg. 23

(2014) 135–140. doi:10.1053/j.sempedsurg.2014.04.004.

[155] R. Georgescu, L. Chiu, R. Neme, I. Georgescu, A. Stoica, E. Georgescu, Possibilities and limits in the treatment of congenital diaphragmatic hernia, 7 (2014) 433–439.

[156] N. Hibino, G. Villalona, N. Pietris, D.R. Duncan, A. Schoffner, J.D. Roh, et al., Tissue-engineered vascular grafts form neovessels that arise from regeneration of the adjacent blood vessel., FASEB J. 25 (2011) 2731–2739. doi:10.1096/fj.11-182246.

[157] T. Breymann, U. Blanz, M. a. Wojtalik, W. Daenen, R. Hetzer, G. Sarris, et al., European Contegra multicentre study: 7-year results after 165 valved bovine jugular vein graft implantations., Thorac. Cardiovasc. Surg. 57 (2009) 257–269. doi:10.1055/s-0029-1185513.

[158] S.A. Antoniou, R. Pointner, F.-A. Granderath, F. Kockerling, The Use of Biological Meshes in Diaphragmatic Defects - An Evidence-Based Review of the Literature., Front. Surg. 2 (2015) 56. doi:10.3389/fsurg.2015.00056.

[159] J. a Burdick, R.L. Mauck, J.H. Gorman, R.C. Gorman, Acellular biomaterials: an evolving alternative to cell-based therapies., Sci. Transl. Med. 5 (2013) 176ps4. doi:10.1126/scitranslmed.3003997.

[160] L. Teodori, A. Costa, R. Marzio, B. Perniconi, D. Coletti, S. Adamo, et al., Native extracellular matrix: a new scaffolding platform for repair of damaged muscle, Front. Physiol. 5 (2014) 1–9. doi:10.3389/fphys.2014.00218.

[161] E. Carlson, Edward CMeezan, J.T. Hjelle, K. Brendel, E.C. Carlson, A simple, versatile, nondisruptive method for the isolation of morpholigcally and chemicallu pure basement membranes from several tissues, Life Sci. 17 (1975) 1721–1732. doi:10.1016/0024-3205(75)90119-8.

[162] S. Baiguera, P. Jungebluth, A. Burns, C. Mavilia, J. Haag, P. De Coppi, et al., Tissue engineered human tracheas for in vivo implantation, Biomaterials. 31 (2010) 8931–8938. doi:10.1016/j.biomaterials.2010.08.005.

[163] J. Harold, L. Drabkin, Spectrophotometry of HbNO and SHb, (n.d.).

[164] J.D. Rosenblatt, A.I. Lunt, D.J. Parry, T.A. Partridge, Culturing satellite cells from living single muscle fiber explants, Vitr. Cell Dev Biol Anim. 31 (1995) 773–779. doi:10.1007/bf02634119.

[165] C. Lagord, L. Soulet, S. Bonavaud, Y. Bassaglia, C. Rey, G. Barlovatz-Meimon, et al., Differential myogenicity of satellite cells isolated from extensor digitorum longus (EDL) and soleus rat muscles revealed in vitro., Cell Tissue Res. 291 (1998) 455–68. http://www.ncbi.nlm.nih.gov/pubmed/9477302.

[166] L. Urbani, M. Piccoli, C. Franzin, M. Pozzobon, P. de Coppi, Hypoxia Increases Mouse Satellite Cell Clone Proliferation Maintaining both In Vitro and In Vivo Heterogeneity and Myogenic Potential, PLoS One. 7 (2012) 1–13. doi:10.1371/journal.pone.0049860.

[167] H.M. Blau, C. Webster, Isolation and characterization of human muscle cells., Proc. Natl. Acad. Sci. U. S. A. 78 (1981) 5623–7. doi:10.1073/pnas.78.9.5623.

[168] G.K. Pavlath, D. Thaloor, T. a. Rando, M. Cheong, A.W. English, B. Zheng, Heterogeneity among muscle precursor cells in adult skeletal muscles with differing regenerative capacities, Dev. Dyn. 212 (1998) 495–508. doi:10.1002/(SICI)1097-0177(199808)212:4<495::AID-AJA3>3.0.CO;2-C.

[169] P. Chapters, C. Franzin, C.A. Secondary, C. Author, C. Franzin, M. Piccoli, et al., Springer Protocols Isolation and expansion of muscle precursor cells from human skeletal muscle biopsies, (2014).

[170] P.M. Group, Platelet-rich Plasma : Properties and Clinical Applications, Growth Factors. 2 (2007) 73–78.

[171] J. Schindelin, I. Arganda-Carreras, E. Frise, V. Kaynig, M. Longair, T. Pietzsch, et al., Fiji - an Open Source platform for biological image analysis, Nat. Methods. 9 (2012) 10.1038/nmeth.2019. doi:10.1038/nmeth.2019.

[172] C.M. Walthers, A.K. Nazemi, S.L. Patel, B.M. Wu, J.C.Y. Dunn, The effect of scaffold macroporosity on angiogenesis and cell survival in tissue-engineered smooth muscle, Biomaterials. 35 (2014) 5129–5137. doi:10.1016/j.biomaterials.2014.03.025.

[173] C. Chiappini, E. De Rosa, J.O. Martinez, X. Liu, J. Steele, M.M. Stevens, et al., Biodegradable silicon nanoneedles delivering nucleic acids intracellularly induce localized in vivo neovascularization., Nat. Mater. (2015) 6–13. doi:10.1038/nmat4249.

[174] A.C. Brown, T.H. Barker, Fibrin-based biomaterials: Modulation of macroscopic properties

through rational design at the molecular level, Acta Biomater. 10 (2014) 1502–1514. doi:10.1016/j.actbio.2013.09.008.

[175] E. Leikina, K. Melikov, S. Sanyal, S.K. Verma, B. Eun, C. Gebert, et al., Extracellular annexins and dynamin are important for sequential steps in myoblast fusion, J. Cell Biol. 200 (2013) 109–123. doi:10.1083/jcb.201207012.

[176] F. Gattazzo, A. Urciuolo, P. Bonaldo, Extracellular matrix: A dynamic microenvironment for stem cell niche, Biochim. Biophys. Acta - Gen. Subj. 1840 (2014) 2506–2519. doi:10.1016/j.bbagen.2014.01.010.

[177] A. Urciuolo, M. Quarta, V. Morbidoni, F. Gattazzo, S. Molon, P. Grumati, et al., Collagen VI regulates satellite cell self-renewal and muscle regeneration., Nat. Commun. 4 (2013) 1964. doi:10.1038/ncomms2964.

[178] F. Calvo, N. Ege, A. Grande-Garcia, S. Hooper, R.P. Jenkins, S.I. Chaudhry, et al., Mechanotransduction and YAP-dependent matrix remodelling is required for the generation and maintenance of cancer-associated fibroblasts, Nat. Cell Biol. 15 (2013) 637–646. doi:10.1038/ncb2756.

[179] S. Calve, S.J. Odelberg, H.-G. Simon, A transitional extracellular matrix instructs cell behavior during muscle regeneration, Dev. Biol. 344 (2010) 259–271. doi:10.1016/j.ydbio.2010.05.007.

[180] R.P. Mecham, Overview of extracellular matrix, Curr. Protoc. Cell Biol. (2012) 1–16. doi:10.1002/0471143030.cb1001s57.

[181] J.K. Mouw, G. Ou, V.M. Weaver, Extracellular matrix assembly: a multiscale deconstruction., Nat. Rev. Mol. Cell Biol. 15 (2014) 771–785. doi:10.1038/nrm3902.

[182] M. Larsen, V. V Artym, J.A. Green, K.M. Yamada, The matrix reorganized: extracellular matrix remodeling and integrin signaling., Curr. Opin. Cell Biol. 18 (2006) 463–71. doi:10.1016/j.ceb.2006.08.009.

[183] M.M. Martino, P.S. Briquez, a. Ranga, M.P. Lutolf, J. a. Hubbell, Heparin-binding domain of fibrin(ogen) binds growth factors and promotes tissue repair when incorporated within a synthetic matrix, Proc. Natl. Acad. Sci. 110 (2013) 4563–4568. doi:10.1073/pnas.1221602110.

[184] S. Higashiyama, J. a Abraham, M. Klagsbrun, Heparin-binding EGF-like growth factor

stimulation of smooth muscle cell migration: dependence on interactions with cell surface heparan sulfate., J. Cell Biol. 122 (1993) 933–40. doi:10.1083/jcb.122.4.933.

[185] G. Neufeld, T. Cohen, S. Gengrinovitch, Z. Poltorak, Vascular endothelial growth factor (VEGF) and its receptors., FASEB J. 13 (1999) 9–22. doi:Doi 10.1210/Er.2003-0027.

[186] C.I. Gama, S.E. Tully, N. Sotogaku, P.M. Clark, M. Rawat, N. Vaidehi, et al., Sulfation patterns of glycosaminoglycans encode molecular recognition and activity, Nat. Chem. Biol. 2 (2006) 467–473. doi:10.1038/nchembio810.

[187] K. Forsten-Williams, C.L. Chu, M. Fannon, J.A. Buczek-Thomas, M. a. Nugent, Control of growth factor networks by heparan sulfate proteoglycans, Ann. Biomed. Eng. 36 (2008) 2134–2148. doi:10.1007/s10439-008-9575-z.

[188] M.A. Schwartz, Integrins and extracellular matrix in mechanotransduction., Cold Spring Harb. Perspect. Biol. 2 (2010) a005066. doi:10.1101/cshperspect.a005066.

[189] J.H. Kim, Y. Ren, W.P. Ng, S. Li, S. Son, Y.-S. Kee, et al., Mechanical Tension Drives Cell Membrane Fusion., Dev. Cell. 32 (2015) 561–73. doi:10.1016/j.devcel.2015.01.005.

[190] K.L. Mui, Y.H. Bae, L. Gao, S.-L. Liu, T. Xu, G.L. Radice, et al., N-Cadherin Induction by ECM Stiffness and FAK Overrides the Spreading Requirement for Proliferation of Vascular Smooth Muscle Cells, Cell Rep. 10 (2015) 1477–1486. doi:10.1016/j.celrep.2015.02.023.

[191] G. Lacraz, A.-J. Rouleau, V. Couture, T. Söllrald, G. Drouin, N. Veillette, et al., Increased Stiffness in Aged Skeletal Muscle Impairs Muscle Progenitor Cell Proliferative Activity, PLoS One. 10 (2015) e0136217. doi:10.1371/journal.pone.0136217.

[192] E. Levi, R. Fridman, H.Q. Miao, Y.S. Ma, a Yayon, I. Vlodavsky, Matrix metalloproteinase 2 releases active soluble ectodomain of fibroblast growth factor receptor 1., Proc. Natl. Acad. Sci. U. S. A. 93 (1996) 7069–7074. doi:10.1073/pnas.93.14.7069.

[193] I. Bellayr, K. Holden, X. Mu, H. Pan, Y. Li, Matrix metalloproteinase inhibition negatively affects muscle stem cell behavior, Int. J. Clin. Exp. Pathol. 6 (2013) 124–141.

[194] W.G. Stetler-Stevenson, Tissue inhibitors of metalloproteinases in cell signaling: metalloproteinase-independent biological activities., Sci. Signal. 1 (2008) re6. doi:10.1126/scisignal.127re6.

[195] J.E. Murphy-Ullrich, E.H. Sage, Revisiting the matricellular concept., Matrix Biol. 37 (2014) 1–14. doi:10.1016/j.matbio.2014.07.005.

[196] S. Ricard-Blum, R. Salza, Matricryptins and matrikines: biologically active fragments of the extracellular matrix, Exp. Dermatol. 23 (2014) 457–463. doi:10.1111/exd.12435.

[197] A. Neve, F.P. Cantatore, N. Maruotti, A. Corrado, D. Ribatti, Extracellular Matrix Modulates Angiogenesis in Physiological and Pathological Conditions, Biomed Res. Int. 2014 (2014) 1–10. doi:10.1155/2014/756078.

[198] C. Bonnans, J. Chou, Z. Werb, Remodelling the extracellular matrix in development and disease, Nat. Rev. Mol. Cell Biol. 15 (2014) 786–801. doi:10.1038/nrm3904.

[199] C.J. Mann, E. Perdiguero, Y. Kharraz, S. Aguilar, P. Pessina, A.L. Serrano, et al., Aberrant repair and fibrosis development in skeletal muscle, Skelet. Muscle. 1 (2011) 21. doi:10.1186/2044-5040-1-21.

[200] T. a Wynn, T.R. Ramalingam, Mechanisms of fibrosis: therapeutic translation for fibrotic disease., Nat. Med. 18 (2012) 1028–40. doi:10.1038/nm.2807.

[201] E. Pegoraro, H. Marks, C.A. Garcia, T. Crawford, P. Mancias, A.M. Connolly, et al., Laminin alpha2 muscular dystrophy: genotype/phenotype studies of 22 patients, Neurology. 51 (1998) 101–110. http://www.ncbi.nlm.nih.gov/pubmed/9674786.

[202] D. Montarras, A. L'Honoré, M. Buckingham, Lying low but ready for action: The quiescent muscle satellite cell, FEBS J. 280 (2013) 4036–4050. doi:10.1111/febs.12372.

[203] D. Fan, A. Takawale, J. Lee, Z. Kassiri, Cardiac fibroblasts, fibrosis and extracellular matrix remodeling in heart disease., Fibrogenesis Tissue Repair. 5 (2012) 15. doi:10.1186/1755-1536-5-15.

[204] A.M. Segura, O.H. Frazier, L.M. Buja, Fibrosis and heart failure, Heart Fail. Rev. 19 (2014) 173–185. doi:10.1007/s10741-012-9365-4.

[205] M.W. Mosesson, Fibrinogen and fibrin structure and functions, J. Thromb. Haemost. 3 (2005) 1894–1904. doi:10.1111/j.1538-7836.2005.01365.x.

[206] S. Rahman, Y. Patel, J. Murray, K. V Patel, R. Sumathipala, M. Sobel, et al., Novel hepatocyte growth factor (HGF) binding domains on fibronectin and vitronectin coordinate a distinct and

amplified Met-integrin induced signalling pathway in endothelial cells., BMC Cell Biol. 6 (2005) 8. doi:10.1186/1471-2121-6-8.

[207] V. Charulatha, A. Rajaram, Influence of different crosslinking treatments on the physical properties of collagen membranes., Biomaterials. 24 (2003) 759–67. doi:10.1016/S0142-9612(02)00412-X.

[208] L. Buttafoco, N.G. Kolkman, P. Engbers-Buijtenhuijs, a. a. Poot, P.J. Dijkstra, I. Vermes, et al., Electrospinning of collagen and elastin for tissue engineering applications, Biomaterials. 27 (2006) 724–734. doi:10.1016/j.biomaterials.2005.06.024.

[209] J.C. Middleton, a J. Tipton, Synthetic biodegradable polymers as orthopedic devices., Biomaterials. 21 (2000) 2335–2346. doi:10.1016/S0142-9612(00)00101-0.

[210] A. Göpferich, Mechanisms of polymer degradation and erosion, Biomaterials. 17 (1996) 103–114. doi:10.1016/0142-9612(96)85755-3.

[211] E. Farkas, Z.G. Meszena, a Toldy, S. Matko, Polymer Degradation and Stability, Polym. Degrad. Stab. 93 (2008) 1205–1213. doi:10.1016/j.polymdegradstab.2008.02.010.

[212] R. Kaur, I. Badea, Nanodiamonds as novel nanomaterials for biomedical applications: Drug delivery and imaging systems, Int. J. Nanomedicine. 8 (2013) 203–220. doi:10.2147/IJN.S37348.

[213] J.S. Miller, K.R. Stevens, M.T. Yang, B.M. Baker, D.-H.T. Nguyen, D.M. Cohen, et al., Rapid casting of patterned vascular networks for perfusable engineered three-dimensional tissues, Nat. Mater. 11 (2012) 768–774. doi:10.1038/nmat3357.

[214] P. a. Gunatillake, R. Adhikari, N. Gadegaard, Biodegradable synthetic polymers for tissue engineering, Eur. Cells Mater. 5 (2003) 1–16. doi:vol005a01 [pii].

[215] E.S. Place, J.H. George, C.K. Williams, M.M. Stevens, Synthetic polymer scaffolds for tissue engineering., Chem. Soc. Rev. 38 (2009) 1139–1151. doi:10.1039/b811392k.

[216] A. V. Boruch, A. Nieponice, I.R. Qureshi, T.W. Gilbert, S.F. Badylak, Constructive Remodeling of Biologic Scaffolds is Dependent on Early Exposure to Physiologic Bladder Filling in a Canine Partial Cystectomy Model, J. Surg. Res. 161 (2010) 217–225. doi:10.1016/j.jss.2009.02.014.

[217] A. Clough, J. Ball, G.S. Smith, S. Leibman, Porcine small intestine submucosa matrix (Surgisis)

for esophageal perforation., Ann. Thorac. Surg. 91 (2011) e15–6. doi:10.1016/j.athoracsur.2010.10.011.

[218] A. Soto-Gutierrez, L. Zhang, C. Medberry, K. Fukumitsu, D. Faulk, H. Jiang, et al., A whole-organ regenerative medicine approach for liver replacement., Tissue Eng. Part C. Methods. 17 (2011) 677–686. doi:10.1089/ten.tec.2010.0698.

[219] H.C. Ott, B. Clippinger, C. Conrad, C. Schuetz, I. Pomerantseva, L. Ikonomou, et al., Regeneration and orthotopic transplantation of a bioartificial lung., Nat. Med. 16 (2010) 927–933. doi:10.1038/nm.2193.

[220] M.J. Elliott, P. De Coppi, S. Speggiorin, D. Roebuck, C.R. Butler, E. Samuel, et al., Stem-cell-based, tissue engineered tracheal replacement in a child: A 2-year follow-up study, Lancet. 380 (2012) 994–1000. doi:10.1016/S0140-6736(12)60737-5.

[221] J.M. Fishman, M.W. Lowdell, L. Urbani, T. Ansari, A.J. Burns, M. Turmaine, et al., Immunomodulatory effect of a decellularized skeletal muscle scaffold in a discordant xenotransplantation model, Proc. Natl. Acad. Sci. 110 (2013) 14360–14365. doi:10.1073/pnas.1213228110.

[222] A.H. Morris, T.R. Kyriakides, Matricellular proteins and biomaterials, Matrix Biol. 37 (2014) 183–191. doi:10.1016/j.matbio.2014.03.002.

[223] J.E. Reing, L. Zhang, J. Myers-Irvin, K.E. Cordero, D.O. Freytes, E. Heber-Katz, et al., Degradation products of extracellular matrix affect cell migration and proliferation, Tissue Eng Part A. 15 (2009) 605–614. doi:10.1089/ten.tea.2007.0425.

[224] K. a Daly, A.M. Stewart-Akers, H. Hara, M. Ezzelarab, C. Long, K. Cordero, et al., Effect of the alphaGal epitope on the response to small intestinal submucosa extracellular matrix in a nonhuman primate model., Tissue Eng. Part A. 15 (2009) 3877–3888. doi:10.1089/ten.TEA.2009.0089.

[225] a J. Allman, T.B. McPherson, S.F. Badylak, L.C. Merrill, B. Kallakury, C. Sheehan, et al., Xenogeneic extracellular matrix grafts elicit a TH2-restricted immune response., Transplantation. 71 (2001) 1631–1640. doi:10.1097/00007890-200106150-00024.

[226] A. Crupi, A. Costa, A. Tarnok, S. Melzer, L. Teodori, Inflammation in tissue engineering: The

Janus between engraftment and rejection, Eur. J. Immunol. 45 (2015) 3222–3236. doi:10.1002/eji.201545818.

[227] T.J. Keane, R. Londono, N.J. Turner, S.F. Badylak, Consequences of ineffective decellularization of biologic scaffolds on the host response, Biomaterials. 33 (2012) 1771–1781. doi:10.1016/j.biomaterials.2011.10.054.

[228] P.M. Crapo, T.W. Gilbert, S.F. Badylak, An overview of tissue and whole organ decellularization processes, Biomaterials. 32 (2011) 3233–3243. doi:10.1016/j.biomaterials.2011.01.057.

[229] W.Q. Sun, H. Xu, M. Sandor, J. Lombardi, Process-induced extracellular matrix alterations affect the mechanisms of soft tissue repair and regeneration., J. Tissue Eng. 4 (2013) 2041731413505305. doi:10.1177/2041731413505305.

[230] R.L.P. Romao, A. Nasr, P.P.L. Chiu, J.C. Langer, What is the best prosthetic material for patch repair of congenital diaphragmatic hernia? Comparison and meta-analysis of porcine small intestinal submucosa and polytetrafluoroethylene, J. Pediatr. Surg. 47 (2012) 1496–1500. doi:10.1016/j.jpedsurg.2012.01.009.

[231] T.W. Gilbert, T.L. Sellaro, S.F. Badylak, Decellularization of tissues and organs, Biomaterials. 27 (2006) 3675–3683. doi:10.1016/j.biomaterials.2006.02.014.

[232] R. Londono, S.F. Badylak, Biologic Scaffolds for Regenerative Medicine: Mechanisms of In vivo Remodeling, Ann. Biomed. Eng. 43 (2015) 577–592. doi:10.1007/s10439-014-1103-8.

[233] T.A. Bertram, E. Tentoff, P.C. Johnson, B. Tawil, M. Van Dyke, K.B. Hellman, Hurdles in tissue engineering/regenerative medicine product commercialization: a pilot survey of governmental funding agencies and the financial industry., Tissue Eng. Part A. 18 (2012) 2187–94. doi:10.1089/ten.TEA.2012.0186.

[234] R.O. Hynes, The extracellular matrix: not just pretty fibrils., Science. 326 (2009) 1216–1219. doi:10.1126/science.1176009.

[235] P.N. Nonaka, N. Campillo, J.J. Uriarte, E. Garreta, E. Melo, L.V.F. de Oliveira, et al., Effects of freezing/thawing on the mechanical properties of decellularized lungs., J. Biomed. Mater. Res. A. 102 (2014) 413–9. doi:10.1002/jbm.a.34708.

[236] D.O. Freytes, R.S. Tullius, S.F. Badylak, Effect of storage upon material properties of lyophilized porcine extracellular matrix derived from the urinary bladder., J. Biomed. Mater. Res. B. Appl. Biomater. 78 (2006) 327–33. doi:10.1002/jbm.b.30491.

[237] W.Q. Sun, S.-S. Gouk, Aging of a Regenerative Biologic Scaffold (AlloDerm Native Tissue Matrix) During Storage at Elevated Humidity and Temperature, (2008).

[238] P. Mazur, Freezing of living cells: mechanisms and implications., Am. J. Physiol. 247 (1984) C125–42.

[239] V. Mirabet, C. Carda, P. Solves, E. Novella-Maestre, F. Carbonell-Uberos, J.M. Caffarena, et al., Long-term storage in liquid nitrogen does not affect cell viability in cardiac valve allografts., Cryobiology. 57 (2008) 113–21. doi:10.1016/j.cryobiol.2008.07.008.

[240] J.O.M. Karlsson, M. Toner, Long-term storage of tissues by cryopreservation: critical issues, Biomaterials. 17 (1996) 243–256. doi:10.1016/0142-9612(96)85562-1.

[241] C. Polge, A. Smith, A. Parkes, Revival of Spermatozoa after Vitrification and Dehydration at Low Temperatures, Nature. 164 (1949) 666–666. doi:10.1038/164666a0.

[242] C.J. Gerson, S. Goldstein, A.E. Heacox, Retained structural integrity of collagen and elastin within cryopreserved human heart valve tissue as detected by two-photon laser scanning confocal microscopy., Cryobiology. 59 (2009) 171–9. doi:10.1016/j.cryobiol.2009.06.012.

[243] D.E. Pegg, Principles of cryopreservation., Methods Mol. Biol. 368 (2007) 39–57. doi:10.1007/978-1-59745-362-2_3.

[244] S. Baiguera, C. Del Gaudio, M.O. Jaus, L. Polizzi, A. Gonfiotti, C.E. Comin, et al., Long-term changes to in vitro preserved bioengineered human trachea and their implications for decellularized tissues., Biomaterials. 33 (2012) 3662–72. doi:10.1016/j.biomaterials.2012.01.064.

[245] D.A. Mladenov, T.D. Tsvetkov, N.L. Vulchanov, Freeze drying of biomaterials for the medical practice., Cryobiology. 30 (1993) 335–48. doi:10.1006/cryo.1993.1033.

[246] C.F. Borgognoni, M.J.S. Maizato, A.A. Leirner, B. Polakiewicz, M.M. Beppu, O.Z. Higa, et al., Effect of freeze-drying on the mechanical, physical and morphological properties of glutaraldehyde-treated bovine pericardium: evaluation of freeze-dried treated bovine

pericardium properties., J. Appl. Biomater. Biomech. 8 (2010) 186–90.

[247] A. Atala, S.B. Bauer, S. Soker, J.J. Yoo, A.B. Retik, Tissue-engineered autologous bladders for patients needing cystoplasty., Lancet. 367 (2006) 1241–6. doi:10.1016/S0140-6736(06)68438-9.

[248] A. Raya-Rivera, D.R. Esquiliano, J.J. Yoo, E. Lopez-Bayghen, S. Soker, A. Atala, Tissue-engineered autologous urethras for patients who need reconstruction: an observational study., Lancet (London, England). 377 (2011) 1175–82. doi:10.1016/S0140-6736(10)62354-9.

[249] B.E. Uygun, A. Soto-Gutierrez, H. Yagi, M.-L. Izamis, M.A. Guzzardi, C. Shulman, et al., Organ reengineering through development of a transplantable recellularized liver graft using decellularized liver matrix, Nat. Med. 16 (2010) 814–820. doi:10.1038/nm.2170.

[250] H.C. Ott, T.S. Matthiesen, S.-K. Goh, L.D. Black, S.M. Kren, T.I. Netoff, et al., Perfusion-decellularized matrix: using nature's platform to engineer a bioartificial heart., Nat. Med. 14 (2008) 213–221. doi:10.1038/nm1684.

[251] T.H. Petersen, E. a Calle, L. Zhao, E.J. Lee, L. Gui, M.B. Raredon, et al., Tissue-engineered lungs for in vivo implantation., Science. 329 (2010) 538–541. doi:10.1126/science.1189345.

[252] G.J. Christ, M.L. Siriwardane, P. de Coppi, Engineering muscle tissue for the fetus: getting ready for a strong life, Front. Pharmacol. 6 (2015) 1–11. doi:10.3389/fphar.2015.00053.

[253] S. Mayer, H. Decaluwe, M. Ruol, S. Manodoro, M. Kramer, H. Till, et al., Diaphragm Repair with a Novel Cross-Linked Collagen Biomaterial in a Growing Rabbit Model, PLoS One. 10 (2015) e0132021. doi:10.1371/journal.pone.0132021.

[254] P.M. Crapo, T.W. Gilbert, S.F. Badylak, An overview of tissue and whole organ decellularization processes., Biomaterials. 32 (2011) 3233–43. doi:10.1016/j.biomaterials.2011.01.057.

[255] S. Dupont, L. Morsut, M. Aragona, E. Enzo, S. Giulitti, M. Cordenonsi, et al., Role of YAP/TAZ in mechanotransduction., Nature. 474 (2011) 179–183. doi:10.1038/nature10137.

[256] F. Trensz, F. Lucien, V. Couture, T. Söllrald, G. Drouin, A.-J. Rouleau, et al., Increased microenvironment stiffness in damaged myofibers promotes myogenic progenitor cell proliferation, Skelet. Muscle. 5 (2015) 5. doi:10.1186/s13395-015-0030-1.

[257] M. Saclier, H. Yacoub-Youssef, A.L. Mackey, L. Arnold, H. Ardjoune, M. Magnan, et al.,

Differentially Activated Macrophages Orchestrate Myogenic Precursor Cell Fate During Human Skeletal Muscle Regeneration, Stem Cells. 31 (2013) 384–396. doi:10.1002/stem.1288.

[258] O. Agbulut, P. Noirez, F. Beaumont, G. Butler-Browne, Myosin heavy chain isoforms in postnatal muscle development of mice, Biol. Cell. 95 (2003) 399–406. doi:10.1016/S0248-4900(03)00087-X.

[259] L.E. Carey, C.L. Dearth, S.A. Johnson, R. Londono, C.J. Medberry, K.A. Daly, et al., In vivo degradation of 14C-labeled porcine dermis biologic scaffold., Biomaterials. 35 (2014) 8297–304. doi:10.1016/j.biomaterials.2014.06.015.

[260] A.J. Beattie, T.W. Gilbert, J.P. Guyot, A.J. Yates, S.F. Badylak, Chemoattraction of progenitor cells by remodeling extracellular matrix scaffolds., Tissue Eng. Part A. 15 (2009) 1119–1125. doi:10.1089/ten.tea.2008.0162.

[261] B.J. Kwee, D.J. Mooney, Manipulating the Intersection of Angiogenesis and Inflammation, Ann. Biomed. Eng. 43 (2015) 628–640. doi:10.1007/s10439-014-1145-y.

[262] J.G. Tidball, S.A. Villalta, Regulatory interactions between muscle and the immune system during muscle regeneration., Am. J. Physiol. Regul. Integr. Comp. Physiol. 298 (2010) R1173–R1187. doi:10.1152/ajpregu.00735.2009.

[263] S. Browne, A. Pandit, Biomaterial-Mediated Modification of the Local Inflammatory Environment, Front. Bioeng. Biotechnol. 3 (2015) 1–14. doi:10.3389/fbioe.2015.00067.

[264] S. Chen, J.A. Jones, Y. Xu, H.-Y. Low, J.M. Anderson, K.W. Leong, Characterization of topographical effects on macrophage behavior in a foreign body response model, Biomaterials. 31 (2010) 3479–3491. doi:10.1016/j.biomaterials.2010.01.074.

[265] U. Klinge, U. Dietz, N. Fet, B. Klosterhalfen, Characterisation of the cellular infiltrate in the foreign body granuloma of textile meshes with its impact on collagen deposition, Hernia. 18 (2014) 571–578. doi:10.1007/s10029-014-1220-1.

[266] M. Piccoli, C. Franzin, E. Bertin, L. Urbani, B. Blaauw, A. Repele, et al., Amniotic fluid stem cells restore the muscle cell niche in a HSA-Cre, SmnF7/F7 mouse model, Stem Cells. 30 (2012) 1675–1684. doi:10.1002/stem.1134.

[267] S. Gregori, D. Tomasoni, V. Pacciani, M. Scirpoli, M. Battaglia, C.F. Magnani, et al.,

Differentiation of type 1 T regulatory cells (Tr1) by tolerogenic DC-10 requires the IL-10-dependent ILT4/HLA-G pathway, Blood. 116 (2010) 935–944. doi:10.1182/blood-2009-07-234872.

[268] B.M. Sicari, J.L. Dziki, B.F. Siu, C.J. Medberry, C.L. Dearth, S.F. Badylak, The promotion of a constructive macrophage phenotype by solubilized extracellular matrix, Biomaterials. 35 (2014) 8605–8612. doi:10.1016/j.biomaterials.2014.06.060.

[269] G.F. Mok, D. Sweetman, Many routes to the same destination: lessons from skeletal muscle development., Reproduction. 141 (2011) 301–12. doi:10.1530/REP-10-0394.

[270] R. Kalluri, M. Zeisberg, Fibroblasts in cancer., Nat. Rev. Cancer. 6 (2006) 392–401. doi:10.1038/nrc1877.

[271] J.S. Burns, M. Kristiansen, L.P. Kristensen, K.H. Larsen, M.O. Nielsen, H. Christiansen, et al., Decellularized Matrix from Tumorigenic Human Mesenchymal Stem Cells Promotes Neovascularization with Galectin-1 Dependent Endothelial Interaction, PLoS One. 6 (2011) e21888. doi:10.1371/journal.pone.0021888.

[272] G.L. Semenza, Vasculogenesis, angiogenesis, and arteriogenesis: Mechanisms of blood vessel formation and remodeling, J. Cell. Biochem. 102 (2007) 840–847. doi:10.1002/jcb.21523.

[273] S.K. Ramasamy, A.P. Kusumbe, R.H. Adams, Regulation of tissue morphogenesis by endothelial cell-derived signals, Trends Cell Biol. 25 (2015) 148–157. doi:10.1016/j.tcb.2014.11.007.

[274] M. Simons, A. Eichmann, Molecular Controls of Arterial Morphogenesis, Circ. Res. 116 (2015) 1712–1724. doi:10.1161/CIRCRESAHA.116.302953.

[275] L.-H. Chu, C.G. Rivera, a. S. Popel, J.S. Bader, Constructing the angiome: a global angiogenesis protein interaction network, Physiol. Genomics. 44 (2012) 915–924. doi:10.1152/physiolgenomics.00181.2011.

[276] E.I. Deryugina, J.P. Quigley, Tumor angiogenesis: MMP-mediated induction of intravasation- and metastasis-sustaining neovasculature, Matrix Biol. 44-46 (2015) 94–112. doi:10.1016/j.matbio.2015.04.004.

[277] S. Moens, J. Goveia, P.C. Stapor, A.R. Cantelmo, P. Carmeliet, The multifaceted activity of

VEGF in angiogenesis – Implications for therapy responses, Cytokine Growth Factor Rev. 25 (2014) 473–482. doi:10.1016/j.cytogfr.2014.07.009.

[278] E.A. Logsdon, S.D. Finley, A.S. Popel, F. Mac Gabhann, A systems biology view of blood vessel growth and remodelling, J. Cell. Mol. Med. 18 (2014) 1491–1508. doi:10.1111/jcmm.12164.

[279] M.D. Brown, O. Hudlicka, Modulation of physiological angiogenesis in skeletal muscle by mechanical forces: Involvement of VEGF and metalloproteinases, Angiogenesis. 6 (2003) 1–14. doi:10.1023/A:1025809808697.

[280] T.T. Rissanen, P. Korpisalo, J.E. Markkanen, T. Liimatainen, M.R. Ordén, I. Kholová, et al., Blood flow remodels growing vasculature during vascular endothelial growth factor gene therapy and determines between capillary arterialization and sprouting angiogenesis, Circulation. 112 (2005) 3937–3946. doi:10.1161/CIRCULATIONAHA.105.543124.

[281] O. Watson, P. Novodvorsky, C. Gray, A.M.K. Rothman, A. Lawrie, D.C. Crossman, et al., Blood flow suppresses vascular Notch signalling via dll4 and is required for angiogenesis in response to hypoxic signalling, Cardiovasc. Res. 100 (2013) 252–261. doi:10.1093/cvr/cvt170.

[282] K.H. Albrecht, P. Gaehtgens, A. Pries, M. Heuser, The Fahraeus Effect in Narrow Capillaries, Microvasc. Res. 18 (1979) 33–47. doi:http://dx.doi.org/10.1016/0026-2862(79)90016-5.

[283] D.G. Harrison, J. Widder, I. Grumbach, W. Chen, M. Weber, C. Searles, Endothelial mechanotransduction, nitric oxide and vascular inflammation, J Intern Med. 259 (2006) 351–363. doi:JIM1621 [pii]\r10.1111/j.1365-2796.2006.01621.x.

[284] E. Rigamonti, T. Touvier, E. Clementi, A. a Manfredi, S. Brunelli, P. Rovere-Querini, Requirement of inducible nitric oxide synthase for skeletal muscle regeneration after acute damage., J. Immunol. 190 (2013) 1767–77. doi:10.4049/jimmunol.1202903.

[285] B. Enholm, K. Paavonen, a Ristimäki, V. Kumar, Y. Gunji, J. Klefstrom, et al., Comparison of VEGF, VEGF-B, VEGF-C and Ang-1 mRNA regulation by serum, growth factors, oncoproteins and hypoxia., Oncogene. 14 (1997) 2475–2483. doi:10.1038/sj.onc.1201090.

[286] A. Bruno, A. Pagani, L. Pulze, A. Albini, K. Dallaglio, D.M. Noonan, et al., Orchestration of Angiogenesis by Immune Cells, Front. Oncol. 4 (2014) 1–13. doi:10.3389/fonc.2014.00131.

[287] N. Jetten, S. Verbruggen, M.J. Gijbels, M.J. Post, M.P.J. De Winther, M.M.P.C. Donners, Anti-

inflammatory M2, but not pro-inflammatory M1 macrophages promote angiogenesis in vivo, Angiogenesis. 17 (2014) 109–118. doi:10.1007/s10456-013-9381-6.

[288] J.E. Fish, J.D. Wythe, The molecular regulation of arteriovenous specification and maintenance, Dev. Dyn. 244 (2015) 391–409. doi:10.1002/dvdy.24252.

[289] E. Fagiani, G. Christofori, Angiopoietins in angiogenesis, Cancer Lett. 328 (2013) 18–26. doi:10.1016/j.canlet.2012.08.018.

[290] D. Shvartsman, H. Storrie-White, K. Lee, C. Kearney, Y. Brudno, N. Ho, et al., Sustained delivery of VEGF maintains innervation and promotes reperfusion in ischemic skeletal muscles via NGF/GDNF signaling., Mol. Ther. 22 (2014) 1243–53. doi:10.1038/mt.2014.76.

[291] A.R. Caseiro, T. Pereira, P.J. Bártolo, J.D. Santos, A.L. Luís, A.C. Maurício, Mesenchymal Stem Cells and Biomaterials Systems – Perspectives for Skeletal Muscle Tissue Repair and Regeneration, Procedia Eng. 110 (2015) 90–97. doi:10.1016/j.proeng.2015.07.014.

[292] M.D. Chamberlain, M.E.D. West, G.C. Lam, M. V. Sefton, In Vivo Remodelling of Vascularizing Engineered Tissues, Ann. Biomed. Eng. 43 (2015) 1189–1200. doi:10.1007/s10439-014-1146-x.

[293] S.N. Christo, K.R. Diener, A. Bachhuka, K. Vasilev, J.D. Hayball, Innate Immunity and Biomaterials at the Nexus : Friends or Foes, 2015 (2015).

[294] S.Y. Jung, S.M. Lim, F. Albertorio, G. Kim, M.C. Gurau, R.D. Yang, et al., The Vroman Effect: A Molecular Level Description of Fibrinogen Displacement, J. Am. Chem. Soc. 125 (2003) 12782–12786. doi:10.1021/ja037263o.

[295] K.L. Spiller, R.R. Anfang, K.J. Spiller, J. Ng, K.R. Nakazawa, J.W. Daulton, et al., The role of macrophage phenotype in vascularization of tissue engineering scaffolds, Biomaterials. 35 (2014) 4477–4488. doi:10.1016/j.biomaterials.2014.02.012.

[296] H. Liu, B. Chen, B. Lilly, Fibroblasts potentiate blood vessel formation partially through secreted factor TIMP-1, Angiogenesis. 11 (2008) 223–234. doi:10.1007/s10456-008-9102-8.

[297] G. Totonelli, P. Maghsoudlou, F. Georgiades, M. Garriboli, K. Koshy, M. Turmaine, et al., Detergent enzymatic treatment for the development of a natural acellular matrix for oesophageal regeneration, Pediatr. Surg. Int. 29 (2013) 87–95. doi:10.1007/s00383-012-3194-

3.

[298] W.R. Otto, N.A. Wright, Mesenchymal stem cells: from experiment to clinic., Fibrogenesis Tissue Repair. 4 (2011) 20. doi:10.1186/1755-1536-4-20.

[299] L.R. Madden, D.J. Mortisen, E.M. Sussman, S.K. Dupras, J. a. Fugate, J.L. Cuy, et al., Proangiogenic scaffolds as functional templates for cardiac tissue engineering, Proc. Natl. Acad. Sci. 107 (2010) 15211–15216. doi:10.1073/pnas.1006442107.

[300] T.T. Lee, J.R. García, J.I. Paez, A. Singh, E. a. Phelps, S. Weis, et al., Light-triggered in vivo activation of adhesive peptides regulates cell adhesion, inflammation and vascularization of biomaterials, Nat. Mater. 14 (2014) 352–360. doi:10.1038/nmat4157.

[301] J.K. Hong, J.Y. Bang, G. Xu, J.-H. Lee, Y. Kim, H.-J. Lee, et al., Thickness-controllable electrospun fibers promote tubular structure formation by endothelial progenitor cells., Int. J. Nanomedicine. 10 (2015) 1189–200. doi:10.2147/IJN.S73096.

[302] M. Simons, K. Alitalo, B.H. Annex, H.G. Augustin, C. Beam, B.C. Berk, et al., State-of-the-Art Methods for Evaluation of Angiogenesis and Tissue Vascularization: A Scientific Statement From the American Heart Association, 2015. doi:10.1161/RES.0000000000000054.

[303] Y.-T. Shiu, J. a Weiss, J.B. Hoying, M.N. Iwamoto, I.S. Joung, C.T. Quam, The role of mechanical stresses in angiogenesis., Crit. Rev. Biomed. Eng. 33 (2005) 431–510. doi:10.1615/CritRevBiomedEng.v33.i5.10.

[304] T. Heck, Computational models of sprouting angiogenesis and cell migration: towards multiscale mechanochemical models of angiogenesis, Math. Model. Nat. Phenom. xx (2015) 1–46. https://lirias.kuleuven.be/handle/123456789/474369.

[305] C. Latroche, C. Gitiaux, F. Chrétien, I. Desguerre, R. Mounier, B. Chazaud, Skeletal Muscle Microvasculature: A Highly Dynamic Lifeline, Physiology. 30 (2015) 417–427. doi:10.1152/physiol.00026.2015.

[306] E. Brzoska, M. Kowalewska, A. Markowska-Zagrajek, K. Kowalski, K. Archacka, M. Zimowska, et al., Sdf-1 (CXCL12) improves skeletal muscle regeneration via the mobilisation of Cxcr4 and CD34 expressing cells, Biol. Cell. 104 (2012) 722–737. doi:10.1111/boc.201200022.

[307] H. Gerhardt, M. Golding, M. Fruttiger, C. Ruhrberg, A. Lundkvist, A. Abramsson, et al., VEGF

guides angiogenic sprouting utilizing endothelial tip cell filopodia, J. Cell Biol. 161 (2003) 1163–1177. doi:10.1083/jcb.200302047.

[308] Z. Chen, A. Htay, W. Dos Santos, G.T. Gillies, H.L. Fillmore, M.M. Sholley, et al., In vitro angiogenesis by human umbilical vein endothelial cells (HUVEC) induced by three-dimensional co-culture with glioblastoma cells, J. Neurooncol. 92 (2009) 121–128. doi:10.1007/s11060-008-9742-y.

[309] P.D. Losty, Congenital diaphragmatic hernia: Where and what is the evidence?, Semin. Pediatr. Surg. 23 (2014) 278–282. doi:10.1053/j.sempedsurg.2014.09.008.

[310] C. Rosnoblet, A.S. Ribba, C.B. Wollheim, E.K. Kruithof, U.M. Vischer, Regulated von Willebrand factor (vWf) secretion is restored by pro-vWf expression in a transfectable endothelial cell line, Biochim. Biophys. Acta. 1495 (2000) 112–119. http://www.ncbi.nlm.nih.gov/pubmed/10634936.

[311] T. Wälchli, J.M. Mateos, O. Weinman, D. Babic, L. Regli, S.P. Hoerstrup, et al., Quantitative assessment of angiogenesis, perfused blood vessels and endothelial tip cells in the postnatal mouse brain, Nat. Protoc. 10 (2014) 53–74. doi:10.1038/nprot.2015.002.

[312] J.M. Anderson, A. Rodriguez, D.T. Chang, Foreign body reaction to biomaterials, Semin. Immunol. 20 (2008) 86–100. doi:10.1016/j.smim.2007.11.004.

[313] P. Stuelsatz, P. Keire, R. Almuly, Z. Yablonka-Reuveni, A contemporary atlas of the mouse diaphragm: myogenicity, vascularity, and the Pax3 connection., J. Histochem. Cytochem. 60 (2012) 638–57. doi:10.1369/0022155412452417.

[314] A.K. Stubbings, A.J. Moore, M. Dusmet, P. Goldstraw, T.G. West, M.I. Polkey, et al., Physiological properties of human diaphragm muscle fibres and the effect of chronic obstructive pulmonary disease., J. Physiol. 586 (2008) 2637–2650. doi:10.1113/jphysiol.2007.149799.

[315] M. a Lopez, P.S. Pardo, G. a Cox, A.M. Boriek, Early mechanical dysfunction of the diaphragm in the muscular dystrophy with myositis (Ttnmdm) model., Am. J. Physiol. Cell Physiol. 295 (2008) C1092–C1102. doi:10.1152/ajpcell.16.2008.

[316] M. Sussman, Duchenne muscular dystrophy., J. Am. Acad. Orthop. Surg. 10 (2002) 138–51.

doi:10.1016/j.nmd.2013.06.373.

[317] L. Leeuwen, D. a. Fitzgerald, Congenital diaphragmatic hernia, J. Paediatr. Child Health. 50 (2014) 667–673. doi:10.1111/jpc.12508.

[318] A. Gaxiola, J. Varon, G. Valladolid, Congenital diaphragmatic hernia: An overview of the etiology and current management, Acta Paediatr. Int. J. Paediatr. 98 (2009) 621–627. doi:10.1111/j.1651-2227.2008.01212.x.

[319] P.P.L. Chiu, New Insights into Congenital Diaphragmatic Hernia - A Surgeon's Introduction to CDH Animal Models., Front. Pediatr. 2 (2014) 36. doi:10.3389/fped.2014.00036.

[320] J. Wynn, L. Yu, W.K. Chung, Genetic causes of congenital diaphragmatic hernia., Semin. Fetal Neonatal Med. 19 (2014) 324–330. doi:10.1016/j.siny.2014.09.003.

[321] L.M. Wessel, J. Fuchs, U. Rolle, The Surgical Correction of Congenital Deformities: The Treatment of Diaphragmatic Hernia, Esophageal Atresia and Small Bowel Atresia., Dtsch. Arztebl. Int. 112 (2015) 357–64. doi:10.3238/arztebl.2015.0357.

[322] Wang L.C, Clark M.E, Edwards M.J, Use of composite polyester/collagen mesh in the repair of recurrent congenital diaphragmatic hernias, J. Pediatr. Surg. Case Rep. 3 (2015) 377–381. doi:10.1016/j.epsc.2015.07.001.

[323] O. Al-Nouri, B. Hartman, R. Freedman, C. Thomas, T. Esposito, Diaphragmatic rupture: Is management with biological mesh feasible?, Int. J. Surg. Case Rep. 3 (2012) 349–53. doi:10.1016/j.ijscr.2012.04.011.

[324] W. Zhao, Y.M. Ju, G. Christ, A. Atala, J.J. Yoo, S.J. Lee, Diaphragmatic muscle reconstruction with an aligned electrospun poly(ε-caprolactone)/collagen hybrid scaffold, Biomaterials. 34 (2013) 8235–8240. doi:10.1016/j.biomaterials.2013.07.057.

[325] V. Ngô-Muller, K. Muneoka, In Utero and Exo Utero Surgery on Rodent Embryos, Methods Enzymol. 476 (2010) 201–226. doi:10.1016/S0076-6879(10)76012-2.

[326] J. Pulido, S. Reitz, S. Gozdanovic, et al, Laparoscopic repair of chronic traumatic diaphragmatic hernia using biologic mesh with cholecystectomy for intrathoracic gallbladder., JSLS. 15 (2011) 546–549. doi:10.4293/108680811X13176785204472.

[327] B. Wiegmann, S. Korossis, K. Burgwitz, C. Hurschler, S. Fischer, A. Haverich, et al., In Vitro

Comparison of Biological and Synthetic Materials for Skeletal Chest Wall Reconstruction, Ann. Thorac. Surg. 99 (2015) 991–998. doi:10.1016/j.athoracsur.2014.09.040.

[328] S. Franz, S. Rammelt, D. Scharnweber, J.C. Simon, Immune responses to implants – A review of the implications for the design of immunomodulatory biomaterials, Biomaterials. 32 (2011) 6692–6709. doi:10.1016/j.biomaterials.2011.05.078.

[329] S. Schiaffino, A.C. Rossi, V. Smerdu, L.A. Leinwand, C. Reggiani, Developmental myosins: expression patterns and functional significance., Skelet. Muscle. 5 (2015) 22. doi:10.1186/s13395-015-0046-6.

[330] B.N. Brown, S.F. Badylak, Extracellular matrix as an inductive scaffold for functional tissue reconstruction, Transl. Res. 163 (2014) 268–285. doi:10.1016/j.trsl.2013.11.003.

[331] H.J. Rippon, A.E. Bishop, Embryonic stem cells, Cell Prolif. 37 (2004) 23–34. doi:10.1111/j.1365-2184.2004.00298.x.

[332] M. Drukker, G. Katz, A. Urbach, M. Schuldiner, G. Markel, J. Itskovitz-Eldor, et al., Characterization of the expression of MHC proteins in human embryonic stem cells., Proc. Natl. Acad. Sci. U. S. A. 99 (2002) 9864–9869. doi:10.1073/pnas.142298299.

[333] K. Takahashi, S. Yamanaka, Induction of Pluripotent Stem Cells from Mouse Embryonic and Adult Fibroblast Cultures by Defined Factors, Cell. 126 (2006) 663–676. doi:10.1016/j.cell.2006.07.024.

[334] M. Eisenstein, IPSCs: One cell to rule them all?, Nat. Methods. 7 (2010) 81–85. doi:10.1038/nmeth0110-81.

[335] J. Chen, H. Liu, J. Liu, J. Qi, B. Wei, J. Yang, et al., H3K9 methylation is a barrier during somatic cell reprogramming into iPSCs., Nat. Genet. 45 (2013) 34–42. doi:10.1038/ng.2491.

[336] Y. Matsui, K. Zsebo, B.L. Hogan, Derivation of pluripotential embryonic stem cells from murine primordial germ cells in culture., Cell. 70 (1992) 841–847. doi:10.1016/0092-8674(92)90317-6.

[337] P. De Coppi, G. Bartsch, M.M. Siddiqui, T. Xu, C.C. Santos, L. Perin, et al., Isolation of amniotic stem cell lines with potential for therapy., Nat. Biotechnol. 25 (2007) 100–106. doi:10.1097/01.ogx.0000261640.52511.eb.

[338] A. Ditadi, P. De Coppi, O. Picone, L. Gautreau, R. Smati, E. Six, et al., Human and murine amniotic fluid c-Kit+Lin- cells display hematopoietic activity, Blood. 113 (2009) 3953–3960. doi:10.1182/blood-2008-10-182105.

[339] A. Zani, M. Cananzi, F. Fascetti-Leon, G. Lauriti, V. V Smith, S. Bollini, et al., Amniotic fluid stem cells improve survival and enhance repair of damaged intestine in necrotising enterocolitis via a COX-2 dependent mechanism., Gut. 63 (2014) 300–9. doi:10.1136/gutjnl-2012-303735.

[340] J.M. Fishman, A. Tyraskis, P. Maghsoudlou, L. Urbani, G. Totonelli, M.A. Birchall, et al., Skeletal Muscle Tissue Engineering: Which Cell to Use?, Tissue Eng. Part B Rev. 19 (2013) 503–515. doi:10.1089/ten.teb.2013.0120.

[341] C.S. Fry, J.D. Lee, J.R. Jackson, T.J. Kirby, S. a. Stasko, H. Liu, et al., Regulation of the muscle fiber microenvironment by activated satellite cells during hypertrophy, FASEB J. 28 (2014) 1654–1665. doi:10.1096/fj.13-239426.

[342] F. Relaix, P.S. Zammit, Satellite cells are essential for skeletal muscle regeneration: the cell on the edge returns centre stage, Development. 139 (2012) 2845–2856. doi:10.1242/dev.069088.

[343] M.M. Murphy, J. a Lawson, S.J. Mathew, D. a Hutcheson, G. Kardon, Satellite cells, connective tissue fibroblasts and their interactions are crucial for muscle regeneration., Development. 138 (2011) 3625–3637. doi:10.1242/jcs098228.

[344] L. Boldrin, A. Neal, P.S. Zammit, F. Muntoni, J.E. Morgan, Donor satellite cell engraftment is significantly augmented when the host niche is preserved and endogenous satellite cells are incapacitated, Stem Cells. 30 (2012) 1971–1984. doi:10.1002/stem.1158.

[345] A.J. Merrell, B.J. Ellis, Z.D. Fox, J.A. Lawson, J.A. Weiss, G. Kardon, Muscle connective tissue controls development of the diaphragm and is a source of congenital diaphragmatic hernias, Nat. Genet. 47 (2015) 496–504. doi:10.1038/ng.3250.

[346] S.J. Mathew, J.M. Hansen, A.J. Merrell, M.M. Murphy, J.A. Lawson, D.A. Hutcheson, et al., Connective tissue fibroblasts and Tcf4 regulate myogenesis, Development. 138 (2011) 371–384. doi:10.1242/dev.057463.

[347] M. Meregalli, A. Farini, M. Belicchi, Y. Torrente, CD133(+) Cells for the Treatment of

Degenerative Diseases: Update and Perspectives., Adv. Exp. Med. Biol. 777 (2013) 229–43. doi:10.1007/978-1-4614-5894-4_15.

[348] C. Bonfanti, G. Rossi, F.S. Tedesco, M. Giannotta, S. Benedetti, R. Tonlorenzi, et al., PW1/Peg3 expression regulates key properties that determine mesoangioblast stem cell competence., Nat. Commun. 6 (2015) 6364. doi:10.1038/ncomms7364.

[349] T. Tamaki, Multipotency and physiological role of skeletal muscle interstitium-derived stem cells The Japanese Society of Physical Fitness and Sports Medicine Multipotency and physiological role of skeletal muscle interstitium-derived stem cells, 1 (2012) 423–436.

[350] A. Dellavalle, M. Sampaolesi, R. Tonlorenzi, E. Tagliafico, B. Sacchetti, L. Perani, et al., Pericytes of human skeletal muscle are myogenic precursors distinct from satellite cells., Nat. Cell Biol. 9 (2007) 255–267. doi:10.1038/ncb1542.

[351] J. Zheng, Y. Wang, A. Karandikar, Q. Wang, Skeletal myogenesis by human embryonic stem cells, Cell Res. (2006). http://www.nature.com/cr/journal/vaop/ncurrent/full/7310080a.html.

[352] M. Shelton, J. Metz, J. Liu, R.L. Carpenedo, S.-P. Demers, W.L. Stanford, et al., Derivation and Expansion of PAX7-Positive Muscle Progenitors from Human and Mouse Embryonic Stem Cells, Stem Cell Reports. 3 (2014) 516–529. doi:10.1016/j.stemcr.2014.07.001.

[353] M. Krampera, G. Pizzolo, G. Aprili, M. Franchini, Mesenchymal stem cells for bone, cartilage, tendon and skeletal muscle repair, Bone. 39 (2006) 678–683. doi:10.1016/j.bone.2006.04.020.

[354] J.A. Kim, Y.H. Shon, J.O. Lim, J.J. Yoo, H.-I. Shin, E.K. Park, MYOD mediates skeletal myogenic differentiation of human amniotic fluid stem cells and regeneration of muscle injury., Stem Cell Res. Ther. 4 (2013) 147. doi:10.1186/scrt358.

[355] S.P. Loukogeorgakis, P. De Coppi, Stem cells from amniotic fluid – Potential for regenerative medicine, Best Pract. Res. Clin. Obstet. Gynaecol. 44 (2015) 1–13. doi:10.1016/j.bpobgyn.2015.08.009.

[356] V. Parazzi, C. Lavazza, V. Boldrin, E. Montelatici, F. Pallotti, M. Marconi, et al., Extensive Characterization of Platelet Gel Releasate From Cord Blood in Regenerative Medicine, 24 (2015) 2573–2584.

[357] A. Picardi, A. Lanti, L. Cudillo, R. Cerretti, T. Dentamaro, G. De Angelis, et al., Platelet gel for

treatment of mucocutaneous lesions related to graft-versus-host disease after allogeneic hematopoietic stem cell transplant, Transfusion. 50 (2010) 501–506. doi:10.1111/j.1537-2995.2009.02439.x.

[358] M. Sánchez, E. Anitua, D. Delgado, P. Sánchez, G. Orive, S. Padilla, Muscle repair: platelet-rich plasma derivates as a bridge from spontaneity to intervention, Injury. 45 (2014) S7–S14. doi:10.1016/S0020-1383(14)70004-X.

[359] Y. Wen, P. Bi, W. Liu, a. Asakura, C. Keller, S. Kuang, Constitutive Notch Activation Upregulates Pax7 and Promotes the Self-Renewal of Skeletal Muscle Satellite Cells, Mol. Cell. Biol. 32 (2012) 2300–2311. doi:10.1128/MCB.06753-11.

[360] M.T. Webster, U. Manor, J. Lippincott-schwartz, C. Fan, M.T. Webster, U. Manor, et al., Intravital Imaging Reveals Ghost Fibers as Architectural Units Guiding Myogenic Progenitors during Regeneration Short Article Intravital Imaging Reveals Ghost Fibers as Architectural Units Guiding Myogenic Progenitors during Regeneration, Stem Cell. (2016) 1–10. doi:10.1016/j.stem.2015.11.005.

[361] J.H. Kim, P. Jin, R. Duan, E.H. Chen, Mechanisms of myoblast fusion during muscle development, Curr. Opin. Genet. Dev. 32 (2015) 162–170. doi:10.1016/j.gde.2015.03.006.

[362] S. Shojaie, L. Ermini, C. Ackerley, J. Wang, S. Chin, B. Yeganeh, et al., Acellular Lung Scaffolds Direct Differentiation of Endoderm to Functional Airway Epithelial Cells: Requirement of Matrix-Bound HS Proteoglycans., Stem Cell Reports. 4 (2015) 419–30. doi:10.1016/j.stemcr.2015.01.004.

[363] A.J. Merrell, G. Kardon, Development of the diaphragm - a skeletal muscle essential for mammalian respiration, FEBS J. 280 (2013) 4026–4035. doi:10.1111/febs.12274.

[364] M.R. Hicks, T. V. Cao, D.H. Campbell, P.R. Standley, Mechanical strain applied to human fibroblasts differentially regulates skeletal myoblast differentiation, J. Appl. Physiol. 113 (2012) 465–472. doi:10.1152/japplphysiol.01545.2011.

[365] S.J. Mathew, J.M. Hansen, a. J. Merrell, M.M. Murphy, J. a. Lawson, D. a. Hutcheson, et al., Connective tissue fibroblasts and Tcf4 regulate myogenesis, Development. 138 (2011) 371–384. doi:10.1242/dev.057463.